SERI/RR--253-1750

DE84 013032

Low-Cost Collectors/ Systems Development Progress Report

C. Kutscher
R. Davenport
R. Farrington
G. Jorgensen
A. Lewandowski
C. Vineyard

July 1984

Prepared under Task No. 1271.00 and 1278.00
FTP No. 256

Solar Energy Research Institute
A Division of Midwest Research Institute

1617 Cole Boulevard
Golden, Colorado 80401

Prepared for the
U.S. Department of Energy
Contract No. DE-AC02-83CH10093

PREFACE

This report describes the combined work performed under two FY 1982 SERI tasks: Task No. 1271, "Materials Research and Development for Low-Cost Collectors" and Task No. 1278, "Low-Cost Collectors." The authors would like to express their thanks to the technicians who supported this effort: Douglas Powell, who constructed the sheet metal collector, and James Pruett, who assembled the low-cost system loop and built the pump speed controller. Support given at various times by James Dolan, Milton Bell, and Cécile Leboeuf is also gratefully acknowledged. Although the final draft version of this report was completed in April 1983, funding for the final publication was not available until 1984.

Charles F. Kutscher
Task Leader

Approved for

SOLAR ENERGY RESEARCH INSTITUTE

for JPT

John P. Thornton, Chief
Thermal Systems and Engineering Branch

L. J. Shannon, Director
Solar Heat Research Division

SUMMARY

Objective

To develop much lower cost (by a factor of 3-4) residential space heating and hot water systems suitable for both retrofit and new construction applications.

Discussion

This report describes the work done in FY 1982 in the Solar Energy Research Institute's low-cost collectors and systems effort. The effort focused on liquid rather than air systems because of their direct applicability to systems that supply only domestic hot water (DHW) as well as combined DHW and space heating systems. The task was divided into two parallel efforts: one concentrating on collectors (since they typically represent one-third of the installed cost), the other concentrating on the remainder of the system. The initial work involved a literature search, compilation of previous work done at SERI, solicitation of ideas via the Commerce Business Daily, and establishment of communication with industry. Since work on a Department of Energy project entitled "Active Program Research Requirements" was similar, close coordination was established with that effort. Based on several market studies found in the literature, specific cost and performance goals were established.

To identify which type of system offered the greatest reliability, performance, and cost reduction potential, we studied and compared 13 system configurations. Once a drainback system was chosen as the best configuration, computer models were used to predict its performance and allow for sizing of its subcomponents. Criteria for filling, draining, and establishing a syphon in drainback systems were determined analytically and experimentally. Since a drainback system requires more pumping power than other configurations, we measured pump efficiencies for a number of solar energy system pumps. Potential solutions for the high pumping power requirements were studied, and a simple pump controller (consisting of a Triac and time delay) to limit pump power was built and successfully tested.

The next step was to identify low-cost materials to be used in the loop construction. We surveyed candidate piping, insulation, and storage tank materials and compared the materials recommended on the basis of costs and physical properties. Polybutylene piping and low-pressure steel storage tanks were identified as major contributors to cost reduction. Overall system cost estimates were made, the appropriate materials were ordered, and a low-cost DHW loop was built and installed at SERI.

To provide a fresh look at what very low cost concepts were feasible for low-cost collectors, two extensive materials surveys were performed. Approximately 90 different absorber materials and 45 different glazing materials were compared based on cost, physical properties, and optical properties. As a result, several low-cost collector concepts were studied and two prototype collectors were built: a glass-reinforced concrete collector and a sheet metal collector. The latter was ultimately integrated into the low-cost system loop.

Collector concepts developed outside of SERI were also examined. Two collectors were evaluated in-house: a thin-film plastic collector developed by Brookhaven National Laboratory and a rigid plastic collector manufactured by Sealed Air Corporation. Both collectors were tested according to ASHRAE 93-77 standards at SERI's Mid-Temperature Collector Research Facility (MTCRF) and recommendations for improvements were made.

Conclusions

Market studies have clearly shown that, in the absence of tax credits, large cost reductions are needed in solar space heating and domestic hot water systems to achieve significant penetration of the residential retrofit market. A study of typical cost figures for contractor-installed solar space heating (DHW systems) indicates the following approximate breakdown: equipment, 56%; labor, 17%; and overhead and profit, 27%. (Companies that market and install their own solar products can have significantly higher overhead and profit costs.) Of the 56 percentage points attributable to equipment, 35 of those points (i.e., 65% of equipment cost) represent collector costs. Of the 17 percentage points in the labor category, 11 (i.e., 65% of labor cost) represent piping (including insulation). Thus reductions in collector material costs and piping installation costs can have a significant impact on overall system costs. Of the various system alternatives, the drainback configuration appears very promising because of its high reliability and potential for cost reduction. Sizing of pipe to provide proper filling and draining is straightforward, and pumping power can be minimized in syphon-return systems by using a simple combination of a Triac and a time delay. By using polybutylene pipe in place of copper and low-pressure steel storage containers, balance-of-system costs can be greatly reduced.

A closed, low-pressure drainback loop allows use of low-cost collector materials that would otherwise corrode or succumb to pressure. For example, both aluminum and steel are considerably less expensive than copper but can be used in a properly designed drainback system. Glass-reinforced concrete and various plastics are also low-cost candidates. Although these and other collector concepts require further research, the total installed cost to the consumer for a combined DHW and space heating system can probably be reduced to approximately $\$150/m^2$ ($14/ft^2$) without tax credits, which is equivalent, on the average, to an energy cost of about \$82/(GJ/yr) [\$87/(MBtu/yr)].

TABLE OF CONTENTS

Page

Part I. Approach

1.0 Introduction 1

1.1 History and Objectives 1
1.2 Task Organization and Strategy 2
1.3 Relationship to Other Programs 2

2.0 Preliminary Studies 4

2.1 Data Gathering 4
2.1.1 Previous Results 4
2.1.2 Commerce Business Daily (CBD) Responses 7
2.1.3 Industry Contacts 12
2.1.4 Coordination with the Active Program Research Requirements Study 13
2.2 System Cost and Performance Goals 13
2.2.1 Cost Goal 14
2.2.2 Performance Goal 22
2.3 References 22

Part II. Low-Cost Systems

3.0 Survey of Candidate Systems 24

3.1 System Descriptions 24
3.1.1 Recirculation (or Pulse) 27
3.1.2 Drainout (or Draindown) 27
3.1.3 Drainback with Air Compressor 29
3.1.4 Drainback with Liquid Level Control 29
3.1.5 Thermosyphon with Electrically Protected Collector 31
3.1.6 Drainout Thermosyphon 31
3.1.7 Breadbox (or Batch) 33
3.1.8 Coil in Tank, Wrap Around, Tank in Tank 33
3.1.9 External Heat Exchanger 35
3.1.10 Drainback with Load-Side Heat Exchanger 35
3.1.11 Drainback with Collector-Side Heat Exchanger 37
3.1.12 Two-Phase Thermosyphon 38
3.1.13 One-Phase Thermosyphon 39
3.2 Drainback Systems 41
3.3 References 44

4.0 System Analysis and Experimentation 46

4.1 Computer Analysis of Heat Exchange Alternatives 46
4.2 Fill and Drain Analysis and Testing 50
4.2.1 Draining 50
4.2.2 Filling 55

TABLE OF CONTENTS (Continued)

Page

4.3 Pump Testing and Analysis..... 62
4.3.1 Calculated Pump Efficiencies..... 67
4.3.2 Measured Overall Pump Efficiencies..... 71
4.4 Conclusions..... 78
4.5 References..... 80

5.0 System Optimization..... 81

5.1 Results of System Materials Survey..... 81
5.1.1 Pipe Materials..... 81
5.1.2 Tank and Liner Materials..... 84
5.1.3 Insulating Materials..... 84
5.2 Design Alternatives..... 89
5.3 System Costs..... 91
5.4 Reference..... 91
5.5 Bibliography..... 94

Part III. Low-Cost Collectors

6.0 Survey of Collector Materials..... 95

6.1 Absorber Materials..... 95
6.1.1 Survey..... 95
6.1.2 Use of Low-Temperature Materials..... 105
6.2 Glazing Materials..... 113
6.3 Glossary of Terms Used in Section 6.2..... 129
6.4 Glazing Materials Bibliography..... 130
6.5 Absorber Materials Bibliography..... 130

7.0 SERI Low-Cost Collector Concepts..... 132

7.1 Introduction..... 132
7.2 Glass-Reinforced Concrete Collector..... 133
7.2.1 Analysis..... 134
7.2.2 Construction..... 142
7.2.3 Cost of GRC Collector..... 145
7.2.4 Conclusions..... 146
7.3 Other Concepts..... 147
7.3.1 Galvanized Sheet Metal Collector..... 147
7.3.2 Glass Cloth Collector..... 151
7.3.3 Polypropylene Collector..... 151
7.3.4 Black Pellet Concept..... 153
7.4 References..... 155

8.0 Collector Testing..... 157

8.1 Description of the Mid-Temperature Collector Research Facility... 157
8.2 Modifications to the Mid-Temperature Collector Research Facility..... 160

TABLE OF CONTENTS (Concluded)

Page

8.3 Test Results..... 161
8.3.1 BNL Collector Test Results..... 161
8.3.2 Sealed Air Collector Test Results..... 163
8.4 References..... 165

9.0 Conclusions and Recommendations..... 167

9.1 Low-Cost Systems..... 167
9.2 Low-Cost Collectors..... 168

Appendix A Analysis of a Combination Tank/Solar Collector..... 170

Appendix B Analysis of Thermal Protection for Plastic Pipe..... 184

Appendix C Experimental Measurement of Pump Efficiencies..... 193

LIST OF FIGURES

		Page
1-1	Milestone and Activity Chart for Low-Cost Collectors Task	3
2-1	Solicitation of Low-Cost Solar Collector Research for Domestic Hot Water/Space Heating Applications in the Commerce Business Daily	7
2-2	Market Acceptance of a Solar Hot Water Heater for a High Home Value	17
2-3	Market Acceptance of a Solar Hot Water Heater for a Moderate Home Value	17
2-4	Consumer Acceptance of Added Heat Pump System Cost	18
3-1	System Configurations	25
3-2	Recirculation (or Pulse) System	28
3-3	Drainout System	28
3-4	Drainback System with Air Compressor	30
3-5	Drainback System with Liquid Level Control	30
3-6	Thermosyphon System with Electrically Protected Collector	32
3-7	Drainout Thermosyphon System	32
3-8	Breadbox (or Batch) System	33
3-9	Coil-in-Tank, Wrap-Around, Tank-in-Tank Systems	34
3-10	External Heat Exchanger System	36
3-11	Drainback System with Load-Side Heat Exchanger	36
3-12	Drainback System with Collector-Side Heat Exchanger	38
3-13	Two-Phase Thermosyphon System	39
3-14	One-Phase Thermosyphon System	39
4-1	Collector-Side Heat Exchange	47
4-2	Load-Side Heat Exchange	47
4-3	Observations of Menisci	52
4-4	Analytical Models for Open-Ended Pipes	52
4-5	Experimental Setup	55

LIST OF FIGURES (Continued)

		Page
4-6	General Form of Fill Curve	56
4-7	Fill Curves, Runs 4, 5, 10, 11, 12, 13, 19, 20	57
4-8	Fill Curves, Runs 21, 22, 23, 28	57
4-9	Pump Performance Curve for Fill Tests	59
4-10	Experimental Setup	60
4-11	Fill Results, Runs 2, 12, 13, 14	61
4-12	Fill Results, Runs 17, 18, 19	61
4-13	Drainback System H-Q Curves	63
4-14	Taco 009 Pump Efficiencies	69
4-15	Myson Pump Efficiencies	70
4-16	Experimental Setup for Richdel Pumps	73
4-17	Experimental Setup for Grundfos and Taco Pumps	74
4-18	Experimental Taco 009 Pump Curve with Pressure Gauges	74
4-19	Published Grundfos UPS 20-42 Pump Curve	76
6-1	Possible Arrangement for Black Liquid Thin-Film Absorber	112
6-2	Thermostatically Controlled Reflectors to Limit Temperature	112
7-1	Open-Channel Absorber	134
7-2	GRC Collector Plate	134
7-3	Fully Wetted Absorber	135
7-4	Fin Efficiency for Cast-in-Place Passages	136
7-5	Collector Efficiency Factor of Cast-in-Place Passages	137
7-6	GRC Absorber Place	138
7-7	Model of Tubes for Stress Analysis	139
7-8	Model of Rib Between Tubes	139

LIST OF FIGURES (Continued)

		Page
7-9	Model for Longitudinal Stress Analysis	140
7-10	Four Possible Configurations for a Galvanized Sheet Metal Absorber Plate	147
7-11	Flat-Plate Sheet Metal Absorber	149
7-12	Glass Cloth Collector	152
7-13	Polypropylene Absorber	153
7-14	Black Sphere Collector	154
8-1	MTCRF Test Loop Schematic	158
8-2	CP2 (Brookhaven) Peak Efficiency Performance	163
8-3	CP2 (Brookhaven) Incident Angle Performance	164
8-4	Sealed Air Collector Efficiency Tests	164
8-5	Sealed Air Collector Peak Thermal Performance Tests	166
8-6	Sealed Air Collector Incident-Angle Modifiers	166
A-1	Sunwizard Domestic Hot Water System	170
A-2	Performance of Sunwizard System	173
A-3	Sunwizard Performance Using Actual Water Temperatures	173
A-4	Geometry for View Factor Calculations	176
A-5	Slope Factor as a Function of the Reflector Radius	177
A-6	Geometry for Incident Radiation Calculation	179
A-7	Thermal Model of Sunwizard System	181
B-1	Geometry for Bare Copper Pipe	186
B-2	Insulated Copper Pipe	190
C-1	Flowmeter Calibration	193
C-2	Richdel 798A Published Pump Curve	197
C-3a	Experimental Curve for Used Richdel R798A Pump, Test I	198

LIST OF FIGURES (Concluded)

		Page
C-3b	Experimental Curve for Used Richdel R798A Pump, Test II.....	199
C-4a	Experimental Curve for New Richdel R798A Pump, Test I.....	200
C-4b	Experimental Curve for New Richdel R798A Pump, Test II.....	201
C-5	Published Grundfos UPS 20-42 Pump Curve.....	202
C-6	Experimental Grundfos UPS 20-42 Pump Curve, Speed 1 (Low).....	203
C-7	Experimental Grundfos UPS 20-42 Pump Curve, Speed 2 (Med.).....	204
C-8	Experimental Grundfos UPS 20-42 Pump Curve, Speed 3 (High).....	205
C-9	Taco 009 Pump Curve with Strain Gauge Differential Pressure Transducer.....	206

LIST OF TABLES

		Page
2-1	Useful Low-Cost Collector Information Gathered Prior to FY 1982...	5
2-2	Summary of Responses to CBD Announcement.....	8
2-3	Industry Contacts in Low-Cost Collector Systems Task.....	12
2-4	APRR System Ranking.....	14
2-5	APRR Collector Ranking.....	15
3-1	Boiling Point of Water at Various Pressures.....	43
4-1	Collector-Side vs. Load-Side Heat Exchanger Results.....	50
4-2	Drain/Fill Results for a 1.27-cm (1/2-in.) Copper Pipe.....	58
4-3	Pressure Drop for a Drainback System.....	64
4-4	Pressure Drop as a Function of Pipe Size and Flow Rate.....	66
4-5	Annual System Operating Cost.....	68
4-6	Myson Pump Efficiencies Calculated from Published Head-Flow Curve.....	70
4-7	Calculated Overall Pump Efficiencies.....	71
4-8	Calculated Pump Motor Efficiencies.....	71
4-9	Equipment List for Pump Tests.....	75
4-10	Measured Pump Efficiencies.....	76
4-11	Measured Power Factor.....	77
4-12	Power Reduction Options for Drainback Systems.....	79
5-1	Industry Contacts for Balance-of-System Materials Survey.....	82
5-2	Pipe Materials.....	83
5-3	Storage Containment Materials.....	85
5-4	Liner Materials.....	86
5-5	Insulating Materials.....	87
5-6	Cost Estimate for a Solar Domestic Hot Water System.....	92

LIST OF TABLES (Continued)

		Page
5-7	Cost Estimate for a Domestic Hot Water System with Plastic Collectors and Piping	93
6-1	Physical Properties of Metal Sheet	97
6-2	Physical Properties of Metal Foil	98
6-3	Physical Properties of Foamed Plastics	99
6-4	Physical Properties of Rigid Plastics	100
6-5	Physical Properties of Thin Film Plastics	102
6-6	Physical Properties of Rubbers	103
6-7	Physical Properties of Textiles	106
6-8	Physical Properties of Forest Products	107
6-9	Physical Properties of Ceramics	108
6-10	Industry Contacts Made During the Absorber Materials Survey	110
6-11	Cost and Availability of Glazing Materials	115
6-12	Optical and Thermal Properties of Glazing Materials	119
6-13	Mechanical and Weathering Properties of Glazing Materials	122
6-14	Industry Contacts Made during the Glazing Materials Survey	128
7-1	Industry Contacts Who Have Considered Concrete Collector Concepts	134
7-2	Calculated Values for Cast-in-Place Fluid Passages	137
7-3	Industry Contacts for Construction of GRC Collectors	144
7-4	GRC Mixture	145
7-5	Estimated Costs for Sheet Metal Collector	150
7-6	Estimated Costs for a Glass Cloth Flat-Plate Collector	152
7-7	Estimated Costs of a Flat-Plate Collector with a Polypropylene Absorber	153

LIST OF TABLES (Concluded)

		Page
8-1	Major Features of the Mid-Temperature Collector Research Facility	157
8-2	Mid-Temperature Collector Research Facility Instrumentation	159
8-3	Test Conditions Required for Valid Data over 5-min Period	160
A-1	Results of Sunwizard Simulations	171
A-2	Sunwizard Simulations Using Actual Water Temperatures	172
A-3	Air Space Conductance Values	174
A-4	Shape Factors as a Function of Radial Distance r	178
A-5	Monthly Cold Water Supply Temperatures (at the source) in ^{o}F for 14 Cities	183
C-1	Turbine Meter Head-Flow Characteristics	194
C-2	Viatran Pressure Transducers	194
C-3	Summary of Instrumentation Uncertainty	196

PART I. APPROACH

SECTION 1.0

INTRODUCTION

This section supplies the background and framework for SERI's Low-Cost Collectors/Systems task. Section 1.1 explains the history of this effort as well as the objectives and scope of work. Section 1.2 explains how the project was organized and gives a brief summary of our progress. Section 1.3 describes the relationship between the SERI effort and work being done at Brookhaven National Laboratory (BNL).

1.1 HISTORY AND OBJECTIVES

In late 1979 a committee was formed at the Solar Energy Research Institute (SERI) to investigate the possibilities for reducing collector costs. The committee identified the collector as the major cost element in solar hot water and space heating systems, so committee members proposed in-depth research toward reducing the cost of collectors.

Although interest in the project was high among committee members, little funding was available at that time and little progress was made. In late December 1981, funding became available and two tasks were created to develop low-cost collectors. These were entitled "Low-Cost Collectors" and "Materials Research and Development for Low-Cost Collectors." The latter task recognized that materials research would need to make important contributions to achieve successful low-cost collector designs. Sections 5.1, 6.0, and 7.0 discuss materials directly.

The two tasks were later combined into one because of their complementary nature, and the mission of the earlier low-cost collector committee was expanded. Since collector cost reductions alone do not guarantee affordable system costs (without tax credits), the project would also study reducing costs for entire systems.

Originally, domestic hot water was identified as the most promising solar application. Even with better insulated houses and passive solar design, there is still a need for domestic hot water (DHW). Since it is more efficient to heat water with liquid collectors than with air collectors and since the task budget was limited, the task members decided to concentrate only on liquid collectors in FY 1982. Shortly after task work began, the scope was expanded to include space heating as well as DHW at the request of DOE.

It is possible to design a solar energy system for a new home that uses relatively low performance collectors in conjunction with a space heating system that can utilize low temperatures (e.g., radiant slab). It is also possible to reduce costs by integrating collectors with the roof structure. Since designing systems suitable for retrofit application was considered to be important, the intent of the task at SERI has been to study stand-alone collector systems that can operate at a reasonable efficiency (30% overall) at

temperatures of 60°C (140°F). We have kept in mind the possibilities for roof integration, however, and two of our concepts (glass-reinforced concrete and galvanized sheet metal) are candidates for this type of integration.

1.2 TASK ORGANIZATION AND STRATEGY

Figure 1-1 shows a milestone and activity chart for the FY 1982 low-cost collector task. This chart shows that the collector and system efforts were addressed separately. The first step was to document work previously done by the low-cost collector committee and elsewhere. Then parallel efforts were aimed at identifying promising collectors from outside SERI as well as developing new concepts in-house. In-house development began with surveys of candidate absorber and glazing materials to identify the most promising items for building lower-cost collectors.

Several promising collector ideas were identified and their costs were estimated. Only two concepts were developed during FY 1982--a glass-reinforced concrete absorber and a galvanized sheet metal collector. The resulting SERI prototypes and two other collectors (the Brookhaven thin film Teflon and a rigid plastic collector by Sealed Air) were tested at SERI's Mid-Temperature Collector Research Facility (MTCRF).

The work on low-cost systems began with a survey of all possible solar hot water and space heating system configurations. The most promising system in terms of cost, reliability, and suitability for a low-cost collector was identified--a closed-loop drainback system. We used computer models to compare the performance of two variations of this system--collector-side heat exchange and load-side heat exchange. An experimental system was assembled to test fill and drain characteristics for this system as well as its pumping power penalty.

We also estimated the costs of variations of the system to identify areas for improvement. A materials survey helped to identify lower-cost materials for piping, storage, and insulation. Finally, we constructed a model system that includes low-cost piping and storage.

1.3 RELATIONSHIP TO OTHER PROGRAMS

Several national laboratories are working on collector development. Besides SERI, however, only Brookhaven is developing a low-cost, flat-plate collector for space heating and hot water applications. Brookhaven's concept emphasizes reducing quantities of materials to reduce costs. For example, the Teflon used for the absorber is not a particularly inexpensive material, but when used in very thin sheets it is inexpensive on a cost per area basis.

SERI's approach, on the other hand, stresses the use of inherently low-cost materials, such as concrete, fiberglass resin, polypropylene, and sheet metal, with weight as a secondary issue. SERI has also not yet settled on one concept but is exploring a number of alternatives, whereas Brookhaven is stressing refinement of their concept. The SERI and Brookhaven programs are thus quite different in approach and are very complementary.

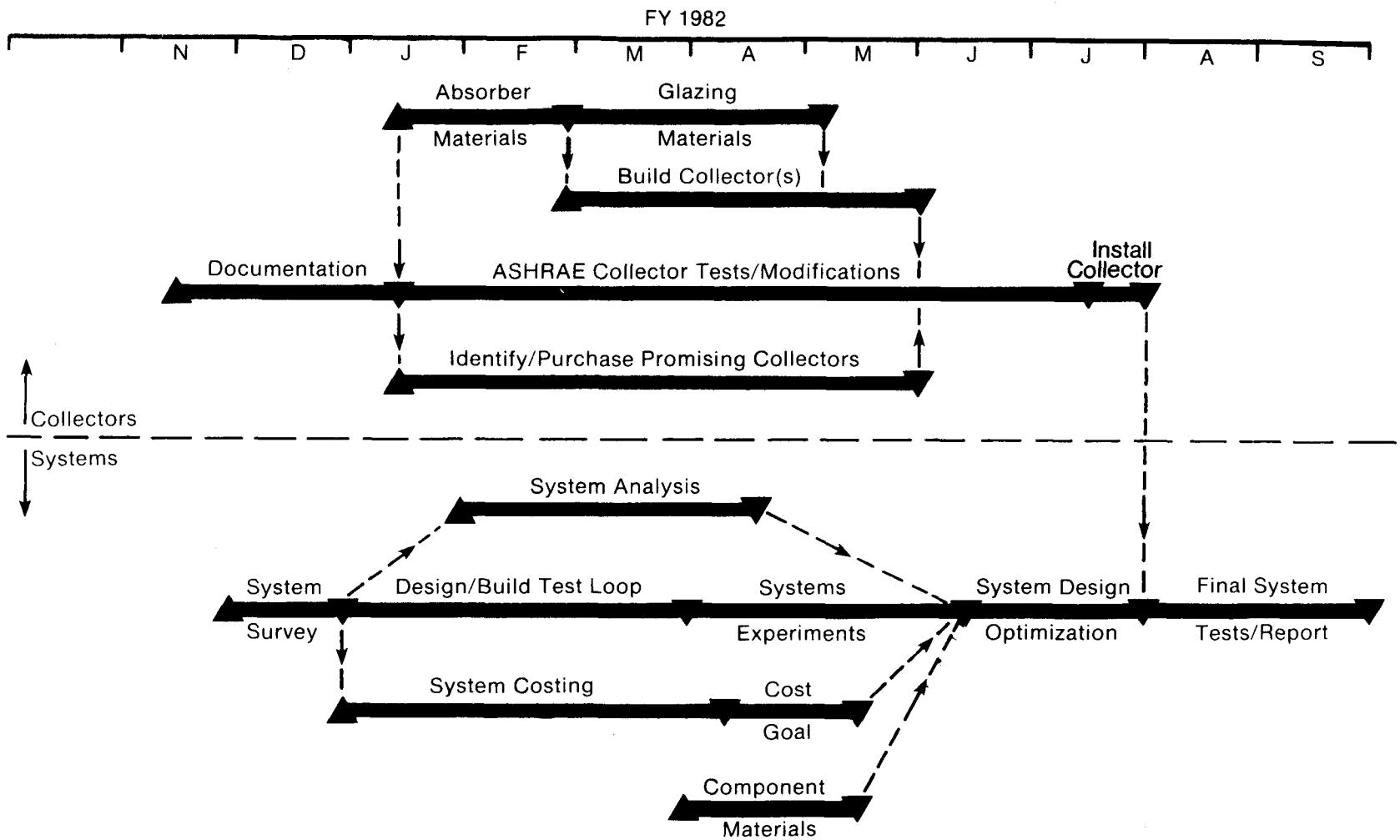

Figure 1-1. Milestone and Activity Chart for Low-Cost Collectors Task

SECTION 2.0

PRELIMINARY STUDIES

In order to decide which low-cost collectors and low-cost system concepts offered the most promise, we gathered information from as many sources as possible and then established specific goals for cost and performance. Section 2.1 describes the data-gathering effort. Section 2.1.1 discusses the earlier work done at SERI by the low-cost collector committee, including building collectors and extensive literature searches. Section 2.1.2 gives the responses to an announcement made in the Commerce Business Daily requesting ideas on low-cost collectors. The numerous contacts made with industry are described in Section 2.1.3. Related work done at SERI in the Active Program Research Requirements study is summarized in Section 2.1.4.

Establishment of costs and performance goals was important to provide the task with a means of measuring progress. The background and development of a cost goal is described in Section 2.2.1 and related to performance in Section 2.2.2.

2.1 DATA GATHERING

We consulted a variety of information sources to help identify all possible alternatives for low-cost collectors and systems. One source was earlier results of the work done by SERI's low-cost collector committee. Another was an announcement placed in the Commerce Business Daily soliciting ideas on new collectors. We also contacted researchers in industry whenever possible and documented our telephone conversations. Another source was a study entitled "Active Program Research Requirements" (APRR), which was being done at SERI for the Department of Energy (DOE). Since SERI has been acting as coordinator of all collector work for DOE, task members have reviewed the progress of work at other laboratories.

2.1.1 Previous Results

The first priority of FY 1982 efforts was to document earlier work at SERI. Information on several collector concepts had been gathered and stored in a general file. Pertinent information was extracted from this file, summarized, and arranged in appropriate categories. Table 2-1 shows the contents of the new file.

Ullman (1981) prepared an informal written summary of earlier SERI work. Instantaneous and day-long efficiency tests had been performed on two innovative collector concepts: a collector incorporating a black polyethylene absorber manufactured by Cryovac and a collector using sand as the absorbing medium. Results of testing these concepts are summarized here.

Table 2-1. Useful Low-Cost Collector Information Gathered Prior to FY 1982

Plastic Film Absorbers
Acurex (laminated polymer films)
BNL (laminated po ymer film/metal foil)
Solar Sets (BNL and fiberglass absorber)
Rigid Plastic Absorbers
Tuffak Twinwall (extruded polycarbonate)
Florida Solar Energy Center (FSEC) (black liquid in twinwall, kalwall glazing)
Upsala College, N.J. (black liquid in twinwall)
FAFCO Inc. (extruded polypropylene, fiberglass glazing, acrylonitrite-butadiene styrene [ABS] headers)
Solar Industries (extruded polypropylene absorber)
Ramada Energy Systems (extruded polysulfone, polycarbonate glazing)
Concrete Absorbers
Two patents of work in Britain
Foam, Foamglass, Ethylene/Propylene Diene Monomer (EPDM) Absorbers
Dynamic Flow (air collector with grooved foamglass, plastic glazing)
Tuxis Corp. (polyethylene foam absorber, polyethylene glazing)
Metal and Glass Absorber
General Motors (GM) (copper absorber in rigid polyurethane foam enclosure)
Optimized radiation trapping at interfaces (ORTI) (flow between black pan and glass sheet)
Center of Energy Studies, Indian Institute of Technology, New Delhi, India (black liquid in glass tubes)
Materials
Paints, coatings, and foils for absorbers
Reflective laminates, condensation reducers, heat exchangers
Literature on Nomex and other miscellaneous materials

2.1.1.1 Cryovac Collector

The Cryovac collector uses a trickle-flow design that has two layers of polyethylene welded together to form flow channels. A layer of polycarbonate or nylon inside each layer of polyethylene enhances sealing. The exposed layer of polyethylene is infused with carbon black to provide ultraviolet (UV) resistance. The absorber is contained in a galvanized box with fiberglass insulation and Tedlar glazing.

The instantaneous efficiency test yielded a y-intercept of 0.50 and a slope of -8.5 $W/m^2\ ^oC$ (-1.5 $Btu/h\ ft^2\ ^oF$). The cost of collector materials was estimated at $\$58/m^2$ ($\$5.39/ft^2$) of aperture area. The test identified problems with low tear resistance of the polyethylene, difficulties connecting a manifold to the absorber, incomplete wetting of the absorber surface, and high heat losses. The test did not measure the collector's stagnation ability, although the high heat losses could be expected to limit stagnation temperatures and protect the polyethylene.

2.1.1.2 Sand Collector

The sand collector uses an absorber consisting of a serpentine copper pipe embedded in a layer of sand that is bonded with a sodium silicate binder and coated with Nextel flat-black paint. The absorber is contained in a galvanized metal housing containing fiberglass insulation and covered with a single layer of Tedlar.

The instantaneous efficiency test yielded a y-intercept of 0.50 and a slope of -5.6 $W/m^2\ ^oC$ (-0.99 $Btu/h\ ft^2\ ^oF$), which is somewhat better than the Cryovac collector in terms of heat loss, but is still relatively low in optical efficiency. The materials cost approximately $\$47/m^2$ ($\$4.37/ft^2$). Problems with this collector include cracking of the sand absorber, poor fin efficiency, and excessive weight (415 kg/m^3, 25.9 lb/ft^3).

2.1.1.3 Other Investigations

Several other collector concepts were investigated but not fully tested. In-house day-long side-by-side testing was performed on a collector incorporating an ethylene/propylene diene monomer (EPDM) mat absorber (Solar-Roll) with a 4-mil Tedlar glazing, fiberglass insulation, and a wooden housing. No instantaneous testing was done. Another collector investigated, built by a Colorado State University student, used two sheets of aluminized Mylar film with a selective coating as the absorber. Water trickled from top to bottom between the sheets. This collector used rigid isocyanurate insulation and an extruded aluminum frame. Problems occurred with leakage and delamination of the aluminum, so the collector was not tested.

Testing of collector concepts in FY 1982 departed somewhat from the earlier philosophy, which was to screen several collectors by using side-by-side day-long testing. Earlier SERI researchers assembled a facility capable of simultaneously testing four different collectors, each with its own tank. Those collectors that looked most promising underwent instantaneous efficiency testing.

The philosophy in FY 1982 was to initially screen concepts based on a study of materials and on engineering judgment. Collector testing thus emphasizes instantaneous testing, which can be done in a rigorous standardized manner.

2.1.2 Commerce Business Daily (CBD) Responses

Although task members made every effort to keep abreast of new ideas in industry (see Section 2.1.3), we decided that a public announcement might attract industry input that would otherwise be missed. Accordingly, an announcement was made in the Commerce Business Daily on 9 April 1982. The contents of this announcement are shown in Figure 2-1.

Table 2-2 gives a summary of the 19 responses to the announcement. Fifteen of these responses involved collector concepts. Since only liquid collectors were considered in FY 1982, we eliminated four responses from further investigation. (Air collectors were not explicitly excluded from the CBD announcement since they may be considered at SERI during FY 1983.) The remaining 11 responses are categorized as follows: three breadbox-type units (one of which is freon-charged), an active freon system, a compound parabolic concentrator (CPC) design, a "terraced trough" collector, a nonevacuated tube design, an inverted flat plate with reflector, a polymer concrete collector, a glass-reinforced concrete (GRC) collector, and a stainless steel sheet collector.

Based on previous SERI studies, the last two responses (items 18 and 19 in Table 2-2) appeared to be the most promising concepts. The SRI concept of an open trough GRC panel with black glass directly on top appears to be more expensive than SERI's integral passage concrete panel but probably warrants further investigation. The Spencer design of a fluid below atmospheric pressure in a collector is interesting and rather similar to a galvanized sheet metal concept developed at SERI. The Spencer collector may not, however, be sufficiently lower in cost than conventional flat plates.

FRIDAY, APRIL 9, 1982

U.S. GOVERNMENT PROCUREMENTS

Services

A Experimental, Developmental, Test and Research Work (includes both basic and applied research)

A -- LOW COST SOLAR COLLECTOR RESEARCH FOR DOMESTIC HOT WATER/SPACE HEATING APPLICATIONS SERI is interested in purchasing, testing and modifying innovative collectors which show promise for being considerably less expensive than current production collectors. Manufacturers/designers of such collectors who are willing to have their product or design considered for participation in this program should send in information regarding the collector concept (e.g. drawings, specifications, test data, etc.) on or before April 30, 1982. SERI intends to buy no more than three or four collectors for this program. Selection will be based upon SERI's assessment of the overall design. Technical inquiries should be directed to Chuck Kutscher, Thermal Systems and Engineering Branch, Solar Energy Research Institute, (095)

Solar Energy Research Institute, 1617 Cole Boulevard, Subcontracts Branch, Golden, Colorado 80401, attn: Joseph C. Wilson, (303) 231-1838

Figure 2-1. Solicitation of Low-Cost Solar Collector Research for Domestic Hot Water/Space Heating Applications in the Commerce Business Daily

Table 2-2. Summary of Responses to CBD Announcement

Name	Description of Response	Remarks
1. R. G. Vandermeil Eng., Inc. 38 Chauncy St. Boston, MA 02111 (Drew Gillett) (617) 423-7243	Offer of assistance in reviewing proposals.	
2. Energy Engineers, Inc. 2501 Princeton Drive, N.E. Albuquerque, NM 87107 (Tom Feldman) (505) 884-1610	"Heatpipe" freon-charged thermosyphon bread-box hot water heater; $3,000 installed cost.	Claim 30% higher efficiency, DHW only.
3. Purdue University Mechanical Eng. Bldg. West Lafayette, IN 47907 (J. T. Pearson) (317) 494-6900	Air collector employing "louvered absorber/convector."	Letter only, no accompanying literature.
4. Multitherm Corp. 125 S. Front St. Colwyn, PA 19023 (Charles Kovacs, Jr.) (800) 523-7590	Description of two heat transfer fluids: PG-1 (nontoxic) and IG-2.	
5. Restoration Data 25 North New Street Staunton, VA 24401 (Andrew L. McCaskey, Jr.) (703) 885-3076	Offer to supply instrumentation assistance.	
6. DSET Laboratories, Inc. Box 1850 Black Canyon Stage I Phoenix, AZ 85029 (M. W. Rupp) (602) 465-7356	Offer of assistance in collector testing.	

Table 2-2. Summary of Responses to CBD Announcement (Continued)

Name	Description of Response	Remarks
7. Shawnee Solar Development Corp. 211-1/2 W. Main P.O. Box 560 Carbondale, IL 62901 (Jeff Graef) (618) 549-3972	Site-built, low-cost breadbox hot water heater (tank is absorber).	Includes construction drawings and instructions, DHW only.
8. Solaron Corp. 1885 W. Dartmouth Ave. Englewood, CO 80110 (Dennis Jones) (303) 762-1500	Passive breadbox solar water heater made of plastic for nonfreezing climates.	Six prototypes under construction, DHW only.
9. Manumark, Inc. Browns Bridge Road P.O. Box 997 Chatsworth, GA 30705 (Paula B. Davis) (404) 695-6764	Air collector systems.	Looks relatively conventional, but one system is an active window-mounted collector.
10. William C. Bauer 175 Cordova Court Boulder, CO 80303 (303) 494-5328	Patent for air collector with fiberglass matrix absorber.	
11. Community Energy Systems, Inc. 1820-1/2 S. MacArthur Blvd. Springfield, IL 62704 (Stu Kainste) (217) 522-2836	Site-built vertical air collectors for $\$17/ft^2$.	Appeals to do-it-yourself market.
12. Synergic Resources Corp. One Bola-Cynwyd Plaza Suite 630 Bola-Cynwyd, PA 19004 (William Steigelmann) (215) 667-2160	A so-called "terraced" collector consisting of horizontal troughs of water.	

Table 2-2. Summary of Responses to CBD Announcement (Continued)

Name	Description of Response	Remarks
13. Eng. Inc. 857 Beacon Street Boston, MA 02115 (Hans P. Huber) (617) 536-4924	Nonevacuated glass tube liquid collector; proposal to supply SERI with four 3 ft x 7 ft panels for $4,000.	
14. Lone Star Polymer Concrete Co. One Greenwich Plaza P.O. Box 5050 Greenwich, CT 06836 (M. Gunasekaran) (804) 461-1945	Propose to manufacture polymer concrete collector panels to specifications.	Had contacted SERI earlier.
15. Nortec Solar Industries, Inc. P.O. Box 288 Century Rd. Manotick Ontario, Canada KOA 2NO (James R. Swartman) (613) 692-2513	Individually thermosyphoning refrigerant charged collectors that are cooled by water flow loop.	
16. Jemico, Inc. 5364 Mud River Lane Columbia, MD 21044 (Michael A. Brown) (301) 730-7776	Inverted flat-plate liquid collectors with reflector supplying 1.5:1 concentration.	
17. New York University Barney Building 26-36 Stuyvesant St. New York, NY 10003 (212) 598-2471	CPC collector design.	Shows little if any cost reduction.
18. SRI International 333 Ravenswood Ave. Menlo Park, CA 94025 (C. F. Hilly, Jr.) (415) 326-6200	Open trough GRC panel with selectively coated glass sheet on top, glass glazing, and foamed concrete insulation.	Includes a cost breakdown.

Table 2-2. Summary of Responses to CBD Announcement (Concluded)

Name	Description of Response	Remarks
19. University of Iowa College of Engineering Division of Energy Eng. Iowa City, IA 52242 (Donald L. Spencer) (319) 353-5638	Absorber panel consists of two stainless steel sheets with water flowing below atmospheric pressure between them.	This concept is described in New Inventions in Low-Cost Solar Heating by William A. Shurcliff, Brick House Publishing Co., 1979.

Because of budget limitations and higher priorities for the study of SERI concepts, none of these collectors were purchased for testing in FY 1982. If the budget permits, one or more of these collectors would be considered for purchase in FY 1983.

2.1.3 Industry Contacts

Communication with people in the solar collector industry is an important aspect of the low-cost collector task. Occasionally we have made face-to-face contacts. (For example, a local representative of Ramada Energy Systems came to SERI to brief task members on the TemTech SDHW system that uses a plastic collector.) However, communication by telephone has been more common. To keep all task members abreast of individual conversations and to provide documentation for future reference, task members have summarized their communication on telephone conversation record forms and distributed them to other task members. A list of companies contacted is given in Table 2-3.

It would be impossible to summarize industry's reaction to a government low-cost collector effort in a single statement. Most of the companies contacted are small and are interested in cooperating with SERI. They seem to realize that systems are too expensive and that drastic measures need to be taken. One well established firm, however, felt that their product was already affordable and questioned the need for SERI's research. Their domestic hot water system has an installed retail price of \$4500, or about \$750/m^2 (\$70/ft^2).

Table 2-3. Industry Contacts in Low-Cost Collector Systems Task

National Bureau of Standards (NBS)	Ramada Energy Systems
Acurex	Stanford Research Institute (SRI)
Brookhaven National Laboratory (BNL)	Sunwizard, Inc.
Springborn Laboratory	Owens Corning
Jet Propulsion Laboratory (JPL)	Aberdeen Research Lab
Colorado State University (CSU)	General Electric Co.
Otto Fabrics	Nortec
Sunco Solar	Shell
Sealed Air Corp.	Solar Oriented Environmental Services
Sun-AG, Inc.	Southern Solar Energy Center
EMC, Inc.	CSIRO, Australia
Solar Specialists	U.S. Army
Solarray	ICI, Australia
Terra-Light	Westinghouse
Novan	Battelle Columbus Laboratory

One small firm (Sunwizard) has experimented with a number of low-cost collector concepts and is currently selling a system that is simply a glazed hot water tank which sits outside a building. A computer analysis performed at SERI of this inexpensive system shows that it can perform very well for domestic hot water heating (see Appendix A for further discussion). Its application could be limited by suitable location, aesthetics, and very cold climates. Also, it will not achieve as high a solar fraction as a typical collector system, but it can have a very low energy cost.

Sealed Air Corporation cooperated with SERI and allowed in-house testing of their collector. Acme Solar, a small firm developing thin-film plastic collectors, has kept SERI informed of their progress. They solve the problem of keeping the absorber surface wet and minimizing wind flagging of the Tedlar glazing by pressurizing the glazing/absorber air gap with a small fan.

Numerous other firms and individuals have shared their advice and materials experience. We obtained a good deal of information on concrete, fiberglass, sealants, plastic piping, and black fluids through telephone contacts. One local concrete company even loaned us a vibrator free of charge when we prepared our concrete absorber. Another provided lightweight aggregate free of charge.

2.1.4 Coordination with the Active Program Research Requirements Study

A DOE study entitled "Active Program Research Requirements" (APRR) was initiated shortly after the present work began. The purpose of this effort was to assess the current state of active solar heating and cooling technologies and determine the need for further research. SERI was assigned the task of preparing the discussion on direct solar heating systems for the APRR study.

The APRR study concluded that based on energy cost, reliability, and potential for cost reduction, a drainback system was the most promising. A ranking of the APRR advanced systems is shown in Table 2-4. As a direct result of the system ranking, a ranking of collector technologies showed that low-cost liquid collectors are the most promising, followed by low-cost air collectors. Table 2-5 gives the ranking of collector technologies together with identified research needs for each. Section 3.0 of this report discusses system comparisons made by the low-cost collector task (which agrees with the conclusions of the APRR study).

2.2 SYSTEM COST AND PERFORMANCE GOALS

The low-cost collector task has concentrated on developing the least expensive solar hot water and space heating system possible. Establishing reasonable cost and performance goals provides a means to measure the task's progress. The delivered energy cost of a solar energy system can be reduced by lowering cost or improving performance or both. While efforts are underway both at SERI and at other laboratories to improve collector efficiencies, a key premise of this task is that most of the improvement must come in reduced costs because of the large energy cost reductions needed (a factor of 4 to 5)

Table 2-4. APRR System Ranking

Ranking		Description
1	Drainback system:	- Low-cost liquid collectors Plastic pipes - Low-cost storage tank Enhanced coil heat exchanger for DHW in solar storage tank - High efficiency circulation pump, syphon-return system - Electronic control unit - Heat pipe heat exchanger to inlet air of conventional furnace
2	Drainback system:	Same as (1) except for storage - Distributed storage--water walls or carpet pad with passive heating
3	Air system:	- Low-cost air collectors - Thermosyphon or heat pipe DHW
4	Drainback system:	Same as (1) except for storage size - Seasonal storage in low-cost tank
5	Air system:	- Low-cost air collectors - Thermosyphon or heat pipe DHW - Phase-change storage
6	District heating system:	- High efficiency collectors - Large centralized storage - Efficient distribution system
7	Closed-loop system:	- Inverse thermosyphon or pumped - Enhanced coil for heat exchange from collector loop - Otherwise similar to (1)

and because of the limited theoretical potential for performance improvement. Also, to achieve sufficiently low costs, some minor degradation in performance might be accepted.

2.2.1 Cost Goal

To arrive at a reasonable cost goal, we must determine the price people are willing to pay for a solar domestic hot water and space heating systems. "People" in this case includes the owners of residential and commercial buildings as well as builders, HVAC engineers, and others who influence pur-

Table 2-5. APRR Collector Ranking

Ranking	Description	Effect on System	Research Needed
1	Low-cost collectors (liquid)	Reduce materials and installation costs	Materials (e.g., high-temperature plastics, concrete, fiberglass, cardboard, thin-film metals, ceramics, black fluids, low-cost cover materials, insulating materials) Design (e.g., trickle-flow collectors, temperature-limiting devices, design to use low-cost, low-temperature materials)
2	Low-cost collectors (air)	Reduce materials and installation costs Improve performance Reduce parasitics	Materials as in (1) Design (improve F_R, reduce losses, reduce air leakage, minimize parasitics)
3	Evacuated collectors, including flat-plate collectors with evacuated glazings	Improve performance Reduce collector area needed	Design (reduce cost, use vacuum properties to best advantage, heat mirrors)
4	Phase-change collectors	Thermal diode affect reduces thermal losses Reduce system piping Reduce parasitics	Low-cost heat pipes Thermal diode panel design
5	CPC collectors	Improve performance	Low-cost reflectors

chasing. A detailed marketing study for several marketing regions is beyond the scope of this task, so national averages were used to calculate an approximate cost goal.

Of course, there is no single cost above which there is no market and below which there is full market penetration, since cost and market penetration are inversely proportional. Also, the cost can be represented in different ways. Payback period (simple or discounted) indicates the real system cost and accounts for fuel saved. The initial cost of a system does not account for its performance but is important to the consumer. (Indeed, a consumer may opt for a system with a longer payback period if its initial cost is lower.)

Since the determination of a cost goal is a sociological problem and not an engineering one, a precise solution is not possible. At best we can make some logical assumptions based on the results of marketing surveys. Several studies predict market acceptance of solar energy.

The most detailed market study containing relevant information was done by Scott (1976) at the University of Delaware. The results are based on questionnaires completed by 300 homeowners in Denver, Colo., and Wilmington, Del. Figure 2-2 shows the probability of purchase versus cost of a solar hot water heater for new construction and retrofit of a high value home. The figure also shows the effect of a difference in the monthly savings. Figure 2-3 shows the same results for owners of a moderate value home.

A factor of 1.6 has been applied to the original cost data presented in these figures to account for inflation from 1976 to 1981. Thus at 1981 prices, a DHW system would have to cost less than $1600 for approximately a 30% market penetration. Note that no obvious point in the curve can be used to define a cost goal.

Shama (1982) has indicated that in Israel solar domestic hot water systems have penetrated 40% of the market in 20 yr. Payback periods of these systems range from 2.5 to 5 yr (many are simple breadbox designs). Figures 2-2 and 2-3 show that 40% penetration corresponds roughly to a price of $750 or $1200, respectively (1981). A system that saves an average of $11.50/month ($18.40/month, 1981) has a simple payback of 5.4 yr. This is just above the high end of the Israeli experience, but is in rough agreement. Market penetration much above 50% is probably optimistic (Shama 1982). Even if a solar heating system were free, many people would not be interested because of aesthetics, apathy, etc. We therefore kept our projections below 50%.

A more recent study by Westinghouse agrees with Scott's results (Kastovech 1982). Figure 2-4 shows payback time versus market acceptance for the incremental cost of a heat pump on a new home. Note that 40% market acceptance corresponds roughly to a 5-yr payback.

Warren (1982) at Lawrence Berkeley Laboratory used the results of a study by OR/MS Dialogue, Inc. of Cambridge, Mass. (OR/MS Dialogue, Inc. 1980) to set cost goals for the APRR study. OR/MS Dialogue predicted 20%, 40%, and 80% market penetrations for systems with payback periods of 9, 5, and 2 yr, respectively. Warren agreed that the 80% number may be unrealistic and is

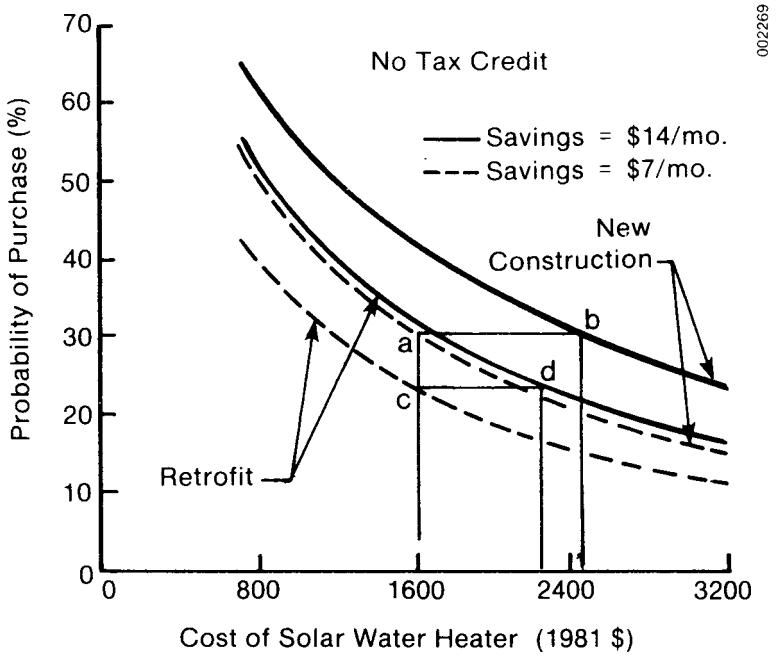

Figure 2-2. Market Acceptance of a Solar Hot Water Heater for a High Home Value

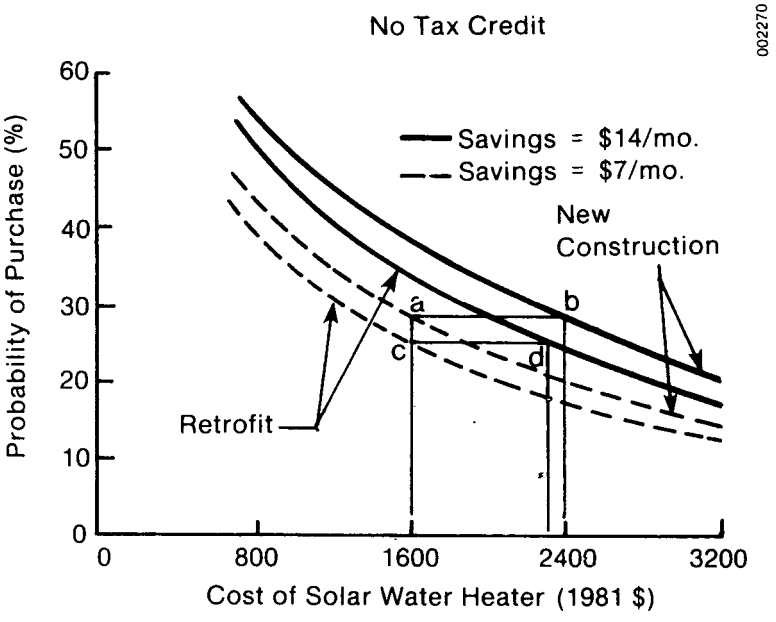

Figure 2-3. Market Acceptance of a Solar Hot Water Heater for Moderate Home Value

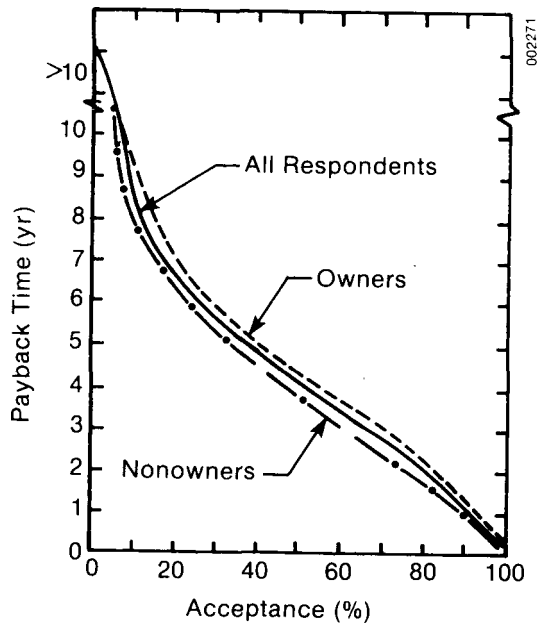

SOURCE: National Family Opinion Inc. Mail Survey
Summer 1980

Figure 2-4. Consumer Acceptance of Added Heat Pump System Costs

using 20% and 40% penetration for the APRR analysis. Although it has not been possible to verify the data reported in the OR/MS Dialogue report, they seem consistent with Scott's results.

These consistencies are encouraging, but the selection of a specific cost goal is still desirable. Since the effect a solar system has on the resale value of a home is not well known, it is reasonable to expect that homeowners will want a system to pay back before they sell their home. Crellin (1982) of the National Association of Realtors stated that residences changed ownership every 9 yr on the average in the late 1970s (latest data available). Thus a payback shorter than 9 yr is required. The OR/MS Dialogue study concludes that industrial respondents and HVAC engineers and architects require payback periods between 3 and 5 yr. Since a 5-yr payback is one of the two targets used by the APRR study and would yield a reasonably high market penetration (40%), we used it as a target criterion for identifying a low-cost collector system.

The relationship between a 5-yr payback and initial cost depends on the cost of competing fuel and on system performance. First, consider natural gas, currently the cheapest fuel. For 1979 the average (residential) price of natural gas in the U.S. was \$2.73/GJ (\$2.88/MBtu); the 1983 price was \$5.68/GJ (\$5.99/MBtu). According to DOE, the average family uses 0.244 m^3 (64.5 gal) of hot water per day. The annual energy use for a natural gas system with a seasonal efficiency of 70%, a required temperature of 60°C (140°F), and inlet water temperature of 10°C (50°F) would be:

$$\frac{1}{0.7} \times \frac{0.244\ m^3}{day} \times \frac{1000\ kg}{m^3} \times \frac{4.187\ J}{kg\ ^oC} \times (60^o - 10^oC) \times \frac{365\ days}{yr} = 26.6\ GJ, \quad (2\text{-}1)$$

or

$$\frac{1}{0.7} \times \frac{64.5 \text{ gal}}{\text{day}} \times \frac{8.3 \text{ lb}}{\text{gal}} \times \frac{1 \text{ Btu}}{\text{lb } ^{o}\text{F}} \times (140^{o} - 50^{o}\text{F}) \times \frac{365 \text{ days}}{\text{yr}} = 25.3 \text{ MBtu} . \quad (2\text{-}2)$$

The average annual cost of hot water in 1983 at $5.68/GJ ($5.99/MBtu) was $151.54. A 5-yr simple payback for a 100% solar system would dictate a system cost of only $757!

The discounted payback is:

$$N = \frac{\log \frac{C(A - 1)}{FA} + 1}{\log A} \quad (2\text{-}3)$$

where

C = initial cost
F = first year fuel savings
G = fuel escalation rate
R = discount rate
A = (1 + G)/(1 + R).

Allowing a 5-yr discounted payback and solving for initial cost, the equation becomes

$$C = \frac{(A^{n} - 1) \text{ FA}}{A - 1} . \quad (2\text{-}4)$$

Using an average annual irradiance of 350 W/m^2 on a horizontal surface and assuming that the radiation on a surface tilted at latitude angle will be 10% greater on the average than the horizontal value (based on SERI's SOLIPH computer program), the annual irradiance is:

$$\frac{350 \text{ W}}{m^2} \times \frac{12 \text{ h}}{\text{day}} \times \frac{365 \text{ days}}{\text{yr}} \times 1.10 = 6.08 \text{ GJ/m}^2 \ (5.36 \times 10^{5} \text{ Btu/ft}^2) . \quad (2\text{-}5)$$

A typical DHW system requires 7 m^2 (75 ft^2) of collector area. Assuming an overall system efficiency of 30%, the annual solar energy delivery will be:

$$6.08 \text{ GJ/m}^2 \times 7 \text{ m}^2 \times 0.30 = 12.8 \text{ GJ (12.1 MBtu)} . \quad (2\text{-}6)$$

The first-year fuel savings F would be:

$$F = \frac{12.76 \text{ GJ}}{0.7} \times \$5.68/\text{GJ} = \$103.54 . \quad (2\text{-}7)$$

Using an Energy Information Agency (EIA) escalation rate (net of inflation) of 4% over the next five years, and a real discount rate of 5% (above inflation),

$$A = \frac{1 + G}{1 + R} = \frac{1.04}{1.05} = 0.991 , \quad (2\text{-}8)$$

which yields an initial cost of

$$C = \frac{(0.991^5 - 1)(103.54)(0.991)}{0.0095} = \$477 \ . \qquad (2\text{-}9)$$

For a 7 m^2 (75 ft^2) array, an installed system would cost \$68.20/m^2 (\$6.34/ft^2)! This goal would obviously be very difficult to attain.

If a \$68.20/m^2 (\$6.34/ft^2) cost goal is unattainable, what can be done? The following options are available:

1. Accept lower market penetration and ease the 5-yr payback requirement
2. Address only those market areas with high insolation or high gas costs or both
3. Conclude that natural gas is now and will continue to be too cheap for solar energy to compete against and concentrate on other fuels (oil, electricity).

(Note that the same situation exists for a combined DHW and space heating system. The allowable cost per unit will be slightly less due to lower collector efficiencies, and fixed costs will be a smaller fraction of total cost. But the required cost would still be \$68.20/m^2 [\$6.34/ft^2]--a difficult goal.)

In adopting option 1, the payback period the same length as the system's life (usually considered 20 yr) could be considered. This would allow an initial system cost of \$1787 or \$255/m^2 (\$23.71/ft^2). This is probably an attainable goal, but would not result in much penetration except for new building construction in which the costs and the system could be amortized along with the mortgage.

Selecting certain markets would help, but a detailed survey of all potential U.S. markets was beyond the scope of this task. Thus, for purposes of this report, natural gas will be ignored and we will now try to determine if low-cost collectors can be competitive with oil and electricity.

The 1983 price of oil was \$8.03/GJ (\$8.47/MBtu). The average escalation rate (net of inflation) through 1989 is 3% (IEA 1984). First-year cost of fuel savings would be:

$$F = \frac{12.76 \text{ GJ} \times \$8.03/\text{GJ}}{0.7} = \$146 \qquad (2\text{-}10)$$

To obtain the initial cost, we first compute

$$A = \frac{1 + G}{1 + R} = \frac{1.03}{1.05} = 0.981 \ , \qquad (2\text{-}11)$$

from which the initial cost is

$$C = \frac{(0.981^5 - 1)(146)(0.981)}{0.981 - 1} = \$689 , \qquad (2\text{-}12)$$

or \$689/7 m^2 = \$98.49/m^2 (\$9.15/ft^2).

The average price of residential electricity in 1983 was \$19.94/GJ (\$21.04/MBtu).

First-year cost of fuel savings would be:

$$F = \frac{12.76\ GJ \times \$19.94/GJ}{1.0} = \$254 . \qquad (2\text{-}13)$$

The expected escalation rate over the next five years (IEA 1984) is only 0.5%.

Again we compute the initial cost as

$$A = \frac{1 + G}{1 + R} = \frac{1.005}{1.05} = 0.957 , \qquad (2\text{-}14)$$

therefore the initial cost is

$$C = \frac{(0.957^5 - 1)(254)(0.957)}{0.957 - 1} = \$1115 \qquad (2\text{-}15)$$

or \$1115/7 m^2 = \$159/m^2 (\$14.80/ft^2) .

Therefore, DHW systems that have a 5-yr payback period need to be available at the following prices to compete with existing fuels:

Natural gas	\$ 68/m^2 or \$ 6.30/ft^2
Oil	\$ 98/m^2 or \$ 9.15/ft^2
Electricity	\$159/m^2 or \$14.80/ft^2

The cost reductions necessary to compete with electricity are probably attainable.

One might argue that the 5-yr payback period is not sufficiently conservative, and that a consumer might reasonably expect a payback of 2 to 3 yr. However, a 7 m^2 (75 ft^2) DHW system that is competitive with electricity would cost \$1115, which is near the value of \$1200 that corresponds to a 40% market penetration (Scott 1976). Since the consumer may want low initial cost rather than short payback, a 5-yr payback may be quite reasonable.

A cost goal of \$150/m^2 would meet the requirement for electricity, while a goal of \$100/m^2 would meet the requirements for oil. If a system efficiency of 40% could be obtained rather than the 30% value that was used, the latter goal of \$100/m^2 would come very close to the requirement for natural gas. The choice of a cost goal is arbitrary. We will use the value of \$150/m^2,

corresponding to a 5-yr payback vs. electricity, but it should be kept in mind that even lower costs are needed to achieve the same payback with oil or gas.

Finally, we based our calculations on a starting year of 1983. If we were to use, for example, 1985 as the starting year for a 5-yr payback, the cost criteria ease somewhat, especially for natural gas. Our analysis is based as much as possible in the present because this yields the greatest certainty in costs. Moving the base year into the future increases the installed system cost necessary to provide a 5-yr payback; however, it also increases the uncertainty associated with making an accurate projection.

2.2.2 Performance Goal

For our cost analysis, we assumed an average system efficiency of 30%. In estimating a typical efficiency value, the day-long performance of a collector array subject to wind and dust must be considered rather than the instantaneous performance of a single clean collector on a test stand. Piping losses (including manifold losses), storage losses, heat exchanger penalties, and load patterns will all affect the performance. Based on operating systems in the field, 35% efficiency is probably typical for a good system in an average climate. A high performance system might be 40% efficient.

High collector efficiencies can be reached using expensive copper absorber plates, but maintaining these efficiencies is difficult with less expensive materials. Because of stagnation temperature limitations of certain plastics, for example, the collector loss coefficient might have to be maintained above a certain level to limit the maximum temperature. Thus, while performance improvement is certainly possible, our present effort will be to reduce costs greatly without a large drop in efficiency.

Perhaps it is best to summarize the cost and performance goals in terms of a single energy cost. Using the 7 m^2 (75 ft^2) system of the cost study, the cost goal of \$150/m^2, and the annual delivered energy figure of 12.76 GJ/yr, the cost of solar energy would be

$$\frac{7\ m^2 \times \$150/m^2}{12.76\ GJ/yr} = \$82.29/(GJ/yr)\ [86.82/(MBtu/yr)]\ . \qquad (2\text{-}16)$$

The total cost of delivered solar energy over the lifetime would therefore depend on the assumed system life.

2.3 REFERENCES

Crellin, Glen, 1982, Telephone conversation, National Association of Realtors.

Energy Information Agency, 1984 (Mar.), Monthly Energy Review, December 1983. Washington, DC: EIA.

Kastovech, J. C., et al., April 1982, Advanced Electric Heat Pump Market and Business Analysis--Final Report ORNL/SUB/79-24712/1, Pittsburg, PA: Westinghouse Electric Corporation.

OR/MS Dialogue, Inc., Sept. 1980, A Market Assessment for Active Solar Heating and Cooling Products, Catalog B: A Survey of Decision Makers in the HVAC Market Place, DOE/CS/30209-T2.

Scott, Jerome E., 1976, Solar Water Heating Economic Feasibility, Captive Potential, and Incentives, NSF/RA-770189, Newark, DE: University of Delaware.

Shama, Avraham, 1982, Personal communication, Solar Energy Research Institute, Golden, CO.

Ullman, Jane, 1981, internal memorandum, Golden, CO: Solar Energy Research Institute.

Warren, Mashuri, 1982, Personal communication, Lawrence Berkeley Laboratory, Berkeley, CA.

PART II. LOW-COST SYSTEMS

SECTION 3.0

SURVEY OF CANDIDATE SYSTEMS

To identify ways to reduce the costs of system components (excluding the collector), we first defined which system configuration offered the greatest potential for performance, reliability, and cost reduction. Section 3.1 describes 13 different domestic hot water configurations and gives advantages and disadvantages of each. (The addition of space heating capability would require only minor additions to these configurations.) The configuration selected for further investigation, the drainback system, is described in more detail in Section 3.2.

3.1 SYSTEM DESCRIPTIONS

The following is a discussion of solar domestic hot water (SDHW) systems and rationale for choosing a two-tank indirect drainback system for the low-cost system. SDHW systems are commonly divided into two major categories: (1) direct systems, which circulate the domestic potable water through the collectors, and (2) indirect systems, which heat domestic potable water indirectly via a heat exchanger (see Figure 3-1). This discussion describes only major types of SDHW systems.

No system is consistently superior to all others. Each has its own peculiarities, and all will work if installed properly. SDHW systems should be designed to meet the following goals:

1. High reliability, which can be achieved by use of redundant components or by minimizing the number of moving parts.
2. Low maintenance, which can be achieved by minimizing moving parts and using a heat transfer fluid and components that do not require periodic replacement.
3. Minimal parasitic energy requirements (low operating cost), which means not using automatic valves or pumps that require electricity or using only those with minimal power requirements.
4. Simplified installation, which usually dictates a packaged system. Proper installation is always critical to eliminate air traps and allow proper venting and draining. Improper installation of systems that require draining of the collectors for freeze protection can lead to system failure.
5. Minimal user participation, which results from eliminating controls (as in a thermosyphon system) or using an automatic controller. This goal leads to greater consumer acceptance and probably greater reliability.
6. Low initial cost, which means minimizing parts, expensive materials, and installation time.

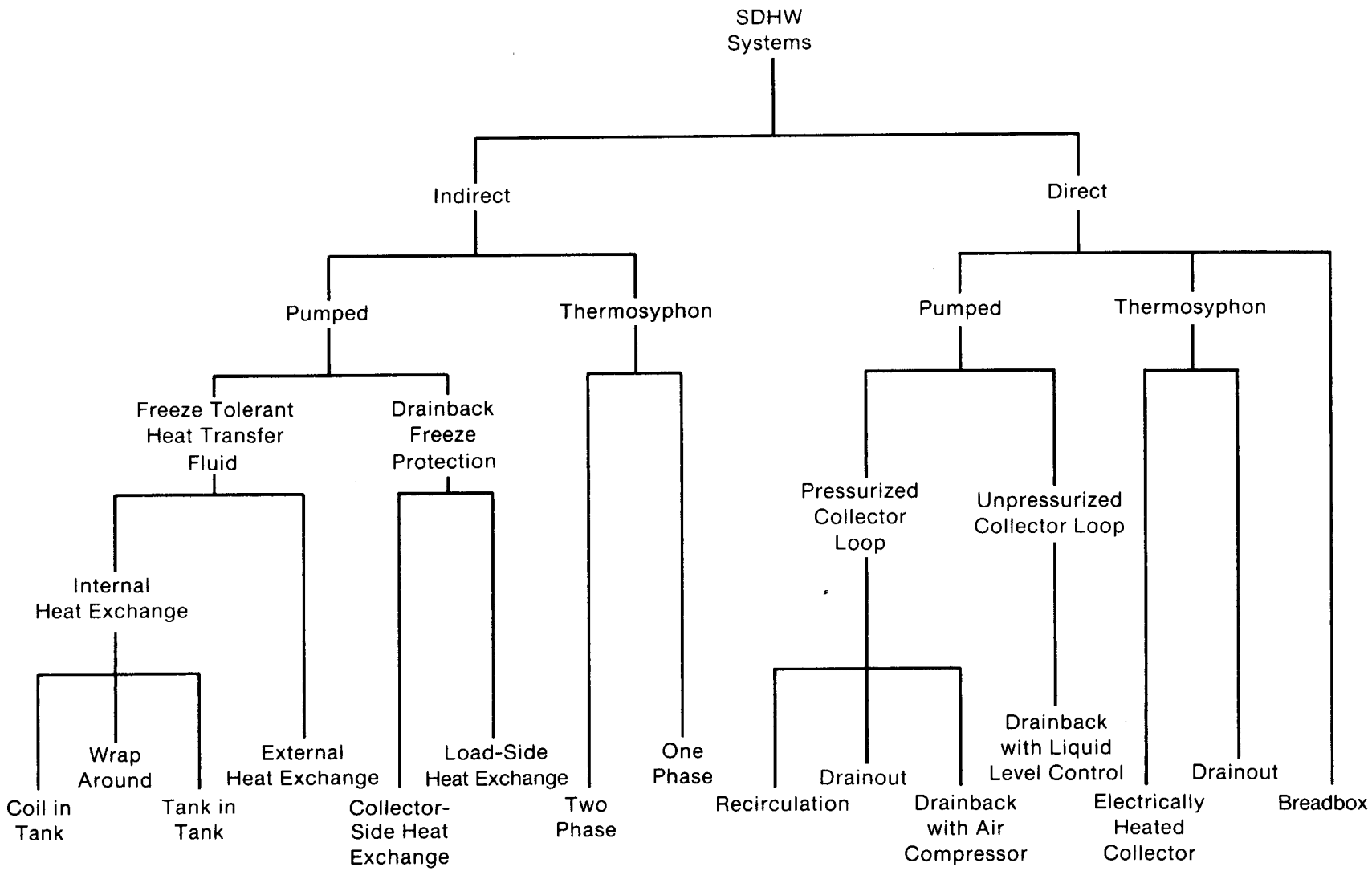

Figure 3-1. System Configurations

7. High system performance, which results from good heat transfer from the collectors to the hot water tank.
8. Durability, which results in extended system lifetimes.

Obviously, some of the goals are not complementary. High efficiency systems require higher initial cost, and high reliability in freezing climates may dictate the use of pumps and valves. The best combination of high performance; long life; and low initial, maintenance, and operating cost will result in the lowest cost of delivered energy. A good system must not only have a low cost of delivered energy but must also displace a significant amount of fuel.

Any of the systems can use either one or two tanks, provided that the one-tank systems have either auxiliary electric heating elements (one-tank auxiliary gas water heaters have recently been introduced to the market) or a backup heating source. Conventional gas DHW tanks are generally used only in two-tank systems because of poor stratification in the storage tank. Both systems require proper installation. A one-tank system has less thermal storage loss (less surface area), requires less space, and costs less in a new installation. However, the storage of hot water in a one-tank system requires the top section of the tank to have an auxiliary heating element, and the collector return line must discharge below that level. Inevitably, water heated by the auxiliary system in the tank will mix with the solar heating water, thereby raising the collector inlet temperature and reducing collector efficiency.

Two-tank systems result in slightly higher collector efficiencies since the collector inlet temperature is not raised by the auxiliary heating system. This configuration can utilize an existing DHW tank in a retrofit situation and has a larger storage capacity. The use of two tanks requires more space and results in greater heat loss. Conventionally insulated tanks that have an R-value of 1.1 m^2 K/W (6.1 ft^2 h ^oF/Btu) have high thermal losses; however, proper insulation to an R-value of 2.1-3.5 m^2 K/W (12-20 ft^2 h ^oF/Btu) will reduce these losses.

The auxiliary tank in a two-tank system is either gas heated or has two electric heating elements. This leads to shorter recovery times and more hot water storage for use during cloudy periods.

A comparison of direct and indirect systems shows the characteristics and advantages of each type. Direct systems have higher efficiencies since they are not penalized by a heat exchanger that uses heat transfer fluids other than water. (An exception is the indirect drainback system which uses water as the heat transfer fluid in the collector loop.) Direct systems also have a lower initial cost since they do not include a heat exchanger, heat transfer fluids, and related equipment. However, they circulate fresh potable water through the collectors, thereby adding oxygen to the system that can lead to corrosion and carbonates that can cause scaling in the collectors. Carbonates, unlike many other substances, become less soluble as the water temperature increases. They precipitate out of the solution and form a hard scale on the metal piping. Since the collector is the hottest part of the collector loop, it will have the greatest amount of scaling. Scaling can lead to a serious reduction in heat transfer, increased pumping costs because of restricted passageways, and increased corrosion. Indirect systems do not circulate fresh potable water through the collectors but have fresh water entering the loop on one side of the heat exchanger. This can be a source of

corrosion and scaling. An indirect system should have a heat exchanger that can be removed for inspection and maintenance. Collectors in direct systems cannot be removed for periodic inspection and are very difficult to clean without damaging the system or contaminating the hot water supply. The collector loop in an indirect system is subject to corrosion if the pH and reserve alkalinity of the heat transfer fluid are not maintained.

Nonmetallic collectors and piping are exceptions to these effects since they will not corrode and carbonate deposits will not adhere to the pipe walls. However, nonmetallic collectors and piping are subject to thermal and ultraviolet degradation, and some are not compatible with certain heat transfer fluids.

The system configurations presented in Figure 3-1 are discussed in the following sections.

3.1.1 Recirculation (or Pulse)

Figure 3-2 shows a simple system suitable for locations where freezing conditions (below 35°F) are infrequent. Potable water is circulated through the collectors. Freeze protection is provided by circulating warm water from the storage tank through the collectors.

Advantages

- Simple
- Efficient, no heat exchanger
- Lower cost (less expensive controls, no heat exchanger)
- No automatic valves.

Disadvantages

- Limited in application (Electric energy consumption increases in colder climates)
- No automatic freeze protection during power failures (Power failures are not uncommon during winter storms)
- Scaling
- Overheating of the system cannot be eliminated easily. The best solution is to use a solenoid valve that drains hot water from the storage tank. Temperatures in excess of 180°F (82°C) will accelerate tank corrosion and may void storage tank warranties.

3.1.2 Drainout (or Draindown)

A drainout (draindown) system (Figure 3-3) isolates the tank and uses automatic valves to drain the collectors and exposed piping (1) whenever a

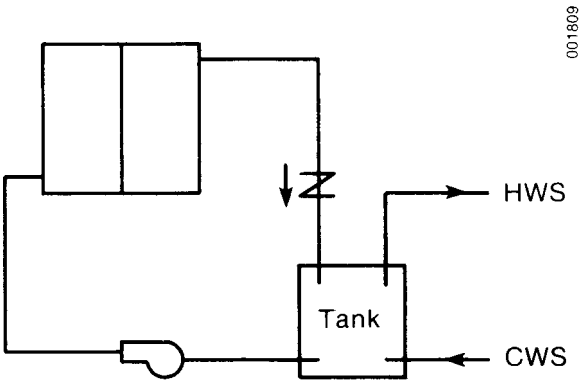

Figure 3-2. Recirculation (or Pulse) System

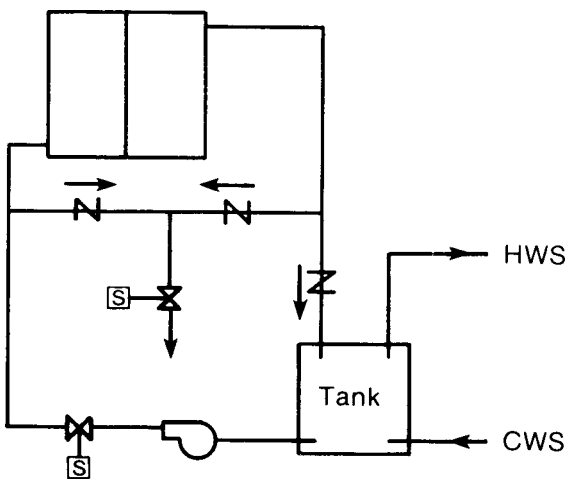

Figure 3-3. Drainout System

freezing condition is sensed, or (2) whenever the pump stops. The first method allows the automatic valves to remain idle for long periods of time, which can lead to valve failure. The second method can waste water if cycled excessively but can increase valve reliability. Solenoid valves in this application have not been very reliable. Debris has collected on the rings, causing leakage, and overheating of the solenoid has caused valve failure. Two 15-W solenoid valves used continually in a system will use more electricity annually than a 100-W pump operating 2500 h/yr. Several new valves are now available that may eliminate these problems. Collectors are filled at city or line water pressure and therefore require only a circulating pump. The pump is not required to overcome a static head.

Advantages

- Efficient, requires no heat exchanger
- Overheating prevented by draining collectors
- Low cost
- Designed to drain during power failure.

Disadvantages

- Corrosion potential (because of the continuous addition of oxygen from the atmosphere and potable water)
- Some automatic valves have low reliability

- Installation is critical for freeze protection
- Scaling potential in collectors due to carbonates in potable water supply
- Wastes water.

3.1.3 Drainback with Air Compressor

A drainback system with an air compressor (Figure 3-4) has been available in the past but seems to have disappeared from the market. It is similar to the drainout system except that water is drained back into the DHW tank. This is possible because the air compressor maintains pressure in the system. Whenever the pump stops, the water in the collectors and exposed piping drains into the storage tank and is replaced by air. When the pump starts, the pressurized air flows back into the tank. Hence, the pump has a static head to overcome (the effect of overcoming a static head is discussed in detail in Section 3.2). The system is not fail-safe during longer power failures since air from leaks in the joints will be absorbed by the water, allowing the water level to reach potentially freezing heights. Without a visual means of monitoring the water level, it is difficult for the user to know if the system is operating properly.

Advantages

- Thermally efficient, no heat exchanger
- Good overheating protection.

Disadvantages

- Initial and operating cost of compressor
- Corrosion potential (primarily from dissolved oxygen in the water supply and makeup air)
- No fail-safe protection during long power failures
- Installation critical for proper draining
- Pump must overcome static head initially
- Difficult to determine if operating properly
- Scaling potential.

3.1.4 Drainback with Liquid Level Control

Drainback systems with liquid level control are not widely marketed but are feasible (Figure 3-5). A liquid-level switch, such as a mechanical float, maintains the water level in an unpressurized tank. Sufficient space is maintained in the tank for water in the collectors and exposed piping whenever the pump stops. This system is fail-safe during a power failure provided that

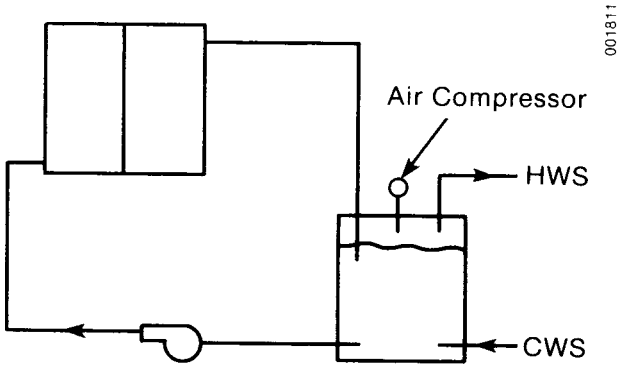

Figure 3-4. Drainback System with Air Compressor

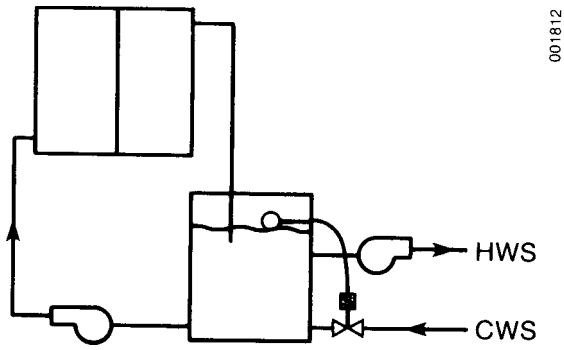

Figure 3-5. Drainback System with Liquid Level Control

the liquid-level switch does not allow the tank to fill during a power failure. This system requires a pump and occasionally a surge tank in addition to the storage tank.

Advantages

- Thermally efficient, no heat exchanger
- Fail-safe freeze protection
- Unpressurized, low-cost storage tank
- Good overheating protection
- Low cost.

Disadvantages

- Two pumps
- Pump must overcome an initially static head
- Installation is critical
- Corrosion potential
- Scaling potential.

3.1.5 Thermosyphon with Electrically Protected Collector

The thermosyphon (Figure 3-6) is the most common SDHW system in the world and is used extensively in Australia, Japan, Republic of China, and the Middle East. It is very simple, with no controls or moving parts, resulting in high reliability and low cost. It is less efficient thermally than a well-designed direct system with a pump as illustrated by its lower Nusselt Number (natural convective heat transfer in a thermosyphon is lower than forced convective heat transfer in a pumped system). However, a thermosyphon may have higher system efficiencies than pumped systems when the parasitic power of the pumps, valves, and controls is included.

The main disadvantages of these systems in the United States are freezing problems and structural considerations. One solution to freezing problems is to protect the collector with an electrical heating element, useful only where freezing conditions are infrequent. This system is common in Arizona, California, Florida, Hawaii, and New Mexico.

Advantages

- Lower initial and operating cost
- Efficient, no heat exchanger or pump
- No automatic valves, pumps, or differential controls.

Disadvantages

- Limited in application (infrequent freezing)
- Not fail-safe during power failure
- Location of storage tank
- Storage tank losses may be high
- Corrosion potential
- Scaling potential
- Overheating protection not easily accomplished.

3.1.6 Drainout Thermosyphon

The drainout thermosyphon system shown in Figure 3-7 was tested by NBS (Fanney and Liu 1979) but has not found widespread use because of previously mentioned disadvantages of thermosyphon systems and the questionable reliability of solenoid valves. In this configuration the valves may remain in one position for extended periods of time and fail to operate properly when needed. All fail-safe automatic valves require a steady source of electricity and can use more energy than a small pump. Manual draindown, based on freezing conditions or seasons, can be used but is generally considered unreliable.

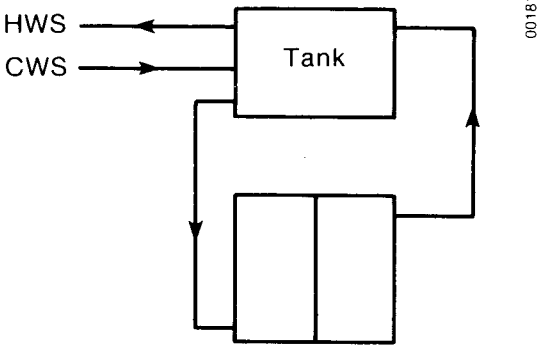

Figure 3-6. Thermosyphon System with Electrically Protected Collector

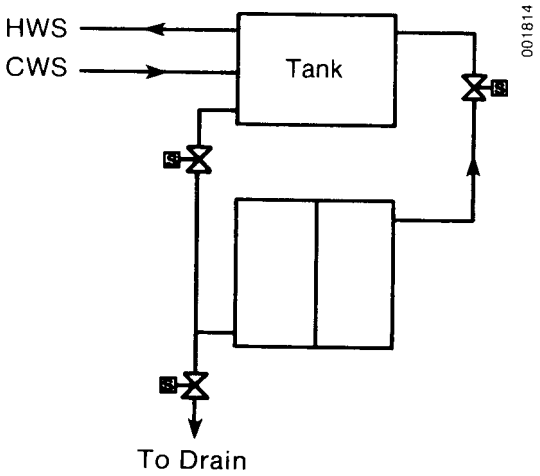

Figure 3-7. Drainout Thermosyphon System

Advantages

- Efficient, no heat exchanger or pump
- Lower initial and operating cost, no pumps or differential controls
- Designed to drain during power failures.

Disadvantages

- Uses automatic valves; adds parasitic energy consumption and added pressure drops
- Location of storage tank
- Storage tank losses can be high
- Installation is critical for draining of collectors
- Corrosion potential
- Scaling potential.

3.1.7 Breadbox (or Batch)

The breadbox system (Figure 3-8) combines storage and collector into one unit. One medium-sized tank or several small tanks are placed in a collector box. The backs and sides of the tanks are well insulated, and the front of the box is covered with one to three layers of glazing. Nighttime storage losses from this system can be large unless insulation is attached manually to the front of the unit at night and during periods of low insolation. With user participation, this system can work well in warm areas.

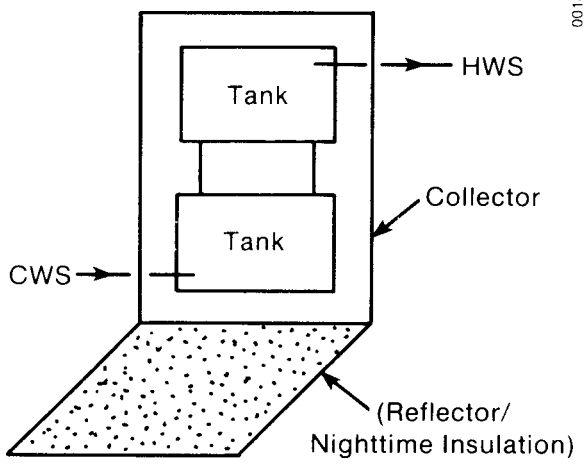

Figure 3-8. Breadbox (or batch) System

Advantages

- Inexpensive
- Easy to build by user
- No pumps, controls, or automatic valve.

Disadvantages

- May require user participation
- Storage losses can be high
- Structural consideration in locating unit
- Is best suited for use in warm regions.

3.1.8 Coil in Tank, Wrap Around, Tank in Tank

Indirect systems with internal heat exchangers are commonly used, and the coil-in-tank heat exchanger is more popular than the wrap-around or the tank-in-tank systems (Figure 3-9). A freeze-resistant fluid (usually a glycol mixture, but occasionally silicone or glycerine) is pumped through the collectors to the tank. Heat transfer on the collector side is by forced convection, and heat transfer on the water side is by natural convection. The collectors are adequately protected from freezing if the collector fluid is maintained. This is often not the case (Meeker and Boyd 1981), and inadequate freeze protection and corrosion result. Some glycol solutions can become acidic above 93°C (200°F), a temperature that will easily be reached during summertime vacations.

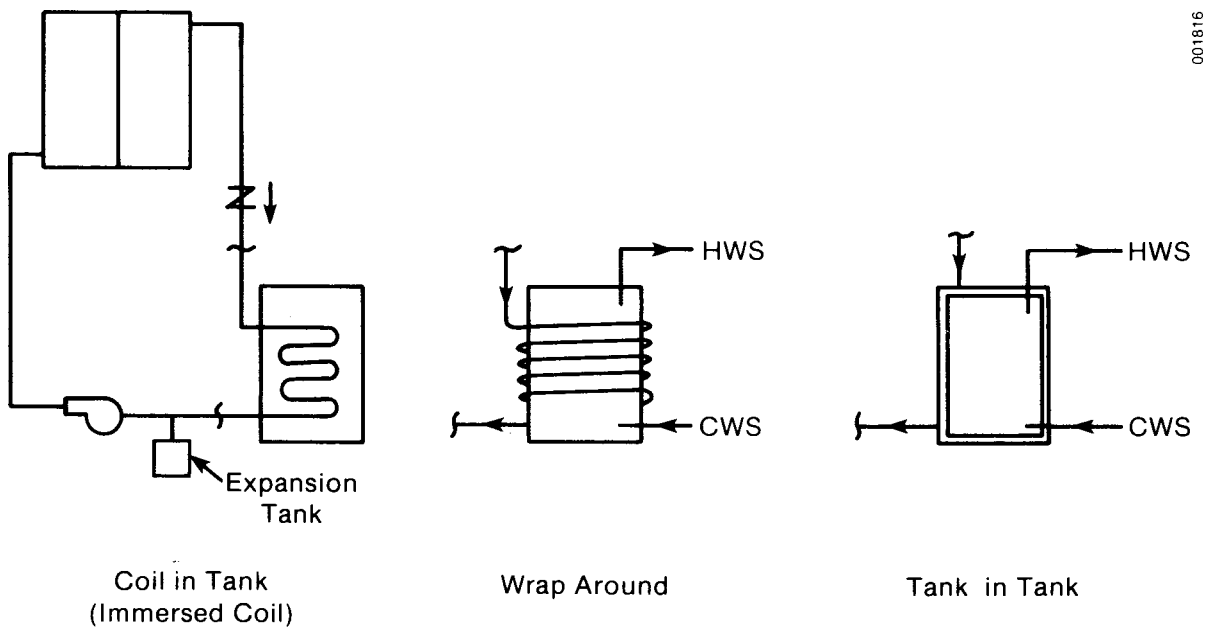

Figure 3-9. Coil-in-Tank, Wrap-Around, Tank-in-Tank Systems

Building codes may require a double-walled heat exchanger even for nontoxic fluids like propylene glycol to prevent accidental water contamination if ethylene glycol is later used in the system and a leak occurs. These heat transfer fluids have a lower specific heat and higher viscosity than water requiring slightly larger pumps and higher flow rates. Because these fluids have lower surface tension than water, they will leak where water does not and therefore require tighter seals and joints.

Advantages

- Good freeze protection if fluid is maintained
- One pump required for circulation only
- Minimal corrosion if use of multiple metals is minimized
- No scaling in collector loop.

Disadvantages

- Double-walled heat exchanger
- Expansion tank required
- Overheating protection not easily accomplished
- Tighter joints required
- Leaks can damage roof

- Heat exchanger and tank often must be replaced together, even if only one fails
- Natural convection inside tank
- Higher initial cost: heat exchanger, fluid inventory, additional components
- Fluid maintenance and replacement.

3.1.9 External Heat Exchanger

The external heat exchanger system (Figure 3-10) is similar to the previous indirect systems except for the location of the heat exchanger. Two pumps are usually used, although some designers have suggested placing the storage tank above the heat exchanger and using natural convection to transfer heat to the storage tank. Using two pumps may require more sophisticated controls and will increase both initial and operating costs. This system is common and allows easy access to the heat exchanger for maintenance or replacement.

Advantages

- Good freeze protection if fluid is maintained
- Heat exchanger accessible for maintenance or replacement
- Good heat transfer from collector fluid to storage
- Minimal corrosion if galvanic corrosion is minimized
- No scaling in collector loop.

Disadvantages

- Two pumps
- Higher initial and operating cost
- Overheating protection is not easily accomplished
- Double-walled heat exchanger required
- Maintenance and replacement of heat transfer fluid
- Expansion tank required
- Tighter joints required
- Leaks can damage roof.

3.1.10 Drainback with Load-Side Heat Exchanger

A drainback system with load-side heat exchanger is similar to the direct drainback system except that the collector loop is generally unpressurized, while the user side, separated by a single-walled heat exchanger, remains pressurized by city water pressure (Figure 3-11). The heat exchanger can be a coil system or a tank-in-tank system as described earlier.

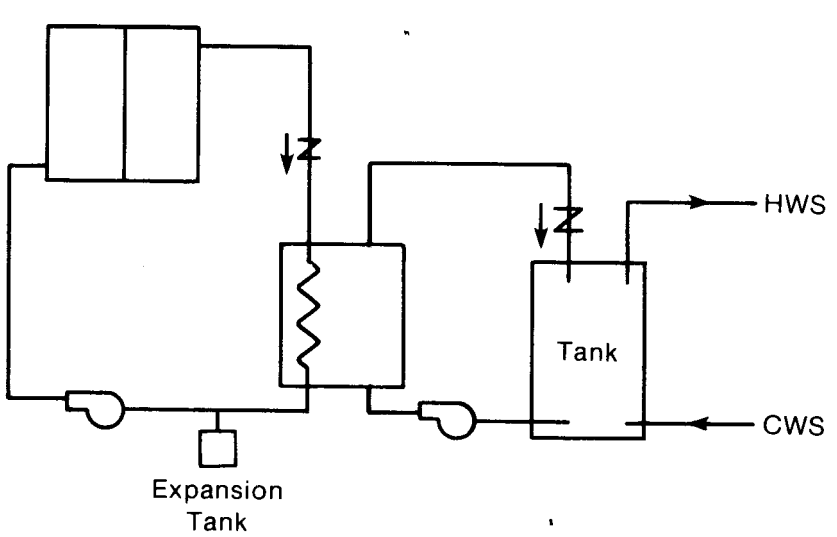

Figure 3-10. External Heat Exchanger System

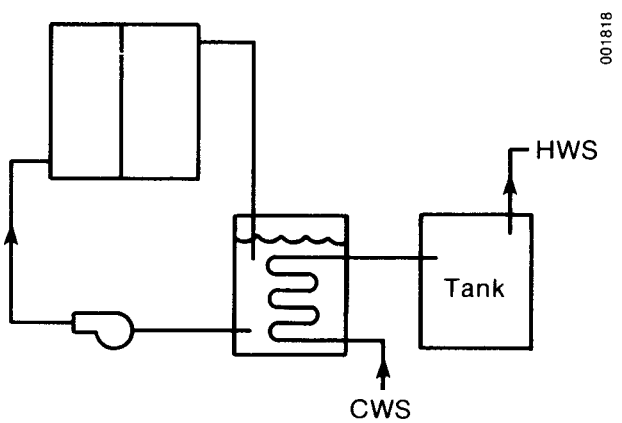

Figure 3-11. Drainback System with Load-Side Heat Exchanger

This drainback system uses an unpressurized solar tank with an air space at the top. As with other drainback systems, water returns to the tank and air fills the collectors whenever the pump stops. Generally, distilled or deionized water is used to minimize corrosion and scaling. Inhibitors may be used also, although a double-walled heat exchanger may then be required. Protection from freezing and overheating is accomplished by stopping the pump, which is a fail-safe procedure. Since fluid passes only once through the heat exchanger, it requires a much larger surface area to accomplish the same heat transfer as in the collector-side heat exchanger (see Section 3.1.11).

Advantages

- Uses one-walled heat exchanger
- Good freeze protection, fail-safe
- Good overheating protection
- Collectors operate at low pressure
- No automatic valves
- No scaling in collector loop
- Low-cost unpressurized solar storage tank.

Disadvantages

- Installation is critical for draining
- Pump must overcome the initial static head
- Potential high operating cost
- Slow recovery time; requires large volume in heat exchanger, and/or heat exchanger with large surface area.

3.1.11 Drainback with Collector-Side Heat Exchanger

The drainback system with a collector-side heat exchanger (Figure 3-12) is similar to the system with a load-side heat exchanger except that the collector loop fluid passes through the tubes of the heat exchanger. It can use any of the previously mentioned heat exchanger designs (coil in tank, tank in tank, wrap around, external).

Advantages

- Uses one-walled heat exchanger
- Good freeze protection, fail-safe
- Good overheating protection
- Collectors operate at low pressure
- No automatic valves

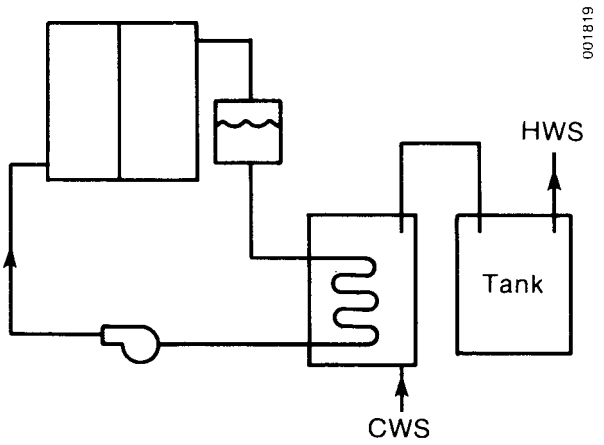

Figure 3-12. Drainback System with Collector-Side Heat Exchanger

- No scaling in collector loop
- Good recovery time.

Disadvantages

- Installation critical for draining
- Pump must overcome the initial static head
- Drainback tank is required
- Potential high operating cost.

3.1.12 Two-Phase Thermosyphon

Figure 3-13 depicts a relatively recent configuration that is currently being manufactured by a few companies. This system transports energy by latent heat transfer. The refrigerant boils in the collector, and vapor rises to the storage tank where it condenses and returns to the tank. This system has the same structural constraints as the direct thermosyphon systems but can provide reliable freeze protection. The performance of these systems is not well known, but initial studies show that they are comparable with pumped systems (Farrington et al. 1981). Some operate at high vapor pressure (1.03 MPa [150 psi]), while others operate at lower vapor pressures but have uncertain thermal stability. All the systems require a skilled refrigeration technician to install and charge the system.

Advantages

- Potential high performance
- No controls, pumps, or automatic valves
- Good freeze protection
- No scaling in collector loop.

Disadvantages

- Refrigeration skills required for installation
- Performance not well known
- Structural considerations
- Storage tank losses may be high
- Overheating protection not easily accomplished.

3.1.13 One-Phase Thermosyphon

A one-phase thermosyphon system (Figure 3-14) would probably use a glycol solution. Though not commercially available, some systems have been custom-built. Mertol et al. (1981) recently modeled this system and concluded that its daily performance would be about 90% of a similar direct thermosyphon system.

Advantages

- No automatic valves, pumps, or controls
- Good freeze protection if maintained
- No scaling in collector loop
- Minimal corrosion.

Disadvantages

- Structural considerations
- Performance not well known
- Storage tank losses may be high
- Overheating protection not easily accomplished
- Expansion tank required.

The most common systems worldwide are the thermosyphon and batch systems, but they are used where freezing problems are not significant. In the United States, use of thermosyphon systems, which are generally the most cost-effective, is restricted by freeze protection and structural considerations. Consumers are often hesitant to place collectors on their roof and are even less likely to place storage tanks on their roof or in their attic. Two major technical drawbacks of thermosyphon systems are the uncertainty of freeze protection and the performance of indirect thermosyphons.

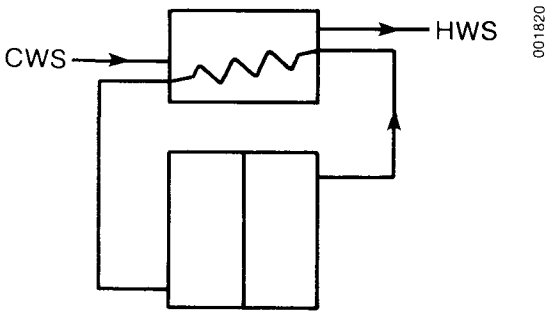

Figure 3-13. Two-Phase Thermosyphon System

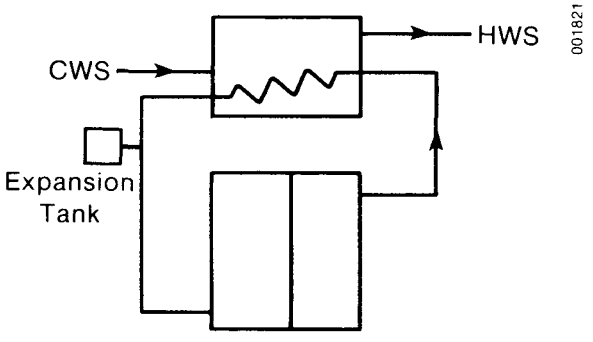

Figure 3-14. One-Phase Thermosyphon System

The SDHW system most likely to be accepted throughout the United States is a pumped system. Of the direct systems, only one is applicable and commonly used: the drainout (draindown) system. All of the configurations of pumped indirect systems discussed here are available commercially. There appears to be growing concern over the use of glycol solutions because of lack of proper maintenance and the necessity of periodic replacement of the heat transfer fluid by the user. A study of SDHW systems (Meeker and Boyd 1981) presented the following examples of design, installation, and maintenance problems found in these systems. The freeze protection of 43 out of 138 glycol systems (34%) was considered inadequate; 6 out of 7 silicone-oil charged systems leaked; all four glycerine-charged systems were acidic; and 39% of the propylene glycol systems using a high temperature shut-off control had a pH of 6.5 or less. In addition, 38 of 128 systems (30%) did not have the required pressure relief valves on the solar loop, and over 20% of the closed loop systems did not have air vents at the high point of the system. Heat transfer fluids in pressurized loops can be effective if properly used, but they can also cause long-term problems if the system is not properly designed, installed, and maintained.

The indirect drainback system has some unique advantages. It is one of two systems (the other is the direct drainback with liquid-level control) that results in low-pressure collector loop, allowing the use of potentially low-cost collectors. Since corrosion can be controlled, collector materials considered unsuitable for use with glycols or untreated water can be considered.

The disadvantages of this system are the static head the pump must overcome and degree of precision required in installation. Some drainback systems use a "syphon" return once circulation is established, while others use an "open-drop" return. The typical dynamic head in a system is about 0.6 m (2 ft) of water with about 75% of this head from the collectors. The energy required to overcome the dynamic head is less than 0.8 W. However, small centrifugal pumps are notoriously inefficient, operating at 5%-10% overall equipment efficiency. We used the following assumptions to calculate the operating costs for this system:

- A flow rate of 1.3×10^{-4} m^3/s (2 gpm)
- A dynamic head of 0.6 m (2 ft) of water and a static head of 6.1 m (20 ft)
- A pump efficiency of 5%
- A cost of 6¢/kWh
- 2500 h/yr of pump operation.

It would cost about $2.25/yr to circulate the water (no static head), $23.70/yr to operate a pump in an open-drop system, and $2.50/yr to operate a syphon-return system. The open-drop system is simple but consumes between one and two months of savings. A syphon return is desirable but requires control modifications to reduce operating costs.

Corrosion in an indirect drainback system must be considered. Drainback systems can be open to the atmosphere, thereby allowing new oxygen into the system whenever the pump stops. Use of plastic collectors and piping may reduce

any corrosion problem. More research is needed to eliminate the problem of corrosion.

The fail-safe freeze protection, overheating protection, low maintenance, potential use of low-cost collectors and storage tanks, and use of single-walled heat exchangers are definite advantages of the indirect drainback system.

3.2 DRAINBACK SYSTEMS

The drainback system has been popular with many manufacturers and users recently. Although it is neither new nor very complicated, there are several basic misunderstandings concerning its operation. A fairly thorough discussion of drainback space heating systems is given in Tully (1981).

Schematics of drainback solar hot water systems are shown in Figures 3-11 and 3-12. This system can have only one high point in the piping for reliable draining. All pipes must be sloped properly to drain and provide freeze protection reliably.

The system begins to collect energy when the temperature at the collector outlet sensor exceeds the storage tank temperature by a set amount, usually 7^{o}-11^{o}C (12^{o}-20^{o}F). When this temperature differential is reached, the controller switches power to the pump and pumping begins. Initially, the pump flow rate is high since the pump does not yet reflect the static head. As the water column in the riser increases, the static head load on the pump increases, resulting in a decrease in the flow rate. The minimum flow rate is reached when the water column reaches the top of the system. At this point the water either trickles down the downcomer (open drop flow) where the flow rate remains at the minimum, or a syphon develops and air is purged from the downcomer. If a syphon develops, the static head is eliminated since the weight of water in the downcomer balances the weight of water in the riser and the flow increases.

Two things happen with a syphon return. First, the static head on the pump is eliminated and the pressure head of the pump drops (and flow increases), but the power to the pump also increases. Developing a syphon return system without altering the pumping arrangement actually increases the parasitic power required by the system. Second, the fluid velocity increases. The increased velocity can exceed the recommended 1.2 m/s (4 fps) for copper piping (Argonne National Laboratory 1981). Several solutions to these problems are presented in Section 4.4.

Some misunderstanding seems to exist about the large change in flow rate that can be obtained by developing a syphon. The actual change in the flow rate depends on system pressure drops (valves, fittings, etc.) and on the system head-flow curve. Very low flow rates will not develop a syphon flow (see Section 4.2 for further discussion). Also, the pressure drop of the system is related to the square of the velocity of the liquid. Small changes in flow will result in larger changes in pressure, which prevent the flow rate from changing dramatically.

Before the pump begins operation, both the riser and downcomer lines are filled with air. As pumping begins, water fills the riser and pushes air ahead of it through the riser, into the downcomer, and into the drainback tank. A syphon develops when the water pushes all of the air out of the downcomer and into the drainback tank. Once a syphon is established, it will remain until the pump stops. The pump will stop operation when the collector sensor drops to within 0.5°-3°C (1°-5°F) of the storage tank sensor. The next occurrence depends on the system configuration and on the downcomer and riser pipe sizes. If the pipe size is larger than 12.7 mm (1/2 in.) then the water column will break up spontaneously and the water will fall down the pipes. The discussion in Section 4.2 shows that pipes above a certain diameter can not support a standing column of water or a syphon return below a minimum flow rate. If the pipe size is 12.7 mm or smaller, then some water will drain down the pipe when the pump stops operation and a reverse syphon will start which will drain the system.

When a syphon is operating, the pressure at the top of the system will be approximately equal to the pressure of the drainback tank minus the pressure of the water column above the height where the tank pressure is measured. This is true if the pressure of the water at the top of the system is greater than the critical pressure for that water temperature. If the drainback tank is open to the atmosphere, then the pressure at the top of the system P_{top} for syphon flow is approximately

$$P_{top} = P_{atmosphere} - P_{height\ of\ water\ column} .$$

Notice that the pressure at the top is always at a vacuum once a syphon is established. Since the boiling point of water is a function of pressure, water can vaporize (boil) at the top of the system. Table 3-1 shows the boiling point of water for different pressures.

Atmospheric pressure is 101.3 kPa (14.7 psi, 33.9 ft of water) at sea level and decreases to about 82.7 kPa (12 psi, 27.7 ft of water) at 1524 m (5000 ft) elevation. The corresponding boiling point of water drops from 100°C (212°F) to about 93°C (200°F). If a SDHW system near Denver has a static head (or downcomer length) of 6.4 m (21 ft), the pressure at the top of the system with a syphon return is

$$P_{top} = 82.7 - 62.8 \text{ kPa (or } 27.7 - 21 \text{ ft)} ,$$

$$P_{top} = 19.9 \text{ kPa (or } 6.7 \text{ ft of water)} .$$

The corresponding boiling point at this pressure is 60°C (140°F), therefore the water at the top of the system will vaporize whenever it exceeds 60°C. Clearly, vaporization is a concern in a system open to the atmosphere. It increases the pressure drop of the system that results from the large volume increase and can break the syphon, resulting in cycling or a no-flow condition if the pump has been switched to a lower pump speed. It also decreases collector efficiency that results from the lower mass flow rate through the collector. There are two ways to avoid this situation: (1) to periodically pressurize the entire collector loop, or (2) to use a vacuum breaker in the collector loop. If a vacuum breaker is used, the pressure corresponding to the maximum collector operating temperature is determined by the height of

Table 3-1. Boiling Point of Water at Various Pressures

Pressure		Boiling Point	
kPa	ft of water	^{o}C	^{o}F
11.7	3.9	48.9	120
19.9	6.7	60.0	140
32.7	10.9	71.1	160
51.8	17.3	82.2	180
101.3	33.9	100.0	212

water column. The vacuum breaker is placed in the downcomer after the collector and at a distance equal to the water column below the high point of the system. The vacuum breaker should be protected from freezing by putting it in an attic or heated space. Placing the vacuum breaker below the level of the collector ensures that the collector operates at a slight vacuum, allowing the use of low-cost collectors that cannot tolerate much pressurization. This approach requires a closed tank that can withstand a gauge pressure equal to the height of the water column between the drainback tank level and the vacuum breaker location. If the drainback tank is open to the atmosphere, then the syphon will stop at the vacuum breaker. The collector pressure is still the atmospheric pressure minus the height of the water column between the vacuum breaker and system high point. However, the pump must continuously overcome a static head equal to the height of the water column between the storage tank and the vacuum breaker. If a drainback system is closed to the atmosphere to reduce corrosion, the storage tank and collector must be able to withstand the vapor pressure at high operating temperatures. For example, if a system has reached 80°C (180°F) and stopped operating, the collector loop and storage tank are at 51.7 kPa (7.5 psig). If the pump starts again (for example, after a cloud has passed by) the collector must withstand the vapor pressure plus the static head of the collector (about 27.6 kPa [4 psi]) as it fills, which is a total pressure of 79.3 kPa (11.5 psig).

The tradeoff between an open and closed drainback system affects the collector requirements. If the collector is to be used in an open system, it need not be capable of operating much above atmospheric pressure. But because oxygen is introduced and loss of fluid by evaporation makes the use of inhibited water difficult, the collector must have good corrosion resistance. If the loop is closed, corrosion can be readily controlled but the collector must be able to withstand pressures of up to 68.9-103.4 kPa [10-15 psig] in a typical residential application (still considerably less than the 413.6 kPa [60 psig] is a direct system).

A properly designed and installed indirect drainback system has several advantages over other systems. A comparison by Argonne National Laboratories (1981) states that the drainback system has a maximum MTBF (mean time between failure) that is approximately 40% greater than the drainout (draindown) system. Drainback systems also appear to be more reliable than water-glycol systems because of the number of valves and their arrangement in the system.

A drainback system combines good freeze protection that is independent of automatic valves, special sensors, or electric power, with a minimal heat exchanger penalty that results from using water as the heat transfer fluid. Scaling in the collector loop is eliminated. Overheating protection is easily

accomplished by permitting the collectors to stagnate. (However, long periods of stagnation should still be avoided by covering the collectors.) A drainback system permits the use of low-cost collectors because of reduced pressure and corrosion problems (but collectors must still withstand stagnation temperatures).

Further reduction in cost may be obtained by using a load-side heat exchanger. A complete discussion of load-side versus collector-side heat exchangers is given in Section 4.1. The load-side heat exchanger configuration permits the use of a low-cost storage tank that needs only to withstand a gauge pressure equal to the water column in the downcomer between the vacuum breaker and the storage tank plus the maximum vapor pressure. The disadvantage of this configuration is the larger heat exchanger surface area required to achieve comparable performance with the collector-side heat exchanger configuration.

One disadvantage of the drainback system is the potentially high operating cost. This is shown in detail in Section 4.3. The cost can be high because of the initial static head that the pump must overcome. If a syphon is established, the power input to the pump increases due to increased flow rate. There are several solutions to this (see Section 4.4). One manufacturer uses the advantage of a small drainback tank used in collector-side heat exchanger configurations and puts the drainback tank in the attic to minimize the static head and operating costs. Both the drainback tank and the connecting pipes must be insulated or heat traced to prevent freezing. However, this approach does not lend itself well to a packaged system concept. Other approaches to reduce the operating cost of packaged systems are discussed later.

A final approach to reduce the initial cost is to use polybutylene piping (see Section 5.1). It is available in straight sections but must be supported to prevent sagging and well protected from damaging ultraviolet radiation. The controller must limit the operating temperature (as it should for the storage tank of any SDHW system) and a section of copper tubing should separate the collector from the plastic piping since the stagnation temperature of flat-plate collectors far exceeds the maximum temperature limits of polybutylene piping. Appendix B contains a method and results for determining the length of copper piping required to isolate the plastic piping from the collector stagnation temperatures.

3.3 REFERENCES

Argonne National Laboratory, Sept. 1981, Final Reliability and Materials Design Guidelines for Solar Domestic Hot Water Systems, ANL/SOP-11, SOLAR/0909-81/70, Argonne, IL: Argonne National Laboratory, p. 159.

Fanney, A. H., and S. T. Liu, 1979, Experimental System Performance and Comparison with Computer Predictions for Six Solar Domestic Hot Water Systems, Washington, D.C.: National Bureau of Standards.

Farrington, R., et al., April 1981, Performance Evaluation of Refrigeration-Charged Thermosyphon Solar Domestic Hot Water System, SERI/TP-721-1140, Golden, CO: Solar Energy Research Institute.

Meeker, J., and L. Boyd, Oct. 1981, "Domestic Hot Water Installations: The Great, the Good, and the Unacceptable," Solar Age, Vol. 6, No. 10.

Mertol, A., W. Place, T. Webster, and R. Greif, 1981, "Detailed Loop Model (DLM) Analysis of Liquid Solar Thermosiphons with Heat Exchangers," Solar Energy, Vol. 27, No. 5.

Tully, Gordon F., Jan. 1981, "Drainback Space Heating Systems: Simple, Reliable and Easy to Repair," Solar Engineering, Vol. 6, No. 1.

SECTION 4.0

SYSTEM ANALYSIS AND EXPERIMENTATION

After selecting a drainback system as the best configuration, our next step was to study it in detail and learn more about its design and performance. Section 4.1 describes computer models of two different drainback systems (using SERI's SOLIPH computer code) to determine their performance and supply heat exchanger sizing data. Since a drainback system must fill whenever the pump starts and drain completely whenever the pump shuts down, criteria for filling and draining were established both analytically and experimentally. These are discussed in Section 4.2.

Since pumping requirements are greater in drainback systems than in other configurations, it was necessary to study pumps in detail. We tested a number of commercially available pumps to determine if their efficiencies were as low as expected, and the results are given in Section 4.3. Section 4.4 summarizes the pumping power problem and offers solutions.

4.1 COMPUTER ANALYSIS OF HEAT EXCHANGE ALTERNATIVES

We concluded in Section 3.0 that the indirect drainback system is a good candidate for a low-cost SDHW system. An indirect drainback system uses one of the following configurations.

- Collector-side heat exchange. This incorporates a pressurized solar hot water tank containing potable water. Treated water in the collector loop flows through a coil, which is immersed in the storage tank. A small reservoir tank holds the collector loop fluid after drainback.
- Load-side heat exchange. This incorporates an unpressurized solar hot water tank, which serves as both the storage tank and drainback tank, containing treated water. Load water flows through a coil immersed in the tank upon demand. Freeze protection is supplied by automatic draining of the collector loop water to the unpressurized tank. The load-side heat exchanger offers some possibility for cost reduction since an unpressurized tank could be made from inexpensive materials such as sheet metal or plastic. (Because pressurized tanks are mass produced, they are surprisingly inexpensive in sizes of 80 gal or less, but a solar energy system can require considerably greater storage volume.)

One problem with the load-side heat exchanger is that the temperature of the load water exiting the heat exchange coil can be well below the tank temperature because it flows at high rates for short time periods yielding low heat exchanger effectiveness. To investigate this problem, we prepared two computer models--one for collector-side heat exchange, CSHX (Figure 4-1), and one for load-side heat exchange, LSHX (Figure 4-2) using SERI's hour-by-hour computer model, SOLIPH. The following specifications apply to both models:

Collector $F_R\eta_o$ = 0.70 where F_R is the collector heat removal factor and η_o is the optical efficiency

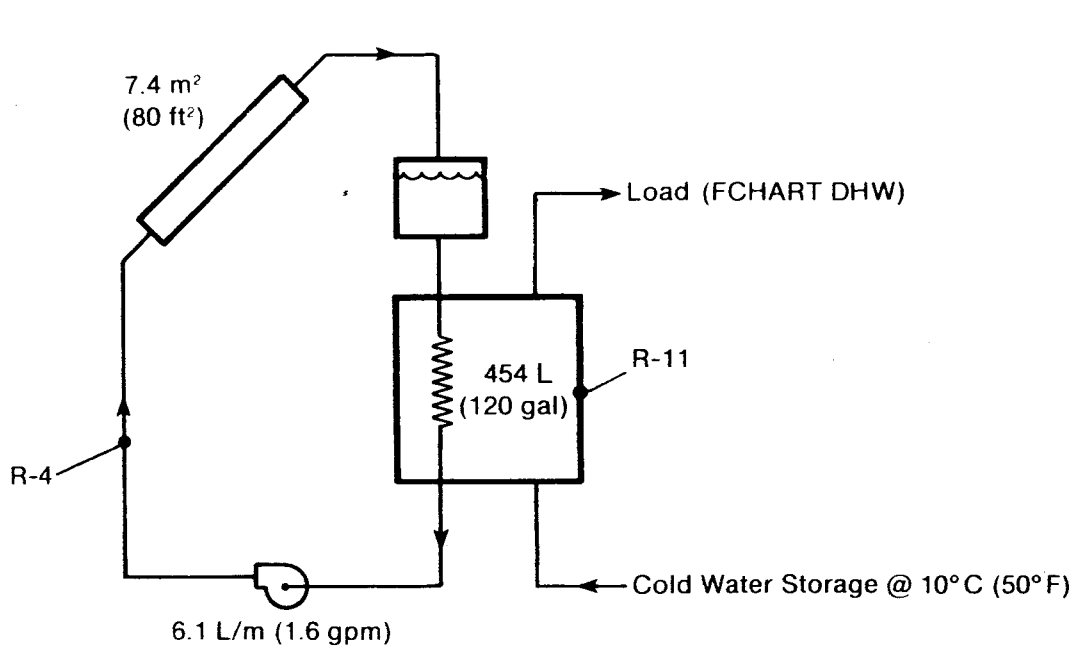

Figure 4-1. Collector-Side Heat Exchange

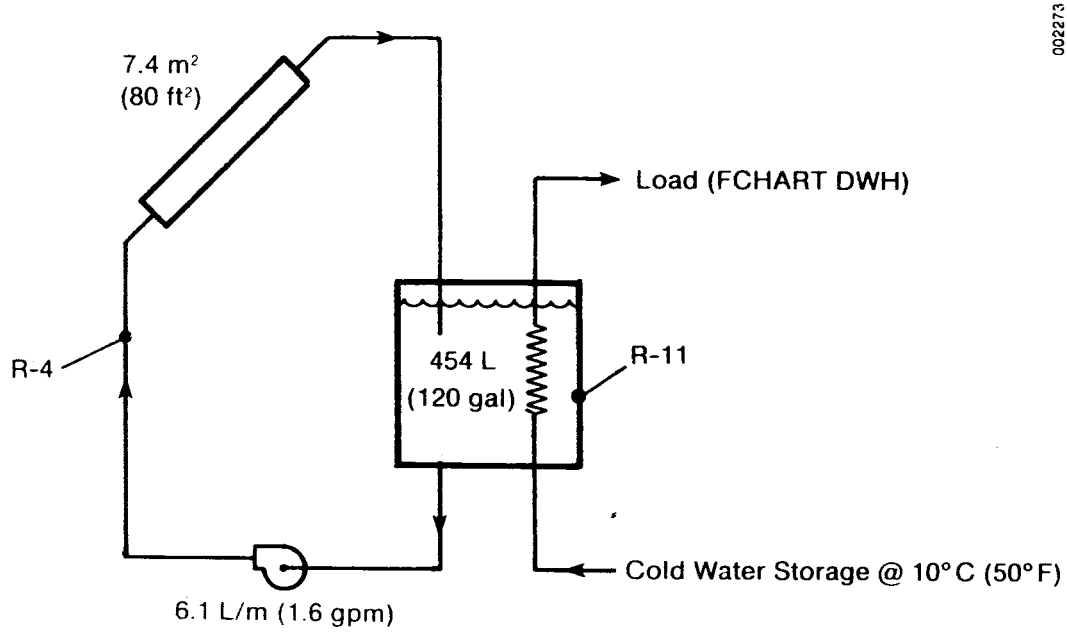

Figure 4-2. Load-Side Heat Exchange

Collector $F_R U_L$ = 5 W/m^2 K (0.88 Btu/h ft^2 ^{o}F) where U_1 is the overall heat loss coefficient

Collector area = 7.43 m^2 (80 ft^2)

Tank volume = 0.454 m^3 (120 gal)

Collector flow rate = 10 x 10^{-5} m^3/s (1.6 gal/min)

Pipe insulation (R-value) = 0.70 m^2 K/W (4 h ft^2 ^{o}F/Btu)

Tank insulation (R-value) = 1.94 m^2 K/W (11 h ft^2 ^{o}F/Btu)

Cold water supply temperature = 10^{o}C (50^{o}F)

DHW load profile = same profile used for F-CHART

Weather = Albuquerque TMY

Immersed coils were simulated by using external heat exchangers.

The UA values (the product of heat loss coefficient and area) for the heat exchangers were determined by modifying the closed-form solution for natural convection heat transfer. On the outside of the tube, the heat transfer coefficient (Lauer 1953) is:

$$h_f = 0.72 \frac{k}{D_o} \left(\frac{D_o^3 \rho^2 \beta g \Delta T}{\mu^2} \frac{C_p \mu}{k} \right)^{1/4}$$

where

k = thermal conductivity
D_o = outer diameter of tube
ρ = density
β = volumetric coefficient of expansion
g = acceleration due to gravity
ΔT = temperature difference
C_p = specific heat
μ = viscosity.

If we assume that all thermal resistance is on the outside of the tube (natural convection), we have the following ordinary differential equation for the collector side heat exchanger:

$$-\dot{m} C_p \frac{dT}{dx} = K \pi D_o (T - T_o)^{1/4} (T - T_o) ,$$

with boundary conditions

$$T\big|_{x=o} = T_{in} ,$$

where $\dot{m}$ is the flow rate, T_o is the temperature outside the tube, T_{in} is the inlet temperature, and

$$K = 0.72 \frac{k}{D_o} \left(D_o^3 \frac{\rho^2 \beta g}{\mu} \frac{C_n \mu}{k} \right)^{1/4} .$$

For a load-side heat exchanger, the equation differs only in sign:

$$\dot{m} C_p \frac{dT}{dx} = K \pi D_o (T_o - T)^{1/4} (T_o - T) .$$

The temperature at x = L are:

$$\text{CSHX:} \quad T_L = T_o + \left[(T_{in} - T_o)^{-1/4} + \frac{K \pi D_o L}{4 \dot{m} C_p} \right]^{-4}$$

$$\text{LSHX:} \quad T_L = T_o - \left[(T_o - T_{in})^{-1/4} + \frac{K \pi D_o L}{4 \dot{m} C_p} \right]^{-4} .$$

For the CSHX, the collector flow rate $\dot{m}$ is 10×10^{-5} m^3/s (1.6 gpm). For the LSHX, $\dot{m}$ is 25×10^{-5} m^3/s (4 gpm). (Runs of a one-dimensional finite difference computer model that steps through an immersed tube suggested that ignoring the inside tube resistance yields a tube ΔT which is about 15% too high.) Using SI units gives the following approximate correlations:

$$\text{CSHX:} \quad T_L \simeq T_o + \left[(T_{in} - T_o)^{-1/4} + 0.0159 \times N \right]^{-4}$$

and

$$\text{LSHX:} \quad T_L \simeq T_o - \left[(T_o - T_{in})^{-1/4} + 0.00669 \times N \right]^{-4} ,$$

where N is the coil length in meters.

Table 4-1 is a summary of results for the computer runs. Note that 30 m (98 ft) of unenhanced coil are needed on the load side to provide the same annual system efficiency as 2 m (6.6 ft) on the collector side. The difference in performance between the two systems with the same coil length (15 m or 49 ft) is reflected by the difference in average storage tank temperature. The tank with load-side heat exchange is 9°C (16°F) hotter than the tank with collector-side heat exchange, since the load-side heat exchanger does not remove heat as efficiently as mixing load water directly in the tank. This higher storage temperature means that warmer water is supplied to the collectors, thereby reducing their efficiency. Also, storage tank losses are higher with load-side heat exchange.

Table 4-1. Collector-Side vs. Load-Side Heat Exchanger Results

Type	Coil Length		Q_{coll}		Q_{del}		$\bar{\eta}_{coll}$ (%)	$\bar{\eta}_{sys}$ (%)	$\overline{T_s}$	
	m	ft	GJ	MBtu	GJ	MBtu			°C	°F
CSHX	2.0	6.6	21	20	16	15	34.4	25.5	45.9	115
CSHX	7.5	25	22	21	17	16	36.0	27.5	48.8	120
CSHX	15.0	49	23	22	17	16	36.5	28.0	49.6	121
LSHX	15.0	49	20	19	14	13	31.8	22.3	58.9	138
LSHX	30.0	98	21	20	16	15	34.4	25.6	54.4	130
LSHX	45.0	148	22	21	17	16	35.3	26.8	52.7	127
LSHX	60.0	197	22	21	17	16	35.7	27.3	51.9	125

These results indicate that a load-side heat exchanger requires considerable surface area. Enhanced tubes would increase the efficiency. Since the CSHX and LSHX SOLIPH models now exist, the effect of changing UA values can readily be determined. Alternatives are to add a closed pumped piping loop between the solar and DHW tanks or use an external heat exchanger in between the two tanks. Both add considerably to the cost. Still another option, the use of an immersed standby tank, is discussed in Section 5.2.

4.2 FILL AND DRAIN ANALYSIS AND TESTING

4.2.1 Draining

Two simple experiments were performed to determine the stability of a column of liquid in vertical pipes open at the lower end. Analytical results were then compared to these results.

The purpose of the first experiment was to determine what range of pipe sizes would support a vertical column of water with the bottom of the pipe open and the top closed. The hypothesis was that pipes that are the same sizes as those used in domestic hot water systems would not be stable and the water would run out, thus providing drainback without the need for a vacuum breaker at the top of the system.

Pipes of various lengths (1-2.5 m) and diameters (0.32-1.9 cm nom. OD [1/8 to 3/4 in. nom. OD]) were filled with water and both ends capped. Then they were supported vertically, the lower end cap was removed, and the flow of water, if any, was timed.

The following results were obtained:

Tube Diameter	Tube Length (m)	Time of Drain (s)
0.32 cm (1/8 in.) nom. OD	~1 m	did not drain
1.0 cm ID	~1 m	did not drain
1.4 cm ID (1/2 in.) nom. OD	~1 m	12
1.4 cm ID (1/2 in.) nom. OD	~3 m	31
1.9 cm (3/4 in.) nom. OD	~3 m	29

The two smallest diameter tubes did not drain by themselves. The 1-cm-ID pipe could be made to drain by striking it. All of the larger pipes (1.4 cm OD or more) drained immediately, and the time they took to drain was approximately proportional to the length. From this experiment, we concluded that the ID at which the fluid/air interface becomes unstable is between 1 cm and 1.4 cm.

The purpose of the second experiment was to further study the range of stability, to attempt to observe what happens when the interface breaks down, and to test different methods of bringing about instability and draining. Short sections of copper tube (~10 cm in length) were connected via Tygon tubing to a water reservoir and a syphon begun. The flow was reduced slowly while the tube section was held steady in a vertical position by closing the suction end of the syphon. The meniscus was observed as the flow was reduced.

Using this technique, stable menisci in pipes up to 1.4 cm in diameter were obtained. A stable meniscus could not be formed in a pipe 1.6 cm in diameter. Stable menisci were formed which were concave, flat, or convex depending on the amount of water in the pipe. Breakdown of the meniscus occurred when an air bubble formed on one side of the tube entrance. We tried two methods for inducing instability: (1) cutting the end of the pipe at an angle and (2) drilling a small hole a few centimeters from the end of the pipe. Both methods gave good results. With an angle cut at the end, the water tended to cling to the longer side as flow was reduced, and bubbles easily formed at the other side (see Figure 4-3). With the small hole, air was entrained while the syphon was running and discharged with the water. When the flow was reduced, the air leak eventually caused the siphon to break and the pipe to drain.

These experiments indicated that a stable meniscus can be formed in tubes of up to 1.4 cm in diameter but not larger than about 1.6 cm. They also showed that the meniscus breaks when air enters along one side of the tube because the surface tension is unable to support a hanging meniscus. This led to the analytical model that follows.

4.2.1.1 Analysis of Stability of Liquids in Open-Ended Pipes—One Dimension

A simple analysis can be made to determine the condition of neutral stability for a 1-dimensional interface, as shown in Figure 4-4. Let $f(x)$ be the vertical displacement of the meniscus from its initial flat position at $z = 0$. The condition for neutral stability is that the surface tension force

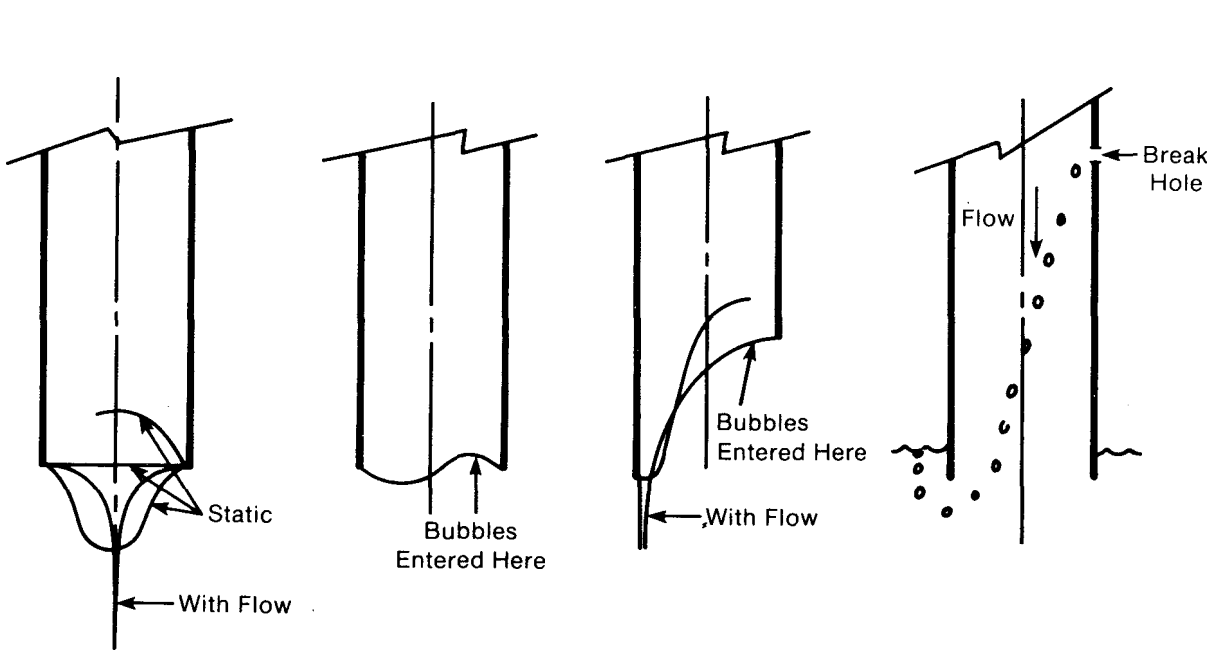

a. Stable Shapes b. Unstable c. Angled Cut d. With Break Hole (no meniscus bond)

Figure 4-3. Observations of Menisci

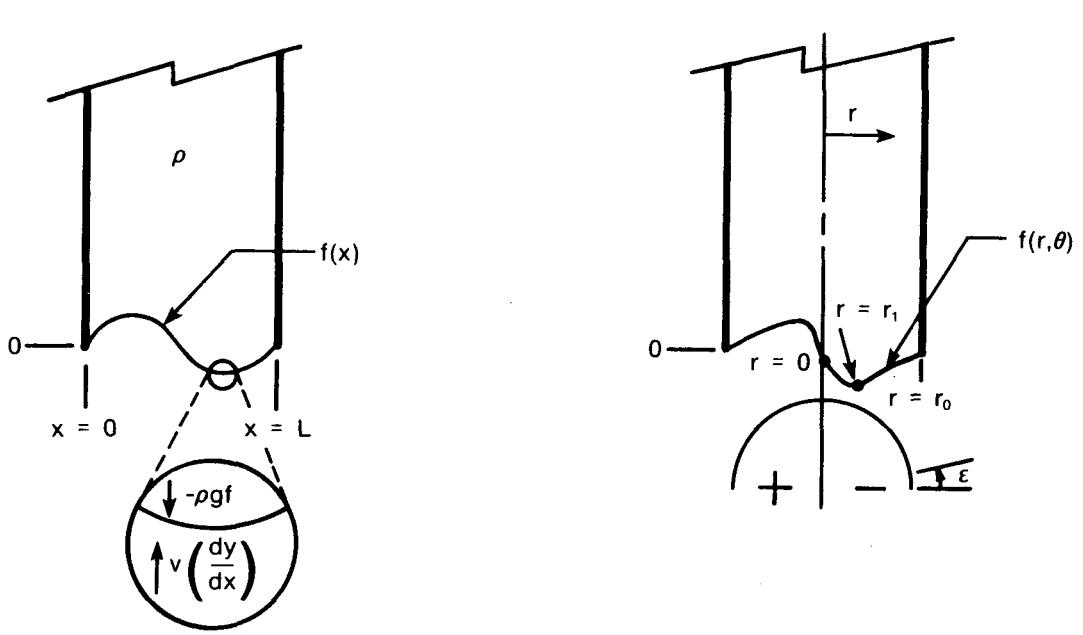

a. 1-Dimension b. 2-Dimension

Figure 4-4. Analytical Models for Open-Ended Pipes

is equal to the force of the pressure across the interface, which initially is zero. This condition can be expressed as

$$\frac{\partial^2 F}{\partial x^2} = -g\rho f \ . \tag{4-1}$$

The boundary conditions are $f(0) = 0$ and $f(L) = 0$. The solution to this differential equation is

$$f(x) = a \sin \frac{g\rho}{\sigma} x + b \cos \frac{g\rho}{\sigma} x \ . \tag{4-2}$$

In this case, $f(0) = 0$ implies that $b = 0$, and $f(L) = 0$ implies that $(g\rho/\sigma)L = n\pi$, where $n = 1,2,3, \ldots$.

Because the total volume of water is constant, n is restricted to even values, and the lowest value is $n = 2$, which corresponds to a full sine wave across the end of the tube. This agrees with the observation of the shape of the meniscus when it breaks down. When $n = 2$, the following expression gives the tube diameter L:

$$L = 2\pi \frac{\sigma}{g\rho} \ , \tag{4-3}$$

where

$\sigma = 0.074$ J/m^2 (surface tension)

$g = 9.8$ m/s^2 (acceleration due to gravity)

$\rho = 1000$ kg/m^3 (density of water).

This gives $L = 1.73$ cm (0.7 in.) as the largest tube diameter that will be stable.

4.2.1.2 Analysis of Stability of Liquids in Open-Ended Pipes—Two Dimensions

The analysis of a two-dimensional meniscus is more complicated, but a similar result can be obtained. The case is analogous to that of the free vibrations of a drum head, which is solved in Butkov (1968). The corresponding solution, in cylindrical coordinates, is

$$f(r,\theta) = \cos \theta \ J_1(3.832 \ r/r_o) \ , \tag{4-4}$$

where J_1 is the Bessel function of order 1 and r_o is the radius of the tube. Applying the same condition for neutral stability as before (2-dimensional):

$$\nabla^2 f = -g\rho f \tag{4-5}$$

In cylindrical coordinates,

$$\nabla^2 f = \frac{1}{r}\frac{\partial}{\partial r}(rf) + \frac{1}{r^2}\frac{\partial f}{\partial \theta}$$

and

$$\nabla^2 f = \frac{\cos\theta}{r}\frac{3.832}{r_o}\frac{dJ_1}{dr} + \frac{3.832^2}{r_o}\frac{d^2J_1}{dr^2} - \frac{\sin\theta}{r^2}J_1 \quad . \tag{4-6}$$

The maximum of $\nabla^2 f$ defines the point of greatest stress for the meniscus and occurs at $\theta = 0$ and where $dJ_1/dr = 0$. This occurs at $r_1 = 0.4805\ r_o$, and therefore $J_1 = 0.5819$ and $d^2J_1/dr^2 = -0.41023$.

Writing Eq. 4-5 at the point $(r_1,0)$ gives

$$\sigma\ \frac{3.832^2}{r_o}\ \frac{d^2J_1}{dr^2} = -g\rho J_1 \quad . \tag{4-7}$$

Solving for r_o gives

$$r_o = 3.832\ \frac{-\sigma}{g\rho}\ \frac{d^2J_1}{dr^2}\ \frac{1}{J_1} \quad . \tag{4-8}$$

If we substitute numerical values, $r_o = 0.88$ cm, so the largest diameter of the pipe for which the meniscus should be stable is 1.77 cm (0.7 in.).

These results indicate that 1.4-cm (1/2-in.) OD pipes should be stable, as we verified in our experiment. The results also indicate that 1.6-cm pipes should be stable, but perhaps the experimental procedure was too crude to achieve stability so near to the limit. Despite the experimental precision, however, the theory fairly accurately predicts the diameter of pipe at the onset of instability, and it is near 1.6-1.8 cm (0.6-0.7 in.).

This analysis led to the development of system testing to understand further the criteria for draining and filling the system to initiate a syphon flow. A test apparatus was constructed to study the draining and filling of 1.27-cm (1/2-in.) and 1.9-cm (3/4-in.) copper pipe. A schematic of the test setup is shown in Figure 4-5. The 1.27-cm, 5.5-m (18-ft) long copper pipe generally drained within one minute without difficulty. However, this pipe occasionally held a standing column of water before beginning the experiment. This did not occur during the testing. It seems possible that 1.27-cm pipe might hold a standing column under certain conditions. We were unable to develop a standing column of water in a pipe of this size during the testing.

If flow is reduced in a 1.27-cm (1/2-in.) pipe (with a throttling valve, for example) after a syphon is established, it will remain stable until reaching a zero flow rate, resulting in a standing column of water in the downcomer. This is consistent with Wallis et al. (1977), whose analysis leads to a critical diameter of 1.36 cm (0.536 in.) for water dropping into air. Pipes

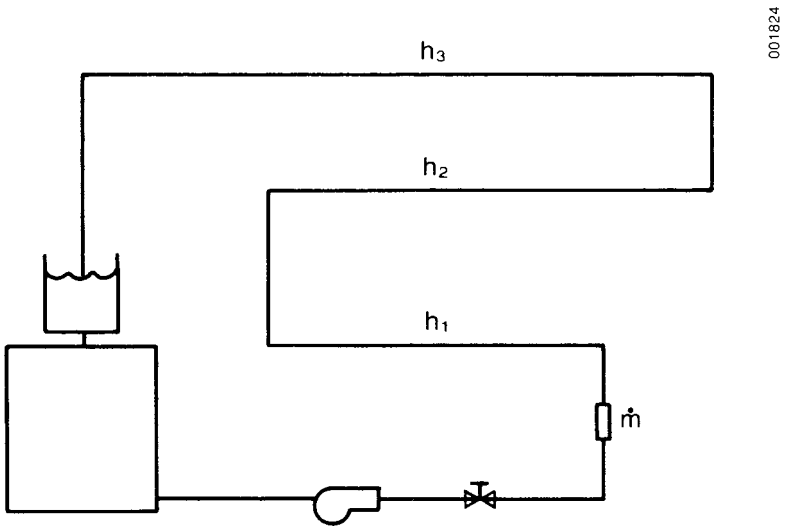

Figure 4-5. Experimental Setup
(1.27 cm [1/2 in.] Fill/Drain Tests)

with diameters greater than this cannot hold a standing column of water. The results of the experiments with 1.9-cm (3/4-in.) pipe were also consistent with the theory that a pipe of this size could not hold a standing column of water.

4.2.2 Filling

A general form of the flow-rate-versus-time curve for filling a 1.27-cm (1/2-in.) pipe is shown in Figure 4-6. The horizontal sections of pipe needed to accommodate structural constraints in the building in which the test loop was assembled (labeled h_1, h_2, and h_3) offer no increase in flow. Therefore, the flow rate is constant as the pump fills these horizontal sections of pipe. The experimental results shown in Figures 4-7, 4-8, 4-11, and 4-12 follow this general curve for syphon flow.

Two arrangements were tested. In the first arrangement, the downcomer tube extended below the water level with a small hole about 2.5 cm (1 in.) above the water level (when the system was drained). In the second arrangement, the downcomer tube ended 0.3 cm (1/8 in.) above the water level when the pump was off and 5.1 cm (2 in.) above the water level when the pump was on. The hole in the pipe for the second arrangement was closed with tape. Both arrangements were noisy at high flow rates because entrained air bubbles from the hole in the first arrangement produced noise and water splashing in the second arrangement. At moderate and low flow rates, both were very quiet.

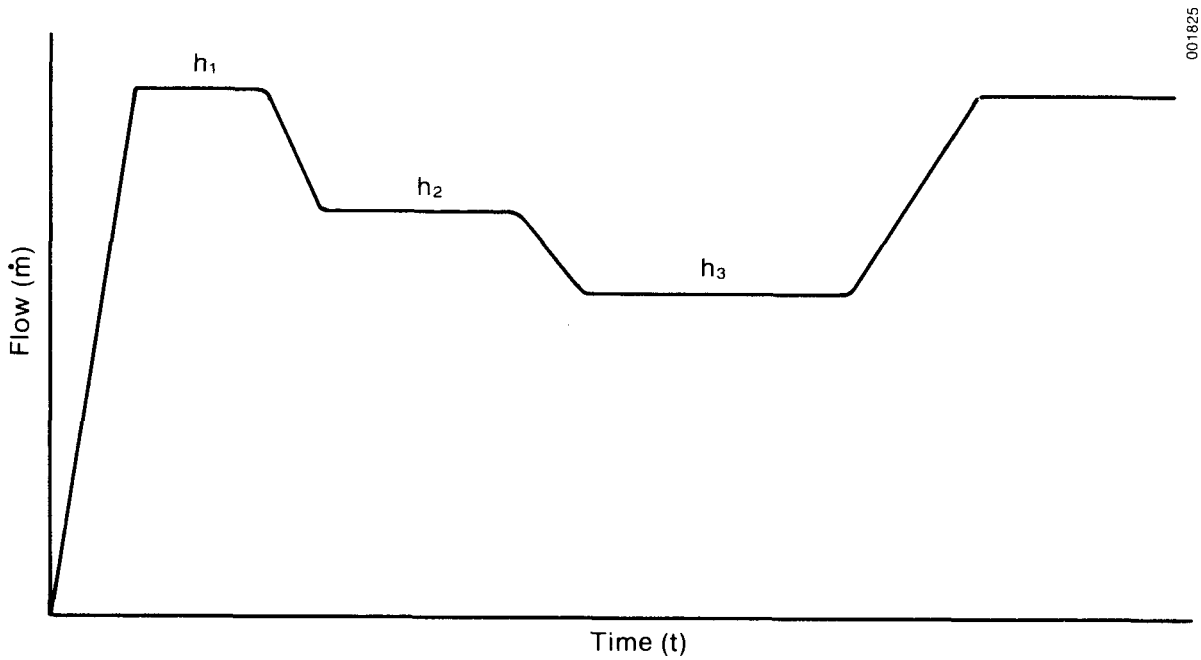

Figure 4-6. General Form of Fill Curve

The first arrangement, which has a hole in the side of the pipe, has no advantage over the second arrangement in developing a syphon. This can be seen by comparing the two arrangements at similar flow rates. Compare runs 4, 5, 10, 11, 12, and 13 with runs 22 and 23; run 19 with run 28; and run 20 with run 21 (see Figures 4-7 and 4-8). The two arrangements fill and drain in comparable time periods (Table 4-2).

At a water temperature of 16°C (60°F) and a pipe length of 1.27 cm (1/2 in.), a syphon will develop at velocities greater than 3.6 m/s (0.70 fps). For a 1.27-cm tube, this corresponds to 1.6×10^{-5} m^3/s (0.51 gpm). This is below typical SDHW flow rates. Hence, a syphon should develop for all SDHW systems using 1.27-cm copper pipe with typical SDHW flow rates.

The throttling valve, as shown in Figure 4-5, was positioned near the pump discharge for convenience. It would have been more realistic to have this large pressure drop near the top of the system to simulate the collector pressure drop. Although this will not affect the syphoning criteria, it will affect the drain and fill time. Draining and filling could be more rapid since there are no substantial pressure drops after the collector is drained or before it is filled.

Note that if the pressure drop is low (runs 4, 5, 10-13, 22, 23) the velocity can exceed the maximum recommended velocity of 1.2 m/s (4 ft/s) for copper tubing (Argonne National Laboratory 1981) (see Table 4-2).

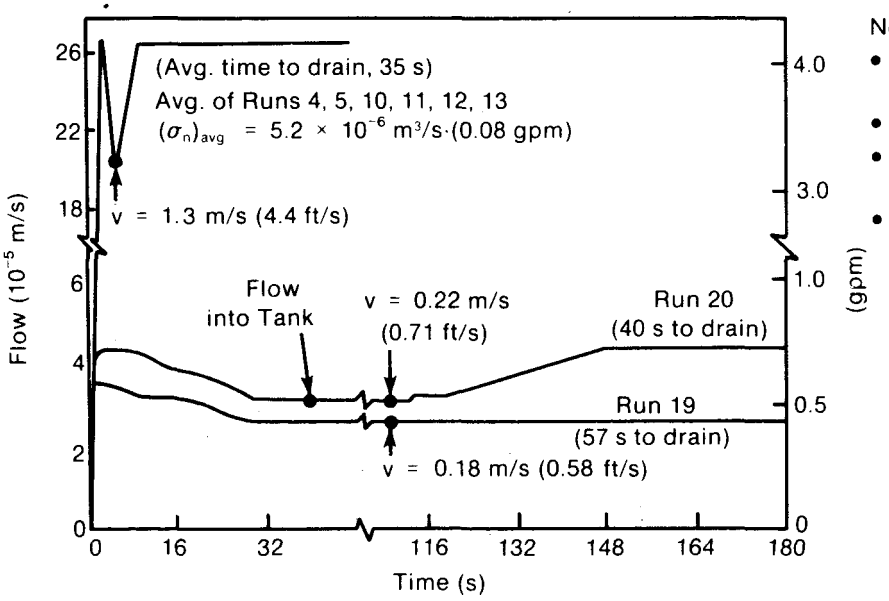

Note:
- Discharge submerged with small hole above water level
- Tank open to atmosphere
- Dump discharge throttled for runs 19, 20
- Scale changes

001826

Figure 4-7. Fill Curves, Runs 4, 5, 10, 11, 12, 13, 19, 20
(1.27 cm [1/2 in.])

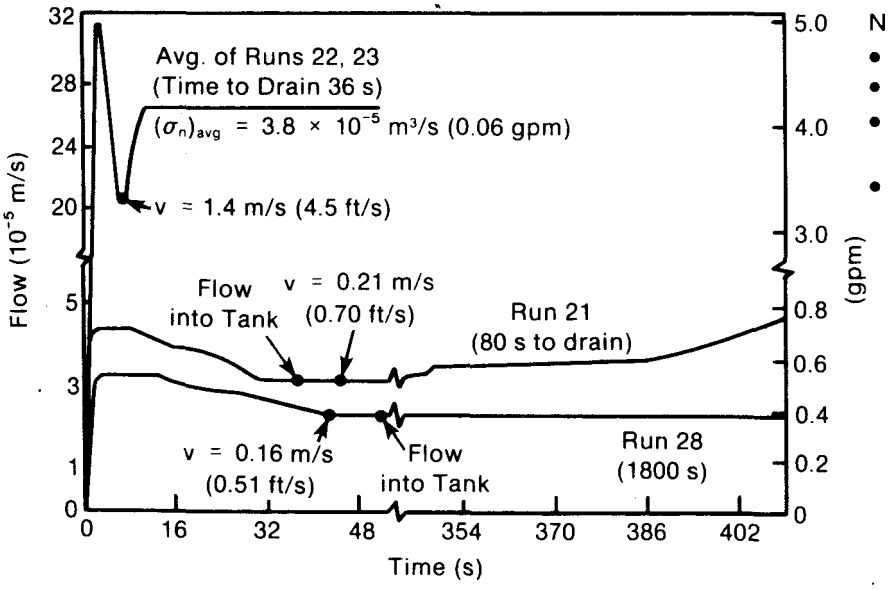

Note:
- Discharge about water level
- Tank open to atmosphere
- Dump discharge throttled for runs 21, 28
- Scale changes

001827

Figure 4-8. Fill Curves, Runs 21, 22, 23, 28
(1.27 cm [1/2 in.])

Table 4-2. Drain/Fill Results for a 1.27-cm (1/2-in.) Copper Pipe

Run	Downcomer Submerged (Y/N)	Syphon (Y/N)	Final Flow 10^{-5} m^3/s (GPM) [m/s (FPS)]	Minimum Flow 10^{-5} m^3/s (GPM) [m/s (FPS)]	Drain Time (s)
4,5,10 11,12,13	Y	Y	26.4 (4.18) [1.75 (5.74)]	20.1 3.19 [1.34 (4.39)]	35
19	Y	N	2.65 (0.42) [0.18 (0.58)]	2.65 0.42 [0.18 (0.58)]	57
20	Y	Y	4.48 (0.71) [0.30 (0.98)]	3.28 (0.52) [0.22 (0.71)]	40
21	N	Y	4.92 (0.78) [0.33 (1.07)]	3.22 (0.51) [0.21 (0.70)]	80
22,23	N	Y	26.4 (4.18) [1.75 (5.75)]	20.6 (3.27) [1.37 (4.50)]	36
28	N	N	2.33 (0.37) [0.16 (0.51)]	2.33 (0.37) [0.16 (0.51)]	N/A

The performance curve for the pump is shown in Figure 4-9. The set-up shown in Figure 4-10 was used to determine filling and draining criteria of two heights of 1.9-cm (3/4-in.) copper pipe. To test the lower height, valves V2, V4, and V6 were closed and V1 and V5 were completely open. To test the greater height, V1 was closed and V2 opened. Valve V3 was used to throttle the flow. The first part of the test was to start the pump at a low flow rate, to slowly increase the flow by opening V3 until a syphon developed, and to record the flow rate at which a syphon started. This flow rate was used for the second part, which was to set V3 at a fixed flow rate, activate the pump, and then monitor the flow rate as a function of time. The flow rate versus time curves for full flow, threshold flow, and no-syphon flow are shown in Figure 4-11 for the shorter pipe and Figure 4-12 for the longer pipe. These curves show that the minimum flow rate to establish a syphon return is a slight function of the system height or static head and also that a flow rate of 7.6×10^{-5} m^3/s or 4.1×10^{-3} m/s (1.2 gpm or 0.8 fpm) is sufficient to develop a syphon in 1.9-cm (3/4-in.) copper pipe for static heads up to 5 m (16 ft).

Wallis et al. (1977) also looked at the effect of the length-to-diameter ratio to determine if the pipe inlet conditions affect the results. In that experiment, length-to-diameter ratios of 8.5, 14, 24, and 50 with 2.54-cm (1-in.) Plexiglas tubes were tested. The results showed that the critical flow rate needed to wash out a bubble did not depend on the distance between the bubble and the end of the pipe. There was a slight difference between the critical flow rates for the two heights, which may result from differences in height or the piping arrangement and location of T1 in Figure 4-10. Since the difference is only 7% of the flow rate and the static heights for SDHW systems do not usually have a large range, this effect did not warrant further investigation.

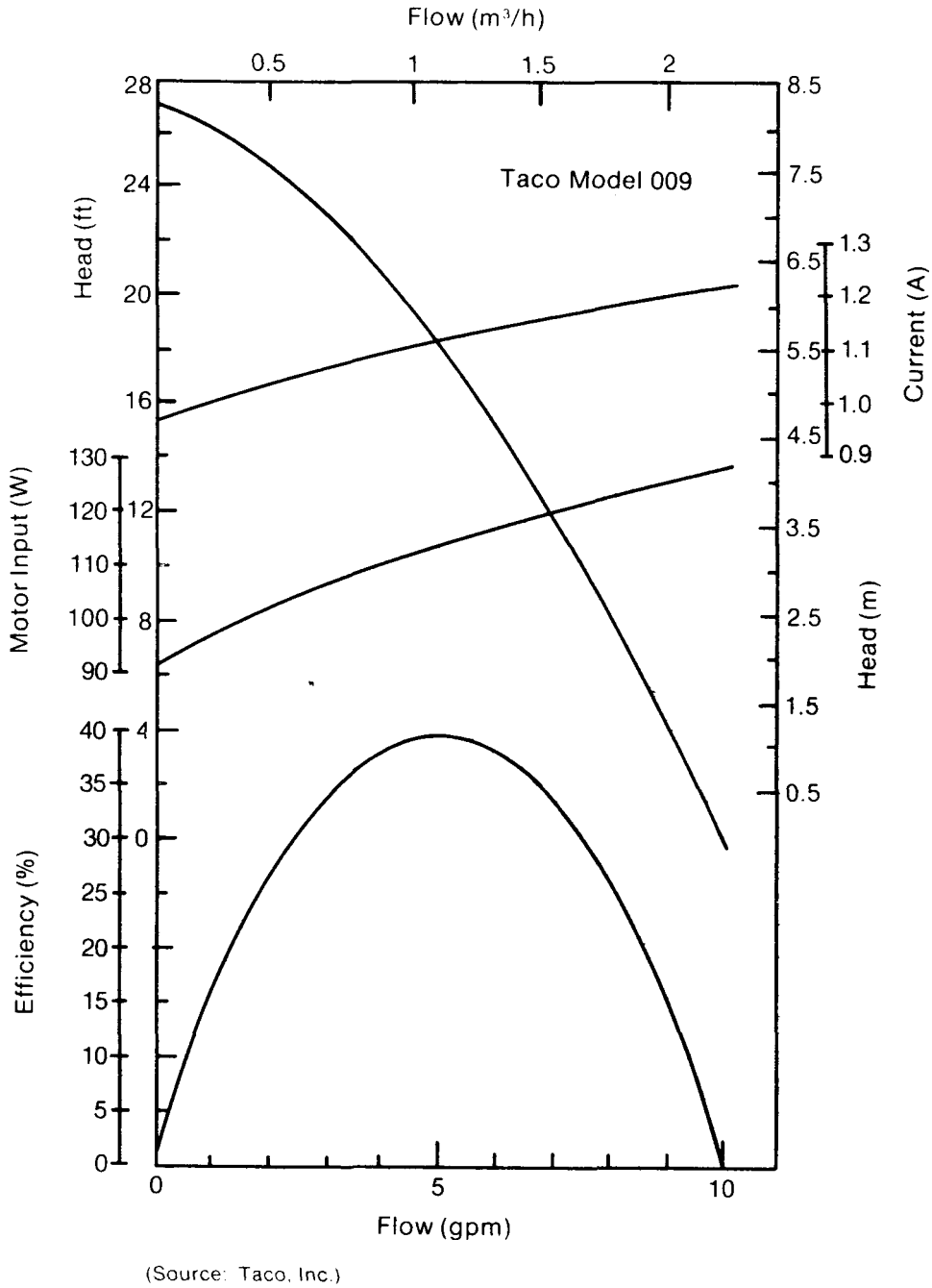

(Source: Taco, Inc.)

Figure 4-9. Pump Performance Curve for Fill Tests
(Source: Taco, Inc.)

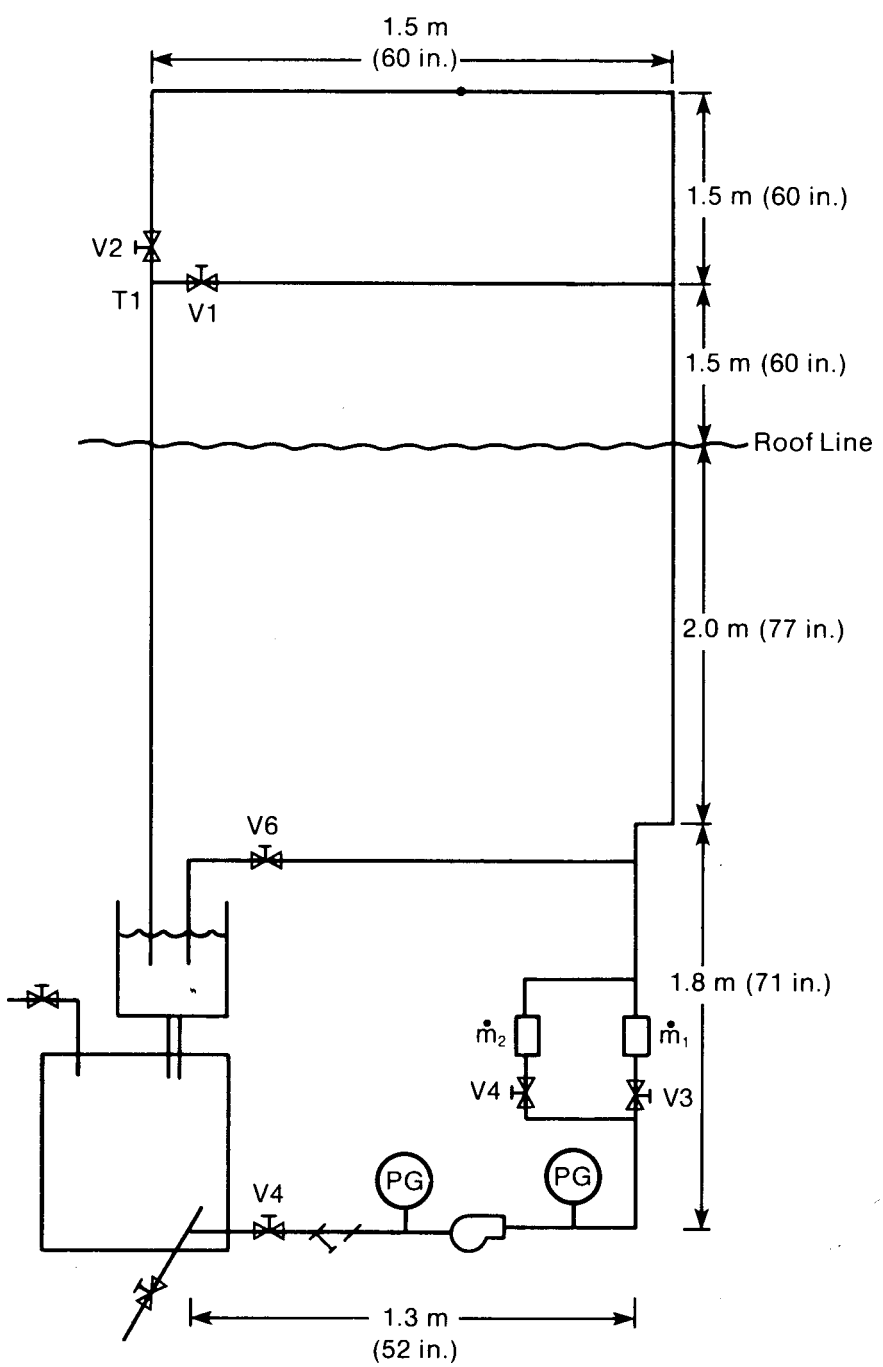

(Not to Scale)

Note:
All piping 1.9 cm (0.75 in.) except flowmeter section which is 1.27 cm (0.50 in.) tubing.
All piping is copper.

Legend:

⋈	Gate Valve
$\dot{m}_1$	Turbine Flowmeter
$\dot{m}_2$	Rotameter Flowmeter
PG	Pressure Gauge

Figure 4-10. Experimental Setup
(1.9 cm [3/4 in.] Fill/Drain Tests)

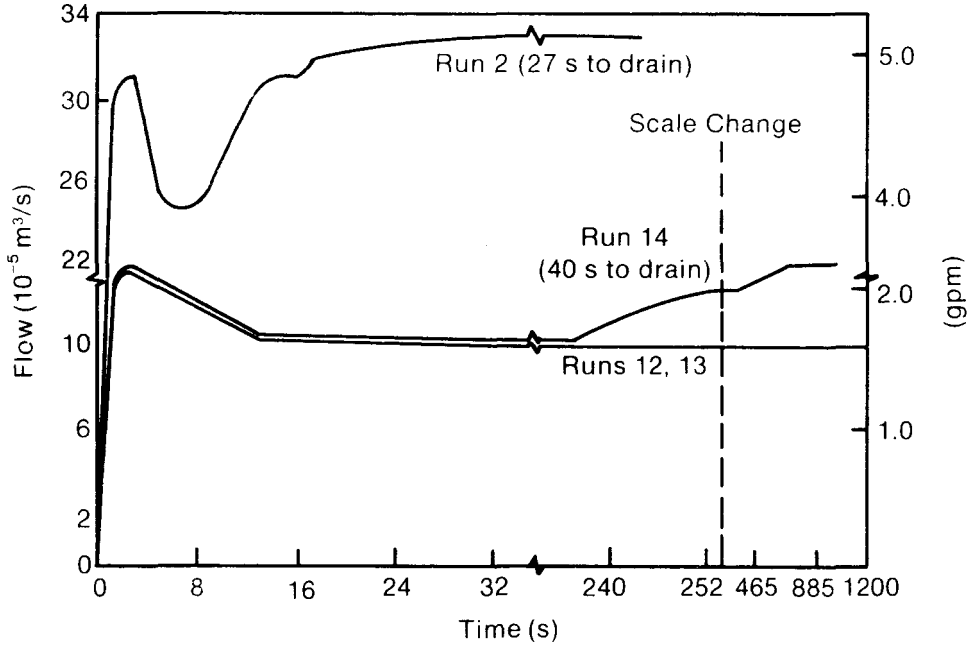

Figure 4-11. Fill Results, Runs 2, 12, 13, 14
(1.9 cm [3/4 in.], 6 m height)

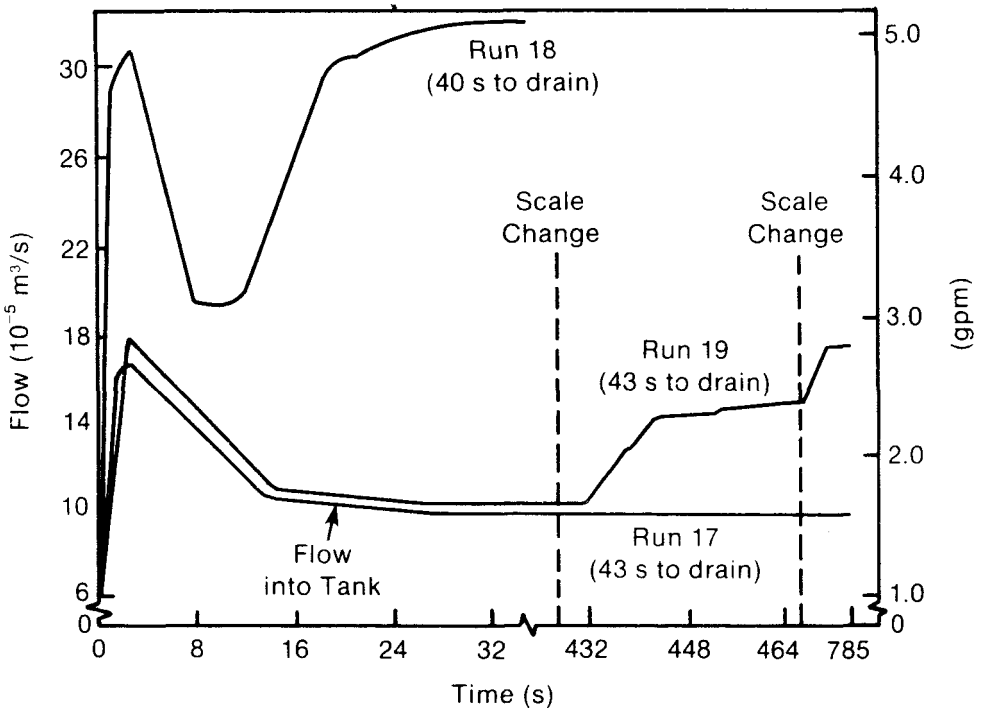

Figure 4-12. Fill Results, Runs 17, 18, 19
(1.9 cm [3/4 in.], 7.5 m height)

Although it is possible to develop a syphon at lower velocities by partially plugging the end of the tube, we did not perform this experiment. Using a smaller diameter tube for the last few inches may lower the flow rate sufficiently to develop a syphon in a 1.9-cm (3/4-in.) tube. A syphon will develop in 1.27-cm (1/2-in.) tube at 3.6 m/s (0.7 fps), which results in a flow rate of 3.2×10^{-5} m^3/s (0.51 gpm) and a fluid velocity of 1.6×10^{-3} m/s (0.31 fps), half the critical flow rate required to develop a syphon in the 1.9-cm pipe.

From our experiments we concluded that a syphon return can be developed for SDHW systems using pipe diameters of 1.27-cm (1/2 in.) and 1.9-cm (3/4 in.). Minimum flow rates necessary for a syphon to occur have been measured. Also, 1.9-cm pipe will drain directly downward without vents or valves. A 1.27-cm pipe can hold a standing column of water but will drain reliably with a sufficient differential pressure head between the downcomer and riser lines of the collector loop. Further testing may be required to determine the conditions, if any, under which a 1.27-cm pipe will not drain. This problem can be avoided by using a hole in the downcomer above the water level or by using a beveled pipe.

4.3 PUMP TESTING AND ANALYSIS

Because the pump in a drainback system must overcome elevation head, parasitic pumping power can be significant. The calculated overall equipment efficiencies of pumps used in SDHW systems are quite low, typically under 15%. Pump efficiencies are defined as hydraulic power divided by electric power, where hydraulic power equals $\dot{V}(m^3/s) \times \Delta P$ (Pa) [or $\rho(lb/ft^3) \times \dot{V}(ft^3/s) \times \Delta P$ (ft of water)] and where electric power is measured in watts (ft lb/s).

The pump efficiency usually found in brochures is the mechanical efficiency of the pump and is defined as hydraulic power divided by shaft power, which ignores the efficiency of the electric motor. The efficiency of the motor is shaft power divided by electric power.

It can be seen that the efficiency of primary interest is the overall equipment efficiency, which is the pump (excluding the motor) efficiency multiplied by the motor efficiency.

The cost to operate a pump is:

$$\text{operating cost(\$)} = [(\text{Power})(t)(CE)(CF)]/\eta \ ,$$

where

ρ = fluid density (kg/m^3 [lb/ft^3])

$\dot{V}$ = volumetric flow rate (m^3/s [ft^3/min])

ΔP = pressure drop; dynamic, static, or total head, (kPa [ft of water])

t = time interval (h/yr)

CE = cost of electricity ($/Wh)

CF = conversion factor [1 for SI units; 2.26×10^{-2} W/(ft-lb/min) for British units]

η = overall equipment efficiency of pump.

A system curve was developed (Figure 4-13) for a typical solar system (Table 4-3). SDHW systems typically operate at flow rates of approximately 1.3×10^{-4} m^3/s (2 gpm) (2 collectors in parallel, 6.3×10^{-5} m^3/s [1 gpm] each). The pressure drop for this hypothetical system at 1.3×10^{-4} m^3/s (2 gpm) is 27.2 kPa (9.1 ft of water) if 1.27-cm (1/2-in.) pipe is used and 6.0 kPa (2.0 ft of water) if 1.9-cm (3/4-in.) pipe is used.

The hydraulic power required for a 1.27-cm (1/2-in.) pipe is 1.26×10^{-4} m^3/s × 27,000 Pa (or 2 gal/min × 8.3 lb/gal × 9.1 ft of water), which is equal to 3.4 W (151 ft-lb/min).

The hydraulic power required for a 1.9-cm (3/4-in.) pipe is 1.26×10^{-4} m^3/s × 5700 Pa (or 2 gal/min × 8.3 lb/gal × 1.9 ft of water), which is equal to 0.7 W (16.6 ft-lb/min).

The 1.27-cm (1/2-in.) pipe size is more common for SDHW systems but requires five times the hydraulic power. However, the hydraulic power required to overcome the friction drop is nearly negligible. We can compute the cost to operate pumps that have an overall equipment efficiency of 10% (i.e., 34-W and

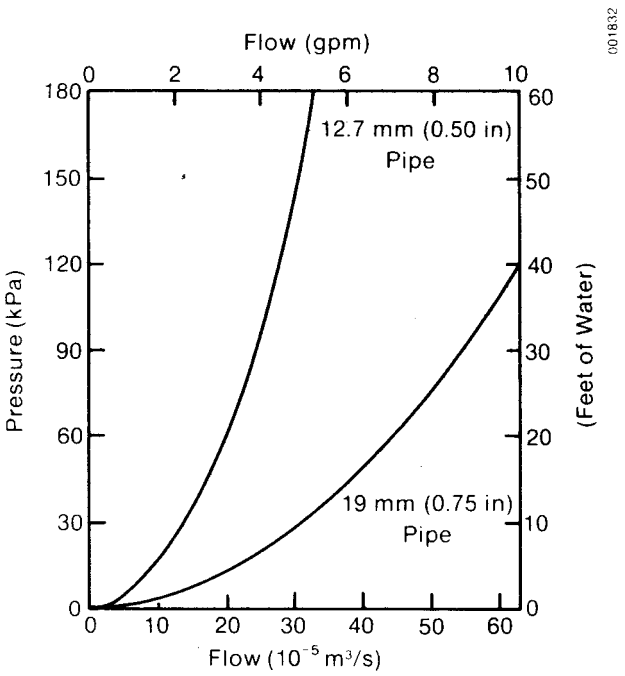

Figure 4-13. Drainback System H-Q Curves
(No Static Head)

Table 4-3. Pressure Drop for a Drainback System

Component	Diameter of Pipe	
	1.27 cm (1/2 in.)	1.9 cm (3/4 in.)
Equivalent Pipe Length, [m (ft)]		
Pipe	15.2 (50)	15.2 (50)
1 globe valve	5.2 (17)	6.7 (22)
1 gate valve	0.2 (0.5)	0.2 (0.5)
1 strainer	9.1 (30)	9.1 (30)
1 drainback tank	1.5 (5)	1.5 (5)
6 standard elbows	2.7 (9.0)	3.8 (12.5)
Total equivalent pipe length m (ft)	34 (112.5)	37 (121.0)
System Measurements		
Pipe ID [cm (in.)]	1.38 (0.545)	1.99 (0.785)
Flow rate [m^3/s (gpm)]	1.26×10^{-4} (2)	1.26×10^{-4} (2)
Velocity [m/s (fps)]	0.84 (2.75)	0.40 (1.3)
Friction factor (approx.)	0.03	0.03
$h_f = f\frac{Lv^2}{D2g}$ kPa (ft of water)	26 (8.7)	4.5 (1.5)
h_c = [2 at 6.3×10^{-5} m^3/s (1 gpm) each], kPa (ft of water)	1.2 (0.4)	1.2 (0.4)
$h_p = h_f + h_c$ [kPa (ft of water)]	27.0 (9.1)	5.7 (1.9)

Note: h_f = friction head
h_c = collector head
h_p = total dynamic pumping head

7-W pumps for 1.27-cm and 1.9-cm [3/4-in.] pipe, respectively) and operate 2500 h/yr, if electricity costs $0.06/kWh. The operating cost for a 12.7-cm (1/2-in.) pipe is (3.4 W)(2500 h/yr)($0.06/kWh)(kW/1000 W)/0.1, which equals $5.10/yr. The operating cost for a 1.9-cm pipe is (0.7 W) (2500 h/yr) ($0.06/kWh)(kW/1000 W)/0.1, which equals $1.05/yr.

The operating cost penalty incurred by using 1.27-cm (1/2-in.) pipe instead of 1.9-cm (3/4-in.) pipe can be seen. If the overall efficiency of the pump were only 5% (which may be more realistic), the operating costs double and the difference in operating costs between the two pipe sizes becomes $8.10/yr. This is a small amount, but it could be significant because 100- to 200-W pumps are often used instead of the 34-W and 7-W pumps used in the example. Proper sizing of the pump will lead to the greatest savings.

This analysis is applicable to any circulating system. The system of particular interest is the drainback SDHW system. The pump in a drainback system must overcome the static head as well as the friction head. In an open-drop system, the static head is always present. In a syphon-return

system, the pump must overcome the static head every time it begins operation. Since the static head is an additive term in the total pump head equation, it can be isolated and studied independently. A typical SDHW drainback system may have a static head of 25 ft. The static head is independent of pipe size. If an open-drop system operates 2500 h/yr with a flow rate of 1.3×10^{-4} m^3/s (2 gpm), a static head of 74.7 kPa, (25 ft) and electricity costs \$0.06/kWh, the annual operating costs will be:

$$\text{operating cost} = [(1.26 \times 10^{-4}\ m^3/s)(74{,}700\ Pa)](2500\ h/yr)(\$0.06/kWh)(1\ kW/1000\ W)/\eta\ .$$

The equivalent cost in English units is:

$$\text{operating cost} = (62.4\ lb/ft^3)\ (2\ gal/min \times 0.1337\ ft^3/gal)(25\ ft)(2500\ h/yr) \times (\$0.06/kWh)(1\ kW/1000\ W)\ (2.26 \times 10^{-2}\ W/ft\text{-}lb\ min)/\eta = \$1.41/\eta\ .$$

If the pump operates at an overall efficiency of 10%, the electric cost to overcome the static head in an open-drop system will be \$14.10/yr. If the efficiency were only 5%, the cost would be \$28.20/yr. Less than 9.5 W of hydraulic power are required to meet this static head. However, a 95-W pump is required for an efficiency of 10%; a 190-W pump is required if efficiency is only 5%. These costs do not include the cost required to overcome the friction head. The friction head in open-drop systems is less than in circulating systems, since the downcomer uses gravity return and presents no pressure drop to the pump. From Table 4-4, it can be seen that the pressure drop from the collector in the 1.27-cm (1/2-in.) pipe system is less than 10% of the total pressure drop for the system. We assumed that the total dynamic pumping head is approximately equal to friction head less the collector head ($h_p \approx h_f$). Thus an error of less than 10% for typical SDHW flow rates in the 1.27-cm pipe system will result. Since the pumping cost varies linearly with h_p, and h_f is linear with L (the equivalent pipe length), then

$$\text{cost} \propto L\ .$$

If the equivalent pipe length is halved by using an open-drop system, then the operating costs to overcome the friction head will be halved for the 1.27-cm (1/2-in.) system. The operating costs for the static head and friction head can then be added. If the pump operates at 10% efficiency, the operating cost will be \$5.10/2 + \$14.10 or about \$17/yr. If the pump is 5% efficient, the cost will be about \$33/yr.

With the 1.9-cm (3/4-in.) pipe system, the operating cost for the open-drop drainback system is approximately the static head pump costs (within 5%), since the cost to overcome the total dynamic friction head is relatively low.

Note that the annual cost of operating an open drop system with 1.27-cm (1/2-in.) pipe and a 74.7 kPa (7.6 m or 25 ft) static head at 1.26×10^{-4} m^3/s (2 gpm) with a 5% efficient pump is equivalent to the cost of operating a 100 W light bulb for 15 h/day for one year. It may be true that it does not cost any more to run a solar system pump than to operate a 100-W bulb, but operating a 100-W light bulb for that duration results in a significant cost.

Assuming a DHW load of 21 GJ/yr (20 MBtu/yr) and a solar fraction of 50%, the annual savings would be 11 GJ/yr (10 MBtu/yr) or 0.92 GJ/month (0.83 MBtu/

Table 4-4. Pressure Drop as a Function of Pipe Size and Flow Rate

Flow		1.27-cm (1/2-in.) Pipe								1.9-cm (3/4-in.) Pipe							
		v		h_f		h_c		h_p		v		h_f		h_c		h_p	
10^{-5} m^3/s	(gpm)	m/s	(fps)	kPa	(ft of water)	kPa	(ft of water)	kPa	(ft of water)	m/s	(fps)	kPa	(ft of water)	kPa	(ft of water)	kPa	(ft of water)
0	(0)	0	(0)	0	(0)	0	(0)	0	(0)	0	(0)	0	(0)	0	(0)	0	(0)
3.2	(.5)	0.21	(0.7)	1.8	(0.6)	0.3	(0.1)	2.1	(0.7)	0.09	(0.3)	0.3	(0.1)	0.3	(0.1)	0.6	(0.2)
6.3	(1.0)	0.43	(1.4)	6.9	(2.3)	0.6	(0.2)	7.5	(2.5)	0.21	(0.7)	1.2	(0.4)	0.6	(0.2)	1.8	(0.6)
9.5	(1.5)	0.64	(2.1)	15.2	(5.1)	0.9	(0.3)	16.1	(5.4)	0.30	(1.0)	2.7	(0.9)	0.9	(0.3)	3.6	(1.2)
13	(2)	0.85	(2.8)	26.0	(8.7)	1.2	(0.4)	27.5	(9.2)	0.40	(1.3)	4.5	(1.5)	1.2	(0.4)	5.7	(1.9)
19	(3)	1.25	(4.1)	57.7	(19.3)	2.1	(0.7)	59.8	(20.0)	0.61	(2.0)	10.2	(3.4)	2.1	(0.7)	12.3	(4.1)
32	(5)	2.10	(6.9)	164.8	(54.8)	2.7	(0.9)	166.5	(55.7)	1.01	(3.3)	28.1	(9.4)	2.7	(0.9)	30.8	(10.3)
63	(10)	4.21	(13.8)	654.6	(219.0)	5.7	(1.9)	660.3	(220.9)	2.01	(6.6)	112.1	(37.5)	5.7	(1.9)	117.8	(39.4)

v = velocity

h_f = friction head

h_c = collector head (Grumman Energy Systems Models 321A/332A at one half of flow rate - two collectors in parallel)

h_p = pumping head, $h_p = h_f + h_c$

month). With energy prices ranging from $3/GJ ($3/MBtu) for gas to $15.65/GJ ($14/MBtu) for electricity, monthly savings can range from $3.94 (assuming a water heater efficiency of 70%) to $14.40/mo. Hence, the operating costs are not negligible. If natural gas is displaced, much of the savings may go to operating the pump. If an open-drop drainback system with a 1.27-cm (1/2-in.) pipe is used with a 5% overall efficiency pump to displace natural gas, the annual operating costs of $33 would nearly equal the annual savings of $47 in our example.

There are several ways to reduce the operating cost of a drainback system. One is to increase the efficiency of the pump equipment since the hydraulic power required is small. Inefficiencies result from both the motor (resistive losses) and the pump (possible friction losses and fluid bypass around the impeller). The other alternative to reduce the operating cost of drainback systems is to use a syphon return. This method reduces electric consumption only if the electric power is reduced after a syphon is established. This can be accomplished by a two-speed pump, by two pumps, or by modulating the speed of the pump with a Triac controller. If this strategy is not followed and a syphon return is established, then operating costs will increase even more since power consumption increases with flow rate. In addition, premature failure of the pipe can occur because of erosion and corrosion at excessively high fluid velocities.

The operating cost for a syphon return system is the cost to circulate the fluid and the cost to develop the syphon. The methodology is the same as that for the open-drop system with a much shorter time interval. If a system starts an average of 4 times/day (a time delay would be needed to prevent cycling) and takes 5 min to establish a syphon, then the pump operates 20 min/day to overcome the static head. For 300 days of operation, this pump would run 100 h/yr. The annual cost to overcome a head of 74.7 kPa (7 m or 25 ft) at 1.26×10^{-4} m^3/s (2 gpm) and a cost of $0.06/kWh would be:

$$\text{operating cost} = (1.26 \times 10^{-4}\ m^3/s)(74{,}700\ Pa)(100\ h/yr)(\$0.06/kWh)(kW/1000\ W) .$$

The equivalent annual cost in English units is

$$\text{operating cost} = (62.4\ lb/ft^3)\ (2\ gal/min \times 0.1337\ ft^3/gal)(25\ ft)(100\ h/yr) \times (\$0.06/kWh)(2.26 \times 10^{-5}\ W/ft\text{-}lb\ min)/\eta = 0.056/\eta.$$

The cost to overcome the static head and initiate a syphon return would be $0.56/yr for a pump with an overall efficiency of 10%, and $1.12/yr for a 5% efficiency pump. The savings from using this strategy instead of an open-drop system or a syphon return without reduced flow would range from $14 to $27/yr. Table 4-5 summarizes the annual operating costs for various system strategies, pipe sizes, and pump efficiencies.

4.3.1 Calculated Pump Efficiencies

Published pump efficiencies are much higher than actual or calculated efficiencies because published efficiencies do not include the motor efficiency.

Table 4-5. Annual System Operating Cost ($)

System Type	η = 5%			η = 10%		
	Friction Head	Static Head	Total Head	Friction Head	Static Head	Total Head
1.27-cm (1/2-in.) pipe:						
Circulating[a]	10.20	--	10.20	5.10	--	5.10
Open drop	5.10	28.20	33.30	2.60	14.10	16.70
Syphon return	10.20	1.12	11.32	5.10	0.56	5.66
1.9-cm (3/4-in.) pipe:						
Circulating[a]	2.10	--	2.10	1.05	--	1.05
Open drop	1.05	28.20	29.25	0.50	14.10	14.60
Syphon return	2.10	1.12	3.22	1.05	0.56	1.61

[a]Would include draindown and other water circulating systems; shown for comparison to demonstrate effect of drainback strategy on operating costs.

Figure 4-14 shows the published mechanical efficiency of a Taco pump and also the overall equipment efficiency of the pump and motor calculated from the published head-flow curve. As expected, there is a substantial difference between the two efficiencies. In general, peak efficiency for these pumps occurs at about half of maximum flow, dropping to zero at each end of the flow-rate range.

Figure 4-15 shows the efficiencies of several Myson pumps calculated from the published head-flow curves. Peak efficiencies vary from less than 1% to over 20%; Table 4-6 gives the peak efficiencies for each pump and the flow conditions at which the peak occurs.

The conclusions that can be drawn from this data are as follows:

- Larger pumps (high values of head times flow) are generally more efficient than pumps with smaller values of head times flow.
- Efficiency increases with head at a constant flow rate (compare the LC 45B and the LC 49B, for instance).
- The variable speed pumps (LA 45, LA 55, LA 58) have very low efficiencies (~1%) at low speeds, which is one-tenth to one-twentieth of their high speed efficiencies. This is caused by a fluid bypass in the particular pumps used to control flow.

Table 4-7 shows the peak overall efficiencies calculated for several Taco pumps. Peak efficiencies are approximately 8% to 20%.

Taco measures the mechanical (shaft to fluid) efficiencies of their pumps without the motor efficiency. The peak pump efficiencies vary from 23% to 52%.

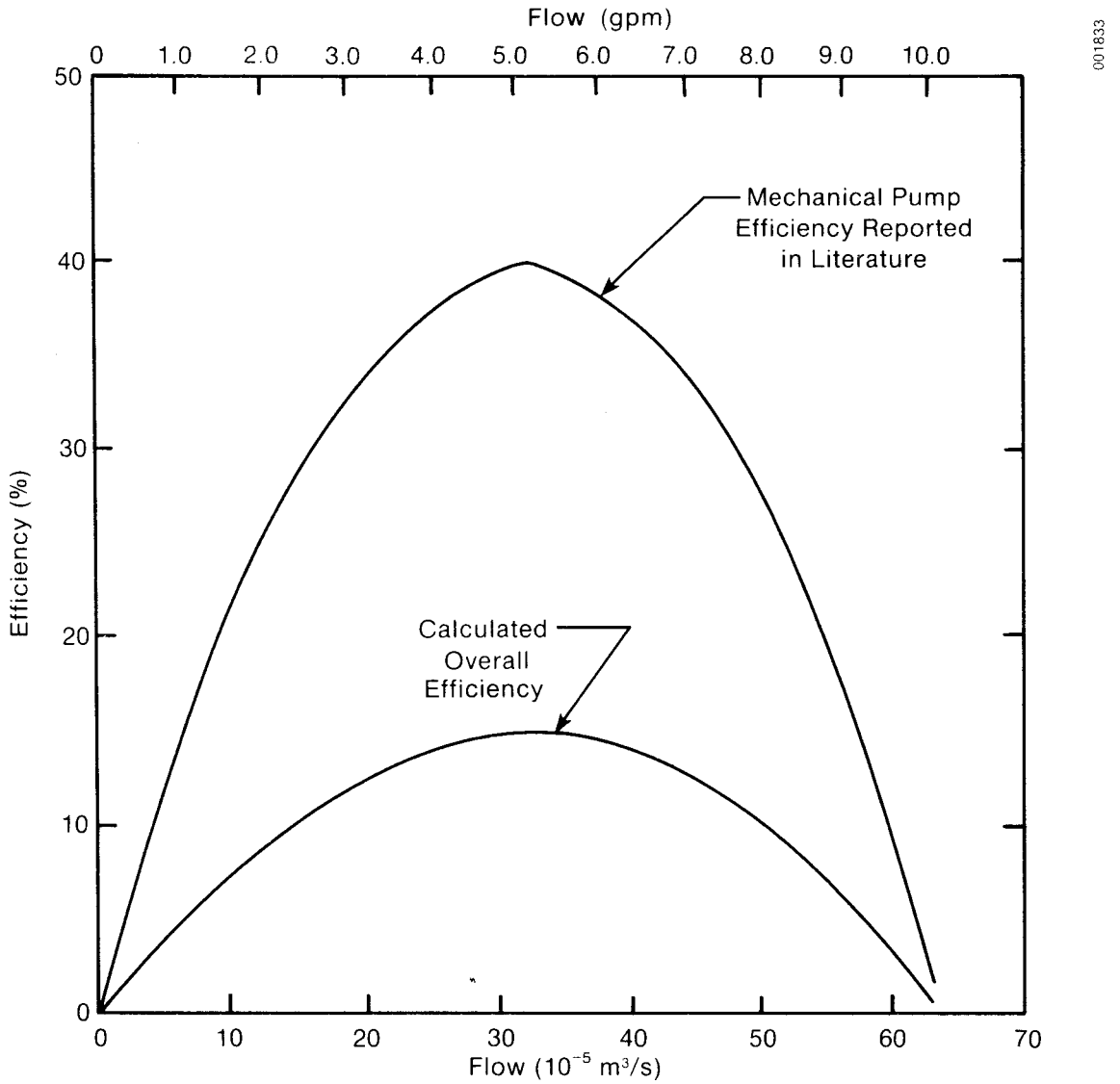

Flow (10^{-5} m^3/s)	Head (Pa)	Published Mechanical Efficiency	Calculated Overall Efficiency
00.0	80703	0.00	0.000
06.3	77714	0.15	0.050
12.6	74127	0.27	0.091
18.9	68747	0.34	0.120
25.2	62171	0.38	0.141
31.5	53802	0.40	0.149
37.8	45732	0.38	0.147
44.1	35270	0.34	0.130
50.4	24510	0.27	0.101
56.7	13151	0.16	0.059
63.0	1195	0.02	0.006

Figure 4-14. Taco 009 Pump Efficiencies

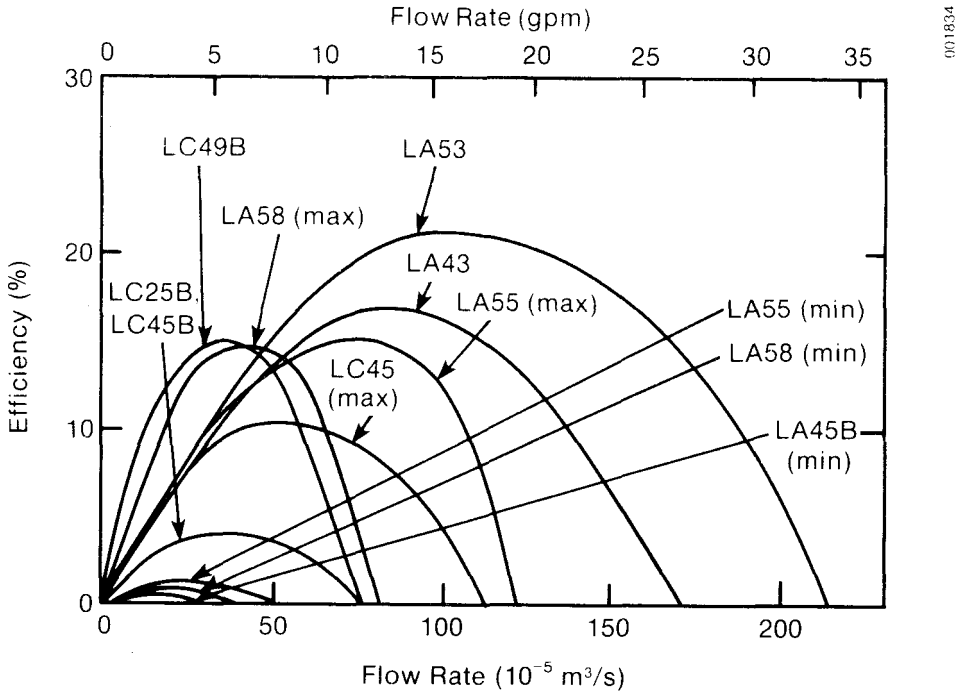

Figure 4-15. Myson Pump Efficiencies

Table 4-6. Myson Pump Efficiencies Calculated from Published Head-Flow Curves

Model	Peak Overall Efficiency	Head		Flow Rate	
		kPa	ft of water	10^{-5} m^3/s	gpm
LA 43	17.1	16.1	5.4	88	14
LA 45 (max)	10.6	16.4	5.5	63	10
(min)	0.6	3.3	1.1	19	3
LA 53	21.4	23.3	7.8	95	15
LA 55 (max)	15.4	22.1	7.4	76	12
(min)	1.5	6.3	2.1	25	4
LA 58 (max)	14.9	38.2	12.8	38	6
(min)	1.1	4.2	1.4	25	4
LC 25B	4.2	9.6	3.2	38	6
LC 45B	4.3	9.8	3.3	38	6
LC 49B	15.4	41.8	14	38	6

Table 4-7. Calculated Overall Pump Efficiencies

Pumps	Overall Peak Efficiency (%)	Head		Flow Rate	
		kPa	ft of water	10^{-5} m^3/s	gpm
008, 008-B, 008V; -2, -3 models	19.0	31.7	10.6	0.50	8
007-3, -B3	18.2	20.9	7	0.76	12
006-B2, -BT2, -BC2	8.2	17.9	6	0.38	6
006-B2Y, -BT2Y, -BC2Y	7.2	16.1	5.4	0.38	6
009-F2, -BF2	15.1	54.4	18.2	0.32	5

Using the calculated overall pump efficiencies and the published mechanical pump efficiencies, we calculated the motor efficiency for each of these pumps. The results are shown in Table 4-8.

These data show that pumps are more efficient when designed for larger flow rates and higher head applications, and all the motors shown are about 30%-40% efficient.

4.3.2 Measured Overall Pump Efficiencies

4.3.2.1 Pump Testing

The initial test setup included a Ramapo target meter to measure flow rate with a flow bypass through a Brooks rotameter. Flow was through a 1.27-cm (1/2-in.) pipe that extended 5.5 m (18 ft) above the water level of an unpressurized tank. A globe valve was used for throttling the flow. The pressure drop through the target meter and piping was too high and did not allow sufficiently high flow rates. A rotameter was installed to measure flow rate of the draining and a flow bypass valve around the pump was installed to measure resistance to backward draining through the centrifugal pump. The pump did not impede drainage measurably.

Table 4-8. Calculated Pump Motor Efficiencies

Pumps	Pump-Alone Efficiency (%)	Motor Efficiency (%)
008	51.8	36.7
007	50.0	36.4
006-B2	23.5	34.9
006-B2Y	23.2	31.0
009	29.5	38.2

The setup was then modified by replacing the target meter with a Cox turbine meter. The piping was changed to allow the fluid to flow from the storage tank through the pump and as directly as possible back to the tank. The globe valve was removed and the 1.27-cm (1/2-in.) line was replaced by 1.9-cm (3/4-in.) line and fittings, except in the flowmeter section. The pressure transducers were removed for calibration but could not be properly calibrated. In addition, the pressure transducers may have been too close to the pump suction and discharge for accurate readings. Fittings immediately before and after the pump (elbows and tees) also may have affected the pump's performance. Therefore, the piping was changed to the final setup that is shown in Figures 4-16 and 4-17. A differential pressure transducer was used instead of the two absolute pressure transducers. However, this configuration also had limitations, which will be discussed in Appendix C. All the instruments were turned on for at least 30 min before testing. An equipment list is shown in Table 4-9. A discussion of the individual instruments is given in Appendix C. A summary of the instrumentation uncertainties is given in Table C-3.

4.3.2.2 Results

In addition to uncertainty in the reading, instrumentation malfunction must also be considered. Appendix C presents the test results for this experimental setup, discusses measurement uncertainty, and identifies possible sources of instrument malfunction. In general, this setup was not adequate to measure pump performance at high flow rates and low pressure heads because of the turbine meter pressure drop. Additionally, high heads at low flow rates could not be measured due to difficulties with the pressure transducers.

Measurements of the head-flow curves for the Taco 009 and Grundfos UPS 20-42 pumps were also generated using two dial pressure gauges. The results are shown in Figure 4-18 for the Taco pump and Figure 4-19 for the Grundfos three-speed pump. These experimental results agree closely with the published performance except for the lowest speed of the Grundfos pump, and there the performance exceeded the published curve. The overall efficiencies of these pumps are shown in Table 4-10. Note that the power to the pump is proportional to the flow rate. Peak efficiencies could not be measured due to the flow measurement limitations. The gauges read the hydrostatic pressure correctly and zeroed properly for atmospheric gauge pressure. The equipment to calibrate the strain-gauge pressure transducers properly was not available. The uncertainty of the Viatran differential pressure transducer appeared to be larger than specified. Only the differential and span could be checked.

After the pump performance testing was completed, equipment was obtained to measure the power factor of the pumps. An Energy Research Associates solid-state kilowatt hour meter (KWH 770) was used to measure the real power of the pump (volts × amps × power factor), and the GE ammeter and Fluke multimeter (see Appendix C) were used to measure the apparent power of the pump (volts × amps). The power factor is equal to the real power of the pump divided by the apparent power of the pump. The results for the Taco 009 and Grundfos UPS 20-42 are shown in Table 4-11. The power factor ranges from 0.83 to 0.875

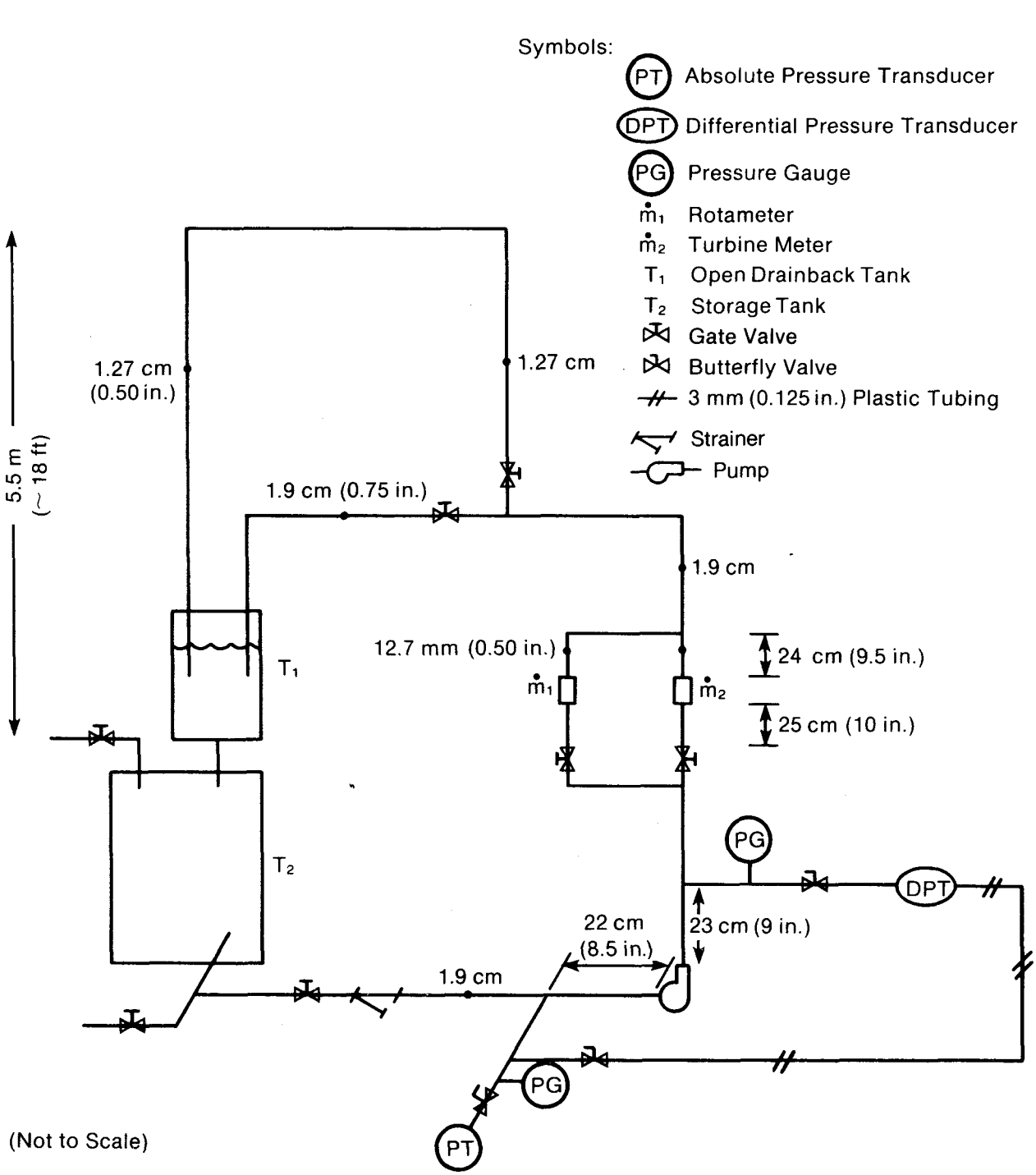

All piping is 1.9 cm (0.75 in.) except the flowmeter section, which is 1.27-cm (0.50-in.) tubing, and a 5.5-m (18-ft) section which is 1.27-cm pipe.

Pump has 1.27-cm threaded fittings (fitting and reducers 5 cm [2 in.] long).

Figure 4-16. Experimental Setup for Richdel Pumps

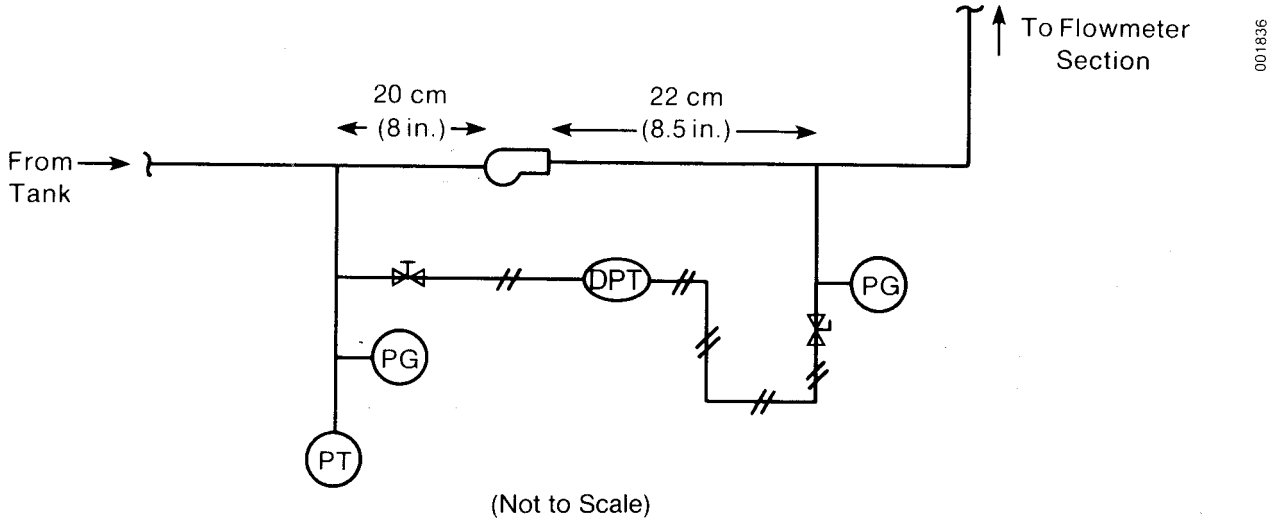

Figure 4-17. Experimental Setup for Grundfos and Taco Pumps (Arrangement is the same as for Richdel pumps except for pump section.)

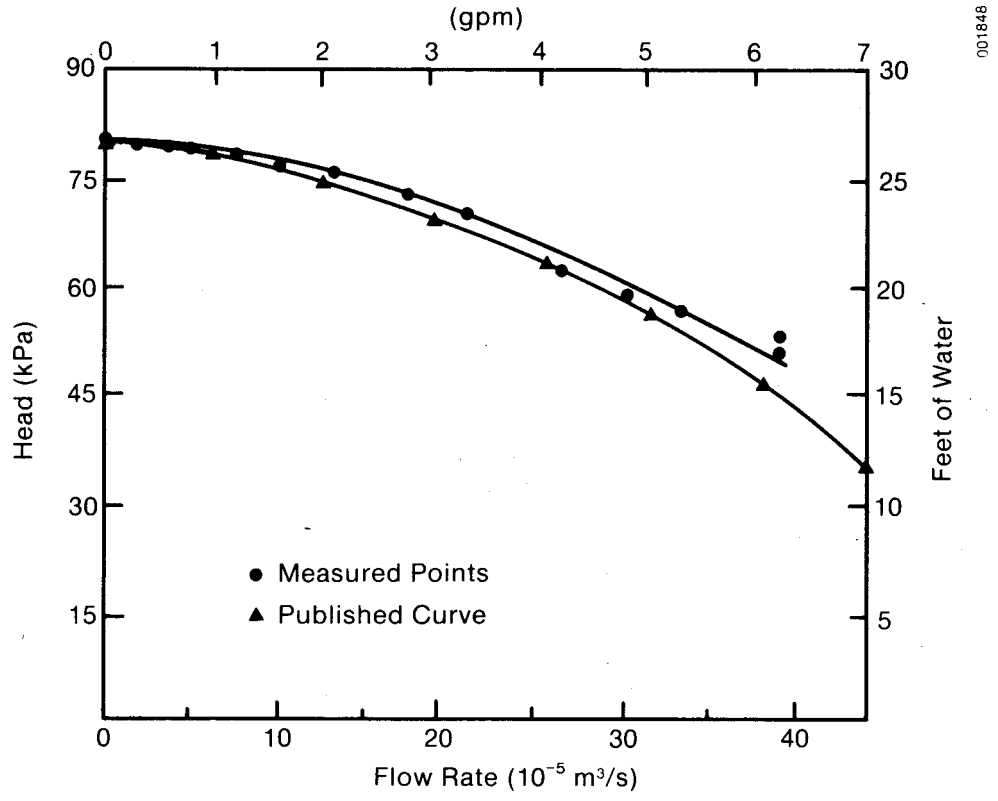

Figure 4-18. Experimental Taco 009 Pump Curve with Pressure Gauges

Table 4-9. Equipment List for Pump Tests

Component	Serial Number	Manufacturer and Model Number	Range of Capacity
Turbine flowmeter	39499	Cox ANC8	0-6.0 × 10^{-4} m/s (0-9.5 gpm)
Digital panel meter	81-162	Cox 8550	
Target meter	7653	Ramapo V-1/2-SS	3.2-3.2 × 10^{-4} m/s (0.5-5.0 gpm)
Transmitter	21666	Ramapo SGA-8350B	0-10 V
Rotameter	8009H57722/3	Brooks S-925-J-204-AAA	0-9.5 × 10^{-5} m^3/s (0-1.5 gpm)
Rotameter	8009H57721/2	Brooks S-925-J-203-AAA	0-5.0 × 10^{-5} m^3/s (0-0.8 gpm)
Storage tank	F80658665	3E2020	0.20 m^3/s (52 gal)
Pressure transducer	210769	Viatran 218-24	0-345 kPa (0-50 psia)
Pressure transducer	171411	Viatran 218-24	0-345 kPa (0-50 psia)
Pressure transducer	210809	Viatran 218-24	0-690 kPa (0-100 psia)
Pressure transducer	17561181	Viatran 220-24	±69 kPa (±10 psid)
Transducer wire		Belden 8426	
Transducer power supply	1331	Raytheon DTM24-4	105-125 V in, 12-25 V out
Digital voltmeter	2575765	Fluke 8024 A	0-200 V
Clamp-on ammeter	DOE 108415	G. E. 942D	
Data logger	2011A00118	H. P. 3497A	
Pump (new)	A8137	Grundfos UPS 20-42	
Pump (new)	B1 934940	Richdel R798A	
Pump (used)	B0 439848	Richdel R798A	

Performance:

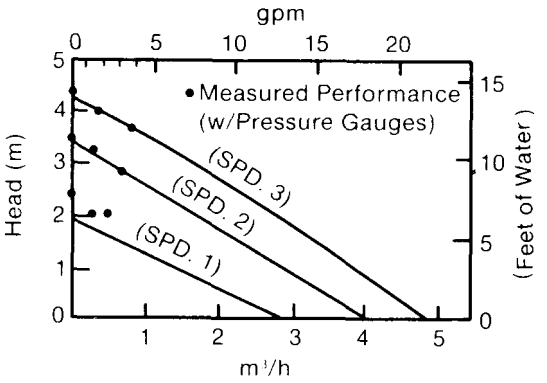

Electrical:

Model	Speed	Hp	Watts	Volts	Amps	RPM	Capacitor
UPS 20-42 F	3	1/20	95	115	0.85	2620	10 MF/180 V
3-Speed	2	1/32	70	115	0.60	2300	
	1	1/64	50	115	0.42	1800	

(Source: Grundfos)

Figure 4-19. Published Grundfos UPS 20-42 Pump Curve

Table 4-10. Measured Pump Efficiencies

Pump	Flow		Head		Power (W)	Overall Efficiency (%)
	L/min	(gpm)	kPa	(psid)		
Taco 009	20.1	(5.3)	60.0	(8.7)	129.2	15.5
	17.0	(4.5)	68.9	(10.0)	127.3	15.4
	11.0	(2.9)	79.3	(11.5)	120.9	12.0
	4.5	(1.2)	86.9	(12.6)	113.9	5.8
	2.3	(0.6)	81.3	(11.8)	111.4	2.8
	0	(0)	82.0	(11.9)	108.1	0.0
Grundfos UPS 20-42						
Speed III	13.6	(3.6)	34.5	(5.0)	96.4	8.1
	6.8	(1.8)	39.3	(5.7)	94.1	4.7
	0	(0)	42.0	(6.1)	91.2	0.0
Speed II	11.4	(3.0)	27.6	(4.0)	76.3	6.8
	5.9	(1.5)	31.7	(4.6)	74.3	4.0
	0	(0)	33.8	(4.9)	71.4	0.0
Speed I	8.3	(2.2)	19.3	(2.8)	54.3	4.9
	4.5	(1.2)	19.3	(2.8)	53.3	2.7
	0	(0)	23.4	(3.4)	51.8	0.0

Table 4-11. Measured Power Factor

Pump	Flow L/min	Flow (gpm)	Voltage[a] (V)	Current[b] (A)	Voltage × Current (V × A)	Wattmeter[c] (W)	Power Factor [W/(V × A)]	Uncertainty[d]
Taco 009	20.1	(5.3)	124.0	1.19	147.6	129.2	0.875	±0.067
	17.4	(4.6)	124.1	1.18	146.4	127.8	0.873	
	17.0	(4.5)	124.0	1.19	147.6	127.3	0.862	
	11.0	(2.9)	124.0	1.12	138.9	120.9	0.871	
	4.5	(1.2)	124.1	1.10	136.5	113.9	0.834	
	2.3	(0.6)	124.1	1.06	131.5	111.4	0.847	
	0	(0)	124.0	1.05	130.2	108.1	0.830	±0.072
Grundfos UPS 20-42								
Speed III	13.6	(3.6)	124.2	0.78	96.9	96.4	0.995	±0.039
	6.8	(1.8)	124.4	0.76	94.5	94.1	0.995	
	0	(0)	124.4	0.74	92.1	91.2	0.991	
Speed II	11.4	(3.0)	124.3	0.63	78.3	76.3	0.974	±0.047
	5.9	(1.5)	124.4	0.62	77.1	74.3	0.963	
	0	(0)	124.4	0.59	73.4	71.4	0.973	
Speed I	8.3	(2.2)	124.5	0.46	57.3	54.3	0.948	±0.062
	4.5	(1.2)	124.5	0.45	56.0	53.3	0.951	
	0	(0)	124.5	0.44	54.8	51.8	0.946	±0.065

[a] ±1.1 V

[b] ±0.09 A for Taco; ±0.03 A for Grundfos

[c] ±0.25% of reading

[d] Root mean square uncertainty

for the Taco pump and from 0.946 to 0.995 for the Grundfos pump. The actual operating cost for a pump is determined by the real power of the pump and not the apparent power, since residential kilowatt hour meters account for the power factor.

4.4 CONCLUSIONS

Drainback systems, though simple in principle, can present complications. The designer should consider the operating cost as well as the initial cost, which requires a system head-flow curve for various pipe sizes and the head-flow curves for various pumps. The designer should consider additional capital costs from increased pipe sizes and insulation as well as increased installation cost; these amounts should then be compared with potential savings.

The designer should decide whether or not to design a syphon flow and then determine if there is sufficient fluid velocity for the syphon to develop. Pipe configuration and pipe slope must allow for drainage of the system.

A major concern with drainback systems is the operating cost that is attributed to the initial static head that the pump must overcome. One solution (Section. 3.2) is to use a collector-side heat exchanger and to mount the drainback tank in the attic. Four other solutions available to the designer lend themselves to a packaged system (Table 4-12). The best choice may depend on the system design, cost of auxiliary energy, and cost and availablility of the options.

If pump speed controllers (option 4) were widely available, they would add little cost to the controller and would provide good control for this system; they also reduce the power to the pump. Options 2, 3, and 4 reduce the pump's input after a syphon is developed. (Savings from this approach were presented in Section 4.3.)

Option 1 is a poor choice if the auxiliary energy is not electricity. Although the pump energy is lost to the water, it is expensive electrical energy. If the auxiliary energy is electric, then the cost for heating the water with the pump is the same as with the auxiliary heating elements. If the back-up is natural gas, then the pump energy to the water is more expensive than the auxiliary energy and is an inefficient way to heat water. In both cases, water flowing to the collectors is preheated electrically, which reduces the collector efficiency.

For a 160-W pump that is operating at an equipment efficiency of 10%, 144 W (490 Btu/h) are expended in heating the water. For a 5.6-m^2 (60-ft^2) collector array and an irradiance of 317 W/m^2 (100 Btu/h ft^2), 8% of the total irradiance on the array is required for energy input from the pump. If the system were 30% thermally efficient, the pump energy input to the water would equal about one-fourth of the delivered energy. Use of a submersible pump has definite adverse effects on the performance of the system.

Table 4-12. Power Reduction Options for Drainback Systems

Option	Advantages	Disadvantages
1. Submersible pump	Reclaims all lost heat	Not suitable for many systems (e.g., systems with sealed drainback tanks)
	No special controls or	Reduces collector timers efficiency by preheating collector loop water electrically
		Maintenance more difficult
		Initial cost is greater than that of conventional pump
		Requires higher temperature materials
		Requires waterproof case and wiring
2. Two pumps with timer for one pump	Conventional pumps Conventional plumbing	Additional initial and installation cost
		Increased maintenance
		Additional controller capability or timer required
3. Two-speed pump with timer	Conventional plumbing	Initial cost greater than that of a single-speed pump
		Requires timer
4. Pump speed controller (SCRs)	Small additional cost Conventional pump Conventional plumbing	Requires compatible motors
		Not currently available commercially

Option 2 can be provided by the installer. Option 3 can be inexpensively added by the controller manufacturer. However, an appropriate pump with both speeds properly chosen would need to be included.

To test Option 4, SERI developed a combination Triac and time delay which drops the pump speed after a set period of time. Initial experiments have demonstrated that this low-cost approach works well and can reduce pumping power on the order of 50%.

4.5 REFERENCES

Argonne National Laboratory, Sept. 1981, Final Reliability and Materials Design Guidelines, ANL/SDP-11, SOLAR/0909-81-70, Argonne, IL: Argonne National Laboratory.

Butkov, Eugene, 1968, Mathematical Physics, Reading, MA: Addison-Wesley.

Lauer, B. E., 1953, "How to Evaluate Heat Transfer Coefficients for Heat Transfer Calculations," Reprinted from The Oil and Gas Journal, Tulsa, OK: The Petroleum Publishing Company.

Wallis, G. B., C. J. Crowley, and Y. Hagi, June 1977, "Conditions for a Pipe to Run Full When Discharging Liquid into a Space Filled with Gas," Journal of Fluids Engineering, Vol. 99.

SECTION 5.0

SYSTEM OPTIMIZATION

With an understanding of how a drainback system works, the next task was to use much lower cost materials in its construction. The first step was to conduct a survey of the various materials available for piping, storage, and insulation and compare them on the basis of cost and physical properties. Results of the survey are given in Section 5-1. The next step was to integrate the best materials into a low-cost design as described in Section 5.2. Finally the estimated costs of the system are given in Section 5.3.

5.1 RESULTS OF SYSTEM MATERIALS SURVEY

In an effort to minimize the overall system cost, we conducted a survey of candidate materials required for fluid containment and thermal insulation. The survey emphasized containment materials--including pipes, tanks, and liners--and insulating materials. Based on system design considerations discussed in Section 5.2, further emphasis was placed on materials compatible with unpressurized, drainback solar domestic hot water (SDHW) systems. For each category, several materials were considered, including commercially available products presently in use and materials not specifically designed for solar applications that have the potential to replace more expensive materials and yield only a small decline in performance. Industry contacts made during this survey are listed in Table 5-1.

5.1.1 Pipe Materials

The accepted pipe material at the present time is copper (Table 5-2). The material qualities of copper are well known, and it is widely accepted by installers and designers. Its main disadvantage is its high price.

Plastic pipe materials cost less than copper and to some degree are easier to install. The major drawbacks of plastic pipes are that they are not as readily accepted by installers and, most importantly, that they have temperature limitations. The only acceptable materials for plastic pipes on the basis of thermal stability are chlorinated polyvinyl chloride (CPVC) and polybutylene (PB). Both are capable of withstanding continuous temperatures of 180°-200°F at elevated pressures. At atmospheric pressure, both are capable of withstanding continuous temperatures as high as 200°F. PB comes in coilable (low modulus) and straight forms and requires continuous support to prevent sagging and water entrapment. Mechanical properties given in Table 5-2 for CPVC are for ambient conditions and degrade by about 50% at working temperatures. This requires supporting rigid CPVC every 81-91 cm (32-36 in.) to prevent sag and subsequent water entrapment except for riser and downcomer pipes. Support is also required for CPVC that is unprotected and exposed to UV radiation. UV aging has no effect on the tensile strength

Table 5-1. Industry Contacts for Balance-of-System Materials Survey

Stan Morake, Plastics Pipe Institute, New York, NY; (212) 573-9400.
Plateau Supply Co., Denver, CO; (303) 292-0990; Glass foam insulation, fiberglass board insulation.
John Popovich, Harbor City, CA; (213) 539-8590; polybutylene pipe.
Jim Finley, Diamond Shamrock, TX; (214) 659-7000; sodium borosilicate foamed glass.
Phil Curtis, Carolina Extruded Plastics, Greensboro, NC; (919) 272-1191; various extruded plastic pipes.
Brent Fletcher, Tetra Plastics, Chesterfield, MO; (314) 632-3655; high density polyethylene pipe.
Standard Plumbing, Salt Lake City, UT; (801) 972-6087; ABS pipe.
Lester Gorsline, The Grosline Company, Tiburon, CA; (415) 726-3211; Neopor cellular concrete.
Andy Corte, B.F. Goodrich Co., Cleveland, OH; (216) 447-6000; PVC and CPVC pipe.
Mick Reeves, Reeves Plastic Pipe Co., Denver, CO.; (303) 399-3760; PB, CPVC, and PVC pipe.
Mell Schard, Shell Chemical Company, Houston, TX; (713) 241-3571; Polybutylene pipe.

of CPVC, so it will be able to maintain working pressures. However, UV aging affects the impact strength of CPVC, and support is required to avoid damage from hail or other such abuse.

One advantage of flexible pipe (PB, PE, or PP) is its ability to withstand freeze-thaw conditions. These pipes also have smooth inner walls, unlike rigid CPVC, PVC, and ABS. The latter have rough inside walls and are more susceptible to clogging.

The most important consideration in using plastic pipe for solar applications is the performance of the fittings. The shapes of these fittings make them more sensitive to thermal cycling and freeze-thaw than straight pipe of the same material. In addition, fittings have not always been tested at continuous-use elevated temperatures, although tests have been performed in short-term, domestic hot water simulations. This problem is critical for PB installations where the fittings are not of the same material and are applied by mechanical crimping. CPVC systems use a solvent cement and joints made from CPVC. Note that adhesives cannot be used with untreated polyethylene and polypropylene.

Based on cost and thermal stability, both CPVC and PB should be strongly considered as substitute pipe materials for copper. PB has an added advantage

Table 5-2. Pipe Materials

Material	Dimensions		Density		Cost		Thermal Properties				Mechanical Properties		UV Resistance
	Outer Diameter (mm)	Wall Thickness (mm)	kg/m^3	kg/m	$/kg	$/m	T_{max} (^oC)	T_{cont} (^oC)	Coef. of Linear Expansion (10^{-6} m/m $^oC^{-1}$)	Thermal Conductivity (W/m K)	Hoop Stress (MPa)	Flexural Modulus (MPa)	
Copper	12.7	2.54	8910	0.722	2.59	1.87		>205	16.6	393			excellent
Steel	12.7	2.54	7830	0.635	3.20	2.03		>205	15.1	45.3			excellent
Acrylonitrite butadiene styrene	31.75	3.175	1040	0.084	8.35	0.79	93.3	23.0	60-130	0.19-0.33	13.79	900-2900	OK
Acetal	12.7	2.54	1415	0.115	3.86	0.44	104.4	23.0	85-100	0.23	17.24	2620	chalks slightly
Cellulose acetate butyrate (CAB)	12.7	2.54	1200	0.097	4.58	0.45	82.0	67.0	144	0.25	11.03	1380	needs UV inhibitor
Chlorinated polyvinyl chloride (CPVC)	12.7	2.54	1535	0.124	5.65	0.70	110.0	82.2-93.3	68-76	0.22	690	172-207	slight with UV additive
Polyvinyl chloride (PVC)	12.7	2.54	1440	0.117	3.25	0.38	79.4	23.0	50-100	0.13	27.59	380-655	varies
Polybutylene (PB)	12.7	2.54	918	0.074	7.93	0.59	107.2	82.2-93.3	128-150	0.14	6.90	2759	crazes rapidly without UV additive
High density polyethylene (HDPE)	12.7	2.54	953	0.077	1.87	0.14	121.1	23.0-60.0	110-130	0.23	5.52-8.62	1000-1550	unprotected crazes rapidly; requires carbon black
Polypropylene (PP)	12.7	2.54	905	0.073	2.21	0.16	93.3	90.0	70-100	0.15		900-1725 (310 @ 93^oC)	

because it has been accepted for use with potable water in most parts of this country, and plumbers are therefore becoming experienced with it. The behavior of PB fittings should be adequately researched to ensure acceptable performance and durability.

5.1.2 Tank and Liner Materials

Storage containment materials must be capable of maintaining their structural integrity (no cracks, disintegration, or sagging) during operating temperature and pressure without loss of the storage fluid (via leaks, corrosion, or absorption). For unpressurized systems, a number of attractive candidate materials are available (Table 5-3) including steel and wood. For drainback systems that use only water as the working fluid, compatibility of the tank material with the working fluid is not a major concern. In this case, a wood or steel tank with a plastic liner provides the most cost-effective option for storage containment. Of those plastic liner materials listed in Table 5-4, polyacrylonitrile should not be used for applications requiring storage temperatures above 65°C, although it has excellent water barrier properties.

5.1.3 Insulating Materials

Solar collection systems require insulating materials to reduce heat losses from pipes, storage tanks, and absorber plates. The ideal insulation would exhibit maximum thermal impedance (R-value) at minimum thickness and cost. Further, it should be capable of withstanding extreme temperatures, be impervious to UV radiation and moisture, and be capable of providing some structural support. Thermal stability should include the absence of out-gas products (from such additives as binder materials, flame retardants, or water proofing) which may be harmful to human health, the environment, or other components of the solar system (for example, the glazing).

Based on thermal resistance per area, the most cost-effective materials listed in Table 5-5 are fiberglass bats and macerated cellulose products. These materials are capable of withstanding temperatures in storage tanks but probably not absorber plate stagnation temperatures (400°F). More temperature-resistant materials such as glass fiberboard or binderless batts can be used as a buffer material between the less expensive insulating material and the high-temperature absorber plate.

The report entitled Survey and Evaluation of Available Thermal Insulation Materials for Use on Solar Heating and Cooling Systems (Versar Inc. and Rittlemann Associates 1980) gives a wealth of comparative information. In particular, the final section offers evaluation of and recommendations for insulation of collectors, piping, and storage. For collectors, a special high-temperature-resistant fiberglass batting and rock wool are strongly recommended. Foam glass is not recommended because it is too brittle. Cellulose exhibits problems with corrosion, settling and compaction, and water absorption and is not recommended as collector insulation. Polystyrene is eliminated from consideration on the basis of poor thermal stability. Polyurethane and polyisocyanurate foams are provisionally recommended because of their potential outgassing problems. Area-based foams are also controversial

Table 5-3. Storage Containment Materials

Material	Thickness (mm)	Density		Cost		T_{cont} (°C)	R-Value (1 in.)	Pressure Limitation	Liner Requirement	Chemical Compatibility
		kg/m^3	kg/m^2	$/kg	$/$m^2$					
Wood	6.35	650-800	4.13-5.08	0.25-0.50	1.25-1.75	90	1.3		yes	
Steel	1.0	8030	8.03	0.34	2.73		0.009	150 psi w/stone liner	yes	
Galvanized steel	0.66	8360	5.52	1.17	6.46				no	
Fiberglass reinforced polyester	12.7	1313	16.68	0.94	15.67	71-82	0.27	unpressurized systems	no	
Polyethylene	4.75-9.5 (4.75)	930	4.42	0.66	2.92	82	0.62	unpressurized systems	no	
Polypropylene	4.75	910	4.32	0.66	2.85	88	0.96	unpressurized systems	no	sensitive to polypropylene glycol

Table 5-4. Liner Materials

Material	Thickness (mm)	Density		Cost		T_{cont} (°C)	Water Permeability	Chemical Compatibility
		kg/m^3	kg/m^2	$/kg	$/$m^2$			
Polyvinyl chlcride (PVC)	0.762	1240	0.945	0.65	0.61			
Chlorosulfonated polyethylene		1305						softens in silicone oil
Polyacrylonitrile (PAN)	0.015-0.1 (0.026)	1150	0.03	6.62	0.20	65	excellent resistance	

Table 5-5. Insulating Materials

Material	Form	Thickness (mm)	Density		Cost		Thermal Properties							UV Resistance	Water Permeability	Flammability
			kg/m^3	kg/m^2	$/kg	$/$m^2$	T_{min} (°C)	T_{max} (°C)	T_{cont} (°C)	$T_{out-gas}$ (°C)	Thermal Conductivity (W/m K)	R-Value (1 in.)	Flexural Modulus (MPa)			
Phenol								135			0.033	4.3				
Phenol formaldehyde	spray or rigid	25.4	40.0	1.0	1.59 (for resin)	2.58	-129	232	177		0.029	5.0		no		low
Urea formaldehyde	foam	25.4	11.2-12.8	0.28-0.33			-184	132			0.33	4.2				
Polyurethane foam	rigid	25.4	8.0-48.0				-196	121	107	140	0.020-0.25	5.9-7.1		no	<2%	
Polyurethane foam and silicone rubber	spray		48.0					150	121		0.020	7.1		good		combustible
Extruded urethane board	rigid	25.4	24.0	0.6	4.94	3.01					0.023	6.2				
Extruded polystyrene (styrofoam)	rigid	25.4	28.8	0.7	2.94	2.15		85			0.036	4.0		yellows and embrittles	<2%	flame retardant added
Expanded polystyrene (bead board)		25.4	16.0	0.4	3.32	1.35		85	74		0.041	3.5		yellows and embrittles	<2%	flame retardant added
Isocyanurate form board	rigid	25.4	28.8-36.8	.73-.94	3.49-4.48	3.28		150	121		0.016	9.0				
Glass-reinforced polyisocyanurate w/Al foil faces	rigid	12.7-57.2 (50.8)	32.0	1.6	4.10	6.67			121		0.020	7.2		foil faces provide protection		flame spread 25
Halocarbon-blown isocyanate	foam						-198		121		0.019	6.8-7.7				self extinguishing
Polyvinylchloride	rigid	3.2-76.2	32-240 (32)				-196		93		0.019-0.022	6.6-7.4		not affected		flame spread 15
Cellular elastomer								104			0.036	4.0				combustible (some are self-extinguishing)
Cellular glass board	rigid	25.4	97	2.5	1.09	2.69					0.058	2.5				
Foam glass	rigid	38.1-101.6 (50.8)	136	6.9	0.95	6.56	-273	316		N/A	0.066-0.107	1.4-2.2		very good	impermeable	incombustible
Cellular concrete	rigid; low density	25.4	400	10.2	4.30	43.69					0.180	0.8	>6900	excellent	must be sealed	nonflammable
Glass fiberboard		25.4-50.8 (25.4)	48.0	1.2	2.94	3.58		343			0.32	4.5	0.12			

Table 5-5. Insulating Materials (Concluded)

Material	Form	Thickness (mm)	Density		Cost		Thermal Properties							UV Resistance	Water Permeability	Flammability
			kg/m^3	kg/m^2	$/kg	$/$m^2$	T_{min} (°C)	T_{max} (°C)	T_{cont} (°C)	$T_{out-gas}$ (°C)	Thermal Conductivity (W/m K)	R-Value (1 in.)	Flexural Modulus (MPa)			
Fiberglass batts	rolls	88.9-152.4 (88.9)	9.6-16.0 (9.6)	0.85	0.52	0.40		538		204	0.045	3.2				
Thermal insulating wool	rolls	25.4-101.6 (25.4)	20.0-38.4 (20.0)	0.5	0.85-1.91	0.43-0.97		538			0.043-0.087	1.7-3.3				
Mineral wool	rigid or granular	25.4-101.6 (25.4)	96.1-160.2 (96.1)	2.4	0.40-0.62	0.97-1.51		454-649			0.036-0.072	2-4				
Industrial felt		25.4-152.4 (25.4)	40.0-128.1 (40.0)	1.0	0.64-1.38	0.65-1.40		204-538			0.039-0.094	1.5-3.7				
Macerated paper or pulp products (cellulose)		25.4	40.0	1.0	0.53	0.54					0.039	3.7				flame retardant added
Wood	rigid	25.4	512.5	13.0	0.12	1.61			90		0.111	1.3	3000	fair if coated	water absorption harmful if untreated	flammable if untreated
Vermiculite	granular	25.4	80.1	2.0	0.49	1.0		538			0.066	2.2				
Perlite (expanded silica)		25.4	32-176 (32)	0.81				816			0.069	2.1				noncombustible
Calcium silicate	granular	25.4	208.2	5.3				650			0.055	2.6			water absorption not harmful	noncombustible
Sodium boro-silicate	formed glass; granular	25.4	21.5	0.6	37.45	20.45		538			0.36	4			disolves in water in 2-3 weeks	

[a]Numbers in parentheses are nominal values chosen as representative of the present application; they are used for cost data calculations.

because of contradictory data on their dimensional stability and resistance to high temperature and humidity. Perlite has good thermal stability and heat resistance characteristics, but its granular nature may cause spillage, settling, or dust production.

The choice of insulation materials for pipes and storage tanks is complicated by design and application (such as underground, above ground exterior, and above ground interior). Versar Inc. and Rittlemann Associates (1980) give primary and secondary considerations for selecting insulation in these cases.

5.2 DESIGN ALTERNATIVES

The most likely areas for cost reduction in a low-cost drainback hot water system are the piping and associated insulation and the tank. The cost of pumps and heat exchangers is difficult to reduce.

Using plastic instead of copper pipe can reduce initial piping costs by a factor of 2. Either CPVC or polybutylene pipe is appropriate based on the materials survey. Since polybutylene pipe is slightly less expensive and is becoming accepted in the plumbing industry, we used it for SERI's low-cost system.

The service temperature limitation of polybutylene pipe ($200^{o}F$) caused concern for the absorber plate-pipe connection. Two protective measures were considered--using a short piece of uninsulated copper pipe or a somewhat longer length of insulated copper pipe between the absorber and the plastic pipe. The analysis in Appendix C shows that the required lengths can be calculated as follows:

bare pipe:
$$L = \frac{kA_c}{\pi D h_e} \cosh^{-1} \frac{T_{hot} - T_a - \frac{\alpha I}{\pi h_e}}{T_\ell - T_a - \frac{\alpha I}{\pi_e h}}, \qquad (5\text{-}1)$$

insulated pipe:
$$L = \frac{kA_c}{\pi D U_e} \cosh^{-1} \frac{T_{hot} - T_a}{T_\ell - T_a}, \qquad (5\text{-}2)$$

where

k = thermal conductivity of copper ($W/m\ ^{o}C$)

A_c = cross-sectional area of metal surface, approximately πDt where t is wall thickness (m^2)

D = outside diameter of copper pipe (m)

h_e = combined linearized convection/radiation heat transfer coefficient ($W/m^2\ ^{o}C$)

T_{hot} = collector stagnation temperature (^{o}C)

T_a = ambient temperature (^{o}C)

T_ℓ = upper temperature limit of plastic pipe (^{o}C)

α = short wave absorptivity of outside surface (pipe or insulation)

U_e = effective heat transfer coefficient based on the difference between copper pipe temperature and ambient air temperature ($W/m^2\ ^{o}C$)

L = required length (m)

I = insolation (J/m^2).

When conservative worst-case assumptions are made, the lengths of copper pipe required are:

- For uninsulated 1.27-cm (1/2-in.) copper pipe, 0.33 m (~1 ft)
- For 1.27-cm copper pipe with 2.5 cm (1 in.) of 0.7 m^2 K/W (R-4 ft^2 h ^{o}F/Btu) insulation, 0.78 m (~2.5 ft).

Since the insulated pipe required is relatively short, it would be preferred over the bare pipe because of lower annual heat loss. A short insulated copper pipe will be included in SERI's low-cost system on the inlet and outlet sides of the collector to protect the plastic pipe.

Opportunities to lower storage tank costs are available only for a load-side heat exchanger system. An unpressurized tank can cost considerably less than a pressurized tank; the latter has little potential for cost reduction because it is already mass-produced. A number of options have been considered for low-cost tanks. Wood, sheet metal, and plastic are potentially inexpensive, as discussed earlier. While plastic has temperature limitations, sheet metal and wood can have high labor costs.

One readily available tank is the 0.21-m^3 (55-gal) oil drum. These drums are currently used to reduce temperature variations in attached sunspaces. A new drum typically costs about $30 and a used drum $7. Two drums can supply sufficient storage for a solar domestic hot water system when one is stacked on top of the other. This method also produces some thermal stratification, thereby improving performance.

The basic problem of load-side heat exchange remains--heat exchanger effectiveness is poor unless a very large coil is used. One alternative is to provide some standby hot water storage (~0.08 m^3 [~20 gal]) on the load side to minimize the need for instantaneous heating. One solution is a tank-in-tank design. Placing a pressurized tank inside the inexpensive oil drum will, of course, add to the system cost, but the tank volume needed is relatively small and thereby minimizes the additional expense.

The use of exhausted freon storage tanks would keep costs for the standby tank quite low. By law these tanks cannot be refilled, so they are typically discarded by air conditioning firms. Like oil drums, however, freon tanks require pipe connections; they would be somewhat more costly for the pressurized freon tank than for the unpressurized oil drum.

Several options exist for the water-filled freon tank. One tank could be placed in the top drum and a preheat coil in the bottom drum, or a freon tank could be placed in each drum, thereby doubling the standby hot water supply (e.g., two 15-gal freon tanks could supply 30 gal of standby hot water). If the concept of a freon tank within an oil drum proved viable, an enterprising manufacturer could sell them as a unit with all fittings attached.

SERI's low-cost system incorporates these concepts to determine their viability.

5.3 SYSTEM COSTS

Table 5-6 shows estimated costs for a typical contractor-installed drainback system that is currently available. The total cost for the installed system is $\$543/m^2$ ($\$50/ft^2$). Replacing the components listed with a low-cost, commercially available collector, polybutylene piping, and stacked oil drums for storage, is shown in Table 5-7. The total cost drops to $\$271/m^2$ ($\$25/ft^2$). By developing a still lower collector it should be possible to approach an installed system cost of $\$150/m^2$ ($\$13.90/ft^2$).

Of course actually building and installing a system for even $\$271/m^2$ ($\$25/ft^2$) is considerably more difficult than doing it on paper. An important assumption has been that overall system efficiency and reliability will be comparable to a conventional system; i.e., the energy cost will reduce by the same amount as installed system cost. Yet, the commercially available $\$5/ft^2$ collector assumed in the analysis has relatively poor performance. Even if such a system could be built, the ideal cost goal of $\$150/m^2$ ($\$13.90/ft^2$) still would not have been reached.

Reducing system costs from $\$271/m^2$ ($\$25/ft^2$) to under $\$150/m^2$ ($\$13.90/ft^2$) would require new engineering ideas or alternative areas for cost reductions. One needed alternative is to reduce the markup between the manufacturer and the consumer. Clearly this area should be explored as a means for reducing system costs.

5.4 REFERENCE

Versar, Inc., and Burt Hill Kosar Rittlemann Associates, Mar. 1980, Survey and Evaluation of Available Thermal Insulation Materials for Use on Solar Heating and Cooling Systems, DOE/CS/3563-TI, Butler, PA: Burt Hill Assoc.

Table 5-6. Cost Estimate for a Solar Domestic Hot Water System

Equipment	Cost	Labor (h)	Rate[a] ($/h)	Total Labor Cost
Collectors: 1.22 m × 2.44 m 2 @ $461.62	$923.24	2.7	18.70	$50.49
Racks: 2 @ 25.00	50.00			
Storage tank: 454 L (120 gal) unpressurized	300.00	2	18.70	37.40
Heat exchanger: 1.91 cm (3/4 in.) copper 30.48 m (100 ft)	67.00	1	18.70	18.70
Pump: 0.06 MPa (20 ft of water) head; 0.126 L/s (2 gpm)	123.45	1	18.70	18.70
Control and sensors	54.14	2	18.70	37.40
Ball valves: 2	15.00	1.5	18.70	28.05
Fittings:	20.00	4.8	18.70	89.76
Pipe: 1.91 cm (3/4 in.) Copper 30.48 m (100 ft)	67.00	7.00	18.70	130.90
Pipe insulation: 30.48 m (100 ft)	65.00	7.00	18.70	130.90
Totals	$1684.83			542.30
Total labor and materials				2227.13
Labor paid by the general contractor (@ 21%)				113.88
Sales tax on materials (@ 6%)				101.09
				2442.10
General contractor's overhead @ 15%				366.31
				2808.41
General contractor's profit @ 15%				421.26
Total System Cost				$3229.68[b]

[a]Data from Means Cost Data, 1983

[b]This represents an installed cost of $543.19/m^2 ($50.46/ft^2) of collector.

Table 5-7. Cost Estimate for a Domestic Hot Water System with Plastic Collectors and Piping

Equipment	Cost	Labor (h)	Rate[a] ($/h)	Total Labor Cost
Collectors: 1.22 m × 3.05 m 2 @ $202.00	$404.00	2.7	18.70	$50.49
Racks: 2	50.00			
Storage tank: 416 L (110 gal) Unpressurized	58.00	3.0	18.70	56.10
Tank Insulation	15.00	1.0	18.70	18.70
Heat exchanger: 1.91 cm (3/4 in.) Copper 30.48 m (100 ft)	67.00	1.0	18.70	18.70
Pump: 0.06 MPa (20 ft of water) head; 0.126 L/s (2 gpm)	123.45	1.0	18.70	18.70
Control and sensors	54.14	2.0	18.70	37.40
Ball valves: 2	15.00	0.75	18.70	14.03
Fittings	10.00	2.0	18.70	37.40
Pipe Insulation	65.00	7.0	18.70	130.90
Pipe (Polybutylene): 1.91 cm (3/4 in.) 30.48 m (100 ft)	31.00	5.0	18.70	93.50
Totals	892.59			475.92
Total labor and materials				1368.51
General contractor's labor contributions ($219.10 @ 21%)				99.94
Sales tax (@ 6%)				53.55
				1522.01
General contractors overhead @ 15%				228.30
				1750.21
General contractor's profit @ 15%				262.55
Total System Cost				$2012.85[b]

[a]Data from Means Cost Data 1983.

[b]This represents an installed cost of $270.83/m^2 ($25.16/ft^2) of collector.

5.5 BIBLIOGRAPHY

Clark, E. J., C. D. Kelly and W. E. Roberts, June 1982, Solar Energy Systems Standards for Screening Plastic Containment Materials, NBSIR 82-2533, Washington, DC: National Bureau of Standards.

Homann, Peter S., C. J. Hilleary, and K. R. Darnal, Jan. 1981, Solar Heating Materials Handbook, DOE/TIC-11474, Albuquerque, NM: AnaChem, Inc.

Ratzel, A. C., and R. B. Bannerat, 1978, "Commercially Available Materials for Use in Flat Plate Solar Collectors," Proceedings of the 1977 Flat Plate Solar Collector Conference, CONF-770253, pp. 387-394.

Granoff, Joan A., ed., 1981, Modern Plastics Encyclopedia, 1981-82, Vol. 58, No. 10A, New York: McGraw-Hill.

Solar Vision, Inc., 1979, Solar Products Specifications Guide, Harrisville, NH: Solar Age Magazine.

McCullagh, James C., ed., 1978, The Solar Greenhouse Book, Emmaus, PA: Rodale Press.

Baumeister, Theodore, ed., 1978, Mark's Standard Handbook for Mechanical Engineers, New York: McGraw-Hill.

SECTION 6.0

SURVEY OF COLLECTOR MATERIALS

In Section 2.2.1 a goal of $\$150/m^2$ ($\$13.90/ft^2$) for installed system cost was established. Roughly one-third of that amount can be attributed to collector costs. One way to reduce the cost of the collector components is to identify alternate materials that, through innovative design or application, are capable of providing nearly the same thermal and optical performance, but are much less expensive. Two major elements of the collector that were targeted as likely areas for cost reduction were the absorber and the glazing. In each of these instances, a survey of alternate materials was conducted. The absorber materials study is described in Section 6.1; the glazing materials are addressed in Section 6.2.

6.1 ABSORBER MATERIALS

6.1.1 Survey

To identify promising new absorber plate candidate materials, we studied a matrix of materials and properties. Categories of materials considered included metal sheets and foil; rigid, foamed, and thin-film polymers; rubbers; fabrics and textiles; forest products; and ceramics. Within each category we listed several specific materials and compiled relevant economic data and thermal, optical, and mechanical characteristics. Durability and remarks concerning ease of processing and performance are also included. Tables 6-1 through 6-9 present the assembled data.

For comparison purposes, 1.0-mm (0.040-in.) copper plate was considered to be the baseline absorber material. Estimates of appropriate thicknesses of other materials were made to allow cost per unit area and weight per unit area comparisons with copper ($\$22/m^2$ [$\$2.04/ft^2$] and 8.9 kg/m^2 [1.8 lb/ft^2], respectively). A second cost constraint is the target of $\$50/m^2$ ($\$4.65/ft^2$) (Section 2.2.1) for the collector. Almost all materials were less expensive than copper, but only a few of these yielded a substantial contribution to the $\$50/m^2$ cost goal.

The primary concern regarding thermal properties was the ability to withstand stagnation temperature (200°C or 400°F) as indicated by the continuous use temperature limit in the matrix. High thermal conductivity was also desirable, although none of the nonmetallic candidates compared favorably with copper. It is possible that this deficiency can be remedied by innovative design application (such as complete wetting of the absorber surface).

Mechanical properties are important because the absorber should support its own weight without sagging. In addition, structural integrity imparted to the collector box is desirable, as is high resistance to thermal shock.

Inherent optical properties provide an indication of the possibility of eliminating costs associated with painting or coating absorber plates. Thus, if a material is intrinsically black, the added expense of an optical coating may not be warranted.

UV stability and hygroscopic behavior were used to characterize lifetime and durability. Some candidate materials--for example, several polymers--are very sensitive to UV exposure and may require either a UV screen (glazing) or the addition of carbon black for protection. This would rule out, for example, the use of clear polyethylene as an absorber material with a black liquid and non-UV screen glazing. Several collector designs being considered require close contact between the working fluid and the absorber material. In these applications, moisture must not be absorbed by the absorber. Several materials could conceivably be treated to prevent absorption (for example, use of a sealant for a concrete design), but the benefit must be weighed against the added cost.

The primary concern in choosing metallic absorber materials (Tables 6-1 and 6-2) has been in maximizing thermal transfer properties (and corrosion resistance). With the exception of brass, tin, and nickel, all other metal sheet materials included are cheaper and lighter in weight than copper, but none have its high thermal conductivity. High cost may have been traded for thermal efficiency in the past, a decision that may warrant reexamination. Another important point is that reducing the thickness of a metallic absorber does not linearly affect cost. In the case of copper, decreasing the thickness by a factor of 8 only cuts the cost per area roughly in half because of increased processing and handling costs associated with foils as opposed to sheet metals. Although substantial weight savings for the absorber plate may be recognized, consideration must also be given to flow passage design. Use of thick metal pipes with a foil absorber may reduce the weight advantage.

For nonmetallic absorber candidate materials, the primary screening parameter chosen was the continuous use temperature limit. Although the maximum temperature attained during stagnation conditions depends on the selection of a particular design for the absorber material and collector, this dependency was not considered, and the ability to survive 204°C (400°F) was assumed to be required. On this basis, none of the foamed plastics (Table 6-3) were deemed viable candidates. Of the rigid polymers (Table 6-4), only a glass-reinforced vinyl ester met the temperature requirement, although it probably did not meet the cost goal. If the absorber is assumed to account for one-third of the collector cost ($\$50/m^2$ or $\$4.65/ft^2$) and a mark-up factor of 3.5 is used, then the cost of the raw material must be less than:

$$(1/3)\ (\$50/m^2)/3.5 = \$4.76/m^2 \text{ or } \$0.44/ft^2 \ .$$

Several thin-film polymer absorber materials (Table 6-5) can be used. Heat-stabilized nylon films may also be appropriate. Of these, Teflon and Tefzel can withstand UV exposure and thus can be used as a clear absorber material (with a black liquid or black rear panel absorber); the addition of darkening agents will slightly increase the cost of the material.

Two elastomeric thin films (Table 6-6) are strong candidates for absorber plates. These are silicone rubber and Viton, a fluorocarbon elastomer. Four mil thicknesses of both products are very stable at elevated temperatures and are relatively inexpensive. Silicone rubber, however, exhibits poor mechanical properties, and its use would probably be limited to unpressurized applications. Increasing the thickness of the absorber would be conceivable for silicone rubber but would be prohibitively expensive for the fluoroelastomers.

Table 6-1. Physical Properties of Metal Sheet

Candidate Material	Material Cost ($/kg)	Material Cost ($/m^2)/(kg/m^2)	Thickness (cm)	Density (kg/m^3)	Temperature Limits Min. (°C)	Temperature Limits Max. (°C)	Temperature Limits Cont. (°C)	Thermal Conductivity (W/m K)	Coef. of Thermal Expansion (m/m K)	Strength[a]	Water Permeability (J/msPa)	Lifetime (yr)	α_S	ε_T
Copper (Centaur Metals)	2.45	21.81/8.90	0.10	8900				377.0	16.6×10^{-6}	E=119, G=45 GPa			0.60 (Oxidized)	0.60 (Oxidized)
Aluminum (Reynolds Al)	1.89	5.12/2.71	0.10	2710				206.0	24.3×10^{-6}	E=71, G=26.2 GPa			0.11 (Oxidized)	0.11 (Oxidized)
Steel (Reynolds Al)	0.34	2.72/8.00	0.10	8000				45.0	17.8×10^{-6}	E=207, G=79.3 GPa			0.79 (Oxidized)	0.79 (Oxidized)
Stainless steel (18-8) (Reynolds Al)	1.89	14.65/7.75	0.10	7750				16.1	17.0×10^{-6}	E=190, G=73.1 GPa				
Galvanized steel	0.54	1.72/3.21	0.04	8032			149	65.3	11.6×10^{-6}	E=207 G=79.3 GPa				
Nickel (200)	18.30	164.24/8.98	0.10	8975				58.8	15.3×10^{-6}	E=221			0.37 (Oxidized)	0.37 (Oxidized)
Tin	17.53	96.28/5.49	0.08	6757				59.0		E=44				
Brass (Centaur Metals)	3.31	28.30/8.55	0.10	8550				104.0		E=106, G=40 GPa			0.60 (Oxidized)	0.60 (Oxidized)

[a]E = Modulus of elasticity; G = modulus of rigidity.

Table 6-2. Physical Properties of Metal Foil

Candidate Material	Material Cost ($/kg)	Material Cost ($/m^2)/kg/m^2	Thickness (cm)	Density (kg/m^3)	Temperature Limits Min. (°C)	Temperature Limits Max. (°C)	Temperature Limits Cont. (°C)	Thermal Conductivity (W/m K)	Coef. of Thermal Expansion (m/m K)	Strength[a]	Water Permeability (J/msPa)	Lifetime (yr)	α_S
Maxorb (Nickel) Foil[b]	--	21.53	0.0013	8900	<-7	>250		92.1	13×10^{-6}	200 MPa tensile			0.97
Solarstrip Foil (Cu)[c]	--	8.6-22.6	0.007-0.030	8900		340	230						0.95
Koor Foil (Al)													
Al Foil[3]			0.012	2710				225.3	2.4×10^{-5}	E=71 GPa, G=26 GPa			0.17
Cu Foil	8.95	9.56/1.07	0.012	8900						E=119 GPa, G=44.7 GPa			
Steel Foil (Ni or C)			0.012	8000						E=207, G=79.3 GPa			
Stainless Steel Foil (annealed 304)	5.34	5.33/1.00	0.013	7858				16.3	1.7×10^{-5}	E=190, G=73.1 GPa			

[a] E = Modulus of elasticity, G = modulus of rigidity.

[b] In quantity, $6.46/m^2; adhesive good to 220°C; data effective October 1979; 6-18 in. width.

[c] Ref. SPSG June 1981; lowest prices without substrate.

Table 6-3. Physical Properties of Foamed Plastics

Candidate Material	Material Cost ($/kg)	Material Cost ($/m^2)/kg/m^2	Thickness (cm)	Density (kg/m^3)	Temperature Limits Min. (°C)	Temperature Limits Max. (°C)	Temperature Limits Cont. (°C)	Thermal Conductivity (W/m K)	Coef. of Thermal Expansion (m/m K)	Strength MOR(MPa)	Water Permeability (J/msPa)[a]
Polyurethane[b]	7.04	5.01/0.71	2.54	28			121	0.03	4.9	413.8	(<0.1-5%)
Polyurethane[b]	1.63	13.75/8.43	2.54	332			149	0.07	4.9	8965.5	(0.2%)
Polystyrene beads	3.83	1.65/0.43	2.54	17		77	77	0.04	6.3	220.7	(2-4%)
Extruded polystyrene	3.83	2.72/0.71	2.54	28		77	77	0.04	6.3	482.8	(0-1%)
ABS structural foam (acrylonitrite-butadiene styrene)	2.21	29.69/13.44	2.54	529			82	0.08	17.5		0

[a]Percentage absorbed in 24 h by plate of 1/8-in. thickness is given in parentheses.

[b]Blown with CO_2.

Table 6-4. Physical Properties of Rigid Plastics

Candidate Material	Material Cost ($/kg)	Material Cost ($/m^2)/kg/m^2	Thickness (cm)	Density (kg/m^3)	Temperature Limits Min. (°C)	Temperature Limits Max. (°C)	Temperature Limits Cont. (°C)	Thermal Conductivity (W/m K)	Coef. of Thermal Expansion (m/m K)	Flexural Strength MOR(MPa)/MOE(MPa)	Water Permeability (J/msPa)[a]
Acrylic	3.13	11.83/3.78	0.3175	1190			77	0.21	7.0×10^{-5}	100.0/2069	(0.2-0.4%)
Polycarbonate	4.06	14.93/3.68	0.3175	1158			121	0.19	6.8×10^{-5}	93.1/2207	8.1×10^{-12} (0.15-0.18%)
Polyurethane	1.70	1.73/1.02	0.3175	320			93	0.21	16.2×10^{-5}	29.0/345	(0.2%)
Glass-reinforced polyester (fiberglass) (premixed chopped glass)[b]	0.94	5.78/6.15	0.3175	1937			163	0.54	2.9×10^{-5}	179.3/11034	(0.06-0.28)
Polystyrene	0.84	2.76/3.28	0.3175	1034			93	0.67	7.2×10^{-5}	69.0/1448	(0.05-0.4%)
Polyvinyl chloride (PVC) (exterior panel)	0.65	2.97/4.57	0.3175	1439			67	0.18	5.4×10^{-5}	89.7/3172	1.2×10^{-12} (0.04-0.4%)
Polypropylene, Black 30% mineral filled	0.66	2.32/3.51	0.3175	1107			129	0.13	2.9×10^{-5}	58.6/2759	3.1×10^{-13} (0.02-0.10%)
Polypropylene, Black 30% glass coupled	1.26	4.60/3.65	0.3175	1151			138	0.13	3.6×10^{-5}	55.2/5862	3.1×10^{-13} (0.01-0.05%)

Table 6-4. Physical Properties of Rigid Plastics (Concluded)

Candidate Material	Material Cost ($/kg)	Material Cost ($/m^2)/kg/m^2	Thickness (cm)	Density (kg/m^3)	Temperature Limits Min. (^{o}C)	Temperature Limits Max. (^{o}C)	Temperature Limits Cont. (^{o}C)	Thermal Conductivity (W/m K)	Coef. of Thermal Expansion (m/m K)	Flexural Strength MOR(MPa)/ MOE(MPa)	Water Permeability (J/msPa)[a]
Glass-reinforced phenolic	0.54	3.04/ 5.62	0.3175	1771			71		1.6×10^{-5}	172.4/ 17241	
Fabric filled phenolic	0.63	3.82/ 6.06	0.3175	1910			71		4.0×10^{-5}	103.4/	(0.12-0.36%)
Polysulfone[c]	8.82	34.72/ 3.94	0.3175	1240			150	0.12	5.4×10^{-5}	106.2/ 2690	(0.22%)
Cellulose acetate	0.92	3.56/ 3.87	0.3175	1218			82	0.25	14.0×10^{-5}	48.3/	9.6×10^{-12} (2-7%)
Asbestos-filled phenolic				1700			150	0.35	3.3×10^{-5}	44.8/	
Glass-reinforced vinyl ester	3.10 for resin	10.33/ 3.33	0.3175	1050			>200	1.73	3.1×10^{-5}	202/ 8750	
Polyacryonitrile											

[a]Percentage absorbed in 24 h by plate of 1/8-in. thickness is given in parentheses.

[b]UV sensitivity depends on pigmentation.

[c]Strength loss due to UV exposure.

Table 6-5. Physical Properties of Thin Film Plastics

Candidate Material	Material Cost ($/kg)	Material Cost ($/m²)/kg/m²	Thickness (cm)	Density (kg/m³)	Temperature Limits Min. (°C)	Temperature Limits Max. (°C)	Temperature Limits Cont. (°C)	Thermal Conductivity (W/m K)	Coef. of Thermal Expansion (m/m K)	Flexural Strength MOR(MPa)/MOE(MPa)	Water Permeability (J/msPa)[a]	Lifetime (yr)	α_S	ε_T
Polyvinyl fluoride (Tedlar)	13.01	1.80/0.14	0.01	1380	-72	107	107		5.0×10^{-5}		6.3×10^{-14} (<0.5%)			
Chlorinated ethylene-propylene (Teflon)	13.23	2.84/0.21	0.01	2145			204	0.25	16.8×10^{-5}	/ 690	(<0.01%)			
Polyvinylidene fluoride[b] (Kynar)	11.03	1.94/0.18	0.01	1760	-80	150	135	0.21	11.6×10^{-5}	/ 1393	(0.04%)			
Polyvinylidene chloride (Saran)				1715		127				110.3/	1.8×10^{-14}			
Polyester (Mylar)	2.34	0.32/0.14	0.01	1386	-70	150		0.15	1.7×10^{-5}		9.6×10^{-14}			
Polyethylene	0.66	0.06/0.09	0.01	940			113	0.42	1.5×10^{-5}	40.7/603	3.8×10^{-11} (<0.01%)			
Ethylene-chlorotrifluoroethylene (Halar 500)	18.74	2.52/0.13	0.01	1345					8.6×10^{-5}					
Ethylene-tetrafluoroethylene copolymer (Terzel 280)	19.85	3.37/0.17	0.01	1700			199		4.2×10^{-5}					
Kel-F	44.10	8.82/0.20	0.01	2000					3.5×10^{-5}		2.5×10^{-12}			
Sylgard 184 (silicone)	19.89	2.09/0.11	0.01	1050					4.5×10^{-5}					
Polyimide (kapton)[c]	99.23	7.04/0.07	0.005	1420	-269	400	252	0.16	2.0×10^{-5}		(1.3%)			
Nylon (type 6 film)[d]							204							
Polypropylene	3.31	0.26/0.08	0.009	895		121	100	0.12	9.0×10^{-5}	48.3/345	(<0.005)		Fair UV resistance	

[a]Percentage absorbed in 24 h by plate of 1/8-in. thickness is given in parentheses.

[b]No weight loss, 1 year at 300°F.

[c]Must paint; cost too high to add carbon black.

[d]Heat stabilized version of Nylon 6 (temperature up to 400°F for several hours).

Table 6-6. Physical Properties of Rubbers

Candidate Material	Material Cost ($/kg)	Material Cost ($/m²)/kg/m²	Thickness (cm)	Density (kg/m³)	Temperature Limits Min. (°C)	Temperature Limits Max. (°C)	Temperature Limits Cont. (°C)	Thermal Conductivity (W/m K)	Coef. of Thermal Expansion (m/m K)	Flexural Strength MOR(MPa)/MOE(MPa)	Water Permeability (J/msPa)
Neoprene	1.33	0.16/0.12	0.01	1230	-40	120	80-95				2.2×10^{-11}
Urethane rubber[a] (Adiprene)	3.33	0.35/0.11	0.01	1060	-60	100	85				
Hydrocarbon rubber (Nordel)	1.08	0.09/0.09	0.01	860	-50	170	145				
Polyester elastomer[b] (Hytrel)	3.26	0.41/0.13	0.01	1250		120	110			483-517	
Synthetic rubber[c] (Hypalon) (chlorosulfonated polyethylene elastomer)	1.61	0.19/0.12	0.01	1170	-20	150	120-135				
Ethylene/acrylic elastomer (Vemac)	2.46	0.27/0.11	0.01	1100	-45		165				
Fluoroelastomer (Viton)[d] (fluorocarbon elastomer)	19.98	3.70/0.19	0.01	1850	-20	260	204				
Butyl rubber	1.13	0.10/0.09	0.01	900							6.0×10^{-12}
Polyacrylic rubber	2.33	0.26/0.11	0.01	1100							9.2×10^{-12}
Vulcaprene[e]											9.4×10^{-12}

Table 6-6. Physical Properties of Rubbers (Concluded)

Candidate Material	Material Cost ($/kg)	Material Cost ($/m^2)/kg/m^2	Thickness (cm)	Density (kg/m^3)	Temperature Limits Min. (°C)	Temperature Limits Max. (°C)	Temperature Limits Cont. (°C)	Thermal Conductivity (W/m K)	Coef. of Thermal Expansion (m/m K)	Flexural Strength MOR(MPa)/MOE(MPa)	Water Permeability (J/msPa)
Natural rubber	0.93	0.09/0.09	0.01	930			85				1.5×10^{-10}
Silicone rubber[f]	5.99	0.90/0.15	0.01	1500	-57		315				2.0×10^{-10}
Polybutadine	1.37	0.13/0.10	0.01	970							1.2×10^{-10}
Polyvinyl butyral	3.31	0.35/0.11	0.01	1050							4.8×10^{-12}
Rigid foamed				72		150		0.03			

[a]Strongest available (mechanical strength) rubber; hardest and very good abrasion resistance.

[b]Good resistance to hot/moist environments.

[c]Excellent resistance to oxidation, UV, ozone, and other weathering.

[d]Costly.

[e]German product from Bayer; similar to neoprene.

[f]Poor mechanical properties; costly.

The textiles (Table 6-7) that have the most appropriate properties are Nomex "paper" and silicone-coated glass cloth. Nomex 410 paper is presently used in some air collectors. The cost estimate for silicone-coated glass cloth is slightly conservative and may eliminate serious consideration of this material. Although Nomex cloth exhibits excellent thermal stability, it is too expensive to be included as a candidate absorber material.

Forest products (Table 6-8) in general can be eliminated from present consideration by their poor resistance to sustained heat. The upper limit for typical continuous use is 90°C (194°F); beyond this threshold, charring, loss of mechanical integrity, and even spontaneous combustion can occur.

From the list of ceramics (Table 6-9), we chose glass-reinforced concrete (GRC) and soda lime silicate cellular glass (Foamglas) as good candidates. Although polymer concrete has several desirable properties compared to GRC (such as smooth flow passages, inherent water resistance, its dark color, and excellent mechanical properties without fiber reinforcement), it cannot withstand stagnation conditions without costly treatment. Problems may occur with the use of Foamglas during freeze-thaw conditions. The ability of GRC to withstand thermal shock should be considered.

Industry contacts made during this survey are given in Table 6-10.

6.1.2 Use of Low-Temperature Materials

Notable in the matrix of materials for absorber plates is the number of candidate materials whose only drawback is their useful temperature limit. We therefore want to consider how to avoid high collector stagnation temperatures and therefore increase the number of viable candidate materials.

There are basically two ways in which high stagnation temperatures can be avoided. One way is to limit absorption of solar energy by the absorber when the temperature is above a safe level for the material or when the collector is not operating. This approach led to the following ideas:

- Black fluid absorber with drainback
- Thermochromic absorber or glazing materials
- Thermochemical reactions in glazing or absorber
- Thermostatically controlled reflectors.

A second way to limit the absorber temperature is by providing some means to remove the heat collected during stagnation at a rate high enough to keep the absorber below its maximum temperature. The following methods accomplish this goal:

- Thermostatically controlled vents
- Heat sink/dissipator
- Phase-change material in collector.

These concepts are discussed in the remainder of this section.

Table 6-7. Physical Properties of Textiles

Candidate Material	Material Cost ($/kg)	Material Cost ($/m²)/kg/m²	Thickness (cm)	Density (kg/m³)	Temperature Limits Min. (°C)	Temperature Limits Max. (°C)	Temperature Limits Cont. (°C)	Thermal Conductivity (W/m K)	Coef. of Thermal Expansion (m/m K)	Flexural Strength MOR(MPa)/MOE(MPa)	Water Permeability (J/msPa)
Nylon (T-728)	3.31	2.64/0.80	0.07	1140			<90	0.250			
Dacron polyester (T-73)	3.31	3.20/0.97	0.07	1380			<120	0.160			
Kevlar weave (Kevlar 29)[a]	22.05-77.18	7.23-25.30/0.33	0.075	437 (for fabric) 1440 (for (raw material)	-46	204	135-150		-2×10^{-6}		
Polypropylene weave											
Nomex cloth (Style X-630)	26.46-45.20	6.28-10.73/0.24	0.069	346		600		0.035			
Nomex "paper" (Type 410)[b]	21.09	2.28/0.11	0.0125	866		220	204				
Canvas (linen, kemp, or cotton)[c]											
Silicone-coated glass cloth[d]	11.04	5.38/0.49	0.03	1625	-45	250					
Glass fiber weave	2.80	0.64/0.23	0.038	600		230				200/8275	

[a]UV sensitive, self abrasive.

[b]Resists UV when coated and used with glass glazing.

[c]Cotton degrades in UV; black dye would fade.

[d]Good UV stability.

Table 6-8. Physical Properties of Forest Products

Candidate Material	Material Cost ($/kg)	Material Cost ($/m^2)/ kg/m^2	Thickness (cm)	Density (kg/m^3)	Temperature Limits Min. (°C)	Temperature Limits Max. (°C)	Temperature Limits Cont. (°C)	Thermal Conductivity (W/m K)	Coef. of Thermal Expansion (m/m K)	Flexural Strength MOR(MPa)/ MOE(MPa)	Water Permeability (J/msPa)	Lifetime (yr)	α_S	ε_T
Plywood	0.46	1.78/ 3.87	0.635	609			90	0.12		82.8/ 6897			0.90	0.90
Wafer board	0.31	1.26/ 4.07	0.635	641			90			17.2/ 3103				
Particle board	0.25	1.36/ 5.45	0.635	858			90	0.14		34.5/ 3448				
Strand board														
Hard board	0.28	1.58/ 5.63	0.635	886			90	0.11		82.8/ 2586				
Paper board	0.55	2.71/ 4.92	0.635	775						113.8/ 552				
Cardboard														

Table 6-9. Physical Properties of Ceramics

Candidate Material	Material Cost ($/kg)	Material Cost ($/m²)/ kg/m²	Thickness (cm)	Density (kg/m³)	Temperature Limits Min. (°C)	Temperature Limits Max. (°C)	Temperature Limits Cont. (°C)	Thermal Conductivity (W/m K)	Coef. of Thermal Expansion (m/m K)	Flexural Strength MOR(MPa)/ MOE(MPa)	Water Permeability (J/msPa)	Lifetime (yr)	α_S	ε_T
Concrete	0.02	0.95/ 47.50	1.9050	2491			540	0.13	1.1×10^{-5}	4.1/				
Glass reinforced concrete (GRC)	0.15	6.70/ 44.67	1.9050	2343			>400		0.9×10^{-5}	16.2/ 13800				
GRC with lightweight aggregate	0.15	4.00/ 26.67	1.9050	1400			>400		0.9×10^{-5}					
Polymer concrete (Polysil)	0.11	4.57/ 41.55	1.9050	2180			93	1.67	2.4×10^{-5}	65.9/				
Borosilicate cellular glass (Foamsil-28)[a]	5.58	27.50/ 4.93	2.5400	194		425		0.07	0.3×10^{-5}	0.76/				
Soda lime silicate cellular glass (Foamglas)[a]	0.95	3.33/ 3.51	2.5400	138		425		0.07	0.8×10^{-5}	0.55/				
Soda lime glass	0.06	0.47/ 7.83	0.3175	2463					0.9×10^{-5}	89.7/			0.84	0.84
Fusion glass	0.73	5.64/ 7.73	0.3175	2435					0.9×10^{-5}	89.7/			0.84	0.84
Tempered glass	0.91	7.21/ 7.92	0.3175	2497		274	246		0.9×10^{-5}				0.84	0.84
Float glass[b]	0.45	3.57/ 7.93	0.3175	2497			38						0.84	0.84
Porcelain[c,d]	0.86-8.60	58.16-581.60/ 67.63	1.9050	3550			1000	1.05	0.4×10^{-5}	78.5 117.2	(up to 0.5%) H_2O absorption			

Table 6-9. Physical Properties of Ceramics (Concluded)

Candidate Material	Material Cost ($/kg)	Material Cost ($/m²)/ kg/m²	Thickness (cm)	Density (kg/m³)	Temperature Limits Min. (°C)	Temperature Limits Max. (°C)	Temperature Limits Cont. (°C)	Thermal Conductivity (W/m K)	Coef. of Thermal Expansion (m/m K)	Flexural Strength MOR(MPa)/ MOE(MPa)	Water Permeability (J/maPa)	Lifetime (yr)	α_S	ε_T
Polymer-cement concrete[e]	0.38	16.23/ 42.71	1.9050	2242			245		2.4×10^{-5}	8.6/				
Polymer-impregnated concrete														
Alumina ceramics[f] (Coors ADO-90)	34.45	108.05/ 3.14	0.0850	3690			1500	11.30	0.64×10^{-5}	365.0/	(0%)[g]			
Polymer concrete (Lone Star)	0.39	17.43/ 44.69	1.9050	2346			260							

[a]Cellular glasses degrade when exposed to temperature 0°C with free standing water present (organic coatings being developed at JPL).

[b]Thermal shock at 100°F.

[c]Requires firing.

[d]15%-20% shrinkage during firing; couple days in kiln; time and capital intensive (Coors Porcelain).

[e]Brookhaven product.

[f]Black; too expensive; only available in 4 in. × 4 in. tiles.

[g]Percentage absorbed in 24 h by plate of 1/8-in. thickness is given in parentheses.

Table 6-10. Industry Contacts Made During the Absorber Materials Survey

Textile and Fabric Product Information; DuPont; Wilmington, Del.; (800) 441-7515; Kevlar, Dacron, Nylon
Peter Palmer; DuPont; Wilmington, Del.; (302) 774-7668; Kapton polyimide
Dennis Nollen; DuPont; Wilmington, Del.; (302) 999-2901; Nomex
Lloyd Simmons; DuPont; Denver, Colo.; (303) 771-8196; elastomers
Centaur Metals Service, Inc.; Denver, Colo.; (303) 299-1190; copper, brass
Scott Williams; Sharon Steel Corp.; Sharon, Pa.; (216) 448-4011; galvanized steel
Jack Sibold; Coors Porcelain; Golden, Colo.; (303) 277-4195; porcelain, ceramics
Jack Fontana; Brookhaven National Laboratory; Long Island, N.Y.; (516) 282-2123 polymer concrete
M. Gunasekaren; Lone Star Polymer Concrete Co.; Greenwich, Conn.; (203) 661-3100, ext. 289; polymer concrete
Bill Jacobs, Louisiana Pacific; Chomburg, Ill.; (312) 397-8833; waferboard, particle board

Black fluid absorber with drainback. This system has several advantages, including high efficiency (bulk absorption instead of convection), reliable operation, and positive verification of operation (visual inspection reveals whether the fluid has drained from the collector). The absorber must be fully wetted, the fluid must be stable, the pigment must not separate or coat passages, and absorptance must be high. Low corrosion, high specific heat, and low viscosity are also desirable.

A collector design using a black fluid might have an open channel through which the fluid flows and a reflector surface on the back wall. The reflector would serve a dual purpose: during operation, it would reflect any sunlight that reached it back through the liquid, and when the collector was shut down, it would reflect solar energy back out of the collector. The first function would raise efficiency because the absorption would occur mostly in the fluid itself, rather than on the back wall. The second function would obviously reduce collector stagnation temperature. The fluid passages in a black fluid absorber must be filled with fluid to be effective, so a trickle-flow design would not work well. Since the passages would be filled, pressure would be higher at the bottom of the collector, and thin-film plastics, for instance,

would have to be supported to form passages. Figure 6-1 shows a possible arrangement. Passages formed in rigid plastics is another possibility.

Thermochromic absorber or glazing material. Thermochromic material would be characterized by a change in transmittance of the glazing or absorptance of an absorber surface with temperature. In the first case, the glazing would darken when it reached a critical temperature, reducing the amount of energy reaching the absorber. It is also possible, but relatively unlikely, that the glazing could be designed to become reflective. In the second case, if the absorptance of the absorber decreased above a critical temperature, less energy would be absorbed and the stagnation temperature would decline. In this case the absorber temperature itself determines the effect, and not the glazing temperature.

Thermochemical reactions in absorber or glazing materials. In this approach, a chemical reaction would occur in the absorber or glazing at a particular temperature, which would change their optical properties as in thermochromic materials. An example of this change is the use of indicators in titrations (e.g., bromthymol blue or phenolphthalein solution), which change from clear to a bright color with a very small change in pH. Appropriate chemicals would be chosen so that the equilibrium between two competing reactions would change at the correct temperature to protect the absorber material.

Thermostatically controlled reflectors. This straightforward solution uses a thermostat mechanism to move reflectors over the collector to scatter away the incoming light (see Figure 6-2). Its major drawback is the reliance on mechanical parts for operation.

All but the last of these ideas seem reasonable for low-cost collectors and worthy of consideration. Thermostatically controlled reflectors are probably too mechanically complicated to work reliably, and their cost would probably be high.

The following paragraphs present three ideas for reducing heat collected during stagnation in the collector (rather than limiting stagnation temperature).

Thermostatically controlled venting. In this idea, vents would open when the collector cavity became too hot, or when the collector was shut off. The mechanical aspects of this idea are similar to those of thermostatically controlled reflectors.

Heat sink/dissipator. In this idea, the collector is fitted with an integral heat rejector for stagnation protection. This type of device is commercially available on some collector models.

Phase-change material in collector. This idea involves placing a phase-change material (PCM) in contact with the absorber; this material would have a phase-change temperature below the absorber's maximum temperature. Sufficient material would be provided to keep the absorber below its maximum temperature all day and allow heat to be radiated away at night.

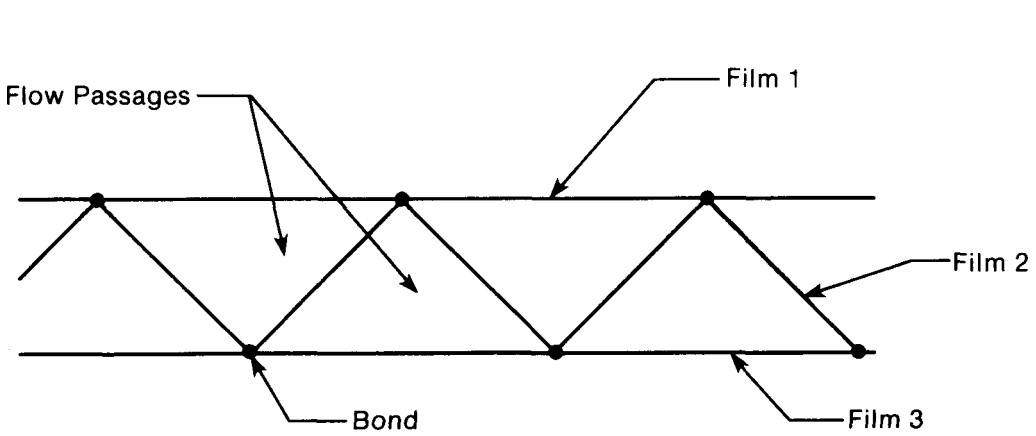

Figure 6-1. Possible Arrangement for Black Liquid Thin-Film Absorber

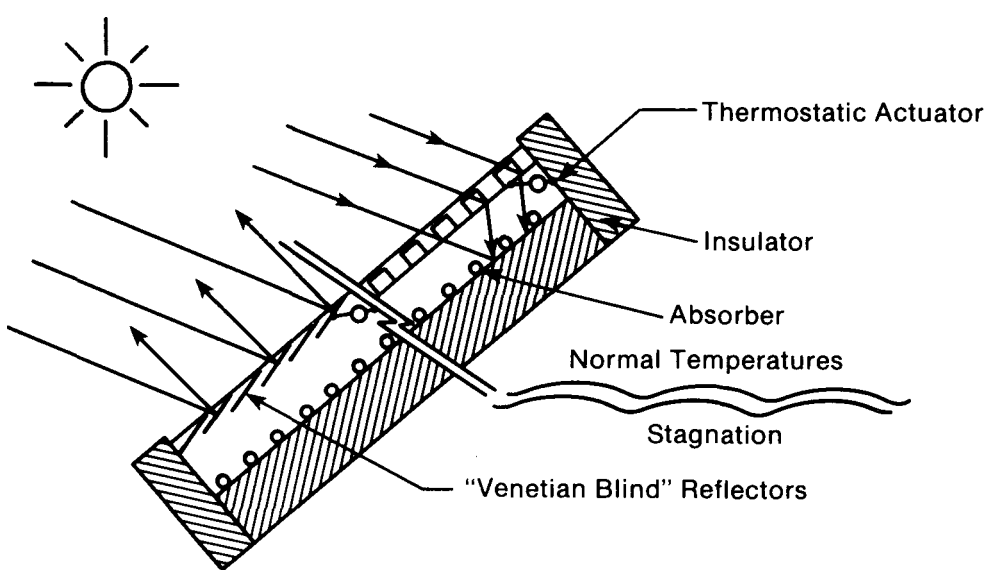

Figure 6-2. Thermostatically Controlled Reflectors to Limit Temperature

A collector might be constructed to use a PCM that is solid at low temperatures and liquid at high temperatures; natural convection would then dissipate heat through a heat rejector. This system might use a batch-type water heater in which the collector would store heat all day in the PCM, and the energy could be extracted at night. In a sense, this collector would have built-in storage. However, this system probably would not work well with low-temperature absorber materials, since the absorber temperature would remain near its maximum throughout the day. In addition, this system would have very poor performance with a morning load profile. Also, collector weight and leakage of the PCM require further consideration.

The major drawbacks to this scheme are (1) the design of a collector with sufficient PCM available to the absorber to allow heat transfer without exceeding the absorber's maximum temperature, and (2) the high cost of phase-change materials.

The complexity of these three ideas for dissipating heat from the collector, combined with their added cost, indicates that pursuing them would be of questionable value. A better solution is to control the excess energy while it is still in the form of light.

The possibilities of using low-temperature materials appear to be reasonably good if the stagnation problem can be overcome. Use of thermochromic materials and thermochemical reactions could lead to profitable materials research results. Using a black fluid absorber is considered to be the most practical method at the present and is discussed further in Section 7.3.3.

6.2 GLAZING MATERIALS

Based on a comparison of cost, performance, and durability data, several polymeric glazing materials have been identified for low-temperature, flat-plate glazing application. These include several fluorocarbon polymer films (Tedlar, Teflon, and possibly Kynar) and an acrylic (Acrylar). Films and scrims made from a silicon-based resin (Sylgard 184) also offer promise. Polymeric laminates offer hope of combining the best aspects of a number of individual polymers to obtain a composite product better adapted to solar application than any single candidate. For example, with the use of an effective UV screening film (Tedlar or Acrylar), a cheaper substrate film that is mechanically stable (polyethylene or polyester) might be employed. From the standpoint of cost and mechanical integrity, the UV stability of polyacrylonitrile should be further investigated. Thin glass (to reduce weight constraints) was also identified as a noteworthy candidate for a glazing material. Corning 7809 thin fusion glass, if produced in sufficient quantities, would be substantially cheaper than present commercial products.

In flat-plate solar collector systems for hot water or space heating applications, the collector units represent roughly one-third of the total installed system cost. A substantial fraction of this amount is due to the cost of the glazing material. To provide direction in reducing collector costs, a survey of glazing materials was performed. Emphasis was placed first on low cost and second on durability and performance of the cover plate materials. All prices listed in the following tables are for large volume orders to obtain comparable baseline costs.

Availability, cost, and weight information for candidate glazing materials is presented in Table 6-11. Relevant optical and thermal properties of each glazing are given in Table 6-12. Table 6-13 lists mechanical properties and weathering characteristics.

Glazings for flat-plate solar collectors can be divided into two general categories: glass or plastic. The ideal glazing transmits all radiation in the visible (solar) spectrum, reflects all infrared (thermal) radiation reemitted by the absorber plate, and has zero thermal conductivity to prevent conductive losses. Further, such a cover plate material should be capable of withstanding continuous service temperatures of 100°C (212°F) and tolerate stagnation temperatures up to 204°C (400°F). Mechanically, it should be highly resistant to the impacts of hail or thrown objects, dynamic loads from wind or snow, and abrasion by airborne particles or cleaning. In addition, all of these desirable qualities should be retained throughout the lifetime of the collector system, making it impervious to degradation by ultraviolet radiation, hydrolysis, or attack by atmospheric pollutants or biological agents. Finally, the ideal glazing material should be inexpensive, lightweight, and easy to handle and install.

As a class, plastics are cost-competitive with glass; they also have relatively lower densities and higher impact strengths and consequently are more shatter resistant and easier to work with than glass. Thin-film polymers can be considerably less expensive and exhibit higher solar transmittance than glass. At the same time, they tend to transmit a greater amount of reradiated thermal energy unless they are sufficiently thick to absorb the emitted infrared radiation. Other disadvantages include a susceptibility to abrasion and scratching (which can scatter incident light or act as degradation centers) and generally poor weathering characteristics.

A direct correlation is evident between durability and cost of polymer glazing materials. Inexpensive candidates such as polyethylene, methylpentene, and nylon 6 are especially prone to ultraviolet degradation. The same is true of some polyesters (such as Petro A and Mylar which are not recommended for solar use); the prices of polyesters increase dramatically with the degree of UV stability. The same is generally true of polycarbonates, which tend to yellow and lose solar transmittance properties if they are not protected from UV exposure.

The problem of poor abrasion resistance can be overcome by the addition of a protective coating, but this tends to greatly increase the price of the glazing. (Compare, for example, the coated Margard versus the uncoated Lexan SG, or Lucite-SAR versus Lucite regular, or Tuffak versus Tuffak CM-2.) CR-39, an allyl ester, is inherently more abrasion-resistant than acrylic or polycarbonate, and this fact is reflected in the price of the product.

One class of polymers that exhibits good inherent UV stability is the polymethylmethacrylate-(PMMA)-based acrylics. Although they are moderately priced, their temperature limitations restrict their use to collector temperatures in the low-to-medium range. Additionally, acrylics are among the most abrasion-susceptible polymers, and they have poorer impact properties than polycarbonates or polyesters. In film form, acrylics similar to Korad A have

Table 6-11. Cost and Availability of Glazing Materials

Material	Product	Manufacturer	Form[a]	Available Dimensions			Density		Cost	
				Thickness (mm)	Length (m)	Width (m)	(kg/m^3)	(kg/m^2)	($/kg)	($/m^2$)
1. Acrylic	Acrylar (X-2417)	3-M	F,S	0.059, 0.076 (0.076)[b]	2.44	1.22	1180	0.0897	21.63	1.94
2. Acrylic	Acrylite SDP (X-O-Lite)	Cy/RO	2S	16	2.4-4.8	1.2	1190			28.18
3. Acrylic	Korad A	Georgia Pacific	F	0.05-0.15 (0.127)	Roll	2.7	1140	0.145		
4. Acrylic	Lucite L	DuPont	S	3.175			1190	3.78	2.56	9.69
5. Acrylic	Lucite-SAR (Super Abrasion Resistant)	DuPont	S	1.5-51 (3.175)			1190	3.78	8.14	30.78
6. Acrylic	Plexiglas G	Rohm & Haas	S	6.35	0.91-3.66	0.61-3.05	1190	7.56	2.78	20.99
7. Acrylic	Plexiglas K	Rohm & Haas	S	3.175	2.44	1.52	1190	3.78	2.79	10.55
8. Acrylic	Plexiglas 55	Rohm & Haas	S	6.35			1190	7.56	11.91	90.00
9. Allyl ester	CR-39	PPG Industries	S	1.6	1.26	0.95	1320	2.11	16.70	35.20
10. Cellulose acetate butyrate	UVEX	Eastman-Kodak	S	1.5-6.35 (3.175)	1.93	1.30	1200	3.81	3.95	15.05
11. E-CTFE fluorocarbon	Halar 500	Allied Chemical	F	0.025-0.25 (0.127)	Roll	1.2	1680	0.213	52.75	11.24

Table 6-11. Cost and Availability of Glazing Materials (Continued)

Material	Product	Manufacturer	Form	Available Dimensions			Density		Cost	
				Thickness (mm)	Length (m)	Width (m)	(kg/m^3)	(kg/m^2)	($/kg)	($/$m^2$)
25. Polycarbonate	Tuffak Twinwall	Rohm & Haas	2S	5.6	2.44	1.22		1.22	13.23	16.15
26. Polyester	Flexigard (7410 & 7415)	3-M	L	0.18, 0.28 (0.18)	Roll	1.25	1214	0.2185	38.44	8.40
27. Polyester	Llumar	Martin Processing	F	0.127	Roll	1.52	1390	0.177	29.29	5.17
28. Polyester	Melinex 072	ICI Americas, Inc.	F	0.05-0.18 (0.1)	Roll	2.03	1400	0.14	13.23	1.85
29. Polyester	Petra A	Allied Chemical	F	0.1-0.635 (0.1)	Roll	1.09	1335	0.1335	3.02	0.40
30. Polyester	Sun Gain	3-M	F	0.1	Roll	1.32				6.67
31. FRP	Filon Solar-E (856 S)	Filon Corp.	L	0.762, 0.940 (0.940)	2.4-3.7	1.22	1623	1.53	10.69	16.36
32. FRP	Sun-Lite Premium II	Kalwall Corp.	S	0.635-1.524 (1.0)	460	1.5	1324	1.324	7.13	9.45
33. Polyethylene			F	0.1			940	0.094	2.34	0.22
34. Polysulfone	Udel P-1700	Union Carbide	F	0.0025-0.762 (0.127)	Roll	1.32	1240	0.158	16.54	2.61
35. Silicone	Sylgard 184	Dow-Corning	F	0.127			1050	0.133	28.91	3.84
36. Vinyl	Esifilm WC-16	Environmental Structures, Inc.	L	0.406	Roll	1.37	1214	0.493	16.36	8.07

Table 6-11. Cost and Availability of Glazing Materials (Continued)

Material	Product	Manufacturer	Form	Available Dimensions			Density		Cost	
				Thickness (mm)	Length (m)	Width (m)	(kg/m^3)	(kg/m^2)	($/kg)	($/$m^2$)
12. ETFE fluorocarbon	Tefzel 500LZ	DuPont	F	0.0127-1.524 (0.127)	Roll	1.5	1700	0.216	58.80	12.70
13. FEP fluorocarbon	Teflon 100A	DuPont	F	0.0127-0.508 (0.0254)	Roll	1.47	2150	0.0546	51.30	2.80
14. CTFE fluorocarbon	Aclar 22A	Allied Chemical	F	0.127			2080	0.264	41.01	10.83
15. CTFE fluorocarbon	KEL-F81	3-M	F						44.10	
16. PVF fluorocarbon	Tedlar 400SE	DuPont	F	0.1	Roll	2.54	1380	0.138	33.08	4.57
17. PVDF fluorocarbon	Kynar	Pennwalt	F	0.1			1760	0.176	16.54	2.91
18. Methylpentene	TPX	Westlake Plastics Company	F	0.076-0.5 (0.1)			830	0.083	8.82	0.73
19. Nylon 6		Allied Chemical	F,S	0.1			1130	0.113	5.51	0.62
20. Polyacrylonitrile (PAN)	Barex 210	Vistron	F	0.015-0.1 (0.026)	Roll	0.885	1150	0.03	6.62	0.20
21. Polycarbonate	Lexam SG	G.E.	S	2-12.7 (3.175)	2.44	1.22	1200	3.81	5.48	20.88
22. Polycarbonate	Margard	G.E.	L	3.175-12.7 (3.175)	2.44	1.22	1200	3.81	11.39	43.38
23. Polycarbonate	Tuffak	Rohm & Haas	S	0.8-12.7 (3.175)	2.44	1.22	1200	3.81	4.15	15.82
24. Polycarbonate	Tuffak CM-2	Rohm & Haas	L	3.175			1200	3.81	9.83	37.46

Table 6-11. Cost and Availability of Glazing Materials (Concluded)

Material	Product	Manufacturer	Form	Available Dimensions			Density		Cost	
				Thickness (mm)	Length (m)	Width (m)	(kg/m^3)	(kg/m^2)	($/kg)	($/$m^2$)
37. Annealed soda lime glass	Float Glass		S	3.175			2500	7.938	0.41	3.23
38. Tempered soda lime glass	Float Glass	LOF	S	3.175	1.83	1.22	2500	7.94	0.95	7.53
39. Tempered soda lime glass	Clearlite	AFG Industries, Inc.	S	3.175, 4.76 (3.175)	2.44	0.86	2460	7.811	0.85	6.67
40. Tempered low-iron glass	Solatex	AFG Industries, Inc.	S	3.175, 3.97, 4.76 (3.175)	2.44	0.86	2460	7.811	0.76	5.92
41. Tempered low-iron glass	Sunadex	AFG Industries, Inc.	S	3.175, 4.76 (3.175)	2.44	0.86	2460	7.811	1.03	8.07
42. Annealed low-iron glass	Solakleer	General Glass International Corp.	S	1, 2.3, 3.2, 4, 4.76 (3.175)	2.13	1.52	2480	7.874	0.52	4.09
43. Tempered borosilicate glass	7740 Pyrex	Corning Glass Works	S	3.175			2230	7.08	15.20	107.64
44. AR-coated tempered borosilicate glass	7744	Corning Glass Works	S				2230			
45. Fusion glass	7809	Corning Glass Works	S	0.5-6.35 (1.5)	3.05	1.45	2440	3.660	1.72	6.29

[a]Defined in Glazing Survey Glossary

[b]Numbers in parentheses are nominal values chosen for this survey

Table 6-12. Optical and Thermal Properties of Glazing Materials

Material	Product	Optical Properties					Thermal Properties				
		Index of Refraction (Sodium D)	τ_S (%)	τ_{IR} (%)	Haze (%)	Gloss [%/Angle of Incidence(°)]	$T_{Min.}$ (°C)	$T_{Max.}$ (°C)	$T_{Cont.}$ (°C)	Thermal Conductivity (W/m K)	Coef. of Thermal Exp. (10^{-5} m/m K)
1. Acrylic	Acrylar		92		0.5	62/20					
2. Acrylic	Acrylite SDP		83						71		7.20
3. Acrylic	Korad A					35/60			80	0.21	
4. Acrylic	Lucite L	1.49	92	46	1				80	0.21	7.0
5. Acrylic	Lucite-SAR	1.43	93	46	0.5				93	0.20	7.0
6. Acrylic	Plexiglas G	1.49	92	46	1.0				82	0.19	8.28
7. Acrylic	Plexiglas K	1.49	92	46	1.0				82	0.19	7.56
8. Acrylic	Plexiglas 55	1.50	92	46	1.0				82	0.17	8.46
9. Allyl ester	CR-39	1.50	90		1-2			150	100	0.20	8.1
10. Cellulose acetate butyrate	UVEX	1.47	87-91					82	67	0.25	14.40
11. E-CTFE fluorocarbon	Halar 500	1.447	81		3-5	85-95/20	Cryogenic	165			8.6
12. ETFE fluorocarbon	Tefzel 500LZ	1.40	92				<-100		150		4.2
13. FEP fluorocarbon	Teflon 100A	1.34	94.6	24			-255	275	200	0.19	8.3
14. CTFE fluorocarbon	Aclar 22A		92							0.22	
15. CTFE fluorocarbon	KEL-F81	1.435									
16. PVF fluorocarbon	Tedlar 400SE	1.46	90	48			-72	177	107		5.0

Table 6-12. Optical and Thermal Properties of Glazing Materials (Continued)

Material	Product	Optical Properties					Thermal Properties				
		Index of Refraction (Sodium D)	τ_S (%)	τ_{IR} (%)	Haze (%)	Gloss [%/Angle of Incidence (°)]	$T_{Min.}$ (°C)	$T_{Max.}$ (°C)	$T_{Cont.}$ (°C)	Thermal Conductivity (W/m K)	Coef. of Thermal Exp. (10^{-5} m/m K)
17. PVDF fluorocarbon	Kynar	1.413	93				-80	150	135	0.19-0.25	13.5
18. Methylpentene		1.46	90					200	100		
19. Nylon 6					2.5-5.0	>70/20			93	0.23	10.5
20. Polyacrylonitrile (PAN)	Barex 210		92.5		5	60/30-45			65	0.26	6.65
21. Polycarbonate	Lexan SG	1.586	84.4	21			Cryogenic	127	71-82	0.19	6.75
22. Polycarbonate	Margard	1.586	84.4	21			Cryogenic	127	71-82	0.19	6.75
23. Polycarbonate	Tuffak	1.586	85-91		0.5-2.0				121-132	0.19	6.84
24. Polycarbonate	Tuffak CM-2										
25. Polycarbonate	Tuffak Twinwall		77	21					132		5.94
26. Polyester	Flexigard (7410 & 7415)		87	46	0.5-1.3		-51	133	121		3.40
27. Polyester	Llumar		88	41			-59	204	177	0.15	
28. Polyester	Melinex 072		88		<0.5					0.15	1.6-1.9
29. Polyester	Petra A				<1	98/45			66	0.15	
30. Polyester	Sun Gain	1.64	93-96					150		0.04	1.7
31. FRP	Filon Solar-E	1.56	82.7	83.4		85/60		93	79	0.187	2.55

Table 6-12. Optical and Thermal Properties of Glazing Materials (Concluded)

Material	Product	Optical Properties					Thermal Properties				
		Index of Refraction (Sodium D)	τ_S (%)	τ_{IR} (%)	Haze (%)	Gloss [%/Angle of Incidence (°)]	$T_{Min.}$ (°C)	$T_{Max.}$ (°C)	$T_{Cont.}$ (°C)	Thermal Conductivity (W/m K)	Coef. of Thermal Exp. (10^{-5} m/m K)
32. FRP	Sun-Lite	1.58	84-88	31				150	93	0.103	2.45
33. Polyethylene		1.5	88.8	82					104	0.23	54.0
34. Polysulfone	Udel P-1700	1.633	80		5			175	140	0.26	5.6
35. Silicone	Sylgard 184	1.43	75				-65	250		0.146	30.0
36. Vinyl	Esifilm WC-16	1.5	83.2						50-65	0.16	6.4
37. Tempered soda lime glass	Float Glass		82.6						110		0.864
38. Tempered soda lime glass	Float Glass		82.5						204	1.48	0.9
39. Tempered soda lime glass	Clearlite	1.52	83.0						204		0.87
40. Tempered low-iron glass	Solatex	1.52	90.1						204		0.87
41. Tempered low-iron glass	Sunadex	1.52	91.6						204		0.87
42. Annealed low-iron glass	Solakleer	1.52	90.1					492			0.866
43. Tempered borosilicate glass	7740 Pyrex	1.474	91					260-288	232-260	1.09	0.325
44. AR-coated tempered borosilicate glass	7744	Graded Index 1.0 1.474	98								
45. Fusion glass	7809	1.509	91.5								

Table 6-13. Mechanical and Weathering Properties of Glazing Materials

Material	Product	Mechanical Properties				Weatherability			Remarks
		Poisson's Ratio	Flexural Modulus (GPa)	Flexural Strength (MPa)	Impact Resistance (J/m)	Ultraviolet Resistance	Water Absorption (%)	Abrasion Resistance	
1. Acrylic	Acrylar					Very good			Possible use as a UV screen
2. Acrylic	Acrylite SDP								
3. Acrylic	Korad A					Good	1.4-1.6 (Evidence that water is very harmful)		
4. Acrylic	Lucite L		2.94	102.7	16.0	Excellent	0.3		
5. Acrylic	Lucite-SAR		2.94	102.7	16.0	Excellent	0.3	Super abrasion resistant	
6. Acrylic	Plexiglas G	0.35	3.10	110.3	21.3	Excellent	0.2		
7. Acrylic	Plexiglas K	0.35	3.10	110.3	21.3	Excellent	0.2		
8. Acrylic	Plexiglas 55	0.35	3.10	110.3	21.3	Excellent	0.2		Designed for aircraft windows; very expensive; significantly superior in crazing characteristics
9. Allyl ester	CR-39		1.72	41.4	10.7	Unknown	0.7 (Dimensional warpage due to water)	Very good	Normally used for eyeglass lens

Table 6-13. Mechanical and Weathering Properties of Glazing Materials (Continued)

Material	Product	Mechanical Properties				Weatherability			Remarks
		Poisson's Ratio	Flexural Modulus (GPa)	Flexural Strength (MPa)	Impact Resistance (J/m)	Ultraviolet Resistance	Water Absorption (%)	Abrasion Resistance	
10. Cellulose acetate butyrate	UVEX		1.38		224.2	Absorbs UV	1.6		
11. E-CTFE fluorocarbon	Halar 500					Good	<0.02 (Good resistance)		Not for use as inner glazing due to temperature limitations
12. ETFE fluorocarbon	Tefzel 500LZ		1.397		No break		<0.03 (Good resistance)		
13. FEP fluorocarbon	Teflon 100A	0.46	0.655		No break	Good	<0.01 (Good resistance)		Inner glazing application
14. CTFE fluorocarbon	Aclar 22A								
15. CTFE fluorocarbon	Kel-F81	0.33							
16. PVF fluorocarbon	Tedlar 400SE	0.40				Good	<0.5 (Good resistance)		Single outer glazing use; embrittles at high temperatures; provides UV screen
17. PVDF fluorocarbon	Kynar	0.34	1.655	13.8	202.8	Excellent	0.04		Film still in developmental stage
18. Methylpentene	TPX					Poor; yellows and embrittles			

Table 6-13. Mechanical and Weathering Properties of Glazing Materials (Continued)

Material	Product	Mechanical Properties				Weatherability			Remarks
		Poisson's Ratio	Flexural Modulus (GPa)	Flexural Strength (MPa)	Impact Resistance (J/m)	Ultraviolet Resistance	Water Absorption (%)	Abrasion Resistance	
19. Nylon 6			0.965	34.5	43.8	Fair	9.5 (Fair resistance)		Heat stabilized (180°C) version available $7.50/kg
20. Polyacrylonitrile	Barex 210		3.3-3.4	97.0	80.0	More data needed; slight yellowing and decreased impact resistance	Excellent resistance		
21. Polycarbonate	Lexan SG	0.37	2.34	93.1			0.15		
22. Polycarbonate	Margard	0.37	2.34	93.1			0.15	Silicone hardcoated surface	
23. Polycarbonate	Tuffak	0.38-0.39	2.34	93.1	854.2	Yellows	0.35		
24. Polycarbonate	Tuffak CM-2	0.38-0.39						Durable, clear, abrasive resistant coating applied to Tuffak	
25. Polycarbonate	Tuffak Twinwall	0.38-0.39							
26. Polyester	Flexigard	0.38-0.40							Polyester/acrylic laminate; should not be use as inner glazing; provides UV screen

Table 6-13. Mechanical and Weathering Properties of Glazing Materials (Continued)

Material	Product	Mechanical Properties				Weatherability			Remarks
		Poisson's Ratio	Flexural Modulus (GPa)	Flexural Strength (MPa)	Impact Resistance (J/m)	Ultraviolet Resistance	Water Absorption (%)	Abrasion Resistance	
27. Polyester	Llumar	0.38-0.40				UV stabilized			10-15 yr life expectancy
28. Polyester	Melinex 072	0.38-0.40					0.6		
29. Polyester	Petra A	0.38-0.40							Not recommended for solar use
30. Polyester	Sun Gain	0.38-0.40				UV protected			AlO_2 anti-reflective coatings on both sides of film
31. FRP	Filon Solar-E		4.14	109.7			0.48		Medium temperature collector glazing application
32. FRP	Sun-Lite		6.90	118.3	261.1		0.60		
33. Polyethylene		0.46				Poor			Total degradation within 2 yr
34. Polysulfone	Udel P-1700	0.40	2.69	106.2	64.1	Poor	0.3 (Good resistance)		
35. Silicone	Sylgard 184					Good	0.1		
36. Vinyl	Esifilm WC-16			117-124	42.7-78.4	2.5×10^{-5} m (1 mil) Tedlar protective over-coat	0.5-3.0		

Table 6-13. Mechanical and Weathering Properties of Glazing Materials (Concluded)

Material	Product	Mechanical Properties				Weatherability			Remarks
		Poisson's Ratio	Flexural Modulus (GPa)	Flexural Strength (MPa)	Impact Resistance (J/m)	Ultraviolet Resistance	Water Absorption (%)	Abrasion Resistance	
37. Annealed soda lime glass	Float Glass				Poor	Excellent	Excellent	Excellent	Problems with thermal shock
38. Tempered soda lime glass	Float Glass				Poor	Excellent	Excellent	Excellent	
39. Tempered soda lime glass	Clearlite					Excellent	Excellent	Excellent	0.12% Iron content
40. Tempered low-iron glass	Sulatex					Excellent	Excellent	Excellent	0.04% Iron content
41. Tempered low-iron glass	Sunadex					Excellent	Excellent	Excellent	0.01% Iron content
42. Annealed low-iron glass	Solarkleer					Excellent	Excellent	Excellent	0.05% Iron content; tempered version available at $\$7.00/m^2$
43. Tempered borosilicate glass	7740 Pyrex	0.20				Excellent	Excellent	Excellent	
44. AR-coated tempered borosilicate glass	7744					Excellent	Excellent	Excellent	In developmental stage (PV and tube application)
45. Fusion glass	7809	0.20				Excellent	Excellent	Excellent	Experimental; projected cost figures

been found to degrade due to UV absorption by the 30% butyl acetate present in the material. A fairly new product, Acrylar (a 100% PMMA film), has shown some encouraging initial results and merits further testing and consideration both as a stand-alone film and as a UV-protective layer in a laminate glazing. One example of such a laminate is 3M Company's Flexigard, in which an acrylic protective overcoat is combined with a polyester substrate, providing enhanced mechanical properties.

Some fluorocarbon polymers are both UV- and temperature-stable, and most are correspondingly expensive. Two moderately priced candidates are Teflon (recommended as an inner glazing because of its extremely high temperature stability and relatively poor mechanical properties) and Tedlar (recommended as an outer glazing because of enhanced mechanical properties and an inability to withstand inner glazing temperatures). Tedlar has also been used as a UV screen in a laminate application (i.e., Filon Solar-E and Esifilm). Kynar, another often-mentioned fluorocarbon polymer candidate, is still in the developmental stage. Projected costs range from moderate for unoriented (low strength) films to high for biaxially oriented films.

A moderately priced silicone film should be considered as a glazing candidate because of its light weight and excellent weather/thermal resistance. Polyacrylonitrile (PAN), a processing and packaging product, is very inexpensive and is an excellent vapor barrier. Its UV stability should be determined by further research.

Glass is a proven cover plate material that provides extended service lifetime, adequate solar transmittance, and high opacity to thermal radiation. Major disadvantages of glass include its fragility and relatively high weight. The cheapest, most common glass is annealed soda lime window glass. One problem with this material is its poor thermal shock response; sudden changes in weather have exposed warm glazings to cool rain, resulting in cracking and fractures. Tempered float glass provides improved thermal shock characteristics and enhances impact resistance but is quite costly.

Solar transmittance properties of glass can be enhanced in several ways. One way is to lower the iron content of the glass. Comparison of the three AFG industry-tempered glass products shows that reducing the iron content from 0.12% to 0.01% improves solar transmittance from 83% to 91.6% at a 21% cost increase. Another way to improve optical performance is the addition of an antireflection coating, although this process is generally prohibitive in cost. Corning Glass Works is presently applying a graded index AR coating (porous silica) to the surface of their low thermal expansion, high-temperature resistant borosilicate glass. Although Corning reports significant improvement in solar transmittance and good weatherability, projected costs are exhorbitant for both the coating process and the base glass.

Thin fusion glass is a more acceptable candidate. Reduction in thickness is accompanied by an obvious reduction in weight. Also, at very high volume production, the projected cost of the material per area could drop to $\$3.70/m^2$ ($\$0.34/ft^2$). Handling very thin glass, however, is still a formidable problem.

Whether thin glass or the more promising polymer coatings are used, they will likely have an important secondary effect on collector costs. Currently, the high weight of glass is a major factor in limiting maximum panel size. Lighter glazings will allow for larger panels with resultant reductions in area-based cost.

Industry contacts made during this survey are listed in Table 6-14.

Table 6-14. Industry Contacts Made During the Glazing Materials Survey

Ron Byron; Kalwall Corp., Manchester, NH; (603)627-3861, and Gladys Kramer; Powers Products Company, Englewood, CO; (303)761-7074; Sun-Lite.

N. Judge King, Bob Lowenberg, and Bud Benson; 3-M Company, St. Paul, MN; (612)733-1287; Flexigard.

Chuck Stuart; G.E., Pittsfield, MA; (413)494-1110, and Penny Voss; G.E., Denver, CO; (303) 320-3026; Lexan and Margard.

Bob Ross; Environmental Structures, Inc., Cleveland, OH; (216)524-9270; Esifilm.

Ed Cessera and Jim Woodridge; Filon Corp., Howthorne, CA; (213)757-5141; Filon Solar-E.

Frank Maccarato and Mike Woldanski; Chemplast, Wayne, NJ; (201)696-4700; Halar, Dumar.

Harry Tenny; Allied Chemical, Morristown, NJ; (201)455-6221; Aclar, Petra A, Nylon 6.

Roger Brekken; 3-M Company, St. Paul, MN; (612)733-1969; Acrylar, Kynar.

Jack Cusp; Rohm and Haas, Philadelphia, PA; (215)592-3000, and Dick Layman; Rohm and Haas, Denver, CO; (303)355-8755; Tuffak and Plexiglass.

Charlie Allen; ICI Americas, Inc., Wilmington, DE; (302)575-4447; Melinex 072.

Millie Carter; Eastman Chemical, Kingsport, TN; (615)246-2111; UVEX.

George Ruth and Gary Krogseng; 3-M Company, St. Paul, MN; (612)778-6214 and 4006; Sun-Gain.

Richard Schwarz; PPG Industries, Inc., Barberton, OH; (216)753-4561, and Charlie Halcome; Welcast Company, Barberton, OH; (216)753-7201; CR-39.

Bob DeBussy and Don Wilson; DuPont, Wilmington, DE; (302)772-5880 and 999-2554; Tedlar.

Bob Mellen; DuPont, Wilmington, DE; (302)773-3703; Lucite.

Table 6-14. Industry Contacts Made During the Glazing Materials Survey (Concluded)

Ralph Williams; DuPont, Wilmington, DE; (302)999-3456; Teflon, Tefzel.

Don Needy and Bev Larson; Plasticrafts, Inc., Denver, CO; (303)433-8801.

Cadillac Plastic and Chemical Company, Commerce City, CO; (303)287-2506.

Regal Plastic Supply Company, Englewood, CO; (303)794-9823.

George Cerden; Dow Corning Corp., Midland, MI; (800)248-2345; Sylgard 184.

Tom Milliot; General Glass International Corp., New Rochelle, NY; (914)235-5900; Solakleer.

Dick Orton and Steve Eptx; AFG Industries, Inc., Kingsport, TN; (615)245-0211; Sunadex, Solatex, Clearlite.

Jerry Jensen; Thermo Systems, Inc., Denver, CO; (303)623-6939; Solatex.

Bernie Baum; Springborn Labs, Enfield, CT; (203)244-2000.

Art Schumarker and Andy Flood; Corning Glass Works, Corning, NY; (607)974-7630 and (607)974-4218; Corning 7744 and 7740 glass.

Jack Williams; Pennwalt Corp., Philadelphia, PA; (215)587-7520; Kynar.

Chuck Anendt (and Darrell Annis); Van Leer Plastics BV, Houston, TX; (713)462-6111; Kynar.

Charlie Miller; Westlake Plastics Company, Lenni, PA; (215)459-1000; Kynar, TPX, Polysulfone.

Steve Waisala and Bill Reagan; Vistron Corp., Cleveland, OH; (216)581-5600; Barex 210 PAN.

6.3 GLOSSARY OF TERMS USED IN SECTION 6.2

Lucite-SAR	= Lucite-super abrasion resistant
Plexiglas II UVA	= Plexiglas II ultraviolet absorbing
E-CTFE Fluorocarbon	= ethylene-chlorotrifluoroethylene copolymer
ETFE Fluorocarbon	= ethylene-tetrafluoroethylene copolymer
FEP Fluorocarbon	= fluorinated ethylene propylene copolymer
CTFE Fluorocarbon	= polychlorotrifluoroethylene copolymer
PVF Fluorocarbon	= polyvinyl fluoride
PVDF Fluorocarbon	= polyvinylidene fluoride
FRP	= fiberglass reinforced polyester
PAN	= polyacrylonitrile

Form designations in Table 6-11:

S = Sheet
F = Film
L = Laminate
2S = Double walled channeled sheet

6.4 GLAZING MATERIALS BIBLIOGRAPHY

Agranoff, Joan, ed., Oct. 1980, Modern Plastics Encyclopedia, Vol. 57, No. 10A, New York: McGraw-Hill.

Agranoff, Joan, ed., Oct. 1981, Modern Plastics Encyclopedia, Vol. 58, No. 10A, New York: McGraw-Hill.

Coyle, R. T., and R. Livingston, Dec. 1981, Evaluation and Market Testing of Corning Code 7809 Thin Solar Glass, SERI/TR-733-1230, Golden, CO: Solar Energy Research Institute.

Egan, G. J., Jan. 1980, "Component Spotlight-Glazing," Solar Heating and Cooling, Vol. 5, No. 1, p. 16.

Eldin, F. E., and D. C. Willhauer, Aug. 1961, "Plastic Films for Solar Energy Applications," Proceedings of the United Nations Conference on New Sources of Energy, Vol. 4, Rome, pp. 519-535.

Films, Sheets, and Laminates; Desk-Top Data Bank, 1979, The International Plastics Selector, Inc., San Diego, CA.

Gilligan, J. G., et al., Apr. 1980, Handbook of Materials for Solar Energy Utilization (Low Temperature Applications), DOE/CH/90034-T1, Chicago: IIT Research Institute.

McGinniss, V. D., et al., July 1980, Compendium of Information on Identification and Testing of Materials for Plastic Solar Thermal Collectors, DOE/CS/30171-1, Columbus, OH: Battelle Columbus Laboratories.

Proceedings of the Solar Glazing 1979 Topical Conference, June 1979, Pomona, NJ: Stockton State College.

Ratzel, A. C., and R. B. Bannerot, 1978, "Commercially Available Materials for Use in Flat-Plate Solar Collectors," Proceedings of 1977 Flat-Plate Solar Collector Conference, CONF-770253, pp. 387-394.

Schissel, P., 1978, "Polymers for Solar Technologies," Golden, CO: Solar Energy Research Institute.

6.5 ABSORBER MATERIALS BIBLIOGRAPHY

Cuddihy, E. F., Apr. 1978, Encapsulation Material Trends Relative to 1986 Cost Goals, JPL-5101-61, Pasadena, CA: Jet Propulsion Laboratory.

Cuddihy, E. F., Jan. 1980, Encapsulation Materials Status to December 1979, JPL-5101-144, Pasadena, CA: Jet Propulsion Laboratory.

Giovan, M., and M. Adams, June 1979, Evaluation of Cellular Glasses for Solar Mirror Panel Applications, DOE/JPL-1060-24, Pasadena, CA: Jet Propulsion Laboratory.

Gunasekaren, M., and R. B. Grekila, May 1977, Development of Polymer-Bonded Silica (Polysil) for Electrical Applications, EPRI EL-488, Pittsburgh, PA: Westinghouse Research and Development Center.

Modern Plastics Encyclopedia, Oct. 1974, Vol. 51, No. 10A.

Ratzel, A. C., and R. B. Bannerot, 1978, "Commercially Available Materials for Use in Flat-Plate Collectors," Proceedings of 1977 Flat-Plate Solar Collector Conference, CONF-770253, pp. 387-394.

Slemmons, A. J., and D. W. Ploeger, Jan. 1981, Conceptual Design of a Glass-Reinforced Concrete Solar Collector, Sandia Contract 49-8468, Menlo Park, CA: SRI International.

Taylor, J. R., June 1980, Low Cost Photovoltaic Concentrator Array: A Novel Design Utilizing Glass-Reinforced Concrete, SAND79-7053, San Ramon, CA: MBAssociates.

VanWert, B., and C. G. Currin, June 1979, "Silicone-Glass Cloth for Solar Glazing," Proceedings of the Solar Glazing 1979 Topical Conference," Pomona, NJ: Stockton State College.

SECTION 7.0

SERI LOW-COST COLLECTOR CONCEPTS

7.1 INTRODUCTION

One approach to lowering overall system costs is to integrate the collector and storage into one unit. This is the approach used in "breadbox" hot water heaters. Because of their simplicity, these devices can be very low in cost; they are now used extensively in Israel and Japan. As mentioned in Section 4.0, they are generally not applicable to very cold climates; also they tend to be suitable only for domestic hot water (DHW) and not space heating.

A similar approach involves the glazing of a blackened hot water tank located on a white concrete pad outside the building. One such system manufactured by Sunwizard Corporation is the subject of the analysis in Appendix B. This system is inexpensive and performs quite well. However, it is limited to DHW, performs best in warmer climates, and is not as widely applicable as roof-mounted systems.

Although these approaches have merit, SERI researchers chose to focus their efforts in FY 1982 on the more widely applicable and better performing concept of separate collectors and storage. As discussed earlier, we also eliminated air collector systems and studied only liquid systems because of their applicability to DHW-only applications. This still leaves room for a myriad of collector concepts such as fin-and-tube, metal plate, open-trough trickle flow, thin-film plastic, thin steel foil, rigid plastic, integral passage slab, and Roll-Bond metal.

Each concept has advantages and disadvantages. For example thin-film (or foil) collectors can be very inexpensive by virtue of the low amount of material used. However, if they are fragile they must be used in an unpressurized system and must rely on a trickle flow. Improper system installation, flow blockage, or trapped vapor could result in collector failure. An open trough (e.g., Thomason concept) eliminates these problems but suffers from the problems associated with fluid evaporation and, being open to the atmosphere, is still susceptible to corrosion.

The Roll-Bond absorbers can be manufactured inexpensively with the proper equipment. The copper typically used in such absorber plates is expensive, however. Aluminum and steel are much less expensive, but these metals may have corrosion problems.

Plastics that can withstand high stagnation temperatures and ultraviolet radiation are expensive and might be limited to thin-film approaches. Lower-cost polymers could be used in rigid absorbers but might cause temperature and UV problems.

The ideal absorber material would be inexpensive, easy to form, strong (in terms of pressure and handling), stable at temperatures of 205°C (400°F), stable under long-term exposure to ultraviolet radiation, nonporous,

lightweight, and completely noncorrosive. Since no material meets all of these criteria, we can only review our materials survey, select promising candidates, and design systems around their weaknesses. This is done with several potential materials and is discussed in the rest of this section. Two concepts developed outside of SERI--a thin-film plastic collector by Brookhaven National Laboratory and a rigid plastic collector by Sealed Air Corporation--are discussed in Section 8.0.

The absorber study discussed earlier identified a number of attractive, low-cost materials for use in a prototype flat-plate collector. Although it was not possible in this effort to explore all of the options, we identified several for more detailed examination. Glass reinforced concrete (GRC) is a very low-cost absorber material; one GRC collector design is discussed in Section 7.2. This concept received most of our attention in FY 1982.

Two readily available metals are considerably less expensive than copper, namely aluminum and steel. In the past these metals were associated with collector failures in the field. For example, Roll-Bond aluminum panels failed when subjected to untreated water or even chlorinated swimming pool water. SERI believes that these considerably less expensive metals can be used in properly controlled closed-loop applications. We constructed a simple collector with off-the-shelf galvanized sheet metal. Since this metal is already mass-produced, it is very low in cost (less than $\$2.15/m^2$ or $\$0.20/ft^2$ wholesale). Construction of this collector is discussed further in Section 7.3.1.

Another low-cost material considered is glass cloth. The problem with using it for a liquid absorber is that it requires a resin capable of withstanding stagnation temperatures. A brief description of a fiberglass collector employing such a resin is presented in Section 7.3.2.

Many low-cost materials covered in the absorber materials matrix were eliminated because of their inability to withstand stagnation temperatures (especially the plastics). Section 7.3.3 discusses using such a material--polypropylene--and protecting it from stagnation by using a black fluid. Finally, Section 7.3.4 describes the innovative idea of using black glass pellets in place of a black fluid.

7.2 GLASS-REINFORCED CONCRETE COLLECTOR

Based on ready availability of materials, ease of fabrication, and low capital cost, glass-reinforced concrete (GRC) was selected as the first collector material to be used and evaluated at SERI. Table 7-1 lists companies that have considered concrete collector concepts. To date most research has been on concrete air collectors. A number of designs were considered, including an open-channel absorber (Figure 7-1) and an absorber with cast-in-place fluid passages (Figure 7-2). Thermal and mechanical analyses were performed on the various designs to optimize performance and structural integrity.

Table 7-1. Industry Contacts Who Have Considered Concrete Collector Concepts

John Popovich, Sunwizard; Harbor City, CA; (213) 539-8590; GRC collectors
Solar Oriented Environmental Systems, Inc.; Miami, FL; (305) 233-7011; solar paving and roofing tile
Louis Dow, Plastic Assembly Corp.; Chagrin Falls, OH; (216) 247-4058; polymer concrete absorber plate
Art Slemmons, SRI International; Menlo Park, CA; (415) 326-6200; GRC panel
F. Peter Lee; Oakland, CA; (415) 482-3068; GRC collectors
Peter Payne, Payne Incorporated; Annapolis, MD; (202) 261-2325

7.2.1 Analysis

The integral flow passage design is different from the typical metal plate with pipes attached to the back because the fluid passages are imbedded in a thick plate made of the absorber material (Figure 7-2). Our research studied how the fin efficiency of the absorber varies with the spacing (w) of the fluid passages.

Consider a fully wetted absorber plate (Figure 7-3) as a best case for comparison. Duffie and Beckman (1980) show that typical values for loss coefficients U_L range from 2 to 8 W/m^2 K (0.4 to 1.4 Btu/h ft^{2o}F), and fluid heat transfer coefficients h_f typically range from 100 to 1000 W/m^2 K (17.6 to

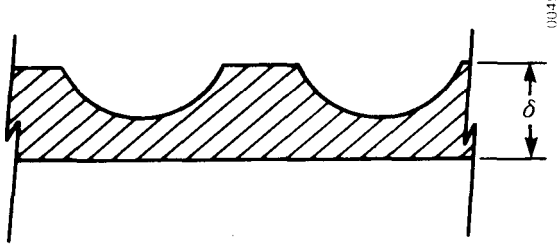

Figure 7-1. Open-Channel Absorber

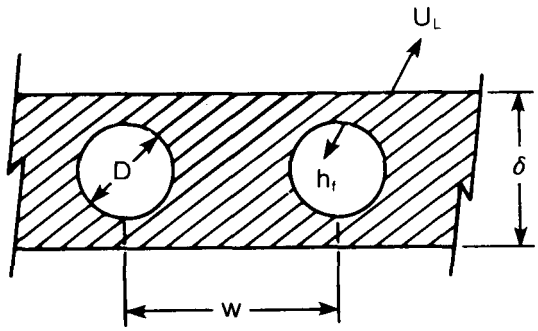

Figure 7-2. GRC Collector Plate

176.0 Btu/h ft^2 ^{o}F). The collector efficiency factor F' is the ratio of the heat transfer coefficient from the fluid U_o to ambient U_L (Duffie and Beckman 1980), so

$$F' = \frac{U_o}{U_L} = \frac{\left(\frac{1}{h_f} + \frac{1}{U_L} + \frac{\delta}{k}\right)^{-1}}{U_L},$$

where

δ = thickness of the absorber plate
k = thermal conductivity of the absorber (~1.5 W/m K [0.9 Btu ft/h ft^2 ^{o}F] for GRC).

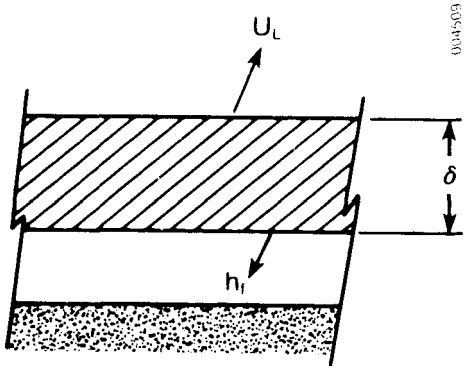

Figure 7-3. Fully Wetted Absorber

It can be shown that for thicknesses of up to 2 cm (0.8 in.), the collector efficiency factor is above 0.85 even for U_L = 8 W/m^2 K (1.4 Btu/h ft^2 ^{o}F), a relatively inefficient collector.

Next, consider fluid passages cast into the absorber plate as shown in Figure 7-2. This arrangement can be treated as a fin and tube because the effect of the back insulation is to reduce the transverse temperature gradients across the thickness of the absorber. For example, a collector with a back loss coefficient of 1 W/m^2 K (0.2 Btu/hr ft^2 ^{o}F) has 6 cm (2.4 in.) of fiberglass insulation below the absorber. A 2-cm (0.8-in.) thick absorber at 100^{o}C (212^{o}F), with an ambient temperature of 20^{o}C (68^{o}F), would only require a 1.1^{o}C (0.6^{o}F) temperature difference across it to conduct the heat through it to the ambient temperature. Thus, the fin can be considered nearly isothermal (along a direction normal to the plate) and the fin efficiency and the collector efficiency factor can be determined. The fin efficiency is:

$$F = \frac{\tan h_f\left[\left(\frac{U_L}{K\delta}\right)^{1/2}\left(\frac{w - D}{2}\right)\right]}{\left(\frac{U_L}{K\delta}\right)^{1/2}\frac{w - D}{2}},$$

where D is the diameter of the fluid passages and w is the channel spacing (Figure 7-2). Assuming that the bond conductance between the tubes and the fins is equal to the GRC thermal conductivity, the collector efficiency factor is

$$F' = \frac{1}{U_L w\left(\frac{1}{U_L[D + (w - D)F]} + \frac{1}{K} + \frac{1}{\pi D h_f}\right)}.$$

For fluid passages of 0.01 m (0.4 in.) in diameter, the fin efficiency is plotted in Figure 7-4 versus w, and the collector efficiency factor is plotted in Figure 7-5. Figure 7-4 shows that fin efficiencies can be high for reasonable tube spacings because of the thickness of the fins. Even for a high heat loss collector, tube spacings of over 7 cm (2.8 in.) are possible with fin efficiencies above 90%. Figure 7-5 shows that both U_L and h_f greatly affect the collector efficiency factor. For a high heat loss collector, very small tube spacing is needed to get reasonable efficiencies (above 0.8). Table 7-2 summarizes the calculated values.

Now consider the mechanical behavior of a 1 m × 2 m (3.3 ft × 6.6 ft) GRC panel with cast-in-place fluid passages. For a 2-cm (0.8-in.) thick panel and 0.3 cm (0.1 in.) minimum wall thickness, we chose a fluid passage spacing of 1.7 cm (0.7 in.) (Figure 7-6). Allowing for mounting of the absorber along the edges results in roughly 50 fluid passages. For this configuration, the mass of the panel can be calculated.

From Table 6-9, the density of GRC is with lightweight aggregate roughly $\rho \approx 1400$ kg/m^3 (87 lb/ft^3). Thus the mass of a base absorber is

$$m = 1400 \text{ kg/m}^3 \left[(0.2 \text{ m})(1 \text{ m})(2 \text{ m}) - 50\pi(0.007 \text{ m})^2\ 2 \text{ m})\right]$$

$$= 34.5 \text{ kg (76 lb)} .$$

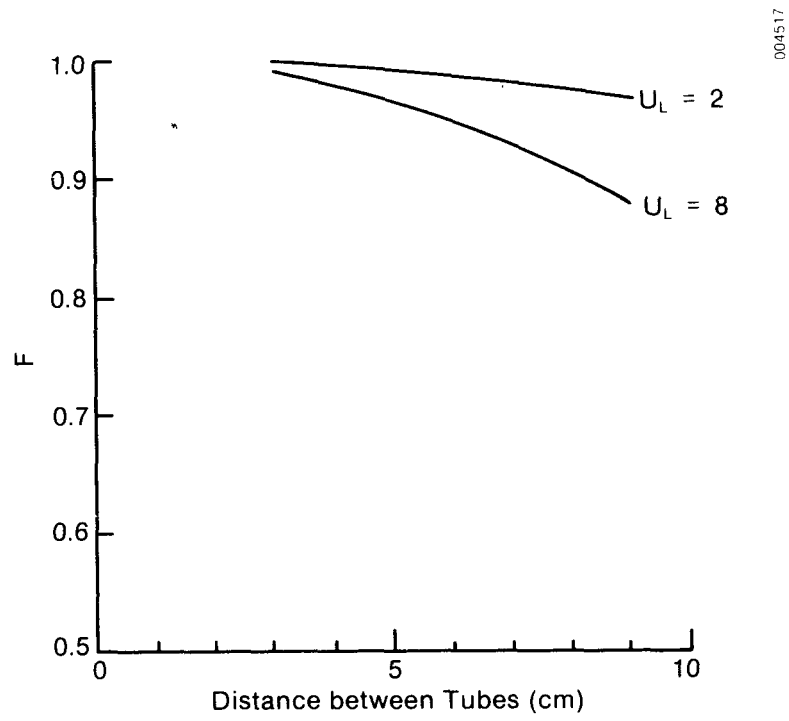

Figure 7-4. Fin Efficiency for Cast-in-Place Passages

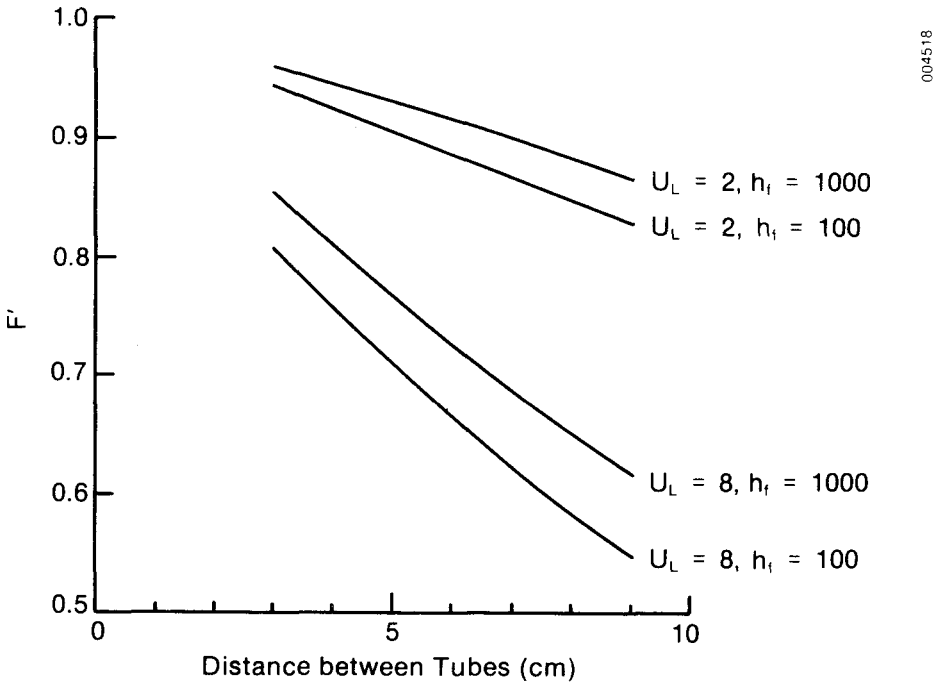

Figure 7-5. Collector Efficiency Factor of Cast-in-Place Passages

Table 7-2. Calculated Values for Cast-in-Place Fluid Passages

UL	HF	W	F	F'
2	100	0.0300	0.99778	0.94288
2	100	0.0500	0.99120	0.90450
2	100	0.0700	0.98047	0.86586
2	100	0.0900	0.96590	0.82743
2	1000	0.0300	0.99778	0.95841
2	1000	0.0500	0.99120	0.92856
2	1000	0.0700	0.98047	0.89701
2	1000	0.0900	0.96590	0.86431
8	100	0.0300	0.99120	0.80496
8	100	0.0500	0.96590	0.70322
8	100	0.0700	0.92700	0.61792
8	100	0.0900	0.87848	0.54636
8	1000	0.0300	0.99120	0.85212
8	1000	0.0500	0.96590	0.76485
8	1000	0.0700	0.92700	0.68592
8	1000	0.0900	0.87848	0.61576

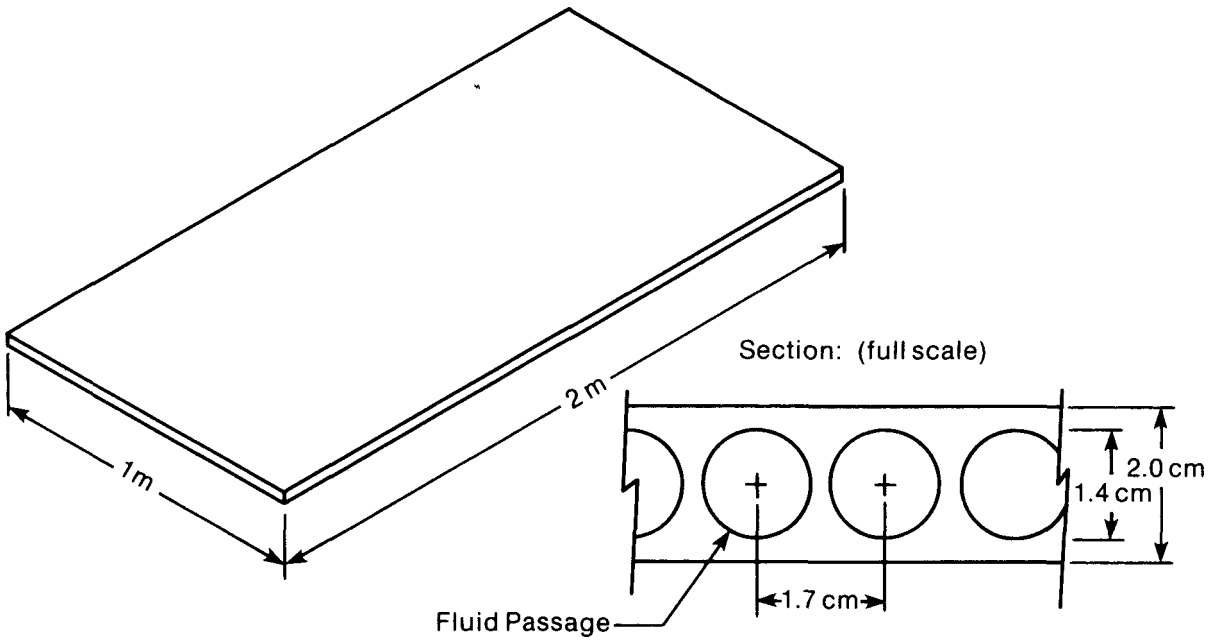

Figure 7-6. GRC Absorber Place

With a 1-cm-thick GRC rim around the absorber, 15 cm in height, the mass of the rim is

$$m = (0.01\ m)(0.15\ m)(2 + 2 + 1 + 1\ m)(1400\ kg/m^3)$$

$$= 12.6\ kg\ (27.8\ lb)\ .$$

Thus the total mass would be 47.1 kg (104 lb).

The force is

$$\frac{mg}{A} = \frac{(47.1\ kg)\ (9.8\ m/s^2)}{2\ m^2} = 231\ Pa\ (5\ psf)\ .$$

Next, consider the mechanical stress experienced by the fluid passages. For the worst case of zero pressure inside the tubes and atmospheric pressure (10^5 Pa) outside the tubes, we can calculate stress. A model of the tubes as circular cylinders with an inner diameter of 1.4 cm (0.6 in.) and an outer diameter of 2.0 cm (0.8 in.) is shown in Figure 7-7. The stress on the outer surface of a cylinder of inner radius a and outer radius b (Shigley 1977) is

$$\sigma_t = -\Delta P \left(\frac{b^2 + a^2}{b^2 - a^2} \right) ,$$

$$= 2.9 \times 10^5\ Pa\ (42.4\ psi)\ compression\ ,$$

where P is atmospheric pressure.

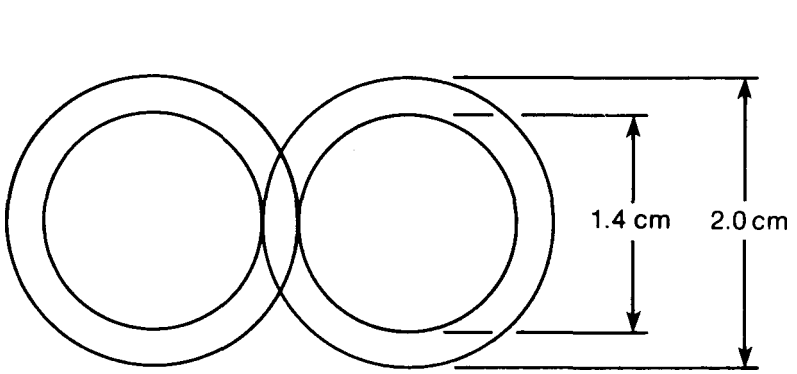

Figure 7-7. Model of Tubes for Stress Analysis

Then, for the compression stress on vertical ribs between the fluid passages, consider the segment shown in Figure 7-8. The compression stress on the connecting rib is

$$\sigma = \sigma_{top} \frac{A_{top}}{A_{middle}} - \sigma_t$$

$$= 2 \times 10^5 \text{ Pa} \frac{0.017 \text{ m}}{0.003 \text{ m}} - 2.9 \times 10^5 \text{ Pa}$$

$$= 8.1 \times 10^5 \text{ Pa (118 psi) compression.}$$

The proportional elastic limit (PEL) of GRC is about 8.3 mPa (1200 psi) (Slemmons and Ploeger 1981). This gives a safety factor of over ten for these conditions. Typical properties for other types of concrete are as follows:

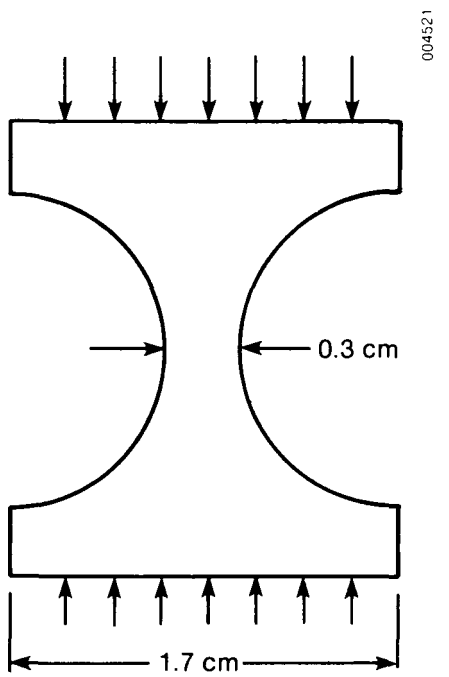

Figure 7-8. Model of Rib Between Tubes

	Density		Compressive Strength		Tensile Strength
	kg/m^3	(lb/ft^3)	MPa	(psi)	MPa (psi)
Normal concrete	--		34.48	(5000)	2.76 (400)
Lightweight concrete	512.5	(32.0)	1.03	(150)	--
	400.4	(25.0)	0.34	(50)	--
	288.3	(18.0)	0.03	(5)	--
Polymer concrete	--		103.45-137.93 (15,000-20,000)		9.66-11.03 (1400-1600)

Thus, normal concrete and polymer concrete would probably be strong enough, but the lightweight concrete would not unless some form of reinforcement is provided.

Besides the fluid forces analyzed above, forces are also present because the panel is supported by its edges. The longitudinal and transverse mechanical stress of the entire plate must be evaluated. Figure 7-9 shows the model used for analyzing the stress in the longitudinal direction for a representative cross section. The maximum stress (Shigley 1977) is $\sigma = Mc/I$, where M = moment, I = moment of inertia, and c is defined in Figure 7-9.

The force per unit length of cross section due to both the mass of the concrete and the water in the tubes is

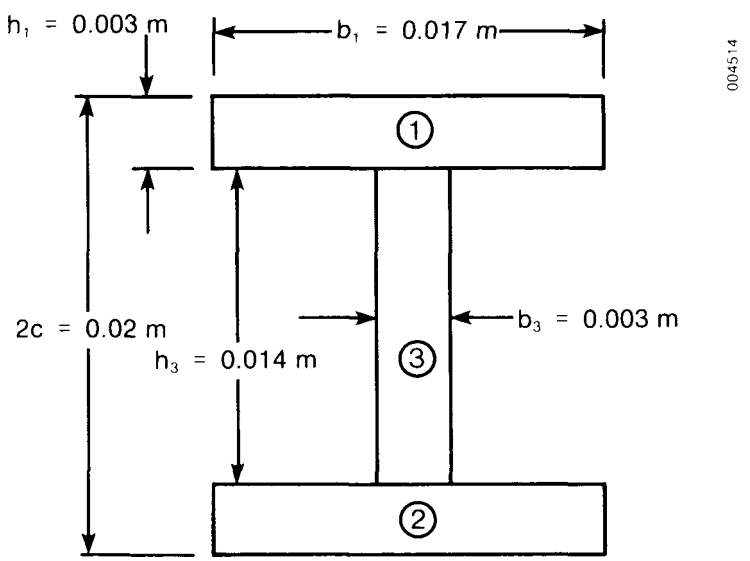

Figure 7-9. Model for Longitudinal Stress Analysis

$$W = [(1400\ kg/m^3)(1.86 \times 10^{-4}\ m^3/m)$$

$$+ (1000\ kg/m^3)(1.54 \times 10^{-4}\ m^3/m)](9.8\ m/s^2)$$

$$= 4.06\ N/m\ (0.28\ lbf/ft)\ .$$

This force gives a moment $M = 1/2\ Wx_\ell^2$, where x_ℓ = longitudinal length (= 2 m) or:

$$M = 1/2(4.06\ N/m)(2\ m)^2 = 8.13\ N\cdot m\ (6.00\ lbf\cdot ft)\ .$$

The moment of inertia of the beam section in Figure 7-9 is calculated as follows:

$$I_1 = I_2 = \frac{b_1 h_1^3}{12} = \frac{(0.017\ m)(0.003\ m)^3}{12} = 3.825 \times 10^{-11}\ m^4\ (4.432 \times 10^{-9}\ ft^4)\ ,$$

where I_1 and I_2 equal the inertia of the top and bottom rectangles about their centroids, and

$$I_3 = \frac{b_3 h_3^3}{12} = \frac{(0.003\ m)(0.02 - 0.006\ m)^3}{12} = 6.86 \times 10^{-10}\ m^4\ (7.94 \times 10^{-8}\ ft^4)\ ,$$

where I_3 is the inertia of the middle rectangle about its centroid.

Therefore, the moment of inertia of the whole structure about its centroid is

$$I = I_3 + (I_1 + A_1 d_1^2) + (I_2 + A_2 d_2^2)\ ,$$

where $d_1 = d_2 = c - h_1/2 = 0.01 - 0.0015\ m = 0.0085\ m$ (0.33 in.). So $I = 1.445 \times 10^{-4}\ m^4\ (1.674 \times 10^{-2}\ ft^4)$.

Finally, from Figure 7-9, c = 0.01 m (0.4 in.), so

$$\sigma = \frac{(8.13\ N\cdot m)\ (0.01\ m)}{1.445 \times 10^{-4}\ m^4} = 563\ Pa\ (0.07psi)\ .$$

For the transverse stress, consider the absorber as a pair of 0.003-m thick plates separated by 0.02 m (0.8 in.) [0.017 m (0.7 in.) inside]. With the entire width taken to be 0.2 m (8 in.), this procedure can be used to obtain:

$$W = \{12.6\ kg + 50[\pi(0.007)^2(2)](1000\ kg/m^3)\}\ (9.8\ m/s^2)$$

$$= 274\ N/m\ of\ width\ (18.8\ lbf/ft)\ .$$

Thus the moment $M = 1/2\ Wx_t^2 = 1/2(274\ N/m)(1\ m^2) = 137\ N\cdot m$ (101 lbf·ft), with x_t = transverse length = 1 m.

The moments of inertia of the two slabs about their centroids is

$$I_1 = I_2 = \frac{bh^3}{12} = \frac{(2\ m)(0.003\ m)^3}{12} = 4.5 \times 10^{-9}\ m^4\ (5.2 \times 10^{-7}\ ft^4)\ .$$

The total moment of inertia about the centroid is

$$I = 2(I_1 + A_1 d_1^2)$$

$$= 2[(4.5 \times 10^{-9}\ m^4) + (0.003\ m)(2\ m)(0.01 - 0.003/2\ m^2)]$$

$$= 1.02 \times 10^{-4}\ m^4\ (1.2 \times 10^{-2}\ ft^4)\ .$$

The maximum stress again occurs at c = 0.01 m, so

$$\sigma = \frac{Mc}{I} \frac{(137\ N \cdot m)(0.01\ m)}{1.02 \times 10^{-4}\ m^4} = 13{,}400\ Pa\ (1.9\ psi)\ .$$

Both the longitudinal and the transverse stress values are well within the capabilities of the GRC.

7.2.2 Construction

Based on the structural analyses in Section 7.1.1, we decided to fabricate two GRC panels for further testing and evaluation. An open channel design (Figure 7-1), which would have a glazing material (probably tempered glass) bonded directly to the absorber, and an integral fluid passage design (Figure 7-2) were proposed. We then built 2 m × 1 m (6.7 ft × 3.3 ft) molds to accommodate these collectors.

To ensure maximum strength, uniformity of mixture and application, and ease of construction, industry contacts (Table 7-3) recommended a spray-up technique. Due to time and budget constraints, we decided to hand-cast the GRC panels in-house.

Alkaline-resistant glass fibers were chosen to provide reinforcement. Alternatives such as metallic fibers may be capable of enhancing the thermal properties of the absorber plate at the expense of added composite weight. A fine-blend, lightweight aggregate was incorporated into the mix to minimize the weight of the collector. Carbon black pigmentation was added to make the absorber black. The actual mixture used is shown in Table 7-4.

The first panel was cast in the open channel design and developed several problems. The cement included a coarse aggregate. Since the nominal thickness of the panel was only 10 mm (3/8 in.), voids were present in the channels. Furthermore, the mold was constructed from wood. Water in the GRC mixture caused the channel strips to swell and buckle, which caused a number of large (10-15-cm [4-6-in.] diameter) indented bubbles in the face of the panel. Because of the irregularities of this panel, we did not evaluate it further.

A finer aggregate was used for the integral passageway collector. In this case, a 6.5-mm (0.25-in.) layer of blackened GRC was cast, 6.5-mm diameter

Tygon tubing was suspended tautly above this initial layer, and a 13-mm (0.5-in.) layer of GRC without colorant was poured over the tubing. After the GRC had cured, the Tygon tube was pulled out (the tubing constricts under tensile force and is easily removed), resulting in 6.5-mm diameter integral passageways of 5-cm spacing.

The next step was to seal the passageways to allow water to flow through the collector. Industrial contacts recommended that we use a product called Sealcrete. We obtained two samples of the sealant--a penetrating sealant and a surface sealant. Laboratory tests on GRC samples treated with various combinations of these two sealants indicated that a pretreatment with the penetrating sealant followed by an application of the surface sealant worked well even at elevated temperatures (72 h at 175°C [347°F]). We therefore decided to treat the flow passages of the GRC absorber plate with the prescribed sealants by plugging one end and filling the channels with the liquid sealants. However, because of small cracks and fissures emanating from the passageways, the sealants seeped through the GRC. Apparently, the mixtures were capable of sealing a porous medium but incapable of plugging cracks. We discussed this problem with industry contacts but failed to identify a product capable of sealing fissures associated with the inaccessible passageways in the GRC.

We also needed to bond the absorber plate to a galvanized steel manifold. The specifications for the sealant included (1) adhesion to both substrate materials, (2) ability to withstand stagnation temperatures, (3) impermeability to water, and (4) resistance to ultraviolet exposure. Additional desirable qualities were the retention of elastomeric properties upon curing, good inherent absorptance, and the absence of out-gassing.

We used an adhesives selector guide (Adhesives; Desk Top Data Book 1979) to survey candidate sealants. We conferred with industrial contacts to further clarify performance specifications and to learn from their field experience. The consensus was that the best sealants to use with concrete are those with either a polysulfide or polyurethane chemical base. Unfortunately, these sealants cannot withstand temperatures above 93°C (200°F). On the other hand, sealants with good temperature resistance such as silicone and some synthetic rubbers usually exhibit poor concrete bonding characteristics.

Although they were skeptical of success, several companies offered to send samples of their products for in-house evaluation. Dow Corning recommended their 795 Silicone Building Sealant as a strong candidate because it contains an internal primer that promotes adhesion to concrete. [A companion product (Dow Corning RTV-790) had been evaluated by Dame (1980) for high-temperature solar applications.] Furthermore, the 795 was locally available in black. A tube of this sealant was purchased along with commercially available acrylic- and silicone-based concrete sealants (Acrylic Mortar Patch from Macklanburg-Duncan Company, and Silicone Concrete Crack Sealant from Dow Corning). These were applied to GRC and galvanized steel test coupons and allowed to cure overnight. We cleaned the galvanized steel samples with acetone and the untreated GRC and treated GRC samples with muriatic acid (an industrial stone and mortar cleaner containing HCl).

Table 7-3. Industry Contacts for Construction of GRC Collectors

Bud Warner, U.S. Bureau of Reclamation, Div. of Research, Concrete Section, U.S. Federal Center; Lakewood, CO; (303) 234-3790; spraying GRC.

Art Slemmons, SRI International; Menlo Park, CA; (415) 326-6200; spraying GRC.

Jim Ford, Owens Corning; Toledo, OH; (419) 248-8000; glass fibers for concrete reinforcement.

Bud Barr, Rio Grande Co.; Denver, CO; (303) 825-2211; black pigment for GRC.

Don Peterson, Clay-Lite; Denver, CO; (303) 292-2345; lightweight aggregate.

George Mackey, Buildex Inc.; Ottawa, KS; (913) 242-2177; GRC mix designs, lightweight aggregate.

Art Green, ICI Americas Inc.; Wilmington, DE; (800) 441-7757; "Mighty" super plasticizer for concrete.

Pat Hood, Rio Grande Co.; Denver, CO; (303) 825-2211; "Mighty" super plasticizer for concrete.

John Lyle, Denver Concrete Vibrator Co.; Denver, CO; (303) 571-1453; vibrator for GRC collector.

Neil Moon and Vernon Jones; Denver, CO; (303) 420-8470; concrete sealants.

Mr. Grimes, Grimes Sealcrete; Oakland, CA; (415) 835-4635; Sealcrete concrete sealant.

Frank Stanko, M&T Chemical Corp.; San Francisco, CA; (213) 247-6210; Epibond 1511 A/B.

Jerry Colter and Michele Tate, SWS Silicones; Adrian, MI; (517) 263-5711; Architectural SWS-930 and Siligan J-500.

Herb Moore, Essex Chemical Corp.; Compton, CA; (213) 537-7600; Pro Seal 700 and 899.

Jack Steiner, General Electric; Waterford, NY; (518) 237-3330; Silpruf.

Bob Schultz, Dow Corning; Midland, MI; (517) 496-4000; 795 construction sealant.

Bud Boyle, General Sealants; City of Industry, CA; (213) 330-3118; GS-79.

Table 7-4. GRC Mixture

Component	Actual Cost	Cost		Wt % in Mix	Cost of Mix	
		$/kg	$/lb		¢/kg	¢/lb
Aggregate	$44/yd^3	0.09	0.04	42.3	3.63	1.65
Cement	$5.50/94 lb	0.13	0.06	25.1	3.24	1.47
Colorant	$1.15/lb	2.54	1.15	6.0	15.21	6.91
Glass	$1.98/lb	4.37	1.98	1.6	6.98	13.17
Water	--	--			--	
				100.0	29.1	13.2

Both commercial products easily peeled off all trial substrates. The Dow Corning 795 also easily peeled off the muriatic-acid-treated GRC. The 795 adhered well, however, to the untreated GRC and the galvanized steel. A sample of GRC bonded to galvanized steel with 795 was subsequently submerged in boiling water for an hour and no adverse effects were noted; excellent adhesion was still evident.

Based on these results, we chose Dow Corning 795 sealant for use in bonding the galvanized steel manifold to the GRC absorber plate. Because of its compatibility with GRC and good sealing properties, this product was also investigated as a possible sealant for the flow channels. Application of Dow Corning 795 (using a long rod and plunger) to the passageway walls successfully sealed the small cracks and prevented water leakage. This sealant also provided a good bond between the GRC panel and the galvanized steel manifold after a 2-week cure time. The rate of cure of silicone sealants is a function of ambient humidity; the local low-humidity environment required an extended curing time to create a good seal between the galvanized steel manifold and the GRC absorber plate.

Following the sealing of the flow passages and bonding of the manifold to the absorber, the GRC plate was placed in a galvanized steel support box with 2.54 cm of polyisocyanurate foam board insulation. A Tedlar glazing was chosen as the cover plate material and was applied roughly 2 cm above the GRC absorber.

7.2.3 Cost of GRC Collector

The following chart shows the material costs of the two GRC absorber plates.

	Mass		Materials Cost ($)	Cost per Unit Area	
	kg	lb		$/m^2	$/ft^2
Open-channel absorber	31.8	70.0	9.25	4.63	0.43
Absorber with cast-in passages	51.05	112.4	14.86	7.43	0.69

The next chart shows the cost breakdown for a 1 m × 2 m (3.3 ft × 6.6 ft) integral passage collector.

Absorber	$14.86[a]
Insulation	$ 4.74[a]
Glazing	$ 0.46[a]
Labor (1/2 hour)	$ 8.00[a]
Headers 0.20 m × 1.83 m = 0.37 m^2 (3.98 ft^2)	
0.37 m^2 × 5.52 kg/m^2 = 2.04 kg @ $1.17/kg	
= $2.38[b]	
(3.98 ft^2) × (1.13 lb/ft^2) = (4.49 lb) @ ($0.53/lb)	
= $36.44	
= $18.22/$m^2$	
($ 1.69/ft^2)	
Price to contractor = $36.44 @ 164% = $59.76	
= $29.88/$m^2$	
($ 2.78/ft^2)	

[a]Mosella 1982.
[b]Richardson 1982.

Note that this cost analysis assumes that a support box would not be required since a GRC frame could be cast as an integral part of the absorber plate.

7.2.4 Conclusions

A collector using glass reinforced concrete as the absorber material was successfully assembled. The ultimate cost to a contractor of such a unit is about $30/$m^2$ ($2.80/$ft^2$), a price well below presently marketed collectors. Based on the theoretical thermal and optical performance of this prototype collector, further R&D is warranted, particularly to find a more effective way to cast the absorber. Spray application of GRC with a lightweight aggregate onto a vibration table is one possibility. Additionally, a more convenient and reliable method of sealing the flow passages must be developed; using an additive with the GRC at the time of mixing is a potential solution.

Several ways of improving performance should be considered. Substitution of metallic fibers for glass fibers may enhance the thermal conductivity of the composite absorber material at the expense of added weight. Durability of the black pigmentation at elevated temperatures should be determined. The use of a black paint either during mixing or after curing should also be investigated. An added advantage of a GRC panel is that it can serve double duty as

a roofing panel. One firm in Oakland that has built GRC roofing panels has already made prototype collectors. Their construction method results in a stronger product than the hand-cast SERI prototype, which was severely damaged when accidentally dropped by the SERI test crew.

7.3 OTHER CONCEPTS

The glass reinforced concrete collector received the bulk of attention in FY 1982 at SERI, but a number of other concepts have been identified as promising and could be explored by SERI in the future. These are discussed in the following sections.

7.3.1 Galvanized Sheet Metal Collector

As discussed earlier, both steel and aluminum are significantly less expensive than copper and are potentially excellent absorber materials for closed-loop, corrosion-inhibited applications. One popular low-cost collector (Shurcliff 1979) consists of a corrugated aluminum absorber plate with a single glazing. Water trickles down the open troughs and is heated by the blackened metal. Because of the open trough design, evaporated water tends to condense on the inside of the glazing, serving as a heat loss mechanism and also reducing transmissivity. The low cost of sheet metal (as shown in the materials survey) has contributed to the use of these collectors for low-temperature hot water heating.

A simple way to improve this collector and make it applicable to a wider range of retrofit applications would be to use two layers of galvanized steel and flow water between them. Although such a collector would not be feasible for an open-loop application, it should function well in a low-pressure, closed-loop, drainback system and improve performance considerably with a relatively small increase in materials cost. Since galvanized steel sheets are mass-produced and readily available, they are very inexpensive ($0.29/ft^2 retail and less than $0.20/ft^2 wholesale). They are appropriate for both factory and on-site fabrication and also offer some possibility for use as roofing material, thus providing further cost reduction. Because of the high thermal conductivity and high degree of surface wetting, they can also achieve high optical efficiency.

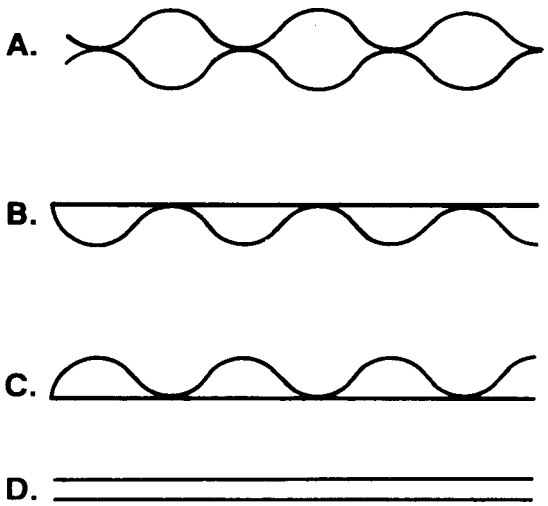

Figure 7-10. Four Possible Configurations for a Galvanized Sheet Metal Absorber Plate

Figure 7-10 shows four possible arrangements for the absorber plate. Part A shows two corrugated sheets. With this arrangement, one long sheet could be folded over to form the two plates and header construction would be simplified. Hydrostatic pressure might more easily be accommodated by this design as well. Part B shows a flat sheet on top of a corrugated sheet.

This design would contain less water (i.e., require a lower flow rate) and have a lower heat loss because of lower surface area. In Part C, the design has the flat sheet on the bottom. If the channels in this design were entrained in the collector, the water will still be in direct contact with most of the absorber surface, but surface area, and therefore heat loss, is as large as in Part A. The design in Part D uses two flat sheets. An external frame would be needed to prevent bulging. It would be more difficult to provide uniform flow with this system, but it is simple to attach the headers to the frame.

Researchers in India did considerable work on galvanized sheet metal collectors in the 1960s (Khanna 1968). He reported that costs were very low. A number of problems occurred, however, as reported by Gupta and Chopra (1976): short life (due to corrosion), bulging under hydrostatic pressure, and leaking rivets. The corrosion problem occurred because the potable water passed directly through the collectors. By using a closed-loop, drainback configuration with treated water, this problem can be overcome. Through discussions with people in the water treatment industry, we found that control of alkalinity with boron nitrate would prevent corrosion at a cost of about $0.66/L ($0.25/gal).

The problems of bulging under pressure and leaking rivets are related. In a piping configuration open to the atmosphere at the top, the bottom of a collector would have a static pressure equal to its elevation head plus the pressure drop across the collector (~3 psi for a single row DHW installation). Addition of more rows in a larger array would increase this pressure, as would closing the loop to the atmosphere, thereby allowing the vapor pressure to build up (e.g., 32.4 kPa at 37.8°C or 4.7 psi at 100°F).

In building a prototype to test this concept, we used two corrugated sheets attached together in a mirror image (Figure 7-11). This provided better longitudinal rigidity, which helped to resist the hydrostatic force concentrated at the bottom of an installed collector. To resist the hydrostatic force acting to separate the plates, a bead of GE Silglaz-N neutral cure silicone caulk was applied between each channel along the absorber's entire length. This provides for a large attachment area thereby spreading out the force.

Headers were made from off-the-shelf corrugated roof peaking sections, providing for a convenient mating of the corrugated sheets. The headers were caulked and riveted in place. To further fasten the absorber in place, four pairs of cross-brackets were made. Each consisted of two lengths on 16-gauge sheet metal bent into an L-shape and connected at each end by a bolt passing through the sheet metal (but outside the outermost flow channel). The brackets at each end of the panel also serve to hold the headers in place. A low-cost selective foil was then applied to the absorber in strips (McChesney et al. 1982).

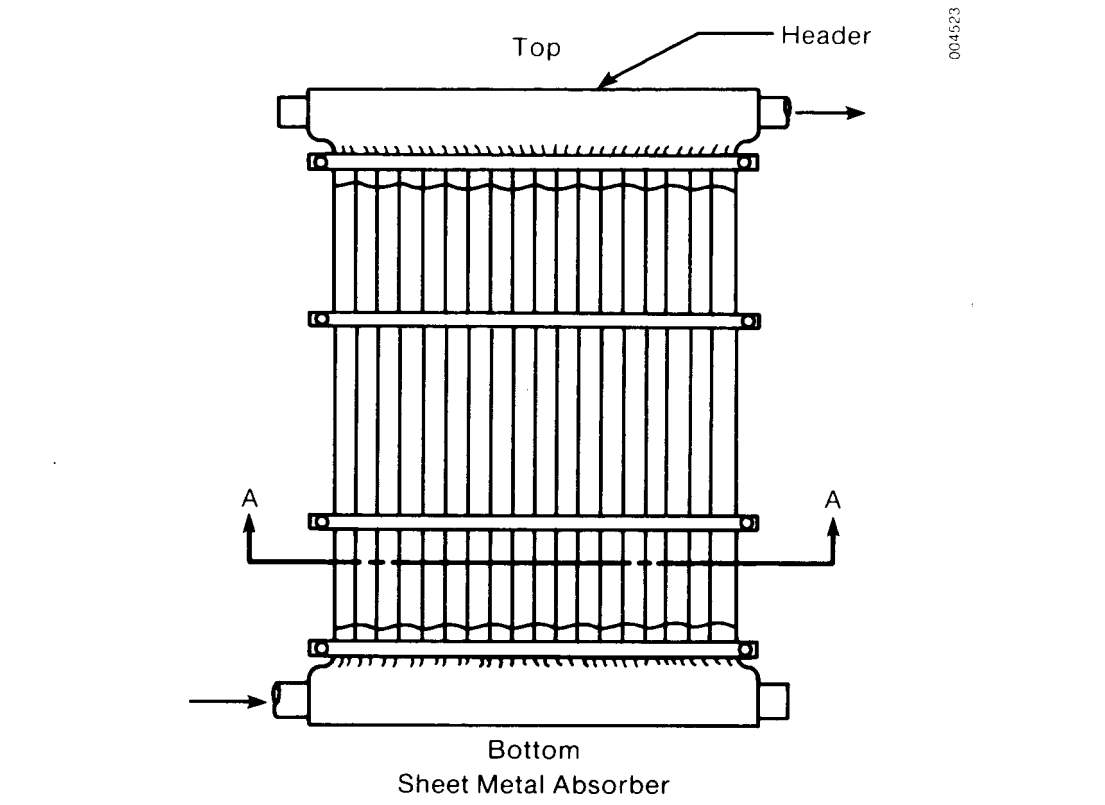

Figure 7-11. Flat-Plate Sheet Metal Absorber

The collector enclosure was made from galvanized sheet metal formed into a U-shaped channel. Sheet metal brackets were fabricated to hold the absorber in place. (These were riveted to the box and the ends of the four pairs of cross-brackets, thereby minimizing heat-loss paths to the frame.) Low-binder fiberglass (2.54-cm thick) was used below the absorber backed by 2.54 cm of polyisocyanurate foam board. A polyethylene sheet was then stretched across the bottom of the enclosure to protect the insulation and attached with tape. Similarly, a single glazing of Tedlar was attached by tape to the top of the enclosure.

Costs of the sheet metal collector are shown in Table 7-5. Although more expensive than the GRC collector, it is considerably lighter and much less fragile. In actual production it is unlikely that fastenings would be the same as the prototype. Spot welding and roller seam welding are alternatives to the caulking/bracket combination. Alternative materials could also be considered, such as aluminum or Galvalume (a galvanized aluminum product).

Table 7-5. Estimated Costs for Sheet Metal Collector (8 ft × 2 ft)

Absorber:	2 sheets of corrugated galvanized steel 30 ga. 32 ft^2 × \$0.23/ft^2	=	\$ 7.36
Headers:	Sheet metal roof peak sections 5 ft @ \$0.73/ft	=	3.65
Sides:	Sheet metal 10 ft × \$0.23/ft^2	=	2.30
Insulation:	Low binder fiberglass: 16 ft^2 @ \$0.13/ft^2	=	2.08
	Isocyanurate foam: 16 ft^2 @ \$0.37/ft^2	=	5.90
Glazing:	Tedlar film 16 ft^2 @ \$0.40/ft^2	=	6.40
Backing:	Polyethylene (4 mil) 16 ft^2 @ \$0.02/ft^2	=	0.32
Selective foil:	16 ft^2 @ \$0.15/ft^2	=	2.40
Adhesive tape:	40 ft^2 @ \$0.02/ft	=	0.80
Fittings:	2 @ \$1 each	=	2.00
Labor:	1 hour @ \$8.00/h	=	8.00
			\$41.21
Cost to manufacture including plant overhead and profit \$41.21 × 1.64 = 67.58 or \$4.22/ft^2			

7.3.2 Glass Cloth Collector

One collector purchased by the SERI low-cost collector committee contained a fiberglass absorber plate. The problem with using fiberglass as an absorber plate is that the resin imbedded in the glass cloth typically can withstand is that off-the-shelf resins are typically rated for temperatures of up to only about 93°C (200°F), thereby greatly limiting collector performance. Thus, either a higher temperature resin must be found or an alternative bonding material must be used.

We located a new, high-temperature resin, Plasticrafts No. 111, capable of withstanding temperatures to 185°C (365°F). Alternatively, the Dow Corning 795 black sealant used for the GRC collector or a high-temperature epoxy could be used for bonding the glass cloth. (High-temperature epoxies are typically expensive, however.) Whichever sealant is used, the absorber would consist of two bonded sheets of cloth separated by about 1 cm (1/2 in.), with flow passages between the cloth sheets separated by the sealing compound. Headers could also be made of fiberglass (Figure 7-12).

Table 7-6 gives estimated costs of a glass cloth collector. The total cost to a contractor is estimated to be $\$41.10/m^2$ ($\$3.82/ft^2$), very similar to the sheet metal collector. A glass cloth collector would be considerably lighter in weight than a sheet metal collector, but it might not be as durable and would be lower in optical efficiency.

7.3.3 Polypropylene Collector

As shown in the materials survey, polypropylene at less than $\$0.54/m^2$ ($\$0.05/ft^2$) is an inexpensive material. It is very susceptible to ultraviolet degradation, however, and cannot withstand high temperatures. A collector could use Flexigard glazing to protect the polypropylene absorber from UV light. Studies have shown (Cuddihy and Laing 1982) that the acrylic component of the acrylic-polyester laminate is a better long-term filter for UV light than Tedlar. To limit stagnation temperature, a black fluid developed by Sperry (Anderson, Jensen, and Kovacic 1980) would be used in a clear polypropylene absorber. The absorber would be backed by a reflective material so that under stagnation conditions with the black fluid drained out of the collector, only minimal heating of the polypropylene absorber would occur.

Polypropylene is chosen over polyethylene because the latter is not transparent. The absorber consists of two sheets of polypropylene with channels formed by heat sealing (Figure 7-13). Headers design is similar to that of the Brookhaven collector (Wilhelm and Andrews 1982).

Estimated costs of the polypropylene collector are given in Table 7-7. The price to the contractor of $\$36.06/m^2$ ($\$3.35/ft^2$) is lower than any of the

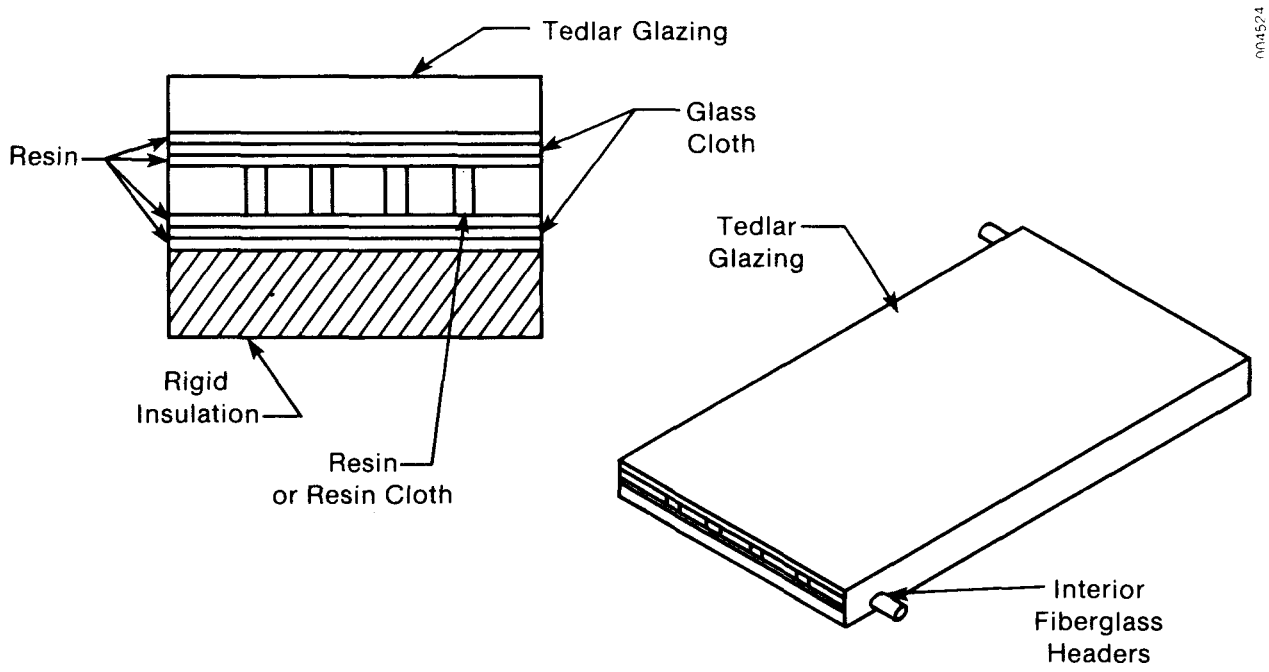

Figure 7-12. Glass Cloth Collector

Table 7-6. Estimated Costs for a Glass Cloth Flat-Plate Collector

Frame	$ 7.64	
Absorber	26.97	
Insulation	5.28	
Header tubes	0.75	
Glazing 2.23 m^2 @ \$3.23/m^2 (24 ft^2 @ \$0.30/ft^2)	7.20	
Labor 0.50 hours	8.00	
	\$55.84	= \$25.08/m^2 (\$2.33/ft^2)
Price to contractor \$55.84 @ 164%		= \$91.58 = \$41.07/m^2 (\$3.82/ft^2)

other designs except the GRC. The polypropylene collector is less fragile and lighter in weight than the GRC collector. Because a black fluid is used, the potential for high efficiency exists, and the fluid temperature is actually above the absorber surface temperature. A major problem is ensuring the longevity of the polypropylene. Periodic (e.g., every eight years) replacement of the Flexigard glazing might be necessary. Also, compatibility of the black fluid with the polymer absorber must be investigated.

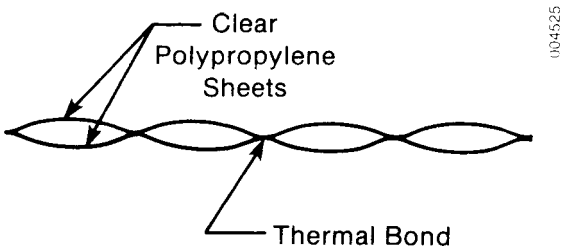

Figure 7-13. Polypropylene Absorber

Table 7-7. Estimated Costs of a Flat-Plate Collector with a Polypropylene Absorber (8 ft × 3 ft)

Absorber:	
Polypropylene--$0.05/ft^2 × 2 surfaces = $0.10/ft^2	
Heat weld channels and edges = 0.03	
$0.13/ft^2	
Total Costs:	
24 ft^2 at $0.13/ft	$ 3.12
Frame	7.12
Insulation	5.28
Header connection tubes	0.75
Glazing (Flexigard)	18.72
Labor (1/2 h)	8.00
	$42.99 ($1.79/ft^2)
Price to contractor: $42.99 @ 164%	$70.50 ($2.94/ft^2)
Black fluid cost:	$80.50 ($3.35/ft^2)

Conversion: 1 ft^2 = 9.29 × 10^{-2} m^2.

7.3.4 Black Pellet Concept

Using small opaque black spheres was investigated as an alternative to using a black fluid to reduce stagnation temperature problems. The spheres have a density just less than that of water and fill the lower header when the collector is drained (Figure 7-14a). When the collector is filled, the spheres

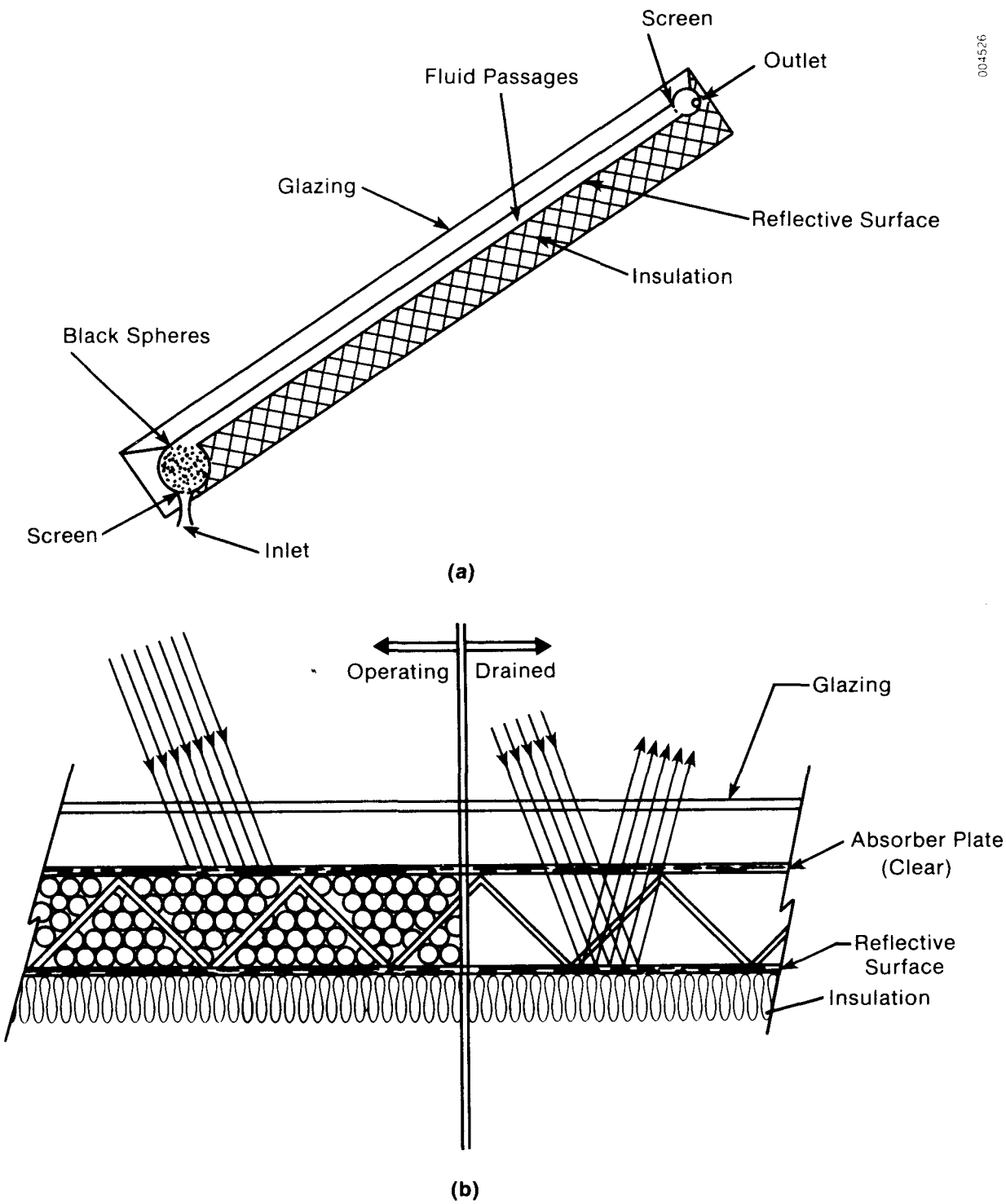

Figure 7-14. Black Sphere Collector

float with the clear water into the fluid passages, forming a packed bed of black spheres. A screen at each end of the collector confines the spheres to the collector. When the collector is drained, the spheres return to the lower header, leaving the reflective back surface of the absorber exposed (Figure 7-14b).

Problems that could arise in such a design include agglomeration and sticking of the spheres in the passages and high parasitics from the large pressure drop through the packed bed. The first problem could probably be alleviated by coating the spheres to make them hydrophobic, and both problems will be reduced if the spheres were made very smooth. Glass spheres would probably be best. The cost of this collector depends on what type of absorber is used.

7.4 REFERENCES

Adhesives; Desk Top Data Book, 1979, San Diego, CA: The Industrial Plastics Selector, Inc.

Anderson, J. H., S. O. Jensen, and J. E. Kovacic, Jan. 1980, Solar Collector Studies for Solar Heating and Cooling Applications, ALO-5355-72, Burnsville, MN: Sunsource Systems Company, and St. Paul, MN: Sperry-Univac.

Cuddihy, E. and R. Laing, 2 June 1982, personal communication, Jet Propulsion Laboratory, Pasadena, CA.

Dame, R. E., June 1980, "Selection and Test of High-Temperature Solar Collector Adhesives," Proceedings of the 1980 Annual Meeting, American Section of the International Solar Energy Society, Vol. 3.1, pp. 470-474.

Duffie, J. A., and W. A. Backman, 1980, Solar Energy Thermal Processes, New York: John Wiley & Sons, p. 218.

Gupta, J. P., and R. K. Chopra, 1976, "Solar Space Heating at High Altitude Conditions," Solar Energy, Vol. 18, pp. 51-7.

Khanna, M. L., 1968, "The Development of a Solar Water Heater and Its Field Trials Under Indian Tropical Conditions," Solar Energy, Vol. 12, pp. 255-61.

McChesney, M. A., R. J. Zimmer, and R. J. H. Lin, 1982, Optimization of Solar Selective Paint Coatings, 5 Sept. 1980--15 June 1982, Minneapolis, MN: Honeywell, Inc.

Mosella, G., editor, 1982, National Construction Estimator, Solana Beach, CA: Craftsman Book Co.

Richardson Engineering Services, Inc., 1982, Process Plant Construction Estimating Standards, 1982-1983, Vol. 2, San Marcos, CA: Richardson Engineering Services, Inc., p. 5-9.

Shigley, Joseph E., 1977, Mechanical Engineering Design, New York: McGraw-Hill.

Shurcliff, W. A., 1979, New Inventions in Low-Cost Solar Heating, Andover, MA: Brick House Publishing Co.

Slemmons, A. J., and D. W. Ploeger, July 1981, Conceptual Design of a Glass-Reinforced Concrete Solar Collector, SAND81-7011, Menlo Park, CA: SRI International.

Wilhelm, W. G., and J. W. Andrews, Aug. 1982, The Development of Polymer Film Solar Collectors: A Status Report, BNL-51582, Upton NY: Brookhaven National Laboratory.

SECTION 8.0

COLLECTOR TESTING

To determine the performance of the various collector concepts, testing according to ASHRAE 93-77 was done at SERI's Mid-Temperature Collector Research Facility (MTCRF). This facility and the modifications required for low-cost collector testing are described in Sections 8.1 and 8.2, respectively. Test results for two collectors (the Brookhaven thin-film plastic and the Sealed Air rigid plastic) are given in Section 8.3. Unfortunately, test results for the SERI collector concepts were not completed.

8.1 DESCRIPTION OF THE MID-TEMPERATURE COLLECTOR RESEARCH FACILITY

All collector testing for this task was performed at SERI's Mid-Temperature Collector Research Facility. The MTCRF is a versatile test facility at which research issues relating to the thermal performance of concentrating collectors are investigated. Several minor modifications, described in Section 8.2, were required to test low-temperature (e.g., flat-plate) collectors.

The facility is a single collector module test loop with the ability to measure thermal performance for a variety of generic collectors over the mid- (121°-343°C, 250°-650°F) and low- (21°-121°C, 70°-250°F) temperature ranges. The basic features of the test loop are listed in Table 8-1. Figure 8-1 is a simplified schematic of the test loop. Two skids hold all the major hardware. The main equipment skid, housed inside a 4.5 m × 6.1 m (15 ft × 20 ft) building, holds the storage tank, circulating pump, warm-up heater, and heat exchangers. Heat rejection takes place in a cooling tower separate from the MTCRF. A flow control valve, flowmeters, temperature controllers, and a conditioning heater are located on a wheeled flow-metering skid that can be moved among three test stations.

Table 8-1. Major Features of the Mid-Temperature Collector Research Facility

Collector work stations	3
Collectors active at one time	1
Heat rejection rate	46.8 kW (160,000 Btu/h)
Fluid flow rate	0.19-45.2 L/min (0.05-12 gpm)
Temperature range	
Water	21°-232°C (70°-450°F)
Heat transfer oil	37°-343°C (100°-650°F)
Maximum working pressure	3.62 MPa (515 psig)

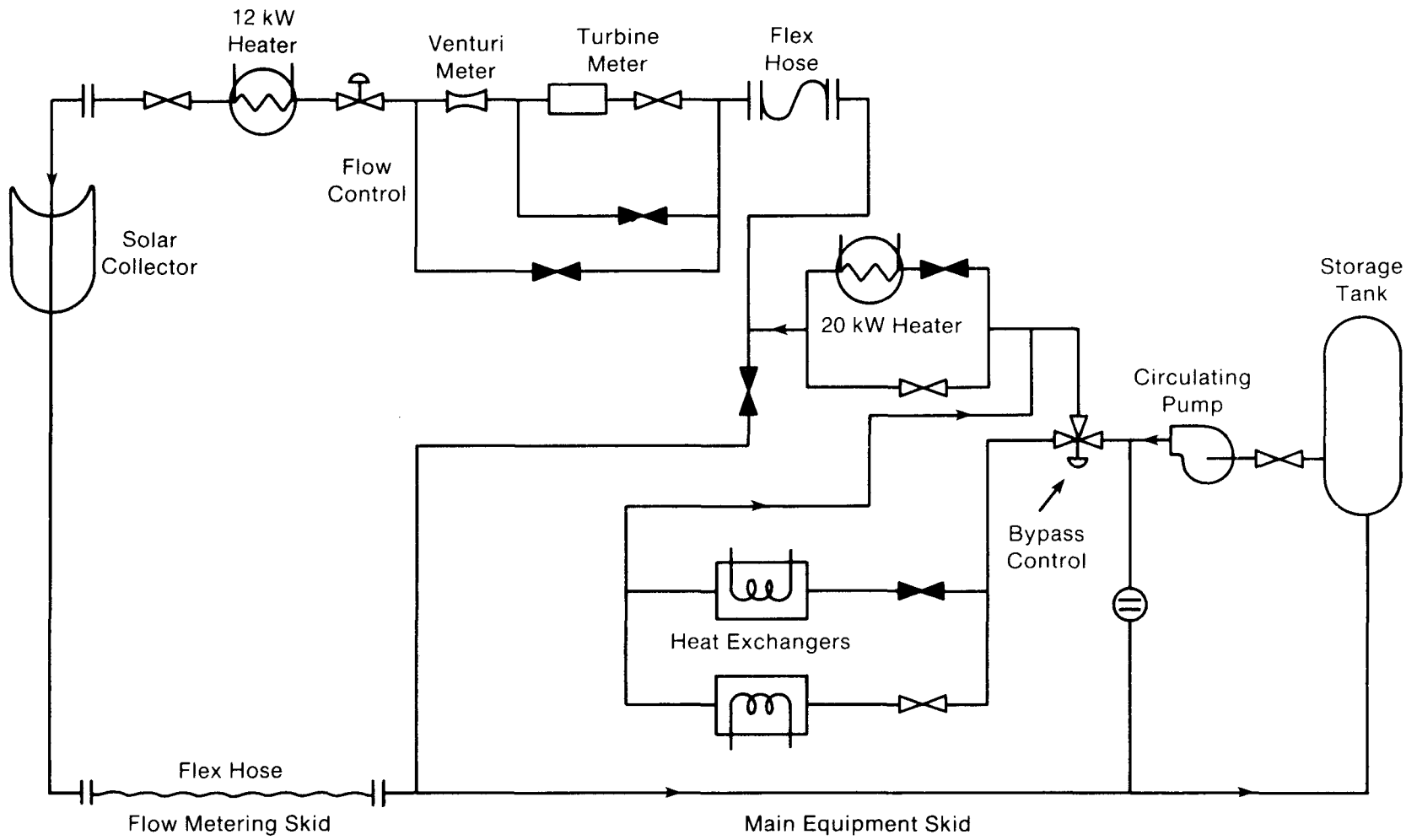

Figure 8-1. MTCRF Test Loop Schematic

All recent collector tests, including those for this task, were performed with collectors mounted on a dual-axis tracking platform. This platform was designed to hold collectors as heavy as 450 kg (990 lb) and as long as 6 m (19.7 ft). Tracking is accurate to within less than 0.1^{o}, which is more than adequate for testing flat plates. Within limitations imposed by latitude, time of day, and date, the platform can maintain an arbitrary incident angle between the sun and the collector aperture plane.

Performance was measured using sensors selected for reliability, high accuracy, and precision. Table 8-2 lists the parameters measured along with the sensors utilized. Data are acquired with an LSI-11 minicomputer and stored on magnetic tape for later detailed analysis. Using manufacturer's accuracy data, an estimate of overall experimental error is 2-3 absolute percentage points, depending on flow rate, temperature level, and collector performance.

The guidelines for conducting flat-plate tests generally followed those of the accepted standard, ASHRAE-93 (1977). Additional requirements were applied to the definition of "quasi-steady state" to define more quantitatively "good" data points. To eliminate all subjective judgment on valid data points, a computer program analyzed data according to a fixed set of required conditions that are presented in Table 8-3. If these conditions are all met for a given 5-min period, the computer averages each variable, prints the average and range, and stores this data as a valid performance data point. Data were recorded once every 15 s.

Table 8-2. Mid-Temperature Collector Research Facility Instrumentation

Measurement	Sensor	Manufacturer	Model	Output	Accuracy
Volume flow	Turbine	Flow Technology	FT-10	Frequency	0.5%
Volume flow	Venturi	Fox Valve	Type N	ΔP	0.5%
Temperature, fluid (inlet, outlet, 2 ea.)	RTD (4 wire)	Hy-Cal	RTS-46	Resistance	0.1^{o}C
Power	Hall effect transducer	OSI	PC5-7D	Voltage	0.5%
Pressure, inlet	Strain gauge	Viatran	218-24	Voltage	1.0%
Pressure, differential	Strain gauge	Viatran	220-24	Voltage	1.0%
Direct irradiance	Pyrheliometer	Eppley	NIP	Voltage	2%
Total irradiance	Pyranometer	Eppley	PSP	Voltage	3%
Temperature, ambient	RTD (3 wire)	Weathertronics	4470[a]	Voltage	0.1^{o}C (0.2^{o}F)
Wind speed	Anemometer	Weathertronics	3020[a]	Voltage	0.1 m/s (0.3 ft/s)
Wind direction	Vane	Weathertronics	1250[a]	Voltage	2^{o}

[a]Includes signal conditioning modules.

Table 8-3. Test Conditions Required for Valid Data Over 5-min Period

Variable	Stability Requirement
Flow rate	±4%
Inlet temperature	±0.5°C (±0.9°F)
Irradiance	±4%
Ambient temperature	±2°C (±3.6°F)
Wind speed	<4.5 m/s (<14.8 ft/s, 10 mph)

8.2 MODIFICATIONS TO THE MID-TEMPERATURE COLLECTOR RESEARCH FACILITY

The MTCRF was originally designed to test a closed, pressurized loop as shown in Figure 8-1. Therefore, to test unpressurized (trickle-flow) collectors, several modifications had to be made. Because of the elevation of the storage tank and the required suction pressure of the circulating pump, it was necessary to disconnect the main and flow-metering equipment skids and provide an independent (open loop) source of fluid to the collector. The flow-metering skid was retained for its temperature and flow control capabilities.

The flow-metering skid was plumbed at local water pressure to provide high enough pressure to push water through the skid and up to the collector. After trickling down the collector and passing through an instrumentation section, the water was discharged.

Initial tests with this configuration showed that the local water pressure varied considerably, causing large fluctuations in flow rate. As a result, very few data points met our requirements as listed in Table 8-3. To overcome this problem a pressure regulator was installed between the water supply and the skid. The regulator stabilized the flow to within marginally acceptable limits.

The use of an open loop configuration with local, untreated water resulted in accelerated corrosion of the test loop piping. While this corrosion by itself is not alarming, the resulting layer of oxidized material coated the only moving parts in the flow skid--the turbine meter rotor and bearings. This corrosion caused the meter to vary from its calibrated performance and resulted in some uncertainty in subsequent flow measurements. The recorded flow rates during the test period were continually checked against timed and weighed samples.

Since flow rates through the flat-plate collectors were nearly an order of magnitude lower than the test loop was designed for, the flow meter operated very near its lower limit of performance. A second flow meter, better suited to the flow ranges in these tests, was procured and installed; however, it was not available until the third test.

Other aspects of test loop operation including flow and temperature control were normal, and no significant problems were experienced.

8.3 TEST RESULTS

Three collectors were tested for this task. Each used either new or innovative absorber and glazing materials. Two were collectors designed for research and one was commercially available.

The first collector tested was built by Brookhaven National Laboratory as part of their ongoing study of low-cost collectors for cooling applications. The Brookhaven Model CP2 utilizes thin-film polymeric materials for both absorber and glazing. A complete description of this unpressurized collector and its forerunners is presented by Wilhelm (1981).

The second collector was a commercially available plastic collector (BGI series) from Sealed Air Corporation, a manufacturer of solar pool blankets. The unique feature of this collector is its extruded absorber panel made from an ethylene-propylene copolymer. The glazing is a corrugated, glass-reinforced polyester. In this design air and rainwater are freely allowed into the absorber-glazing space. A specification sheet (BGI 7-3/81) contains details on construction and materials of this low-temperature collector designed for pool and domestic hot water applications.

The third collector was a GRC type designed and built at SERI and described in Section 7.1.

The test plan for each of these collectors contained three basic tests: time constant, thermal efficiency, and incident-angle modifier. Constraints on time or equipment modified the test plan in some cases and are described in Sections 8.3.1, 8.3.2, and 8.3.3 that discuss individual test results. ASHRAE-93 (1977) was used for these tests, and definitions of terms used here are taken from that document.

8.3.1 BNL Collector Test Results

The Brookhaven Model CP2 was tested while on loan from Colorado State University (CSU) prior to installation there. The basic parameters of this collector include a nominal gross area at 2.2 m^2 (24 ft^2) and weight of only 7.3 kg (16 lb). The measured dimensions were 243 × 90.8 cm (95.7 × 35.7 in.), for a gross area of 2.206 m^2 (23.75 ft^2). The nominal flow rate was 2.3 L/min (0.6 gpm) or 0.038 kg/s (5.03 lb/min) at 15°C (59°F) fluid temperature. An attempt to maintain this mass flow rate throughout the tests was made. Because of variation in local water pressures, this was not always possible.

Since this collector is an unpressurized or trickle type, we tested an open loop configuration. During the test period, several flow rate problems occurred. Recorded flow rate data were corrected by factors determined from timed and weighed measurements. This correction resulted in some uncertainty in the performance data. Unfortunately, before a complete set of validation tests could be completed, the collector had to be shipped to CSU. Of the

three tests that were conducted on the CP2--time constant, thermal efficiency, and incident-angle modifier--the thermal efficiency and incident-angle modifier tests were not entirely completed prior to shipment of this collector to CSU.

The time-constant test was performed by allowing the collector to reach steady state at the following conditions:

$$\dot{m} = 0.042 \text{ kg/s } (5.56 \text{ lb/min})$$

$$T_{f,i} = 13.1^{\circ}C \ (55.6^{\circ}F)$$

$$T_a = 5^{\circ}C \ (41^{\circ}F)$$

$$I_t = 1111 \text{ W/m}^2 \ (352 \text{ Btu/h ft}^2)$$

where

$\dot{m}$ = flow rate

$T_{f,i}$ = inlet fluid temperature

T_a = ambient temperature

I_t = insolation.

The collector was then covered. Decay of the outlet temperature nearly followed the classic exponential form with the time constant determined to be 1.6 min. Since this time constant is less than the 5-min interval required by ASHRAE for quasi-steady-state data, all subsequent data represent 5-min averages.

Figure 8-2 shows the results of the thermal efficiency tests. Note that two distinct sets of data appear: data at $\dot{m}$ = 0.038 kg/s (5.03 lb/min) and data at $\dot{m}$ = 0.042 kg/s (5.56 lb/min). The data at the lower flow rate agrees quite well with unpublished data from another test facility on another CP2 collector. The slope of the data at the higher flow rate does not agree with other data and previous experience at BNL. There are several possible explanations for this discrepancy. First, since there is some uncertainty in the flow measurement, the data may have some systematic error. Another explanation, assuming that the data are accurate, is that as flow is increased, better wetting of the flow channels occurs, causing better heat transfer and higher efficiency. A complete series of tests would have resolved this question.

Data at $\Delta T/I \simeq 0.08$ m^2 $^{\circ}C/W$ (4.5 ft^2 $^{\circ}F$/Btu) tend to fall above the slope indicated by lower temperature points. These data were taken at $I \simeq 750$ W/m^2 (238 Btu/h ft^2). It is possible that some plastic collectors have optical properties that depend on the level of irradiance. This effect has been experienced at SERI previously in unreported data taken on a plastic Fresnel lens collector.

In general, the results from the thermal efficiency tests were not consistent. Unfortunately, additional tests were not possible.

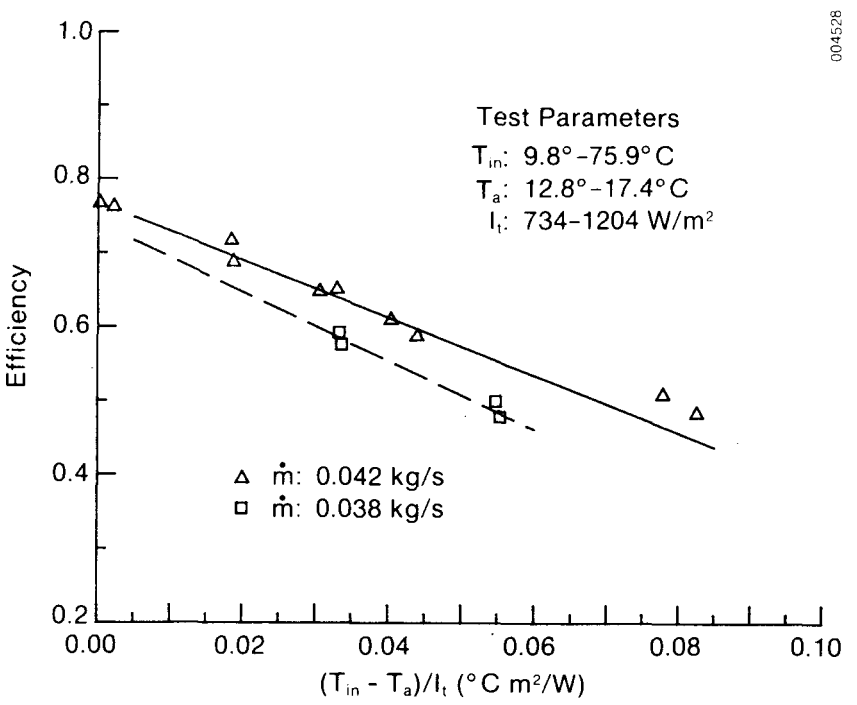

Figure 8-2. CP2 (Brookhaven) Peak Efficiency Performance

Partial results from the incident-angle test are presented in Figure 8-3. The collector had to be returned to CSU before all data could be collected. The incident angle tested was that angle between the collector normal and the sun in the plane including the normal and the long axes of the collector. This orientation minimized the already small shading factor of the frame.

8.3.2 Sealed Air Collector Test Results

A Sealed Air Corporation BGI-32 collector was purchased from the manufacturer so we could test a low-cost commercial collector. The nominal 1.22 m × 2.44 m (4 ft × 8 ft) dimensions of this unit were measured at 119.5 cm × 244.2 cm (3.92 ft × 8.01 ft) for a total gross aperture of 2.92 m^2 (31.4 ft^2). The collector has an inlet manifold at the bottom with connections at either side. The outlet manifold at the top is the same. Plugs were inserted into the inlet and outlet manifolds on one side. The test loop was plumbed to the BGI-32 on the other side using threaded adapter assemblies provided by Sealed Air.

The recommended flow rate was 1.9-3.2 × 10^{-4} m^3/s (3-5 gpm), almost five times the nominal ASHRAE flow rate of 0.02 kg/s m^2 (0.246 lb/min ft^2). An initial test to determine the effect of flow on performance was conducted. The results of that test are given in Figure 8-4. Since it was impractical to equate the inlet fluid temperature to the ambient temperature, the data have some heat losses or gains that must be corrected. For example, the lower flow rates resulted in higher outlet fluid temperatures and therefore higher heat losses. The data were corrected to $\Delta T/I=0$. As shown in the figure, there is a slight increase (~10%) in efficiency with increasing flow rate. At higher flow rates, the average fluid temperature is lower and hence heat losses are lower and efficiencies are higher.

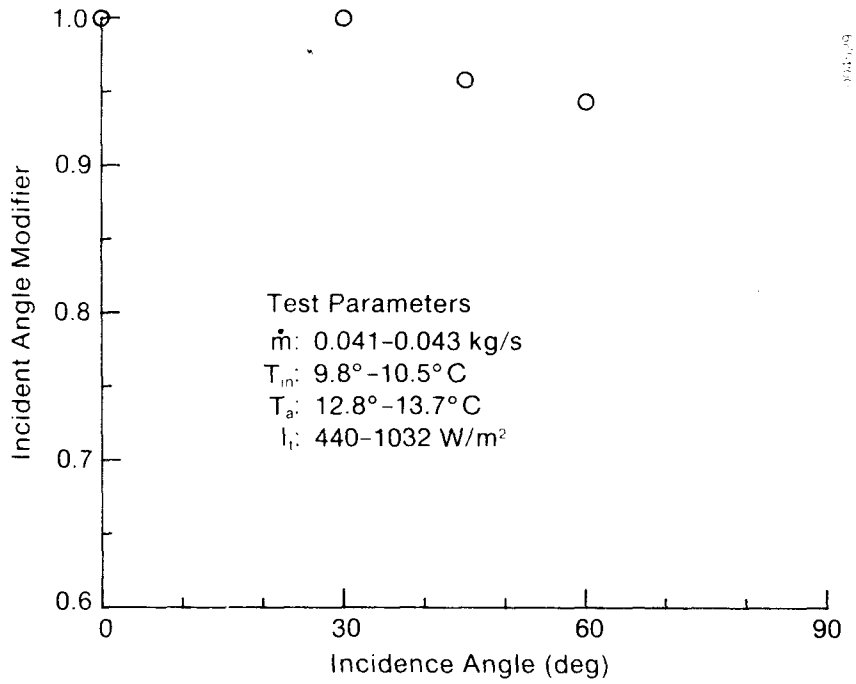

Figure 8-3. CP2 (Brookhaven) Incident Angle Performance

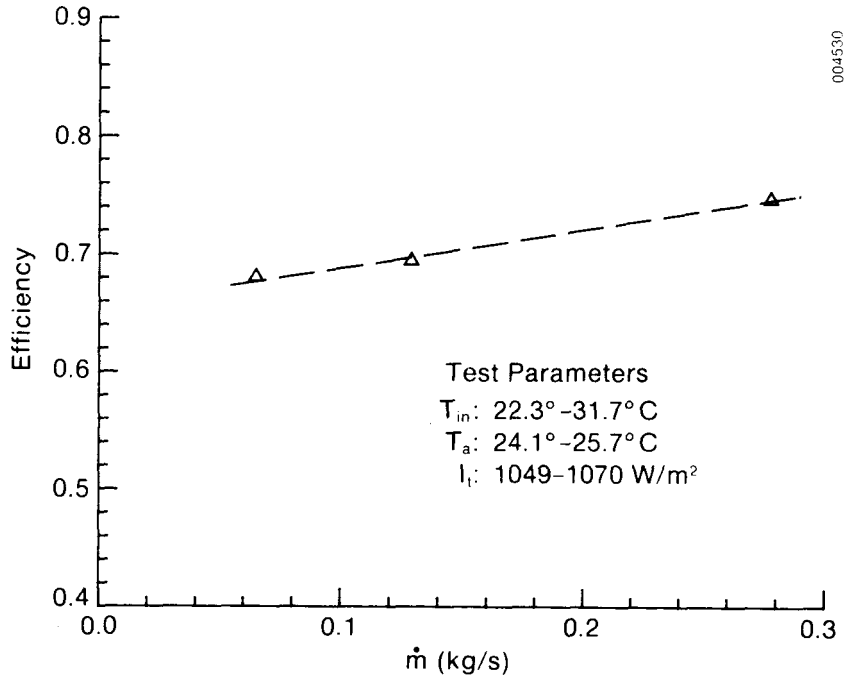

Figure 8-4. Sealed Air Collector Efficiency Tests

A time constant test was not conducted because the low thermal mass of this collector virtually ensured a very low time constant and therefore a quasi-steady-state period requirement of 5 min.

Results of the peak thermal performance tests are shown in Figure 8-5. Also shown is a curve taken from the Sealed Air BGI series data sheet. As indicated, this collector has a rather high heat-loss coefficient. According to Sealed Air, this is intentional to protect the absorber from high stagnation temperatures.

The incident-angle modifier results are shown in Figure 8-6. The incident angle is in the plane including the normal and cross sections of corrugations of the glazing. The curve is fairly flat to 45 deg, when performance begins to drop off rapidly. This is probably controlled by the glazing transmittance; i.e., the effective transmittance remains constant until the incident angle increases to a point where shading between corrugations occurs.

Because of its low cost, moderate performance, and commercial availability, this collector could be the basis for a reasonably cost-effective SDHW system. If the higher temperature performance could be improved, this would be an attractive system. Using the performance data from Figure 8-6, the stagnation point of this collector at T_a = 30°C and I_t = 1000 W/m^2 is approximately 105°C (221°F). The maximum temperature recommended for this absorber material is 143°C (290°F). This indicates that some improvement in heat loss could be made before any potential damage to the absorber would take place. If the performance curve were improved to the maximum absorber temperature, the heat-loss coefficient would show a 32% improvement. At an inlet temperature of 65.5°C (150°F), an irradiance of 1000 W/m^2 (317 Btu/h ft^2), and an ambient temperature of 30°C (86°F) the collector efficiency would improve from 35% to 46%. At an inlet temperature of 93°C (200°F) the improvement would be from 9% to 28%, a considerable increase. It appears that the design is quite conservative and has much room for improvements in performance.

If some form of venting were added to allow natural convective cooling above and below the absorber plate during no-flow conditions, performance could be improved still further. (A recent study by Trinity University showed that venting above the plate in a conventional flat-plate collector could lower the stagnation temperature 80°F.)

8.4 REFERENCES

ASHRAE Standard 93, Feb. 1977, Method of Testing to Determine the Thermal Performance of Solar Collectors, New York: American Society of Heating, Refrigerating and Air-Conditioning Engineers.

Wilhelm, W. G., June 1981, Low Cost Solar Energy Collection for Cooling Applications, BNL 51408, Upton, NY: Brookhaven National Laboratory.

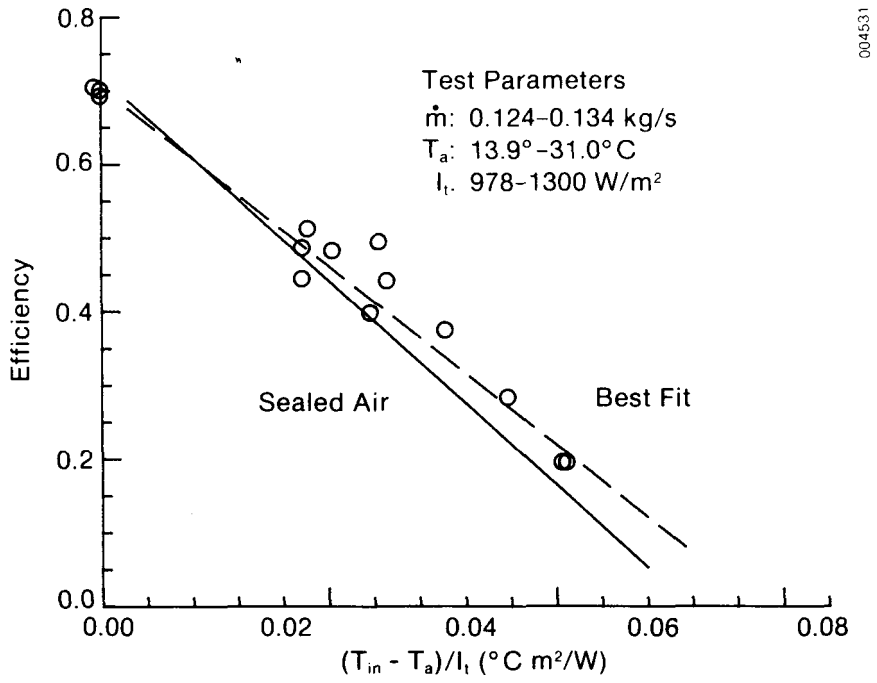

Figure 8-5. Sealed Air Collector Peak Thermal Performance Tests

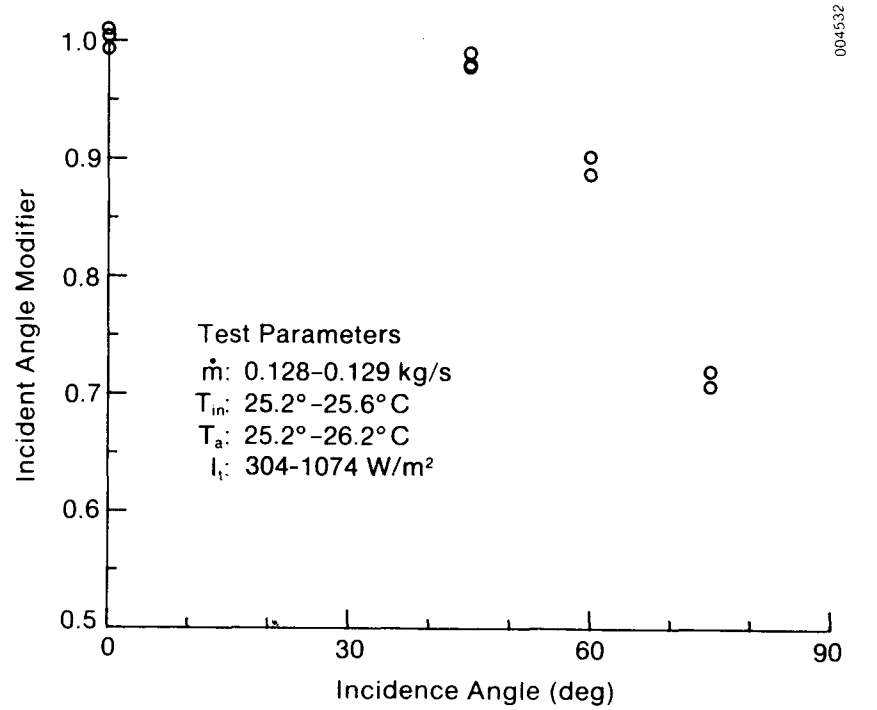

Figure 8-6. Sealed Air Collector Incident-Angle Modifiers

SECTION 9.0

CONCLUSIONS AND RECOMMENDATIONS

This section summarizes what was learned from SERI's Low-Cost Collectors/ Systems task and identifies what areas require further work. Section 9.1 lists conclusions and recommendations for further low-cost systems research; Section 9.2 offers a similar summary for low-cost collectors.

9.1 LOW-COST SYSTEMS

SERI's low-cost systems research during fiscal year 1982 has led to the following conclusions:

- Based on present cost, potential for further cost reduction, installation simplicity, reliability, and performance, a drainback liquid solar energy system appears best for domestic hot water and space heating.
- It is straightforward to design a drainback system which will establish a syphon, yet drain at pump shutdown without need for a vent line.
- A disadvantage of the drainback system is that because the pump must operate at two different heads (static head at fill, and frictional head after syphon establishment), parasitic power is higher than in other systems. This can be a significant cost because of the very low efficiencies (typically under 10%) of small solar pumps. SERI's experimental work has shown that this problem can be solved with a TRIAC control of the pump speed in conjunction with a time delay.
- Both collector-side and load-side heat exchange systems are possible. The latter can be built with cheaper, low-pressure tanks but require more careful design to ensure good performance.
- Piping is a major cost item. The best candidate materials for reducing piping costs are CPVC and polybutylene. The latter is somewhat less expensive and is becoming accepted in the plumbing industry, but requires careful sloping (due to its flexibility) to ensure proper drainage.
- Total installed costs of the system must be approximately $\$150/m^2$ ($\$14/ft^2$) to provide 40% market penetration of residential electricity consumers if no tax credits are allowed.
- Although wood, plastic, and sheet metal are promising low-cost materials for an unpressurized storage tank, simple $0.21\text{-}m^3$ (55-gal) oil drums ($35 each) might be the most cost-effective alternative.
- Small discarded freon tanks containing city water and placed inside the unpressurized storage tank might be a cost-effective alternative to the long copper pipe needed for adequate heat transfer in a load-side heat exchange system.
- Use of currently available low-cost collectors, plastic pipe, and low-cost storage can potentially reduce installed system costs from $\$452/m^2$ ($\$42/ft^2$) to $\$271/m^2$ ($\$25/ft^2$). New low-cost collector concepts are needed for further cost reductions.

The following are recommendations for research still needed in the systems area.

- Analysis is needed to determine optimum design configurations for load-side heat exchange systems.
- Experience must be obtained with a low-cost loop incorporating plastic pipe and low-cost storage to provide the proof of this concept and discover practical problems. Temperature stability of piping to the collectors and of the plastic fittings need to be tested.
- Studies should be made to determine ways to reduce the mark-up costs inherent in currently marketed solar energy systems.
- Means for obtaining improved performance in cold climates from breadbox (integrated collector/storage) systems should be pursued. Expansion of these systems to include space heating should also be investigated.

9.2 LOW-COST COLLECTORS

SERI's low-cost collector work during FY 1982 has led to the following conclusions:

- The cost to the contractor of a flat-plate collector can conceivably be reduced from an average of $\$151/m^2$ ($\$14/ft^2$) to about $\$32/m^2$ ($\$3/ft^2$) (current low-cost concepts being investigated by SERI have estimated costs to the contractor of \$29.88 to $\$41.10/m^2$ [\$2.78 to $\$3.82/ft^2$]).
- A glass-reinforced concrete collector is the least expensive collector being investigated by SERI. According to SERI's analysis, plate thickness will make up for low thermal conductivity. The concrete material is inexpensive and eliminates the need for a collector frame. Weight is comparable to a conventional copper collector. Although the hand-laid SERI prototype was too susceptible to damage, other construction techniques should result in a sufficiently strong product.
- Sealing of a concrete collector can be a problem. Although Dow Corning 795 was used to seal the passageways of our prototype, it is anticipated that less expensive commercial products such as Sealcrete might be sufficient for a spray-up GRC panel.
- Other promising concepts identified by SERI are a sheet steel collector, fiberglass collector, and polypropylene black-fluid collector.
- Brookhaven's thin-film Teflon collector performed very well in SERI's instantaneous efficiency tests. We are uncertain of its potential cost but suspect that it might cost more than other collectors we are exploring because of the lamination process needed. We feel that further efforts should be made to consider using either Teflon sheets or metal foils. As is the case with any innovative collector (but particularly a plastic one), longevity is also a question.
- The Sealed Air collector was relatively low in performance (based on manufacturer's data) but very low in cost--$\$54/m^2$ ($\$5/ft^2$ to the contractor). It is possible to improve performance by adding a selective foil and increasing back insulation. At the same time, stagnation temperature

might be kept below 250°F by venting the spaces between the glazing and the absorber as well as between the absorber and back insulation.

- Depending on collector design, a number of viable candidate materials have been identified. For collectors having high stagnation temperatures, thin-film polymers such as Teflon and Tefzel seem viable. A resin-impregnated glass cloth, glass reinforced concrete, and off-the-shelf sheet metal also offer promising benefits. Both steel and aluminum are excellent lower cost alternatives to copper if properly used in a corrosion-inhibited closed loop. If stagnation conditions can be avoided, a large number of very low-cost polymeric materials could be used for absorber plate application. Use of an ultraviolet-screening glazing would also allow a variety of alternate materials to be used.
- Several polymeric glazing materials have been identified for flat-plate glazing application. These include several fluorocarbon polymer films (Tedlar, Teflon, and possibly Kynar) and an acrylic film (Acrylar). Polymeric laminates offer hope of combining the best properties of a number of polymers to obtain a composite product better adapted to solar application than any single candidate. Thin glass is also a noteworthy candidate.

The following are recommendations for further work in the collector area:

- Potential costs of the GRC collector are so low that construction of a new panel would be warranted. Spray-up would help to overcome problems with the hand-laid model. Problems that need to be addressed are the ability to withstand freezing and thawing, fragility, and the identification of a better sealing technique. A spray-up panel should also incorporate integral headers and a built-in concrete frame.
- The other SERI concepts should be explored further, and if they continue to look promising, prototype panels should be built and tested. Concepts that use aluminum and steel are quite promising in the short term.
- Efforts should continue to discover or develop other low-cost collector concepts. Development of improved polymers should receive high priority.
- Efforts should continue in the area of reducing production costs for the BNL collector. Also, eliminating the need for lamination by choosing either Teflon or metal foil for the absorber should be considered.
- The Sealed Air collector is so low in cost that it warrants further investigation to determine if performance can be improved while maintaining the integrity of the plastic collector. Application of stagnation-limiting devices should be considered.

APPENDIX A

ANALYSIS OF A COMBINATION TANK/SOLAR COLLECTOR

The Sunwizard system pictured in Figure A-1 consists of a pressurized 120-gal tank wrapped with a selective foil (Microsorb) and then placed in an acrylic shell. Water at city line pressure is piped through the tank and then to a conventional water heater to preheat the incoming water. The system is placed out of doors, and the manufacturer recommends that an area around it be painted with a special white paint ("Solarwhite" by Permalume Plastics Corp., Vancouver, Wash.) to act as a diffuse reflector. In Figure A-1, the reflector is shown as a horizontal circle; however, vertical surfaces may also be used and give better winter performance.

The following three types of analyses have been conducted: (1) back-of-the-envelope type checking of correlations, equations, etc., (2) calculation of the enhancement possible due to a horizontal diffuse reflector, and (3) computer modeling activities of the system using an adapted version of SOLIPH. These three are detailed later.

A.1 SUMMARY OF RESULTS

Tables A-1 and A-2 and Figures A-2 and A-3 summarize the results of the simulations. The system performed well, with system thermal efficiencies (based on the energy incident on the absorber and the energy delivered) ranging from about 40% to 50% on an annual basis. The systems delivered 50% to 65% as much energy as a conventional system of 7.4 m^2 (80 ft^2) in Albuquerque, N. Mex., depending on reflector size. In very cold climates, some freezing problems may occur, but their significance is not known.

The reflector enhancement appears to be significant. The tank surrounded by a reflector absorbs about 2/3 more solar energy than the tank without the reflector. However, these results assumed a reflectance of 0.9, which may be optimistic for systems in the field that are exposed to weathering. Vertical reflectors can augment winter performance when the sun is at low elevation angles. They would probably be less susceptible to degradation since they would not be walked upon, and rain would help keep them clean.

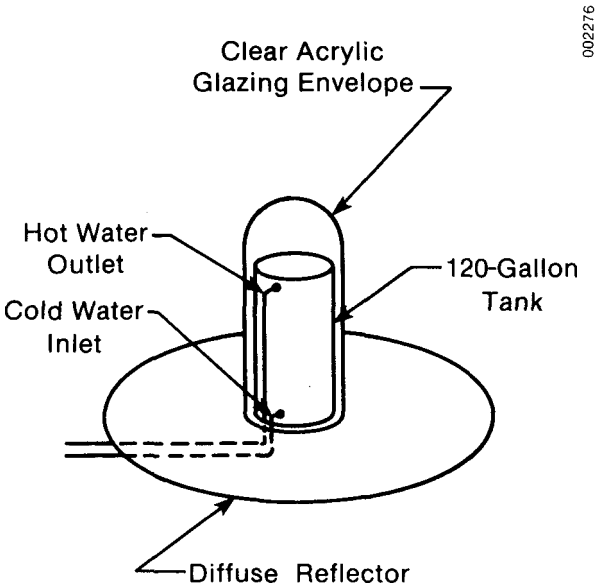

Figure A-1. Sunwizard Domestic Hot Water System

Table A-1. Results of Sunwizard Simulations

Location	Reflector Radius (m)	Q_{coll} (GJ)	Q_{del} (GJ)	System Thermal Efficiency (%)	Q_{loss} (GJ)	Storage T_{max} (°C)	Tank $\overline{T}$ (°C)	Temp. T_{min} (°C)	Fraction of Q_{coll} from Reflector
For comparison with back-of-the-envelope calculations:									
1. Albuquerque, N. Mex.	1.0	14.2	9.1	54.5	5.2	51.1	30.9	9.8	18.3
	2.0	16.3	10.3	53.7	6.0	56.9	33.7	10.7	28.7
	3.0	17.4	11.0	53.7	6.4	60.1	35.2	11.2	33.2
	4.0	18.0	11.3	53.4	6.7	61.9	36.1	11.4	35.5
Using average monthly ambient temperatures:									
2. Albuquerque, N. Mex.	1.0	14.2	8.5	50.9	5.7	59.9	32.7	5.0	18.3
	1.5	15.4	9.2	50.8	6.2	63.4	34.4	5.5	24.7
	2.0	16.3	9.8	51.1	6.5	66.2	35.6	5.9	28.7
	2.5	16.9	10.1	50.8	6.8	68.4	36.5	6.2	31.4
	3.0	17.4	10.4	50.8	7.0	70.1	37.2	6.4	33.2
	3.5	17.7	10.6	50.9	7.1	71.5	37.7	6.5	34.5
	4.0	18.0	10.8	51.0	7.3	72.6	38.1	6.6	35.5
	4.5	18.2	10.9	50.9	7.4	73.5	38.4	6.7	36.3
	5.0	18.4	11.0	50.8	7.4	74.2	38.7	6.8	37.0
3. Boston, Mass.	1.0	7.2	4.3	50.8	2.9	53.4	20.4	-1.9	21.2
	2.0	8.5	5.1	51.0	3.4	58.8	22.1	-1.4	32.9
	3.0	9.1	5.5	51.4	3.7	61.6	23.1	-1.2	37.7
	4.0	9.5	5.7	51.0	3.8	63.3	23.6	-1.1	40.2
4. Caribou, Maine	1.0	7.4	4.5	51.7	3.0	50.6	14.5	-11.1	20.0
	2.0	8.7	5.2	50.8	3.5	55.1	16.1	-10.9	31.2
	3.0	9.3	5.6	51.2	3.7	58.1	17.0	-10.7	36.0
	4.0	9.7	5.8	50.8	3.9	59.6	17.5	-10.6	38.4
5. Santa Maria, Calif.	1.0	11.1	6.6	50.5	4.5	46.6	28.4	11.3	20.2
	2.0	12.9	7.7	50.7	5.2	51.9	31.0	11.6	31.4
	3.0	13.9	8.3	50.8	5.6	54.7	32.3	11.8	36.1
	4.0	14.4	8.6	50.8	5.8	56.3	33.0	12.0	38.6
	5.0	14.8	8.8	50.5	5.9	57.3	33.5	12.0	40.1

Table A-2. Sunwizard Simulations Using Actual Water Temperatures

Location	Reflector Radius (m)	Q_{coll} (GJ)	Q_{del} (GJ)	System Thermal Efficiency (%)	Q_{loss} (GJ)	Storage T_{max} (^{o}C)	Tank $\overline{T}$ (^{o}C)	Temp. T_{min} (^{o}C)	Fraction of Q_{coll} from Reflector
1. Albuquerque, N. Mex.	1	14.2	7.0	41.9	7.2	58.1	38.0	16.6	18.3
	2	16.3	8.2	42.8	8.1	64.0	40.9	17.5	28.7
	3	17.4	8.9	43.5	8.5	67.1	42.4	18.0	33.2
	4	18.0	9.2	43.4	8.8	68.9	43.3	18.2	35.5
2. Boston, Mass.	1	7.2	4.1	48.4	3.1	53.9	21.2	-0.9	21.2
	2	8.5	4.8	48.0	3.6	59.3	22.9	-0.5	32.9
	3	9.1	5.2	48.6	3.9	62.1	23.8	-0.2	37.7
	4	9.5	5.5	49.2	4.1	63.7	24.4	-0.1	40.2
3. Fort Worth, Tex.	1	10.0	5.8	49.3	4.1	56.6	32.5	5.5	20.9
	2	11.7	6.9	50.1	4.8	61.4	34.8	5.9	32.3
	3	12.6	7.4	49.9	5.2	64.0	36.0	6.1	37.1
	4	13.1	7.7	50.0	5.4	65.5	36.8	6.3	39.5
4. Washington, D.C.	1	7.9	3.6	38.7	4.3	54.9	27.3	3.5	21.4
	2	9.3	4.5	41.1	4.8	59.4	29.2	4.1	33.1
	3	10.0	4.9	41.7	5.1	61.8	30.2	4.4	38.0
	4	10.4	5.2	42.5	5.3	63.2	30.8	4.6	40.5

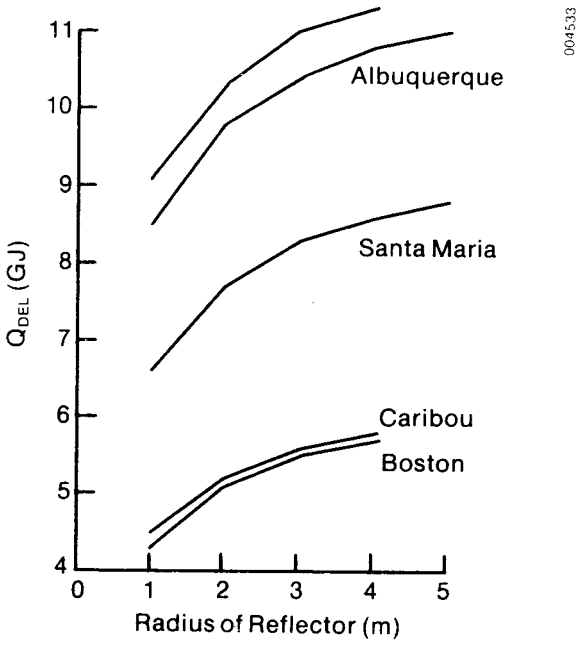

Figure A-2. Performance of Sunwizard System

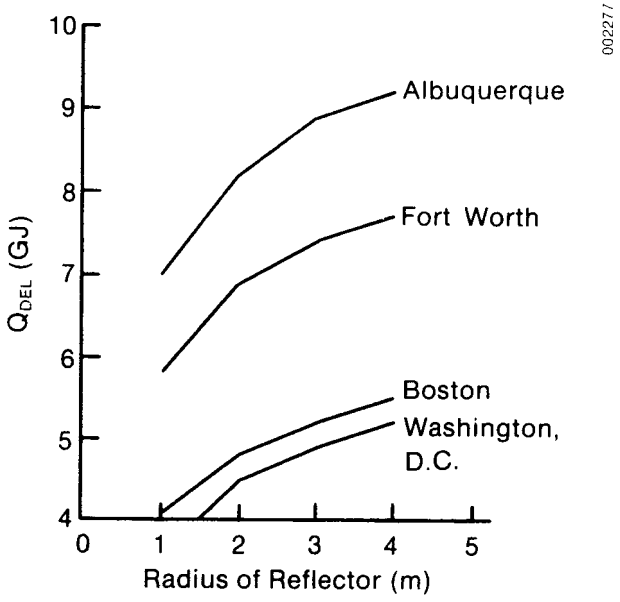

Figure A-3. Sunwizard Performance Using Actual Water Temperatures

Application of this system to space heating loads might also be satisfactory. The sensitivity of the performance of this system to temperature can be estimated from two of the results generated later in this appendix.

In a simulation run for Albuquerque, the cold water supply temperature was 10°C and the system efficiency was 53.4% with a 4 m reflector. Rerunning the Albuquerque simulation using the water temperature of 22.2°C gives a system efficiency of 43.4%. The sensitivity of the system efficiency to cold water supply temperature is [(43.4 - 53.4)%]/[(22.2 - 10)°C] = -0.82%/°C; a 1% increase in the inlet water temperature reduces the efficiency by about 0.8%. If a heating system requires a minimum temperature of 30°C to operate, the calculated system efficiency is still a respectable 35.2%. The major limitation on this system for space heating is that each unit requires an unobstructed area for a reflector and weighs over 1000 lb, so that space or structural (for roofs) limitations could prohibit its use. Also, the useful energy delivery from each unit would be low because of the reduced efficiency from increased inlet water temperature and the seasonal nature of heating loads.

A.2 FIRST-ORDER ANALYSIS

As a first-order analysis, the heat loss coefficient was considered. The final value of U_L = 2.84 W/m^2 °K (0.5 Btu/h ft^2 °F) claimed by the Sunwizard literature was compared with a table of conductances found in Chapman (1974).

Table A-3. Air Space Conductance Values

Mean Temperature of Air Space [°C (°F)]	WT [°C (°F)]	Conductance [W/m² K (Btu/h ft² °F)]		ε = 0.9
		ε = 0.167	ε = 0.67	
10 (50)	5.6 (10)	2.39 (0.42)	3.92 (0.69)	0.99
10 (50)	16.7 (30)	2.95 (0.52)	4.49 (0.79)	1.08
32.2 (90)	5.6 (10)	2.61 (0.46)	4.54 (0.80)	1.16

The table, reproduced here as Table A-3, gives average conductance values for combined radiation and free convection in air spaces such as those found in walls. The values are suitable for air spaces between 1.9 cm and 10.2 cm (3/4 in. and 4 in.) thick. Chapman assumed that the emittances were the same for both surfaces, but they can be used for surfaces with different emittances since the emittances are computed by $(1/\varepsilon_1 + 1/\varepsilon_2)$. For the Sunwizard system the emittance of the tank is given as ~0.08. Assuming that the acrylic shell has $\varepsilon \simeq 1$, $1/\varepsilon_1 + 1/\varepsilon_2$ $(1/0.08 + 1/1) = 13.5$, which is equivalent to $(1/\varepsilon_1 + 1/\varepsilon_2)$ with $\varepsilon_2 \simeq 0.15$. Thus the results in Table A-3 for $\varepsilon = 0.167$ are closest to the Sunwizard case. The table values at higher temperatures are within 10% of 0.5 Btu/h ft² °F, which agrees with the Sunwizard literature. Thus this value seems reasonable.

The temperature decay characteristics of the tank were also checked using the loss coefficient and the mass of water stored in the tank. The surface area of the tank is given as 3.25 m² (35 ft²). For 454 L (120 gal) of water, a heat capacity of about 1.8×10^6 J/°C (950 Btu/°F) can be calculated. With the addition of the tank heat capacity, the value 1.95×10^6 J/°C (1028 Btu/°F), used in the technical information package is reasonable. Using Sunwizard's values, the time constant of the system Mc_p/UA is 58.7 h. This means that the temperature difference between the tank and ambient will decay to 1/e of the original temperature difference in just less than 2.5 days.

The final check was of the temperature rise experienced by this system during a typical hour of sunlight. Taking a value of 946.5 W/m² (300 Btu/ft² h) for the total horizontal irradiance, an exposed area of approximately 1.39 m² (15 ft²), and an absorptance-transmittance product of 0.85, the energy input for an hour would be (946.5 W/m²)(1.39 m²)(0.85)(1 h) = 1118 W (3825 Btu).

This would cause an increase of 2.1°C (3.7°F) in the tank temperature. If the average tank temperature were 38°C (100°F) and the ambient temperature were 10°C (50°F), a loss of 256 W (875 Btu) would occur over the same hour, leading to a net increase of 865 W (2950 Btu) and a net temperature increase of 1.6°C (2.9°F).

If a ground reflector added an additional 50% to the energy input, the net temperature increase would be 2.6°C (4.7°F) in one hour.

A.3 ENHANCEMENT FROM DIFFUSE REFLECTORS

The Sunwizard technical information package presents a long and detailed analysis of reflector enhancement for many configurations. The results can best be summarized by considering the amount of extra energy made available to the system by use of the reflector. Sunwizard's literature states that a 61-m (20-ft) diameter diffuse reflector can increase the output of the Sunwizard system by 60%-100%. To check this, the contribution of a flat, circular, completely diffuse reflector was calculated.

The analysis consists of calculating the view factor from the reflector to a vertical cylindrical tank at the center of the reflector. Letting subscript 1 refer to the reflector surface and subscript 2 refer to the tank surface, the view factor can be expressed as

$$F_{1\to 2} = \frac{1}{A_1} \int_{A_1} \int_{A_2} \frac{\cos \phi_1 \cos \phi_2}{\pi |\vec{r}|^2} \, dA_1 \, dA_2 \, , \qquad \text{(A-1)}$$

where

A_1 = area of the reflector

A_2 = area of the tank

dA_1 = area element on the reflector

dA_2 = area element on the tank

$\vec{r}$ = vector from area element dA_1 to dA_2

ϕ_1 = angle between $\vec{r}$ and the vector normal to the reflector surface at dA_1, $\hat{n}_1$

ϕ_2 = angle between $\vec{r}$ and the vector normal to the tank surface at dA_2, $\hat{n}_2$.

Figure A-4 shows the geometry of this calculation.

The cylindrical coordinate system shown in Figure A-4 was used to calculate the integrals, and the Cartesian system was used to calculate the length of $\vec{r}$ and to evaluate the cosine terms using the dot product between the surface normal vectors and $\vec{r}$.

Area element dA_1 is located at $(x_1, y_1, z_1) = (r_1, \cos \theta_1, r_1 \sin \theta_1, 0)$, and element dA_2 is located at $(x_2, y_2, z_2) = (r_0 \cos \theta_2, r_0 \sin \theta_2, z)$. Thus, $\vec{r}$ is $(x_2 - x_1, y_2 - y_1, z_2 - z_1)$, and

$$|\vec{r}|^2 = (r_0 \cos \theta_2 - r_1 \cos \theta_1)^2 + (r_0 \sin \theta_2 - r_1 \sin \theta_1)^2 + z^2 \, , \qquad \text{(A-2)}$$

$$\cos \phi_1 = \frac{(\hat{r})(\hat{n}_1)}{|\vec{r}|} = \frac{(x_2 - x_1, y_2 - y_1, z_2 - z_1)(0, 0, 1)}{|\vec{r}|} = \frac{z}{|\vec{r}|} \, , \qquad \text{(A-3)}$$

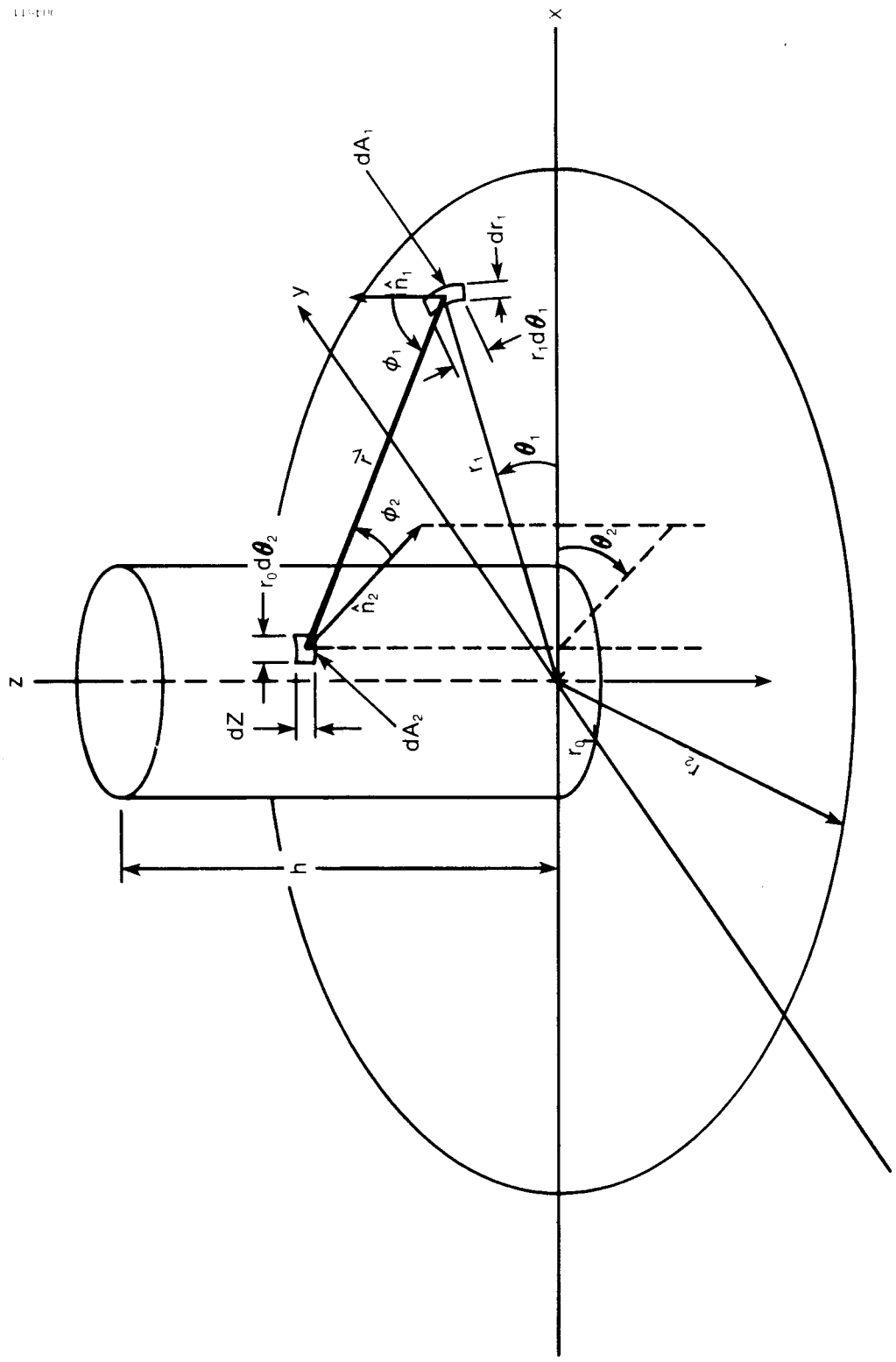

Figure A-4. Geometry for View Factor Calculations

$$\cos \phi_2 = \frac{(-\hat{r})(\hat{n}_2)}{|\vec{r}|} = \frac{-(x_2 - x_1, y_2 - y_1, z_2 - z_1)(\cos \theta_2, \sin \theta_2, 0)}{|\vec{r}|}, \quad \text{(A-4a)}$$

$$\cos \phi_2 = \frac{(-\hat{r})(\hat{n}_2)}{|\vec{r}|} = \frac{-(x_2 - x_1)\cos \theta_2 - (y_2 - y_1)\sin \theta_2}{|\vec{r}|}. \quad \text{(A-4b)}$$

The area element $dA_1 = r_1 dr_1 d\theta_1$ and area element $dA_2 = r_0 d\theta_2 dz$.

The integral was calculated by summing the contributions from area elements at a radius r_1 to a single element at a height z on the cylinder using these equations. Because of the cylindrical symmetry, the integral over each of the elements at a given height on the cylinder is the same, so the value for one element was simply multiplied by the number of elements to give the total integral for that height. Finally, the values at each height were summed to give the total integral for a given r_1 loop in which this occurs. The results were printed and plotted as a function of r_1.

Results from the simulation are presented in Table A-4 and in Figure A-5. In Table A-4 F is the shape factor $F_{1\to2}$ and F * A_1 corresponds to $F_{1\to2}A_1$. This table shows that the maximum enhancement from such a horizontal reflector approaches about 1.2 m^2 (12.9 ft^2) of additional horizontal collector area, compared with the total tank area for absorption of about 3.25 m^2 (35 ft^2).

A.4 SOLIPH MODEL OF SUNWIZARD SYSTEM

To find the annual performance of this system and the enhancement from a horizontal reflector, a SOLIPH-like model for the system was constructed.

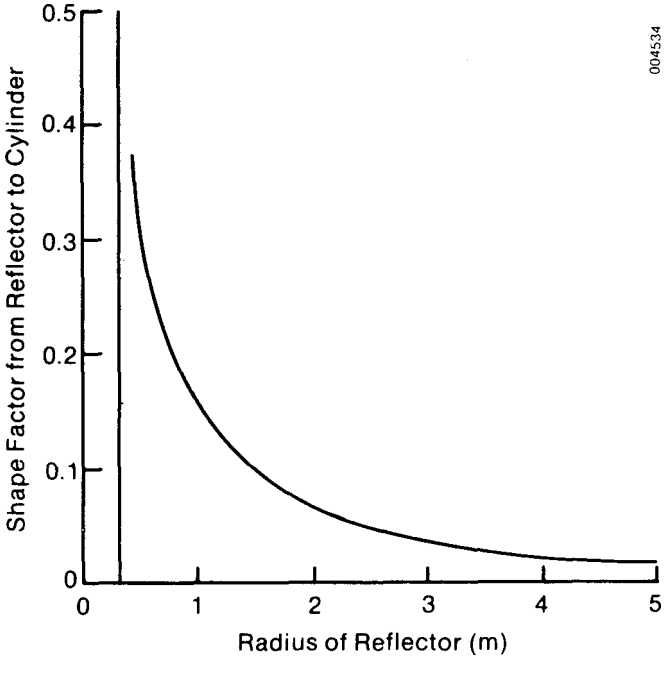

Figure A-5. Slope Factor as a Function of the Reflector Radius

Table A-4. Shape Factors as a Function of Radial Distance r

r_1 (m)	F	F * A_1
0.40	0.3742	0.0823
0.50	0.2947	0.1481
0.60	0.2473	0.2098
0.70	0.2137	0.2685
0.80	0.1877	0.3244
0.90	0.1669	0.3776
1.00	0.1498	0.4281
1.10	0.1353	0.4759
1.20	0.1228	0.5209
1.30	0.1120	0.5632
1.40	0.1026	0.6028
1.50	0.0943	0.6401
1.60	0.0870	0.6750
1.70	0.0804	0.7076
1.80	0.0746	0.7382
1.90	0.0693	0.7668
2.00	0.0646	0.7936
2.10	0.0603	0.8187
2.20	0.0564	0.8422
2.30	0.0529	0.8642
2.40	0.0497	0.8849
2.50	0.0467	0.9043
2.60	0.0440	0.9226
2.70	0.0415	0.9398
2.80	0.0393	0.9561
2.90	0.0372	0.9714
3.00	0.0352	0.9858
3.10	0.0334	0.9995
3.20	0.0318	1.0124
3.30	0.0302	1.0247
3.40	0.0288	1.0363
3.50	0.0274	1.0474
3.60	0.0262	1.0579
3.70	0.0250	1.0678
3.80	0.0239	1.0774
3.90	0.0229	1.0864
4.00	0.0219	1.0951
4.10	0.0210	1.1034
4.20	0.0202	1.1113
4.30	0.0194	1.1189
4.40	0.0186	1.1261
4.50	0.0179	1.1331
4.60	0.0172	1.1397
4.70	0.0166	1.1461
4.80	0.0160	1.1523
4.90	0.0154	1.1582
5.00	0.0149	1.1639

(Because the system is much different from a typical solar energy system, many changes had to be made in SOLIPH, and the final program bears little resemblance to SOLIPH. The two most important changes were in calculating the energy collected and in eliminating an iteration, since a closed-form solution could be derived for each hour.) The development of the algorithm for computing energy collected and the closed-form solution follow.

A.4.1 Solar Energy Incident on a Sunwizard System

Figure A-6 shows the geometry of the calculations. The reflector is assumed to be a perfectly diffuse reflector with a solar reflectance of ρ_s. The diffuse radiation is assumed to be isotropic. The only consideration given to the effect of the tank shadow is to deduct from the total the amount of reflector area that has no beam radiation when considering the reflector contribution. The sun is at an elevation angle of α, and because of the symmetry of the system, no consideration of azimuth is required. If $(\tau\alpha)_s$ is the effective transmittance-absorptance product of the system (0.95 for the Sunwizard), the total radiation absorbed by the tank can be written as:

$$\dot{Q}_{coll} = (\tau\alpha)_s[\dot{Q}_{top} + \dot{Q}_{beam\ side} + \dot{Q}_{diffuse\ side} + \dot{Q}_{reflected\ side}] \ . \qquad (A\text{-}5)$$

The radiation on the top of the tank is the area of the tank top multiplied by the horizontal irradiance:

$$\dot{Q}_{top} = I_h \pi r_0^2 \ . \qquad (A\text{-}6)$$

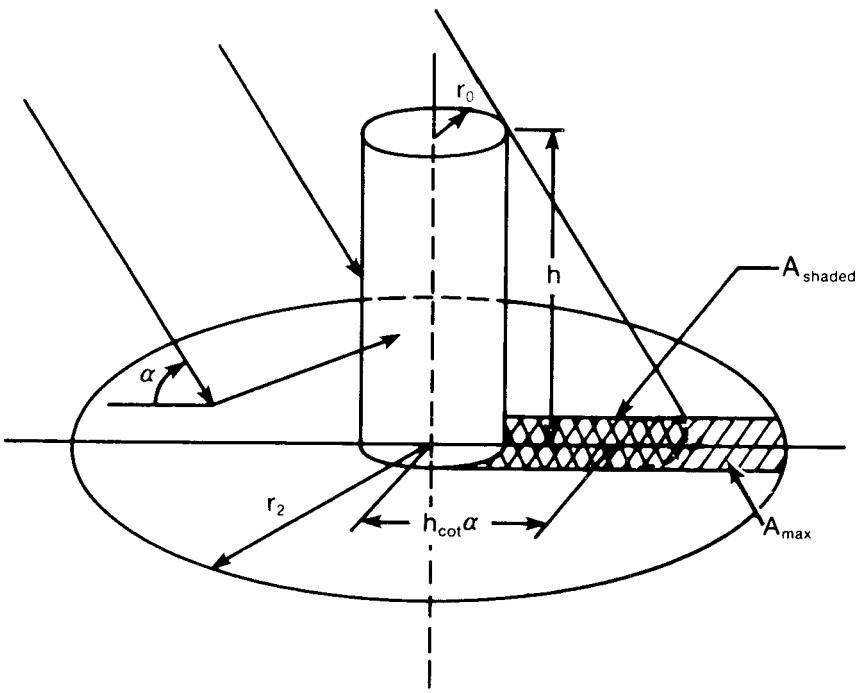

Figure A-6. Geometry for Incident Radiation Calculation

The contribution of beam radiation on the side of the tank is the beam irradiance multiplied by the projected area of the tank side:

$$\dot{Q}_{\text{beam side}} = I_b 2 r_0 h \cos \alpha \ . \tag{A-7}$$

The diffuse radiation on the sides of the tank can be easily calculated since each element of area sees half of a hemisphere of sky, and since the diffuse irradiance is assumed to be isotropic. Thus,

$$\dot{Q}_{\text{diffuse side}} = (I_h - I_b \sin \alpha)\, \pi r_0 h/2 \ . \tag{A-8}$$

Finally, the radiation reflected from the diffuse reflector can be calculated with a slight complication arising because of the shadow of the tank. For a first-order approximation, it was assumed that the portion of the reflector in the shade of the tank would absorb only the diffuse portion of the incident radiation. Thus,

$$\dot{Q}_{\text{reflected side}} = I_h \rho_s F_{1\to 2} A_{\text{unshaded}} + (I_h - I_b \sin \alpha)\, \rho_s F_{1\to 2} A_{\text{shaded}} \ . \tag{A-9}$$

A_{shaded} refers to the area of reflector shaded by the tank, which is

$$A_{\text{shaded}} = \min \left\{ 2 r_0 h \cot \alpha,\ r_2^2 \sin^{-1} (r_0/r_2) + r_0 (r_2^2 - r_0^2)^{1/2} - \frac{\pi r_0^2}{2} \right\} \tag{A-10}$$

The first term in the curly brackets is the area of the shadow at sun elevation α, and the second is the maximum area of reflector that can be shaded by the tank (since as $\alpha \to 0$, $\cot \alpha \to \infty$). The unshaded area of reflector is given by

$$A_{\text{unshaded}} = \pi (r_2^2 - r_0^2) - A_{\text{shaded}} \ . \tag{A-11}$$

Substituting Eqs. A-6 to A-9 into Eq. A-5 the total radiation collected by the system is

$$\begin{aligned} \dot{Q}_{\text{coll}} = (\tau\alpha)_s \big(& I_h \pi r_0^2 + 2 I_b r_0 h \cos \alpha + (I_h - I_b \sin \alpha)\, \pi r_0 h/2 \\ & + \rho_s F_{1\to 2} \left\{ I_h [\pi (r_2^2 - r_0^2) - A]_{\text{shaded}} + (I_h - I_b \sin \alpha)\, A_{\text{shaded}} \right\} \big) \end{aligned} \tag{A-12}$$

where A_{shaded} is given by Eq. A-10 above.

A.4.2 Model of Sunwizard System

The analytical model of this system is much like that for the storage component in SOLIPH, with the addition of energy input directly as radiation.

Figure A-7 shows a schematic of the model used in this analysis. An energy balance on the tank yields

$$Mc_p \frac{dT}{dt} = \dot{Q}_{coll} + \dot{m}c_p T_{in} - \dot{m}c_p T - UA(T - T_a) , \qquad (A-13)$$

where

Mc_p = heat capacity of the system (J/K)

T = temperature of the water in the tank (^oC)

t = time (s)

$\dot{Q}_{coll}$ = energy collected, from Eq. A-12 (W)

$\dot{m}c_p$ = heat capacity flow rate of the load (W/K)

T_{in} = cold water supply temperature (^oC)

UA = heat loss coefficient of the tank (W/K)

T_a = ambient temperature (^oC).

Letting

$$\beta = \frac{\dot{Q}_{coll} + \dot{m}c_p T_{in} + UAT_a}{Mc_p}$$

and

$$\gamma = \frac{\dot{m}c_p + UA}{Mc_p} ,$$

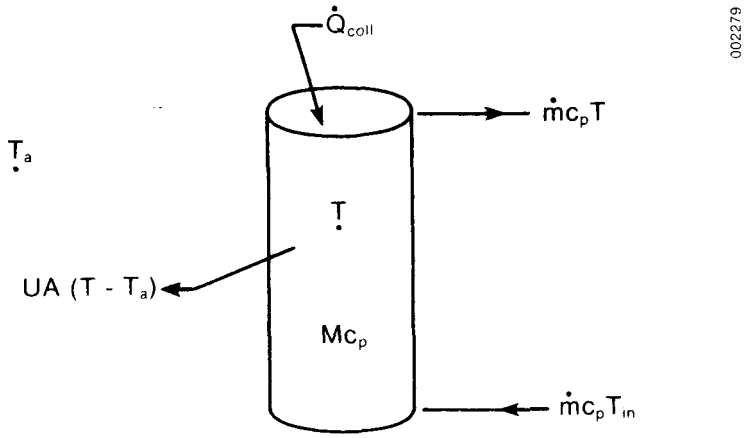

Figure A-7. Thermal Model of Sunwizard System

then $dT/dt = \beta - \gamma T$, which is easily integrated with initial condition $T(0) = T_o$ to yield

$$T(t) = \beta/\gamma + (T_o - \beta/\gamma)\, e^{-\gamma t} . \qquad \text{(A-14)}$$

As in the SOLIPH storage tank model, this can be integrated over time to yield an average tank temperature over the time step dt as follows:

$$\overline{T} = \frac{\int_o^{dt} T(t)\, d\tau}{dt} = \beta/\gamma - (T_o - \beta/\gamma)\, \frac{e^{-dt} - 1}{\gamma dt} . \qquad \text{(A-15)}$$

The energy delivered by the system over a time step is

$$Q_{del} = \dot{m} c_p (\overline{T} - T_{in}) dt . \qquad \text{(A-16)}$$

The energy lost as heat to the atmosphere is

$$Q_{loss} = \dot{m} c_p (\overline{T} - T_a) dt . \qquad \text{(A-17)}$$

In the computer model, Eq. A-14 is used to calculate the storage tank temperature at the end of each time step, and Eqs. A-12, A-16, and A-17 are used to calculate the energy collected, delivered, and lost by the system each hour.

A.4.3 Results from Computer Modeling of Sunwizard System

Simulations of the Sunwizard system for various reflector sizes and in several locations were run. For comparison with the performance of a conventional hot water system, the same load profile used in comparing load-side versus collector-side heat exchangers (Section 4.1) was used here. For direct comparison with those results, the same cold water supply temperature and TMY location (Albuquerque, N. Mex.) were used for one run. Runs for several cities (Albuquerque, N. Mex.; Santa Maria, Calif.; Boston, Mass.; and Caribou, Maine) using the monthly average ambient temperature for the cold water supply temperature were made. These results are summarized in Table A-1 and plotted in Figure A-2. Finally, monthly water supply temperatures (see Table A-5) were obtained and simulations for four cities (Albuquerque, N. Mex.; Boston, Mass.; Fort Worth, Tex.; and Washington, D.C.) were performed using these data. Results from these simulations are presented in Table A-2 and in Figure A-3.

A.5 REFERENCE

Chapman, Alan J., 1974, Heat Transfer, 3rd ed., Table 13.1.

Table A-5. Monthly Cold Water Supply Temperatures (at the source) in °F for 14 Cities

Location	J	F	M	A	M	J	J	A	S	O	N	D
Albuquerque	72	72	72	72	72	72	72	72	72	72	72	72
Boston	32	36	39	52	58	71	74	67	60	56	48	45
Chicago	32	32	34	42	51	57	65	67	62	57	45	35
Denver	39	40	43	49	55	60	63	64	63	56	45	37
Fort Worth	46	49	57	70	75	81	79	83	81	72	56	46
Los Angeles	50	50	54	63	68	73	74	76	76	69	61	55
Las Vegas	73	73	73	73	73	73	73	73	73	73	73	73
Miami	70	70	70	70	70	70	70	70	70	70	70	70
Nashville	46	46	53	63	66	69	71	75	75	71	58	53
New York	36	35	36	39	47	54	58	60	61	57	48	45
Phoenix	48	48	50	52	57	59	63	75	79	69	59	54
Salt Lake City	35	37	38	41	43	47	53	52	48	43	38	37
Seattle	39	37	43	45	48	57	60	68	66	57	48	43
Washington	42	42	52	56	63	67	67	78	79	68	55	46

APPENDIX B

ANALYSIS OF THERMAL PROTECTION FOR PLASTIC PIPE

Since polybutylene pipe has a maximum operating temperature of 200°F, it must be protected from high stagnation temperatures if it is used in low-cost solar hot water/space heating systems. One way to protect it is to use a short length of copper pipe between the collectors and the plastic pipe. Determining the appropriate length of copper pipe is addressed here.

This appendix gives the solutions for the two cases of bare and insulated copper pipe for a drainback system (i.e., no fluid in the collector loop during stagnation conditions). The calculation of the length of the bare pipe follows a typical fin calculation with the addition of direct solar heating of the pipe. Mathematically, the problem can be summarized as follows:

O.D.E.
$$\frac{d^2T}{dx^2} - \frac{\pi D h_e}{kA_c} T = \frac{\pi D h_e}{kA_c} T_a + \frac{D\alpha I}{kA_c} , \tag{B-1}$$

B.C.
$$T_{x=o} = T_{hot} , \tag{B-2}$$

and
$$\left.\frac{dT}{dx}\right|_{x=L} = 0 \tag{B-3}$$

SOLN.
$$T(x) = \left(T_{hot} - T_a - \frac{\alpha I}{\pi h}\right) \frac{\cosh\beta(L - x)}{\cosh\beta L} + T_a + \frac{\alpha I}{\pi h} \tag{B-4}$$

and for x = L,
$$L = \frac{kA_c}{\pi D h_e} \cosh^{-1} \frac{T_{hot} - T_a - \frac{\alpha I}{\pi h_e}}{T_\ell - T_\alpha - \frac{\alpha I}{\pi h_e}} , \tag{B-5}$$

where

k = thermal conductivity of copper (W/m °C)

A_c = cross-sectional area of metal surface, approximately πDt where t is wall thickness (m^2)

D = outside diameter of copper pipe (m)

h_e = combined linearized convection/radiation heat transfer coefficient (W/m^2 °C)

T_{hot} = collector stagnation temperature (°C)

T_a = ambient temperature (°C)

T_ℓ = upper temperature limit of plastic pipe (°C)

α = short wave absorptivity of outside surface (pipe or insulation)

L = required length (m)

I = insolation (J/m^2).

For the insulated pipe, a heat balance is also done on the copper pipe alone. In this case, therefore, the solar radiation term $D\alpha I/KA_c$ does not appear in the differential equation since the solar radiation strikes the insulation. It does affect the surface temperature, however, which in turn influences the effective heat loss coefficient U_e at the metal pipe surface. To find U_e, it is necessary to iterate on the surface temperature since it is unknown. Mathematically this case can be summarized as follows:

O.D.E. $$\frac{d^2T}{dx^2} - \frac{\pi DU_e}{kA_c} T = \frac{\pi DU_e}{kA_c} T_a \ , \tag{B-6}$$

B.C. $$T\big|_{x=o} = T_{hot} \ , \tag{B-7}$$

and

$$\frac{dT}{dx}\bigg|_{x=L} = 0 \ . \tag{B-8}$$

SOLN. $$T(x) = \left(T_{hot} - T_a\right) \frac{\cosh \beta(L - x)}{\cosh \beta L} + T_a \ , \tag{B-9}$$

and for x = L,

$$L = \frac{kA_c}{\pi DU_e} \cosh^{-1} \frac{\left(T_{hot} - T_a\right)}{\left(T_\ell - T_a\right)} \ . \tag{B-10}$$

where

U_e = Effective heat transfer coefficient based on the difference between copper pipe temperature and ambient air temperature ($W/m^2\ ^oC$).

In calculating the values for L, we made the following conservative assumptions: I = 1150 W/m^2; $T_a = 46^oC$; $T_{hot} = 204^oC$; and wind velocity = 0.

The accuracy of the result is affected by the accuracy of the empirical natural convection heat transfer coefficient, the linearization of the radiative and convective heat transfer coefficients at an average pipe temperature, and the assumptions made for absorptivities and emissivities. Results should be considered no more accurate than ±20%, and values for h_e and U_e should be calculated for any given case.

Case A: Bare Copper Pipe

The geometry for the bare copper pipe is shown in Figure B-1. An energy balance can be performed on the copper pipe as follows:

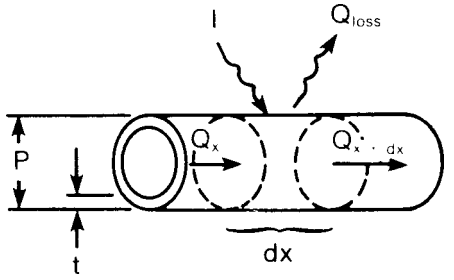

Figure B-1. Geometry for Bare Copper Pipe

$$Q_x - Q_{x+dx} = \pi D(dx)h_e(T - T_a) - \alpha D(dx)I - \frac{dQ}{dx}$$

$$= \pi Dh_e(T - T_a) - D\alpha I \ , \qquad \text{(B-11)}$$

$$Q = -kA_c \frac{dT}{dx} \text{ where } A_c \simeq \pi Dt \ ,$$

$$kA_c \frac{d^2T}{dx^2} = \pi Dh\ (T - T_a) - D\alpha I \ ,$$

$$\frac{d^2T}{dx^2} - \frac{\pi Dh_e}{kA_c} T = - \frac{\pi Dh_e}{kA_c} T_a - \frac{D\alpha I}{kA_c} \ , \qquad \text{(B-12)}$$

where h_e = the combined convection/radiation heat transfer coefficient.

The particular solution is

$$T = T_a + \frac{\alpha I}{\pi h_e}, \qquad \text{(B-13)}$$

and the homogeneous equation is

$$\frac{d^2T}{dx^2} - \frac{\pi Dh_e}{kA_c} = 0. \qquad \text{(B-14)}$$

The solution to this equation has two exponential terms with coefficients which are roots of:

$$\beta^2 - \frac{\pi Dh_e}{kA_c} = 0 \ ,$$

namely,

$$\beta = \pm \left(\frac{\pi Dh_e}{kA_c}\right)^{1/2} . \qquad \text{(B-15)}$$

The general solution is then:

$$T = C_1 e^{\beta x} + C_2 e^{-\beta x}$$

or

$$T = B_1 \sinh \beta x + B_2 \cosh \beta x \ . \qquad \text{(B-16)}$$

The total solution is the sum of the general and the particular solutions:

$$T(x) = B_1 \sinh \beta x + B_2 \cosh \beta x + T_a + \frac{\alpha I}{\pi h_e} \ . \qquad \text{(B-17)}$$

Evaluating B_1 and B_2 at the boundary conditions gives:

$$T|_{x=0} = T_{hot} = B_1 \sinh (0) + B_2 \cosh (0) + T_a + \frac{\alpha I}{\pi h_e} \ ,$$

$$B_2 = T_{hot} - T_a - \frac{\alpha I}{\pi h_e} \ , \qquad \text{(B-18)}$$

$$\left.\frac{dT}{dx}\right|_{x=L} = 0 \text{ (no axial heat conduction at copper/plastic interface)} \ ,$$

$$\beta B_1 \cosh (\beta L) + \beta B_2 \sinh (\beta L) = 0 \ ,$$

$$B_1 = -B_2 \tanh \beta L = \left(-T_{hot} + T_a + \frac{\alpha I}{\pi h_e}\right) \tanh \beta L \ , \qquad \text{(B-19)}$$

Substituting these values for B_1 and B_2 into Eq. B-17 gives

$$T = \left(-T_{hot} + T_a + \frac{\alpha I}{\pi h_e}\right) \tanh \beta L \sinh \beta x + \left(T_{hot} - T_a - \frac{\alpha I}{\pi h_e}\right) \cosh \beta x$$

$$+ T_a + \frac{\alpha I}{\pi h_e} \ ,$$

$$T = -\left(T_{hot} - T_a - \frac{\alpha I}{\pi h_e}\right) [\tanh \beta L \sinh \beta x - \cosh \beta x] + T_a + \frac{\alpha I}{\pi h_e} \ , \qquad \text{(B-20)}$$

$$\text{But } \tanh \beta L \sinh \beta x - \cosh \beta x = \frac{\sinh \beta L \sinh \beta x - \cosh \beta L \cosh \beta x}{\cosh \beta L}$$

$$= \frac{-\cosh \beta (L - x)}{\cosh \beta L}$$

Therefore

$$T(x) = \left(T_{hot} - T_a - \frac{\alpha I}{\pi h_e}\right) \frac{\cosh \beta (L - x)}{\cosh \beta L} + T_a + \frac{\alpha I}{\pi h_e} \ . \qquad \text{(B-21)}$$

At $x = L$, $T = T_\ell$ = upper temperature limit of plastic pipe:

$$T_\ell = \left(T_{hot} - T_a - \frac{\alpha I}{\pi h_e}\right) \frac{1}{\cosh \beta L} + T_a + \frac{\alpha I}{\pi h_e} , \tag{B-22}$$

$$\frac{1}{\cosh \beta L} = \frac{T_\ell - T_a - \frac{\alpha I}{\pi h_e}}{T_{hot} - T_a - \frac{\alpha I}{\pi h_e}} ,$$

and

$$L = \frac{1}{\beta} \cosh^{-1} \frac{T_{hot} - T_a - \frac{\alpha I}{\pi h_e}}{T_\ell - T_a - \frac{\alpha I}{\pi h_e}} . \tag{B-23}$$

To solve for L, we need to determine h_e (per m of pipe):

$$Q_{conv} + Q_{rad} = h_e(\overline{T} - T_a)\, \pi D . \tag{B-24}$$

We will use the log mean pipe temperature

$$\overline{T} = T_a + \frac{[T_\ell - T_a] - [T_{hot} - T_a]}{\ln \frac{T_\ell - T_a}{T_{hot} - T_a}} . \tag{B-25}$$

This should be a conservative approximation.

Using:

$$T_{hot} = 400^oF = 204^oC = 477\ K ,$$

$$T_\ell = 200^oF = 93^oC = 366\ K ,$$

$$T_a = 115^oF = 46^oC = 319\ K ,$$

$$D = 0.0159\ m\ (0.625\ in.) ,$$

$$T = 0.00102\ m\ (0.040\ in.) ,$$

we can compute $\overline{T}$ as follows:

$$\overline{T} = \frac{[200 - 115] - [400 - 115]}{\frac{200 - 115}{400 - 115}} = 280^oF = 138^oC = 411\ K .$$

Then the radiative heat term is

$$Q_{rad} = \sigma A \left(\varepsilon_1 \overline{T}^{\,4} - a_1 T_a^4\right) . \qquad \text{(B-26)}$$

Assuming $\varepsilon_1 \approx a_1 \approx 0.30$:

$$Q_{rad} = 5.67 \times 10^{-8}\ \text{W/m}^2\ \text{K}^4 \cdot \pi\,(0.0159\text{m})(0.30)[(411^4 - 319^4(\text{K}^4)]$$

$$= 15.4\ \text{W per m of pipe} .$$

In English units, $h_f = 0.27\left(\frac{\Delta T}{D}\right)^{1/4}$, and the convective heat term is:

$$Q_{conv} = 0.27\left(\frac{\Delta T}{D}\right)^{0.25} \pi D\,(\Delta T)$$

$$= 0.27\left(\frac{300 - 115^{\circ}\text{F}}{0.0521\ \text{ft}}\right)^{1/4} \pi\,(0.0521\ \text{ft}) \times 1\ \text{m} \times \frac{1\ \text{ft}}{0.3048\ \text{m}}\,(280 - 115)$$

$$= 180\ \text{Btu/h per m of pipe} . \qquad \text{(B-27)}$$

$$Q_{conv} = 180 + 0.293\,\frac{\text{W}}{\text{Btu/h}} = 52.7\ \text{W/m of pipe}$$

$$Q_{conv} + Q_{rad} = 52.7\ \text{W} + 15.4\ \text{W} = 68.1\ \text{W}$$

Then

$$h_e(\overline{T} - T_a)\,\pi D = 68.1\ \text{W} , \qquad \text{(B-28)}$$

or

$$h_e = \frac{68.1\ \text{W}}{(138^{\circ}\text{C} - 46^{\circ}\text{C})\pi(0.0159)} = 14.8\ \text{W/m}^2\ ^{\circ}\text{C} .$$

Using $I = 1150\ \text{W/m}^2$, $\alpha = 0.30$:

$$\frac{\alpha I}{\pi h_e} = \frac{0.30\,(1150)}{\pi(14.8)} = 7.4^{\circ}\text{C}$$

Now the thermal conductivity for copper is

$$k_{cu} = 386\ \text{W/m}\ ^{\circ}\text{C} ,$$

and so

$$\beta = \left(\frac{\pi D h_e}{k A_c}\right)^{1/2} = \left[\frac{\pi\,(0.159)(15.3)}{386 \times \pi \times 0.0159 \times 0.00102}\right]^{1/2} = 6.13\ \text{m}^{-1} .$$

Then, using Eq. B-23,

$$L = \frac{1}{\beta} \cosh^{-1} \frac{T_{hot} - T_a - \frac{\alpha I}{\pi h_e}}{T_\ell - T_a - \frac{\alpha I}{\pi h_e}},$$

$$= \frac{1}{6.13} \cosh^{-1} \frac{(204 - 46 - 7.4)}{(93.3 - 46 - 7.4)},$$

and finally L = 0.327 m (12.9 in., or about 1 ft).

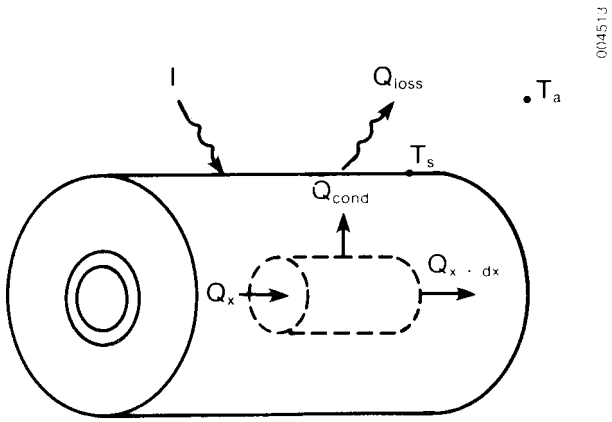

Figure B-2. Insulated Copper Pipe

Case B: Insulated Copper Pipe

Figure B-2 shows the insulated copper pipe case. Since the temperature along the copper pipe is the quantity of interest, a heat balance is performed on the metal pipe itself. The insulation and solar radiation will affect the conduction loss from the copper.

$$Q_x - Q_{x+dx} = \pi D(dx)U_e(T - T_a)$$

$$-\frac{dQ}{dx} = \pi D U_e (T - T_a) \qquad \text{(B-29)}$$

$$kA_c \frac{d^2T}{dx^2} = \pi D U_e (T - T_a)$$

$$\frac{d^2T}{dx^2} - \frac{\pi D U_e}{kA_c} T = -\frac{\pi D U_e}{kA_c} T_a \qquad \text{(B-30)}$$

The particular solution is $T = T_a$.

By analogy with Case A,

$$T = (T_{hot} - T_a) \frac{\cosh \beta (L - x)}{\cosh \beta L} + T_a \,. \qquad \text{(B-31)}$$

and

$$L = \frac{1}{\beta} \cosh^{-1} \frac{T_{hot} - T_a}{T_e - T_a} \qquad \text{(B-32)}$$

To find the insulation surface temperature T_s and the conduction heat loss, we must solve for each in terms of T_s and iterate on T_s until the energy balance becomes $Q_{cond} + Q_{solar} = Q_{conv} + Q_{rad}$.

Then

$$Q_{cond} = \frac{\overline{T} - T_s}{\left[\frac{\ln(r_2/r_1)}{2\pi kL}\right]}, \qquad \text{(B-33)}$$

$$K_{ins} = 0.21 \text{ Btu/h ft } ^{o}F = 0.0364 \text{ W/m K},$$

$$Q_{cond} = \frac{411 \text{ K} - T_s}{\left[\frac{\ln\left(\frac{0.0333 \text{ m}}{0.00794 \text{ m}}\right)}{2\pi\ (0.0364)(1 \text{ m})}\right]} = 0.160\ (411 - T_s)\ .$$

In English units, the convective heat term is:

$$Q_{conv} = 0.27\ \left(\frac{T_s - T_a}{D}\right)^{1/4} \pi D(T_s - T_a)$$

$$= 0.27\ \left(\frac{T_s - 115}{0.219}\right)^{1/4} \times \pi \times 0.219\ (T_s - 115)$$

$$= 0.271\ (T_s - 115)^{1/4} \text{ Btu/h ft of pipe}\ . \qquad \text{(B-34)}$$

Converting the formula to K and SI units gives:

$$Q_{conv} = 0.543(T_s - 319)^{1/4} \text{ W/m of pipe}\ .$$

Now,

$$Q_{solar} = \alpha ID. \qquad \text{(B-35)}$$

Using $\alpha = 0.20$ for insulation,

$$Q_{solar} = 0.20\ (1150 \text{ W/m}^2)(0.067)$$
$$= 15.4 \text{ W/m of pipe}\ . \qquad \text{(B-36)}$$

$$Q_{rad} = \sigma A\ (\varepsilon T_s^{\,4} - \varepsilon T_a^{\,4})$$
$$= 5.67 \times 10^{-8} \times \pi \times 0.067 \text{ m } (0.20)(T_s^{\,4} - 319^4)$$
$$= 2.39 \times 10^{-9}\ (T_s^{\,4} - 1.036 \times 10^{10})\ . \qquad \text{(B-37)}$$

$$Q_{cond} + Q_{solar} = Q_{conv} + Q_{rad} \qquad \text{(B-38)}$$

$$0.160\ (411 - T_s) + 15.4 = 0.543\ (T_s - 319)^{1.25} + 2.39 \times 10^{-9}\ (T_s^4 - 1.036 \times 10^{10})$$

Iterating on T_s, at T_s = 338 K, 11.7 + 15.4 ≃ 21.5 + 6.4.

So $Q_{cond} = U_e A\ (149^oC - 46^oC)$.

Solving for U_e gives:

$$U_e = \frac{11.7\ W}{\pi(0.0159\ m)(1\ m)(149 - 46^oC)}$$

$$= 2.27\ W/m^2 .$$

Thus:

$$\beta = \left(\frac{\pi D U_e}{k A_c}\right)^{1/2} = \left[\frac{\pi(0.0159)(2.27)}{386\ v\ 5.09 \times 10^{-5}}\right]^{1/2} = 2.40\ \bar{m}^1$$

$$L = \frac{1}{\beta} \cosh^{-1} \frac{T_{hot} - T_a}{T_e - T_a}$$

$$= \frac{1}{2.40} \cosh^{-1} \frac{204 - 46}{93.3 - 46}$$

$$= 0.782\ m\ (or\ 31\ in.) .$$

To protect the plastic pipe under the worst conditions it must be isolated with roughly 0.33 m (1 ft) of bare 1/2-in. Cu pipe or 0.78 m (2-1/2 ft) of insulated (R-4) pipe. The latter is preferred since it will not greatly increase operating thermal losses.

APPENDIX C

EXPERIMENTAL MEASUREMENT OF PUMP EFFICIENCIES

This appendix provides a discussion of the instrumentation used for the testing of pumps and the results of the tests.

C.1 FLOWMETER

Originally a Ramapo target meter was used to measure the flow rate. However, the pressure drop was too high to obtain a significant number of data points along the pump curve. Maximum flow obtained with the Grundfos pump on high speed (speed 3) with the Ramapo meter was about 1.0×10^{-4} m^3/s (1.6 gpm). With the change in configuration and the use of the Cox turbine meter, maximum flow obtained with this pump was about 2.4×10^{-4} m^3/s (3.8 gpm). The Cox turbine meter can be mounted at any orientation and has flow straighteners preceding it. The manufacturer recommends a minimum of ten diameters of the same size tubing as the fittings to proceed the flowmeters. With 1.27-cm (1/2-in.) fittings, the recommended length is 0.127 m (5 in.). Tubing with a diameter of 1.27 cm was situated so that 0.254 m (10 in.) tubing preceded the flowmeter and 0.24 m (9.5 in.) followed the flowmeter. Results of the flowmeter calibration are shown in Figure C-1. Two standard deviations, or a 95% confidence level, result in 0.8% uncertainty in the flow measurement. This is $\pm 2.0 \times 10^{-7}$ m^3/s (±0.032 gpm) at 2.5×10^{-4} m^3/s (4 gpm) and $\pm 2.5 \times 10^{-7}$ m^3/s (±0.004 gpm) at 3.2×10^{-6} m^3/s (0.5 gpm).

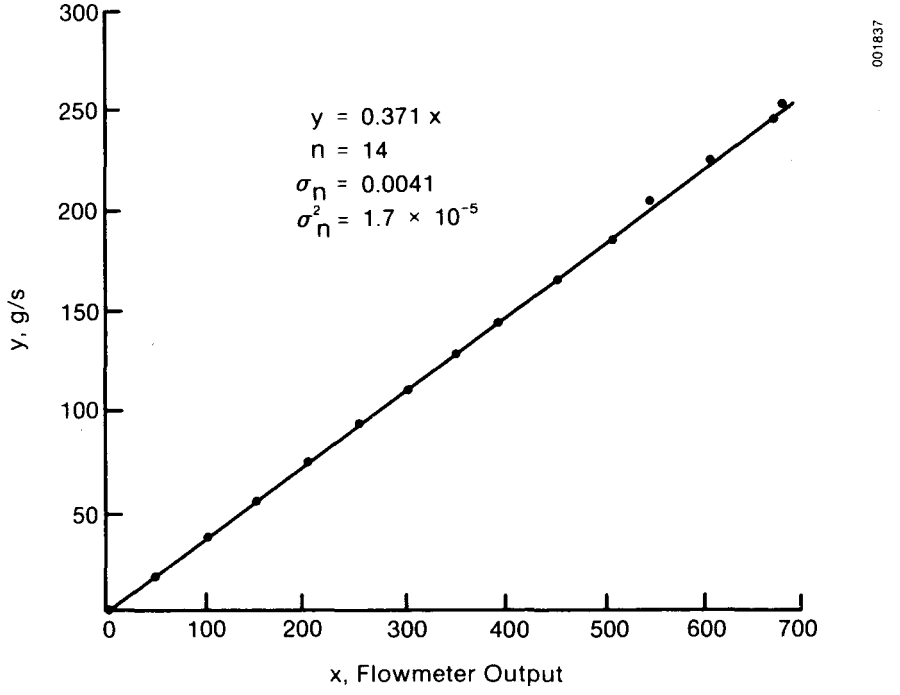

Figure C-1. Flowmeter Calibration

The flowmeter has a specified pressure drop of 82.7 kPa (12 psi or 28 ft of water) at 6.0×10^{-4} m^3/s (9.5 gpm) and varies in approximate proportion to the square of the volumetric flow $\dot{V}$. Therefore,

$$\Delta P \simeq a\dot{V}^2 .$$

Since ΔP = 82.7 kPa at 6.0×10^{-4} m^3/s (28 ft of water at 9.5 gpm),

$$a = \Delta P/\dot{V}^2 = 2.30 \text{ kPa}/(m^3 \text{ s})^2 \text{ (0.31 ft of water/gpm}^2).$$

The approximate pressure drop through the turbine meter is shown in Table C-1.

Table C-1. Turbine Meter Head-Flow Characteristics

Flow		ΔP	
10^{-5} m^3/s	gpm	kPa	ft of water
0	0	0	0
3.2	0.5	0.3	0.1
6.3	1.0	0.9	0.3
9.5	1.5	2.1	0.7
12.6	2.0	3.6	1.2
15.8	2.5	5.7	1.9
18.9	3.0	8.4	2.8
22.1	3.5	11.4	3.8
25.2	4.0	14.6	4.9
31.5	5.0	23.0	7.7

C.2 PRESSURE TRANSDUCERS

Originally three Viatran absolute pressure transducers (Table C-2) were used. The first transducer (210769) was mounted at the top of the system to record the vacuum at the top. It did not produce an output signal and was rejected. Two others (171411 and 210809) were connected with the transducers on the same level (to eliminate hydrostatic differences) and tests were run on four pumps (three centrifugal and one small drill-operated pump). After repeated attempts to calibrate them, they were also rejected.

Table C-2. Viatran Pressure Transducers

Serial Number	Model Number	Range	Location
210769	218-24	0-345 kPa (0-50 psia)	top of system
171411	218-24	0-345 kPa (0-50 psia)	pump inlet
210809	218-24	0-690 kPa (0-100 psia)	pump outlet
17861181	220-24	±69 kPa (±10 psid)	across pump

A Viatran differential pressure transducer (17861181) was installed to replace the two absolute pressure transducers. The zero adjustment and span adjustment were set and remained fairly constant. They generally were within a few hundredths of a psi of their specified value. It was later found that the differential pressure transducer did not reach its full scale. Although the zero and span were adjusted properly, the output did not match the output of two pressure gauges that properly registered atmospheric and hydrostatic pressure.

The 24-V power supply to the transducers was operated for at least 30 min before any testing or calibration was performed. The lines to the transducers were purged of air before any readings were taken. We worked carefully to prevent any twisting of the transducer body which produced significant changes in the reading (on the order of 1 kPa [0.1 psi]).

The pressure transducers have a specified error of ±0.4% of full scale. This includes errors due to nonlinearity, hysteresis, and nonrepeatability. The measurement uncertainty for the 0-345 kPa (0-50 psia) transducers was ±1.4 kPa (±0.2 psia). For the 690 kPa (0-100 psia) transducer,measurement uncertainty was ±2.8 kPa (±0.4 psi) and for the ±69-Pa (±10-psid) transducer, it was ±0.28 kPa (±0.04 psi).

C.3 AMMETER

A General Electric Snapper 942D hook-on meter was used to measure current. The accuracy was ±3% of full scale for 60-Hz circuits or ±0.3 A on the 10-A scale. Five windings of the pump wire were used on a 10-A scale to reduce the reading error, and the current reading to the motor was accurate to ±0.06 A. The response time was 3 s, and the instrument was used within its environmental operating specifications.

C.4 VOLTMETER

A Fluke 8024A Digital Multimeter was used to measure voltage. At 60 Hz it is accurate to ±0.75% of reading plus two digits. For a range of 200 V, a resolution of 0.1 V, and a reading of 125 V, the accuracy is ±(125 × 0.0075) + 0.2 = ±1.1 V.

The accuracy is valid for voltages between 120 V and 127 V. All of the voltages measured were in this range. The meter was calibrated on March 2, 1982 by the Fluke Technical Center.

C.5 DATA ACQUISITION SYSTEM

The data acquisition system (DAS) was a Hewlett Packard (HP) 3054 DL. Its performance was checked during May 1981. The total specified accuracy of the HP 3497 voltage measurement with 5-1/2 digits displayed for a 0.1-V range is ±(0.007% of reading + 5 counts), and for the 10-V range is ± (0.006% of reading + 1 count).

Voltages measured from the pressure transducers ranged from 0.1 V to just over 5 V. The accuracy for the 0.1-V measurement with 5-1/2 digits displayed is (0.1 V × 0.00007) + 0.00005 V = 0.00051 V. The accuracy for the 5-V measurement is (5 V × 0.00006) + 0.00001 V = 0.00031 V. Clearly the error introduced by the HP measurement is negligible for the accuracies needed in this experiment. A summary of the instrumentation uncertainties is presented in Table C-3.

Table C-3. Summary of Instrumentation Uncertainty

Measurement	Uncertainty
Flow	±0.8% of reading
Pressure	
0-50 psia	±1.4 kPa (±0.2 psia, ±0.5 ft of water)
0-100 psia	±2.8 kPa (±0.4 psia, ±0.9 ft of water)
0-10 psid	±0.28 kPa (±0.04 psid, ±0.1 ft of water)
Current	±0.06 A
Voltage	±1.1V
Data acquisition system	negligible

C.6 RESULTS OF PUMP TESTING

Figures C-2 and C-5 show the manufacturers' published head-flow (H-Q) curves for the pumps tested. Note in Figures C-3a, C-3b, C-4a, and C-4b that there is a flat section in the H-Q curve. This is not characteristic of the pumps. Figures C-6, C-7, and C-8 do not show this flat section because of the lower pressure head of the Grundfos pump. Additional instrument error in the differential pressure transducer can be seen by comparing the H-Q curves in Figures C-3a and C-3b and also Figures C-4a and C-4b. Figures C-3a and C-3b have the flat section at about 75.8 kPa (11 psid or 25.4 ft of water). Figures C-3b and C-4b have the flat section at about 53.8 kPa (7.8 psid or 18.1 ft of water). The differential pressure transducer is rated at ±69 kPa (±10 psid or 23.1 ft of water) and can be raised to six times that amount without damage. However, the transducer did not appear to operate properly at the higher pressure differentials. The zero set and span set were checked before and after each test and were found to be very close to the specifications.

Even though tests could not be conducted at higher flow rates, the flow rates critical to an SDHW system ($9.4\text{-}22.1 \times 10^{-5}$ m^3/s or 1.5-3.5 gpm) were tested. These tests confirm very low pump efficiencies and increased electrical power with increased flow rates.

At higher flow rates, the H-Q curves of Figures C-3a and C-4a agree fairly well with the manufacturer's curve. The pressure head at the lower flow rates for the Richdel pumps, however, could not be measured.

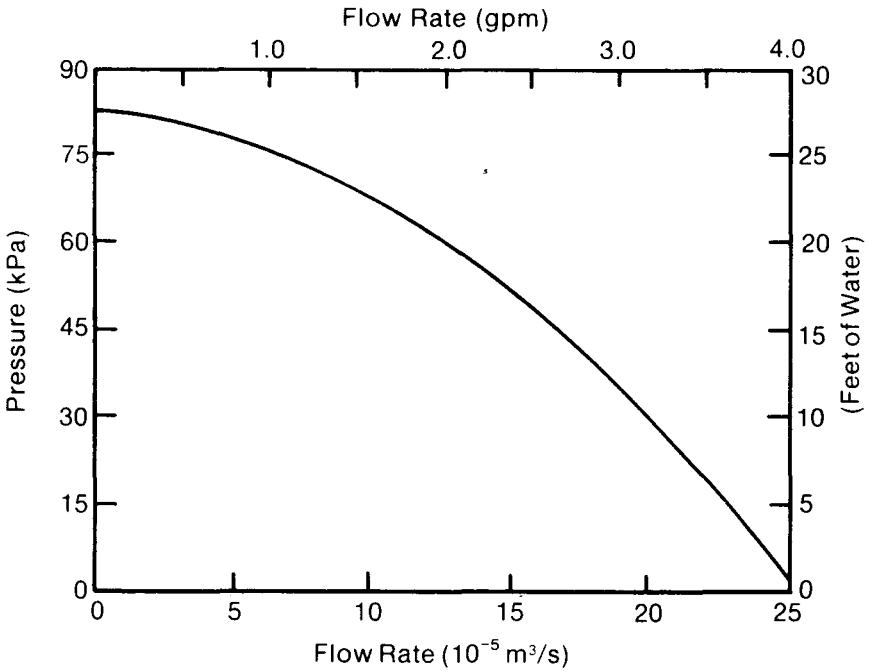

(Source: Richdel, Inc.)

Figure C-2. Richdel R798A Published Pump Curve
(Hot Water Recirculation Pump)

The Grundfos pump supplies very little head but can provide high flow rates. Because of this, only the left portion of the curve could be measured. The H-Q curve for speed 1 (Figure C-6) agrees well with the manufacturer's curve (Figure C-5). However, the measured H-Q curves for speeds 2 and 3 (Figures C-7 and C-8) do not agree with the published curve. This is probably because the uncertainty of the differential pressure transducer was larger than specified.

Within the tested range of flow rates, the overall pump efficiency (electric input to hydraulic power) peaks at about 6%, somewhat lower than anticipated. The difference may come from increased power for both pumps, somewhat lower H-Q curves in one case, and instrumentation uncertainty. There is a small increased power rating for the Grundfos pump. Since there is instrumentation error in the H-Q curves at the higher pressure differences, there is also a greater uncertainty in the pump efficiencies at the corresponding low flow rates. There is a large difference--150 to 190 W--between the published power rating for the Richdel pumps and the measured power rating. Richdel publishes a power rating of 80 W at 120 V and 1.3 A.

A new Taco 009 pump was also tested. The results are shown in Figure C-9. Overall pump equipment efficiency peaked at 10.3% at 3.2×10^{-4} m³/s (5.15 gpm). Instrumentation limitations prevented efficiency measurements at high head (above 55.5 kPa [18.5 ft of water or 8.1 psid]). The manufacturer's published results are shown in Figure C-9. The power of the pumps shown is only the volts-amps measurement and does not account for the power factor. The power factor was measured for two of the pumps and is discussed later. Because of the flat response of the differential pressure transducer and flow

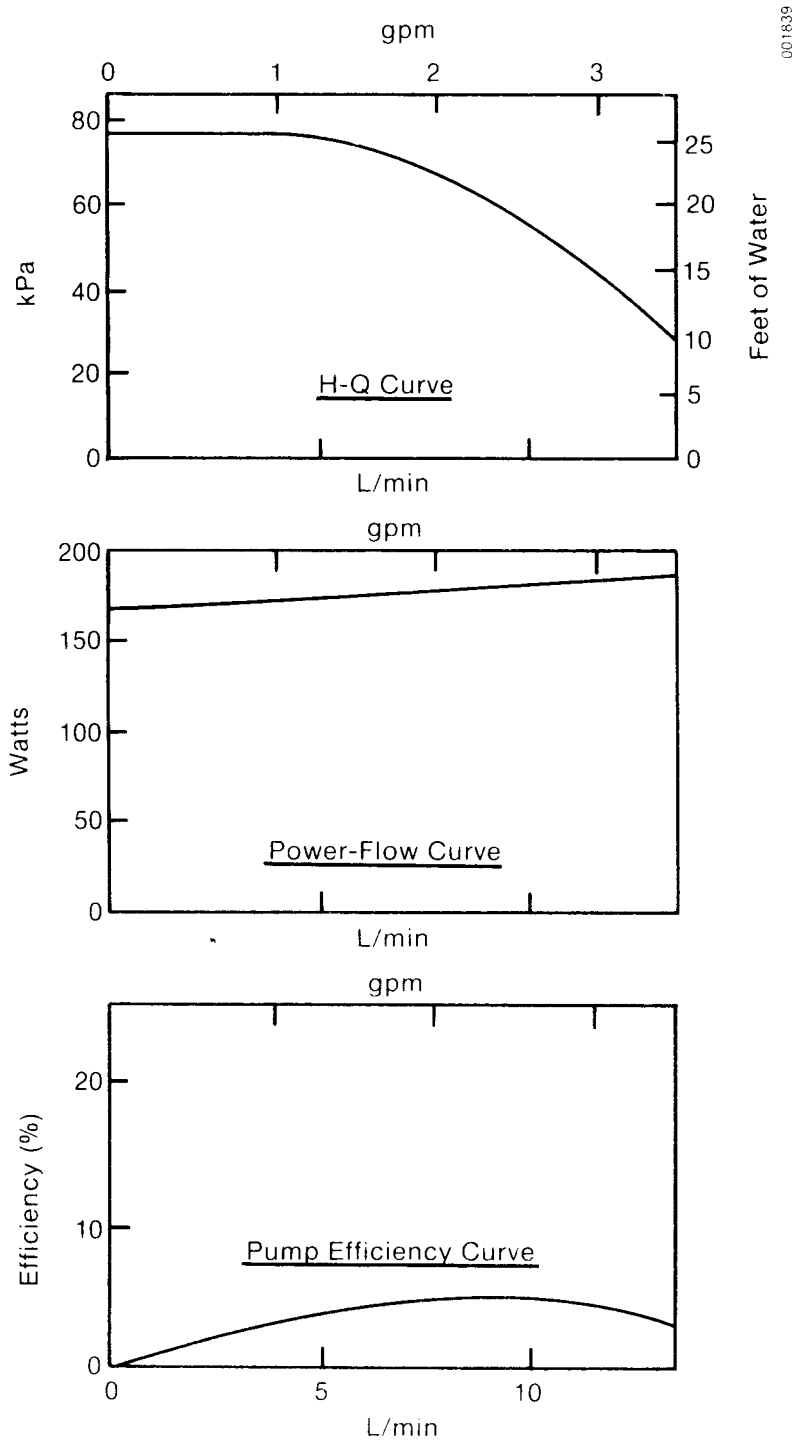

Figure C-3a. Experimental Curve for Used Richdel R798A Pump, Test I

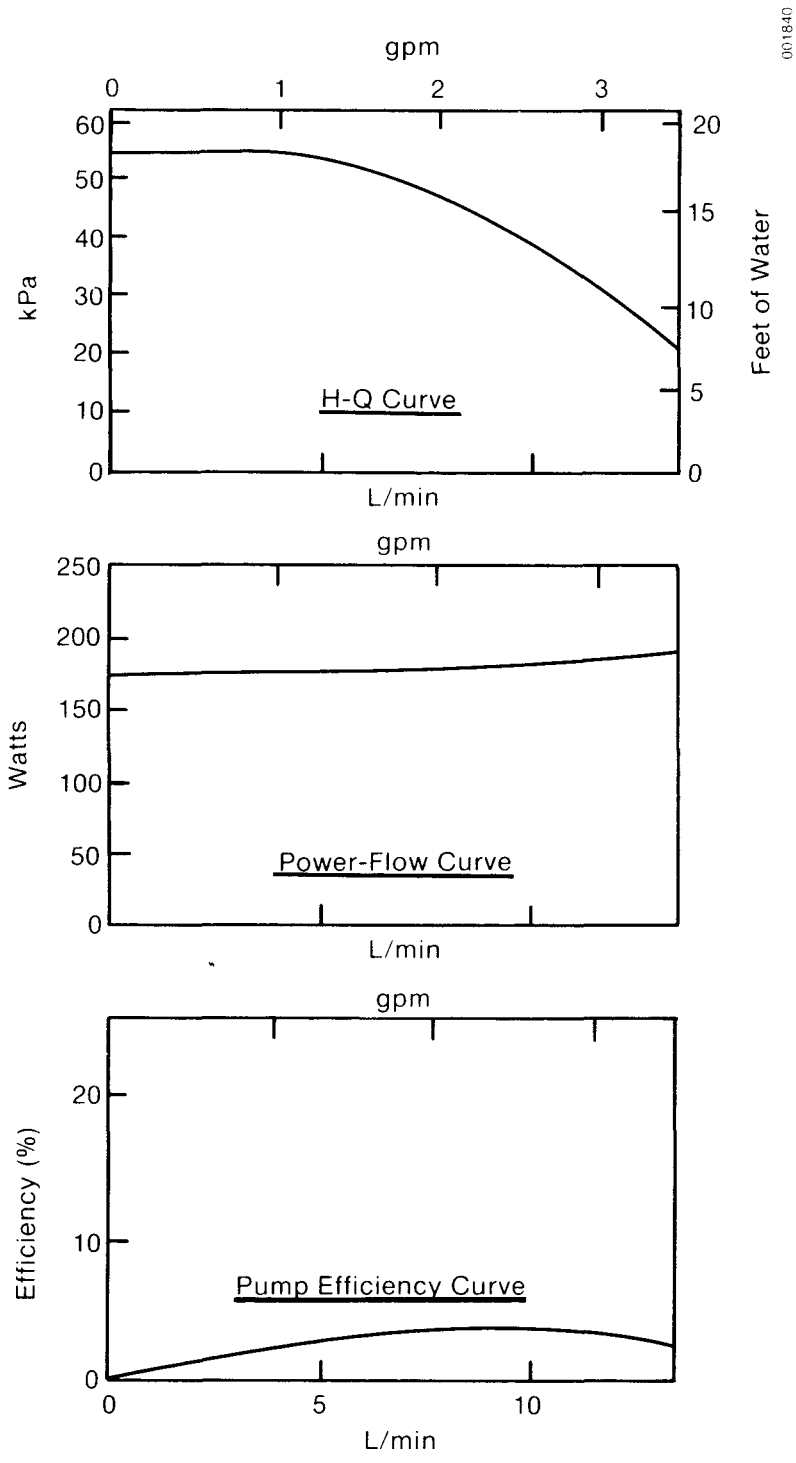

Figure C-3b. Experimental Curve for Used Richdel R798A Pump, Test II

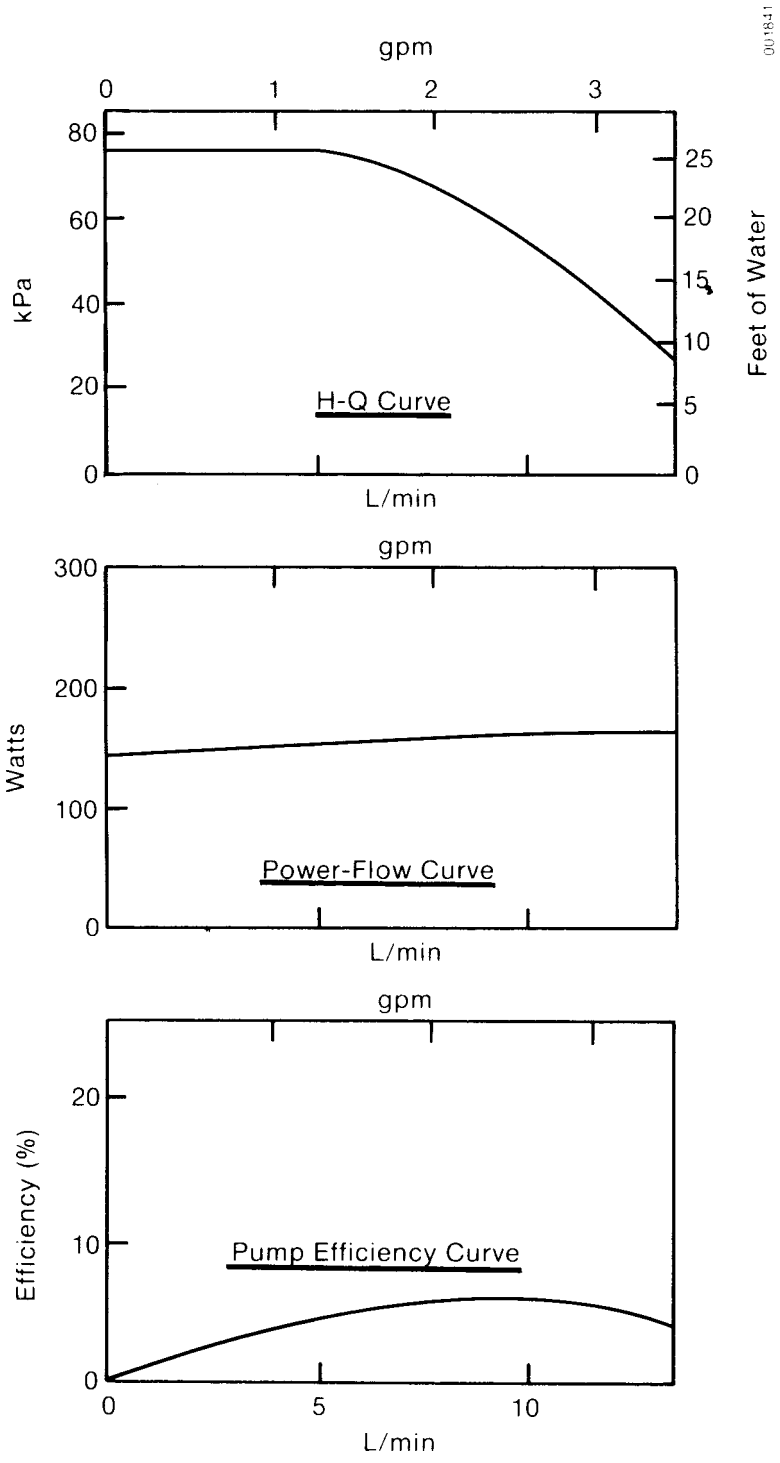

Figure C-4a. Experimental Curve for New Richdel R798A Pump, Test I

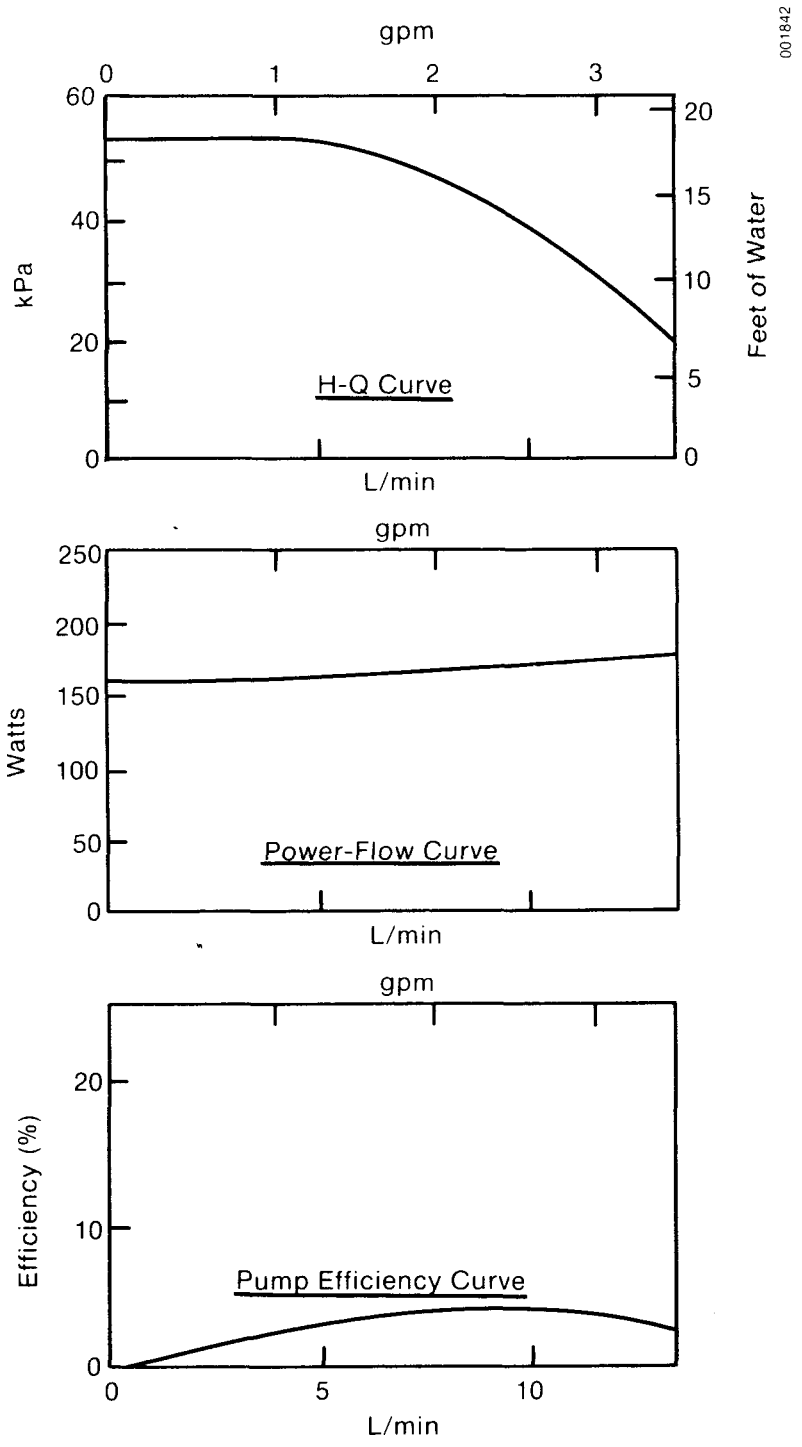

Figure C-4b. Experimental Curve for New Richdel R798A Pump, Test II

Performance:

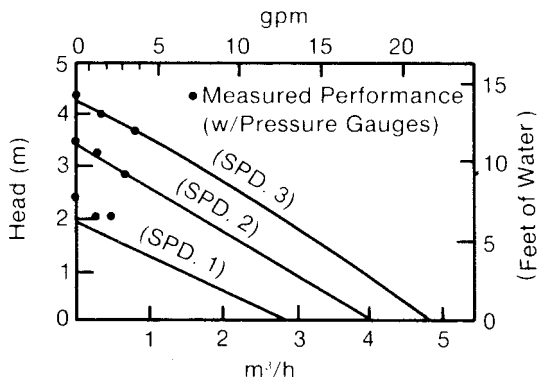

Electrical:

Model	Speed	Hp	Watts	Volts	Amps	RPM	Capacitor
UPS 20-42 F	3	1/20	95	115	0.85	2620	10 MF/180 V
3-Speed	2	1/32	70	115	0.60	2300	
	1	1/64	50	115	0.42	1800	

(Source: Grundfos)

Figure C-5. Published Grundfos UPS 20-42 Pump Curve

range limitations, the H-Q curve and pump efficiency curve in Figure C-9 have meaning only between the flow rates 1.8×10^{-4} m^3/s (2.9 gpm) and 3.2×10^{-4} m^3/s (5.15 gpm).

At a typical SDHW flow rate of 1.9×10^{-4} m^3/s (3 gpm), the overall equipment efficiency of the pump is 7.4%.

The equation for the overall equipment efficiency of the pump is:

$$\eta = \frac{Q(m^3/s) \times H\ (kPa) \times 1000\ kg/m^3}{i(amps) \times V(volts)} ,$$

or

$$\eta = \frac{Q(gpm) \times H\ (ft\ water) \times 8.3\ (lb/gal)}{i(amps) \times V(volts) \times 44\ (ft \cdot lb/W \cdot min)} .$$

The root mean square uncertainty of the overall pump efficiency η is

$$w_\eta = \left[\left(\frac{\partial \eta}{\partial Q} w_Q\right)^2 + \left(\frac{\partial \eta}{\partial H} w_H\right)^2 + \left(\frac{\partial \eta}{\partial i} w_i\right)^2 + \left(\frac{\partial \eta}{\partial V} w_V\right)^2\right]^{1/2} ,$$

where w_j is the uncertainty in the measurement of quantity j.

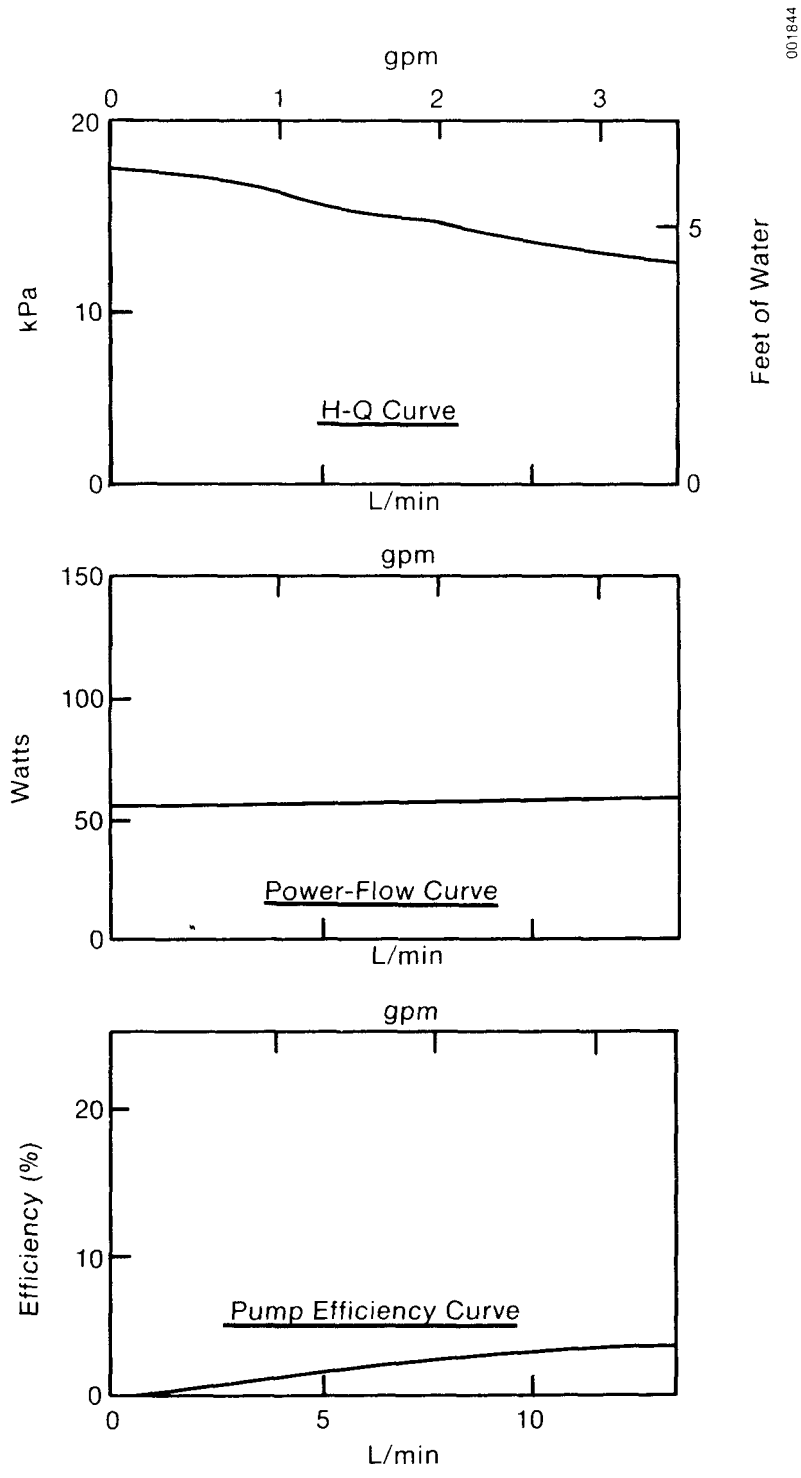

Figure C-6. Experimental Grundfos UPS 20-42 Pump Curve, Speed 1 (Low)

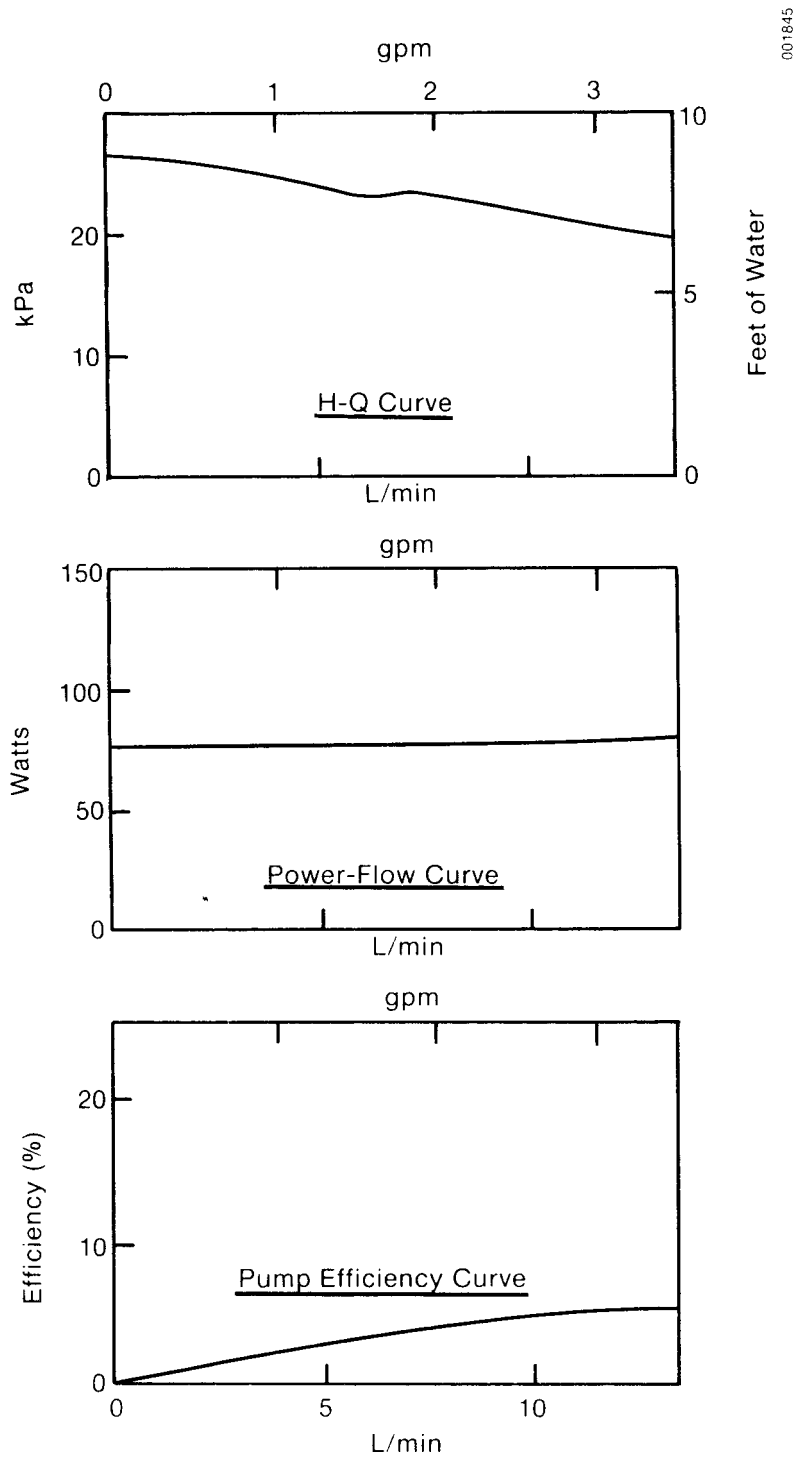

Figure C-7. Experimental Grundfos UPS 20-42 Pump Curve, Speed 2 (Med.)

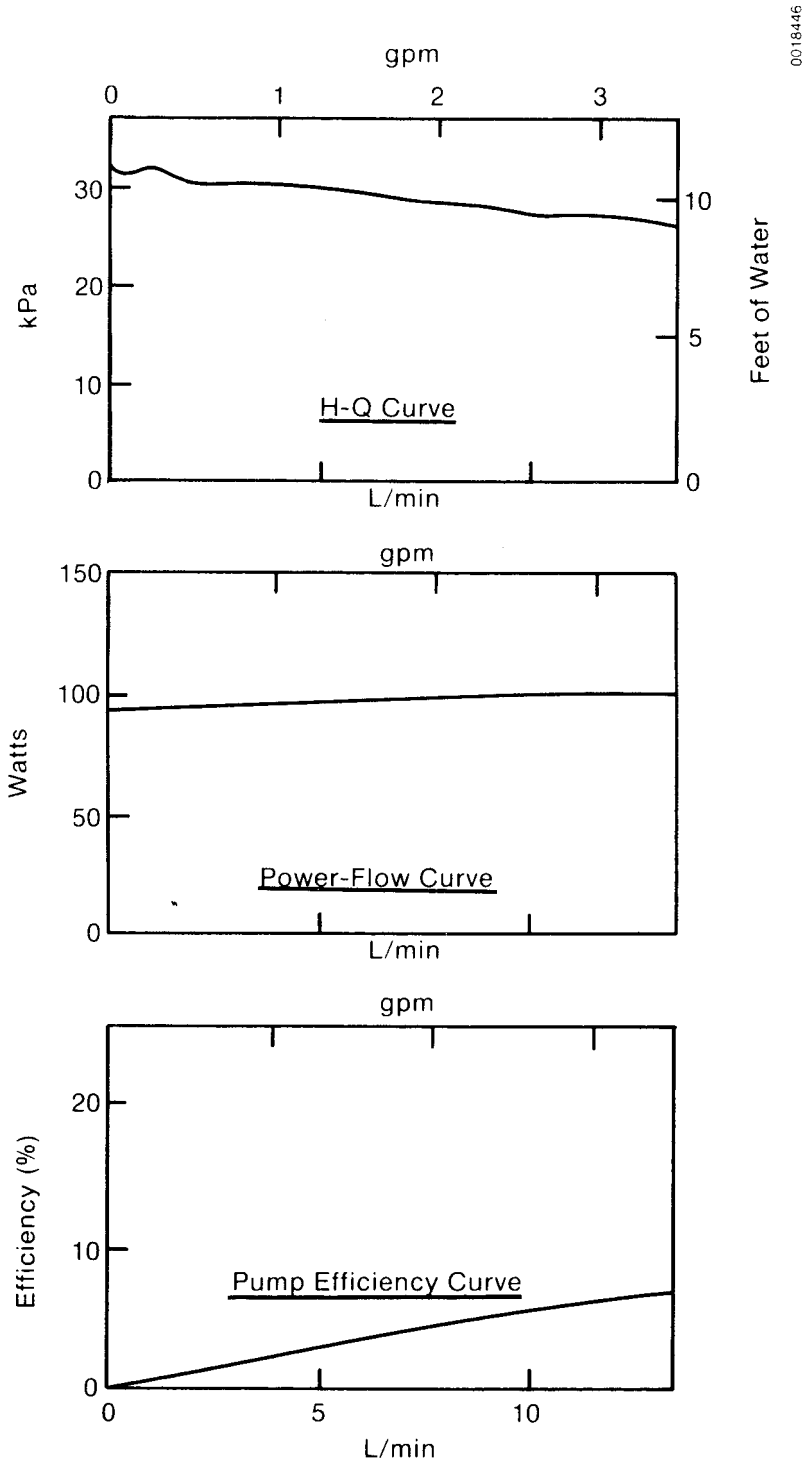

Figure C-8. Experimental Grundfos UPS 20-42 Pump Curve, Speed 3 (High)

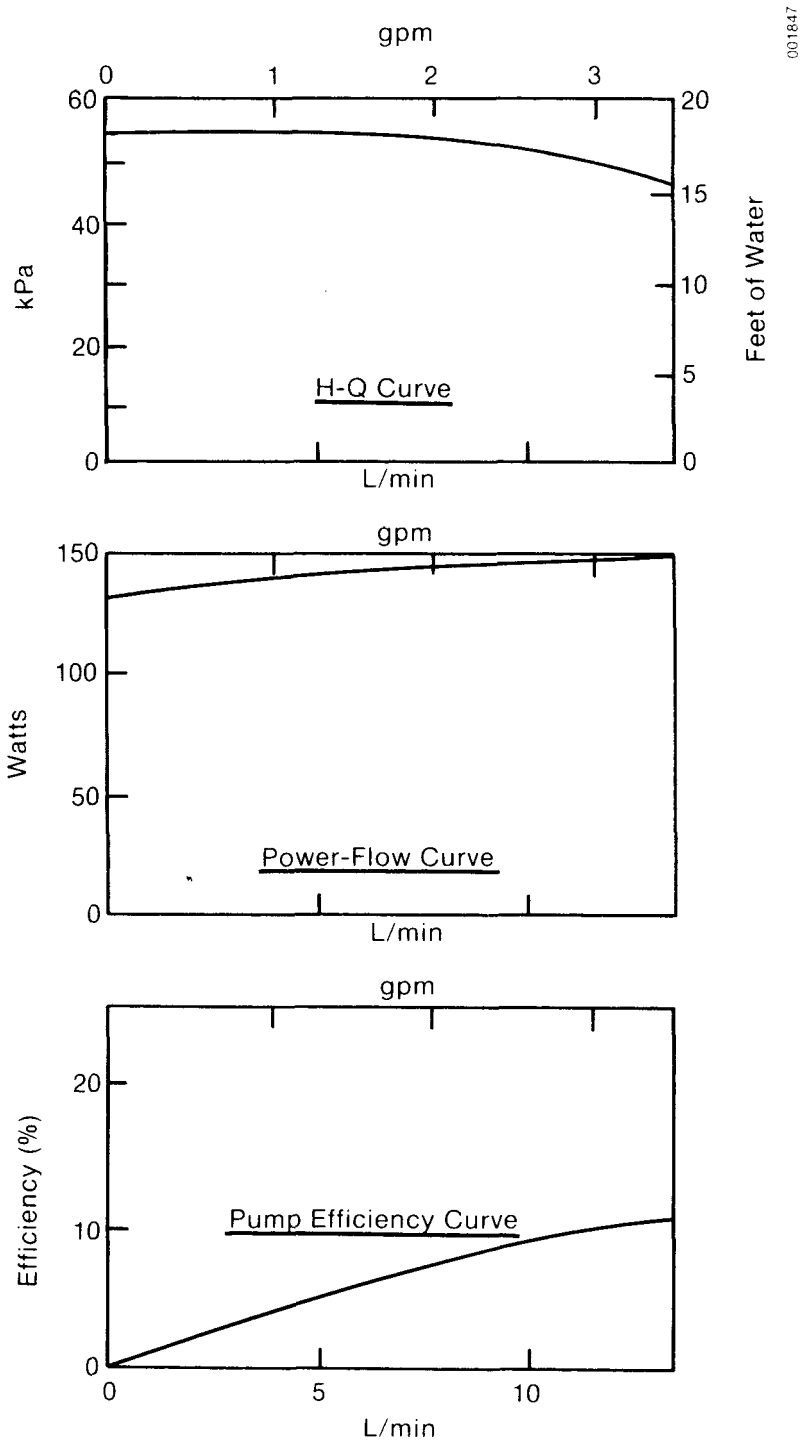

Figure C-9. Taco 009 Pump Curve with Strain Gauge Differential Pressure Transducer

If the differentiation is performed and the instrument uncertainty included, then w_η becomes

$$w_\eta = \left[\left(\frac{H}{iV}\right)^2 (0.008Q)^2 + \left(\frac{Q}{iV}\right)^2 (0.28)^2 + \left(\frac{-QH}{i^2V}\right)^2 (0.06)^2 + \left(\frac{-QH}{iV^2}\right)^2 (1.1)^2\right]^{1/2} (1000) ,$$

or

$$w_\eta = \left[\left(\frac{H}{iV}\right)^2 (0.008Q) + \left(\frac{Q}{iV}\right)^2 + (0.04)^2 + \left(\frac{-QH}{i^2V}\right)^2 (0.06)^2 + \left(\frac{-QH}{iV^2}\right)^2 (1.1)^2\right]^{1/2} \left(\frac{8.3}{44}\right) .$$

For the case of 1.9×10^{-4} m^3/s (3 gpm),

$H = 55.3$ kPa (18.5 ft of water)

$i = 1.14$ A

$V = 123.9$ V

$\eta = 7.4\%$.

The uncertainty in the pump equipment efficiency using the specified instrumentation uncertainty is ±0.004 or about 5.4% of the measured efficiency.

The measured H-Q curve between 1.9×10^{-4} and 3.2×10^{-4} m^3/s (3 and 5 gpm) is below the published curve by 9 to 15 kPa (3 to 5 ft of head). The measured power-flow curve is above the published one by 30 to 40 W. The pump is rated at 115 V and was operated at about 124 V. In addition, the measured power does not account for the motor's power. The published efficiency (Figure 4-9) is the estimated pump efficiency, excluding the motor. The measured efficiency is an overall equipment efficiency. At 1.9×10^{-4} m^3/s, the measured pump equipment efficiency is 7.4%. The published pump efficiency is about 33%. If the power factor is assumed to be near unity, the motor efficiency is 7.4/33 or about 22%. If the power factor is 0.9, then the motor efficiency is about 25%.

The pump equipment efficiency derived from the published H-Q curve (Figure 4-9) is 12% at 1.9×10^{-4} m^3/s (3 gpm). The measured overall pump efficiency at that flow rate is 7.4%.

SELECTED DISTRIBUTION LIST

Mr. Clarence B. Beaver
Beaver Brothers
1029 West Innes Street
Salisbury, NC 28144

Mr. Donald Bowden
Solar Unlimited, Inc.
37 Traylor Island
Huntsville, AL 35801

Mr. Dan Cautley
Division of State Energy
101 South Webster Street, 8th Floor
P.O. Box 7868
Madison, WI 53707

Mr. Jack T. Cole
Energy, Mines, and Resources Canada
Renewable Energy Division
580 Booth Street
Ottawa, Canada K1A 0E4

Dr. Kirk Collier
Route 2, Box 240
Cave Creek, AZ 85331

Mr. Carl Conner
U.S. Department of Energy
CE-311, Room 5H-095
Forrestal Building
1000 Independence Avenue, S.W.
Washington, D.C. 20585

Mr. Robert Dikkers
National Bureau of Standards
Technology B-148
Washington, D.C. 20234

Mr. Webb Farber
U.S. Solar Corporation
P.O. Drawer K
Hampton, FL 32044

Mr. John Goldsmith
U.S. Department of Energy
CE-311, Room 5H-065
Forrestal Building
1000 Independence Avenue, S.W.
Washington, D.C. 20585

Mr. P. Golobic
Ministry of Energy
56 Wellesley Street
Toronto, Ontario
Canada L5K193

Mr. Robert Hassett
U.S. Department of Energy
CE-311.1, Room 5H-065
Forrestal Building
1000 Independence Avenue, S.W.
Washington, D.C. 20585

Mr. Steve Herzenberg
DHR, Inc.
6858 Old Dominion Drive
McLean, VA 22101

Mr. Jacques Hull
Acurex Solar Corporation
485 Clyde Avenue
Mountain View, CA 94042

Mr. Walter Ingle
ETEC
P.O. Box 1449
Canoga Park, CA 91304

Mr. Peter Jacobs
Novan Energy, Inc.
1630 North 63rd Street
Boulder, CO 80301

Mr. Bill Jones
Energy Systems Group
2231 Perimeter Park, Suite 11
Atlanta, GA 30341

Dr. Susumu Karaki
Colorado State University
Department of Mechanical Engineering
Fort Collins, CO 80523

Mr. Kim Jong Kyu
East-South Engineering
Daegu P.O. Box 297
Daegu 630 Korea

Mr. Ray Larsen
Acme Solar Works, Inc.
873 East Pine Street
Lodi, CA 95240

Mr. Robert LeChevalier
Department of Energy
San Francisco Operations Office
1333 Broadway
Oakland, CA 94612

Mr. Benno Lebkuchner
Taco, Inc.
1600 Cranston Street
Cranston, RI 02920

Dr. Peter Lunde
Hartford Graduate Center
275 Windsor Street
Hartford, CT 06120

Dr. John Mitchell
University of Wisconsin-Madison
Engineering Research Bldg. #1341
1500 Johnson Drive
Madison, WI 53706

Mr. Stan Moore
Los Alamos National Laboratory
MS K-571
P.O. Box 1663
Los Alamos, NM 87545

Dr. Fred Morse
U.S. Department of Energy
CE-31, Room 5H-095
Forrestal Building
1000 Independence Avenue, S.W.
Washington, D.C. 20585

Mr. Andrew Parker
Mueller Associates, Inc.
1900 Sulphur Spring Road
Baltimore, MD 21227

Mr. John Popovich
Sunwizard, Inc.
1424 West 259th Street
Harbor City, CA 90710

Mr. David Robison
Oregon Department of Energy
Renewable Resources
102 Labor and Industries Bldg.
Salem, OR 97310

Mr. M. P. Schard
Shell Chemical Company
One Shell Plaza
P.O. Box 2463
Houston, TX 77001

Mr. Harold Seielstad
PG&E Research Center
3400 Crown Canyon Road
San Ramon, CA 94583

Mr. B. E. Sibbett
National Research Council of Canada
Division of Energy
Ottawa, Canada K1A OR6

Mr. Morris Skalka
U.S. Department of Energy
CE-311, Room 5H-065
Forrestal Building
1000 Independence Avenue, S.W.
Washington, D.C. 20585

Mr. R. P. Spears
Reynolds Metals Company
Research and Development
Richmond, VA 23261

Mr. Burt Swerdling
Grumman Energy Systems Co.
445 Broadhollow Road
Melville, NY 11747

Mr. Alan Turick
Sealed Air Corporation
Park 80 Plaza East
Saddle Brook, NJ 07662

Mr. Guy Rohlfs Voss
Energy Contractors Group
13161 Newhope Street
Garden Grove, CA 92643

Mr. Michael Wahlig
Lawrence Berkeley laboratory
University of California
1 Cyclotron Road
Berkeley, CA 94720

Dr. Mashuri Warren
Lawrence Berkeley Laboratory
University of California
1 Cyclotron Road
Berkeley, CA 94720

Dr. Harry Whitehouse
Pacific Sun, Inc.
439 Tasso Street
Palo Alto, CA 94301

Mr. William S. Wilhelm
Brookhaven National Laboratory
Department of Applied Science
Upton, NY 11973

Mr. Brian Williams
Energy Center
128 West Pearl Alley
Santa Cruz, CA 95060

Mr. Gunnar Wilson
Special Projects and Solar Energy
Aluminiumteknik
S-612 21 Finspong, Sweden

Dr. Byron Winn
Colorado State University
Department of Mechanical Engineering
Fort Collins, CO 80523

Mr. Marvin Yarosh
Florida Solar Energy Center
300 State Road 401
Cape Canaveral, FL 32820

Mr. John Yellott
901 West El Caminito
Phoenix, AZ 85021